University of Massachusetts Amherst
ScholarWorks@UMass Amherst

Doctoral Dissertations 1896 - February 2014

1-1-1992

# Synthesis and adsorption of polymers :: control of polymer and surface structure/

Molly Sandra Shoichet
*University of Massachusetts Amherst*

Follow this and additional works at: https://scholarworks.umass.edu/dissertations_1

Recommended Citation
Shoichet, Molly Sandra, "Synthesis and adsorption of polymers :: control of polymer and surface structure/" (1992). *Doctoral Dissertations 1896 - February 2014*. 802.
https://scholarworks.umass.edu/dissertations_1/802

This Open Access Dissertation is brought to you for free and open access by ScholarWorks@UMass Amherst. It has been accepted for inclusion in Doctoral Dissertations 1896 - February 2014 by an authorized administrator of ScholarWorks@UMass Amherst. For more information, please contact scholarworks@library.umass.edu.

31206601075147 5

# SYNTHESIS AND ADSORPTION OF POLYMERS: CONTROL OF POLYMER AND SURFACE STRUCTURE

A Dissertation Presented

by

MOLLY SANDRA SHOICHET

Submitted to the Graduate School of the
University of Massachusetts in partial fulfillment
of the requirements for the degree of

DOCTOR OF PHILOSOPHY

September 1992

Polymer Science and Engineering Department

# SYNTHESIS AND ADSORPTION OF POLYMERS: CONTROL OF POLYMER AND SURFACE STRUCTURE

A Dissertation Presented

by

MOLLY SANDRA SHOICHET

Approved as to style and content by:

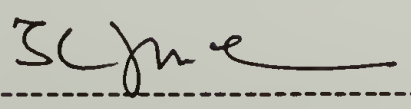

Thomas J. McCarthy, Chair

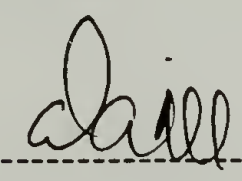

David A. Tirrell, Member

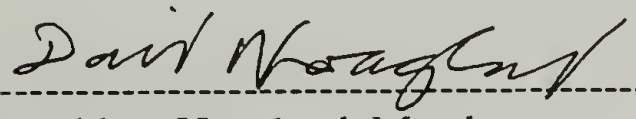

David A. Hoagland, Member

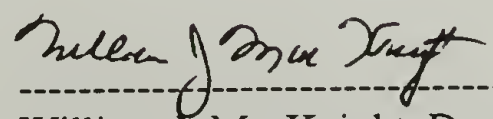

William J. MacKnight, Department Head
Polymer Science and Engineering

To my parents, Dorothy and Irving Shoichet

# ACKNOWLEDGMENTS

During graduate school I met interesting scientists, made good friends, had a supportive advisor and worked on challenging research projects. I entered graduate school with hopes of expanding the "bubble of science"; I leave graduate school with the same aspirations. Tom McCarthy and I were able to combine our interests, mine in biopolymers and his in surface science, to develop an interesting and integrative project. Tom is a great advisor; his creativity and enthusiasm for science fueled my own and made my experience in graduate school much more enjoyable. While giving me the opportunity to try new ideas and make mistakes, Tom also provided sage advice and brought me back on track when I drifted too far afield. Dave Tirrell and Dave Hoagland were both very supportive; they always made time to advise me on different aspects of both my project and future. I had a superb committee and am grateful for their interest. I wish to thank a number of people from various disciplines for their guidance: Jim Prescott and Professor R.L. Rowell (PCS); Rich McCarron, Donna Beer, and Professor Bruce Jacobson (biological cell study); Jim Thomas and Professor Scott Barton (surface tensiometer); Jay Goldfarb and Professor Dick Farris (peel tests); and Judy Landin and Professor David Dooley (CD spectroscopy at Amherst College).

The McCarthy research group is partly responsible for the success of this project. I enjoyed working with and learning from Cady, Joan, Brant, Nicole, Katrina, Damo, Tim, Eric, Bob F., Bob B., Rick, Anthony, and of course Jack. Special thanks are due to Brant who was always willing and able to help.

I have gained strength in the friendships I have made throughout my life. Michele Maden, Mardye Lindway, and Mike Graff enriched my life at UMass and made the experience more worthwhile. Hillary Thompson, Andrea Ghez, Marilyn Oberhardt, and Tina Cortesi, are especially dear to me and continue to challenge and support me.

I dedicate this dissertation to my parents, Dorothy and Irving Shoichet, who have given me the strength of my convictions and the will to strive for the stars. My parents have paved for me a wonderful road of opportunity constructed of pebbles of curiosity and learning. My brothers Brian and Richard are great friends and mentors; together we gain the strength that enhances the love and respect we have for one another.

My fiancé, Kevin Bartus, has been a great distraction throughout graduate school, making my life much more fun and diverse. As we embark on a wonderful adventure through life together, we hope to explore new and challenging venues filled with laughter.

ABSTRACT

SYNTHESIS AND ADSORPTION OF POLYMERS:

CONTROL OF POLYMER AND SURFACE STRUCTURE

SEPTEMBER 1992

MOLLY SANDRA SHOICHET,

S.B., MASSACHUSETTS INSTITUTE OF TECHNOLOGY

M.S., UNIVERSITY OF MASSACHUSETTS

Ph.D., UNIVERSITY OF MASSACHUSETTS

Directed by: Professor Thomas J. McCarthy

Polymer surface modification can be accomplished by several techniques including chemical reaction and adsorption. In Chapter I, a simple and versatile technique to introduce carboxylic acid functionality to the surfaces of three fluoropolymer film samples is described. In Chapter II, the adsorption of neutral poly(L-lysine) (PLL) from solution to the water - fluoropolymer interface is described. Chapter III combines the methods of surface modification described in Chapters I and II and discusses the adsorption of charged PLL to a carboxylic acid-functionalized fluoropolymer film surface. The hydrophobic interaction as a driving force for adsorption is further studied in Chapter IV where the synthesis and adsorption of poly(ethylene oxide) (PEO) and its derivatives are discussed.

The syntheses of carboxylic acid-functionalized fluoropolymer films rely upon a two step mechanism where unsaturation, introduced in the first step, is oxidatively removed in the second step; one acidic group per twelve to sixteen repeat units was introduced to the surface. Contact angles ($\theta_A/\theta_R$) of the acid-functionalized fluoropolymer films decrease with increasing pH: $PVF_2$-$CO_2H$ (77°/39° decreases to 68°/25°); PCTFE-$CO_2H$ (93°/55° decreases to 93°/43°); and FEP-$CO_2H$ (101°/78° decreases to 97°/61°).

The adsorption of poly(L-lysine) (PLL) to the water - FEP interface was controlled by pH of the aqueous solution and PLL solution conformation. Only neutral, α-helical

PLL adsorbed to FEP (FEP-PLL). The adsorption of PLL to carboxylic acid-functionalized FEP, FEP-$CO_2H$, was controlled by an electrostatic interaction; both a hydrogen bonding interaction between FEP-carboxylic acid and PLL backbone and an ionic interaction between FEP-carboxylate and PLL-ammonium enhanced adsorption. Both FEP-PLL (80°/16°) and FEP-$CO_2H$-PLL (78°/29°) are more hydrophilic than FEP. FEP-PLL-ε-amine reacts with 3,5-dinitrobenzoyl chloride in 65% yield whereas FEP-$CO_2H$-PLL-ε-amine reacts in 100% yield. Adsorption of PLL to FEP and FEP-$CO_2H$ improves the peel strength of adhesive joints prepared with these substrates and the adhesion and growth of biological cells on these film samples.

PEO (5,000 to 50,000 g/mole and polydispersity indices of 1.07 to 1.17) was synthesized by anionic ring opening polymerization of ethylene oxide in THF with triethylene glycol monomethyl ether potassium initiation. PEO was end-capped (PEO-R) by reaction with a (perfluoro)alkyl acid chloride in THF with pyridine catalysis. A polar interaction between substrate and segment controlled adsorption at the fluoropolymer - water interface; PEO adsorbed preferentially to $PVF_2$ over PCTFE and FEP. Both PEO and PEO-R adsorbed to the polystyrene latex - water interface; the latter formed a thicker adsorbed layer. PEO-R showed increased surface activity over PEO at the air - water interface; PEO-perfluorodecanoate decreased the surface tension of water to 35 dyn/cm.

TABLE OF CONTENTS

LIST OF TABLES

LIST OF FIGURES

# LIST OF SCHEMES

# CHAPTER I

# CONVENIENT SYNTHESES OF CARBOXYLIC ACID-FUNCTIONALIZED FLUOROPOLYMER SURFACES

## Overview

Carboxylic acid functionality was introduced to the surfaces of film samples of three fluoropolymers by two-step chemical modifications: the initial reactions introduced thin layers of unsaturation which were subsequently oxidatively removed to render carboxylic acid functionality at the film surfaces. The density of carboxylic acid functionality on the three fluoropolymer films was estimated by x-ray photoelectron spectroscopy: for poly(vinylidene fluoride) ($PVF_2$) at $(CH_2CF_2)_{13}(CO_2H)_1$, for poly(chlorotrifluoroethylene) (PCTFE) at $(CF_2CFCl)_{12}(CO_2H)_1$, and for poly(tetrafluoroethylene-co-hexafluoropropylene) (FEP) at $(CF_2CF_2)_{16}(CO_2H)_1$. The acid functionality on the films was further modified by chemical reaction to thallous carboxylate and to primary alcohol that was esterified with trichloroacetyl chloride. A titration curve of contact angle vs. pH showed the pH sensitivity of the carboxylic acid group. The acid functionalized fluoropolymer films were prepared for adsorption studies. As discussed in Chapter III, adsorption is controlled by ionic interactions between surface carboxylate and an ammonium-functionalized polymer dissolved in solution. Chapter II addresses the adsorption of a neutral amine-functionalized polymer to unmodified fluoropolymer. The reactions described herein were characterized by x-ray photoelectron spectroscopy, contact angle, attenuated total reflection infrared spectroscopy, ultraviolet-visible spectrophotometry, scanning electron microscopy and gravimetric analysis.

# Introduction

Surface modification plays an important role in several industries where lubricity, repellency, adhesion or antistatic properties are required.[1] Because objects interact with other objects and their environment via their surfaces, it is important to understand surface structure and properties.[2] The surface is the interface between the object and the environment in which it is immersed. For polymers, the surface can be thought of as mobile if the temperature is greater than the polymer's $T_g$ or if the surroundings swell or permeate the polymer. There are several ways to modify a surface[2] including plasma treatment, surface graft polymerization, adsorption, photochemical modification,[3] and chemical modification. This chapter focuses on chemical modification of fluoropolymer films.

In chemical surface modification, organic chemistry is applied at the polymer film - solution interface in an attempt to derivatize the surface in the same way that one would derivatize a small molecule dissolved in solution.[4] Geometric constraints and the location of functional groups on the surface affect both chemical transformations and their stability in different surroundings. Because the reaction is confined to a surface, the side products and impurities are also located at the surface; a surface reaction should occur in high yield to ensure that the surface functionality - property relationship can be defined. Ideally, one would prepare specifically functionalized polymer surfaces with well defined composition and functionality density where a relation between surface structure and property and surface structure and reactivity could be assigned.[5] More specifically, one could manipulate the surface properties by introducing a specific functional group which would be useful in controlling adsorption, wetting or adhesion.[6]

Fluoropolymers offer unique opportunities in the preparation of specifically functionalized surfaces for a number of reasons.[4,7] Because they are chemically resistant, several reactions can be studied on the surface without affecting the bulk of the

fluoropolymer; a wide variety of functional group transformations can be applied by taking advantage of those developed in organic chemistry. Fluoropolymers offer an advantage over hydrocarbon polymers, such as polyethylene, due to their chemical insensitivity. For polyethylene, it is difficult to distinguish surface functionality from the bulk because the surface - bulk interface is rather diffuse.[8,9] In addition, fluoropolymer films are amenable to several analytical techniques; they are spectroscopically distinct such that most chemical transformations can be be easily followed. Fluoropolymer films are transparent to ultraviolet-visible (UV-vis) radiation, have few peaks above 1500 $cm^{-1}$ in the infrared spectrum, have a lucid carbon region in x-ray photoelectron spectroscopy (XPS or ESCA), and have the integrity for both gravimetric analysis and scanning electron microscopy (SEM). Since fluoropolymers are low surface energy materials, introduction of polar functionality is easily detected by contact angle analysis.

A simple and versatile technique was developed where a thin layer of carboxylic acid functionality was introduced to fluoropolymer film samples.[10] The surface chemistry was developed for use in adsorption studies of amine-functionalized polymers. The adsorption of polymers dissolved in solution to polymer films would be controlled by discrete ionic interactions between the carboxylic acid-functionalized fluoropolymer surface and the amine-functionalized dissolved polymer[11] (cf. Chapter III). The ideal substrate for adsorption studies would contain a "monolayer" (or "sub-monolayer") of carboxylic acids attached to a chemically inert, non-swellable, polymeric support.

Carboxylic acid-functionalized polymer films, specifically polyethylene, have been extensively studied.[12-20] Prior to the research reported herein, the synthesis of two carboxylic acid-functionalized fluoropolymer surfaces were reported; neither, however, was convenient to prepare nor ideal. Carboxylic acid functionality was introduced to poly(tetrafluoroethylene) (PTFE) by reduction with dipotassium benzoin dianion, radical addition of maleic anhydride and subsequent hydrolysis.[6] Because the initial reduction was corrosive, the resulting product was heterogeneous and a thin layer of functionality could

not be prepared. Poly(chlorotrifluoroethylene) (PCTFE) was carboxylic acid-functionalized by reaction with 2-(lithiomethyl)-4,4-dimethyloxazoline and subsequent hydrolysis;[4] since the hydrolysis was complicated and did not proceed to completion, oxazoline functionality was left unreacted on the polymer film surface. Another way to derivatize PCTFE with carboxylic acid functionality was recently reported; PCTFE was reacted with trimethyl 4-lithioorthobutyrate and the orthoester was then hydrolyzed with an aqueous solution of trifluoroacetic acid and acetone.[21] Four of every five surface PCTFE repeat units was derivatized with a chain extended (3 methylene groups) carboxylic acid functional group.

In this chapter, a two step chemical modification is discussed which was developed to introduce carboxylic acid functionality to the surfaces of poly(vinylidene fluoride) ($PVF_2$), PCTFE, and poly(tetrafluoroethylene-co-hexafluoropropylene) (FEP). The strategy, depicted in Scheme 1.1, involves a surface-selective reaction which introduces a thin layer (<100 Å) of unsaturation. The modified product is oxidatively removed leaving carboxylic acid groups covalently attached to the fluoropolymer at the modified - unmodified polymer interface; the fluoropolymer is inert to the oxidation conditions. The topography of the acid functionalized surface is controlled by that of the initial reaction product. The simplicity, versatility, and surface-selectivity of this technique make it useful.

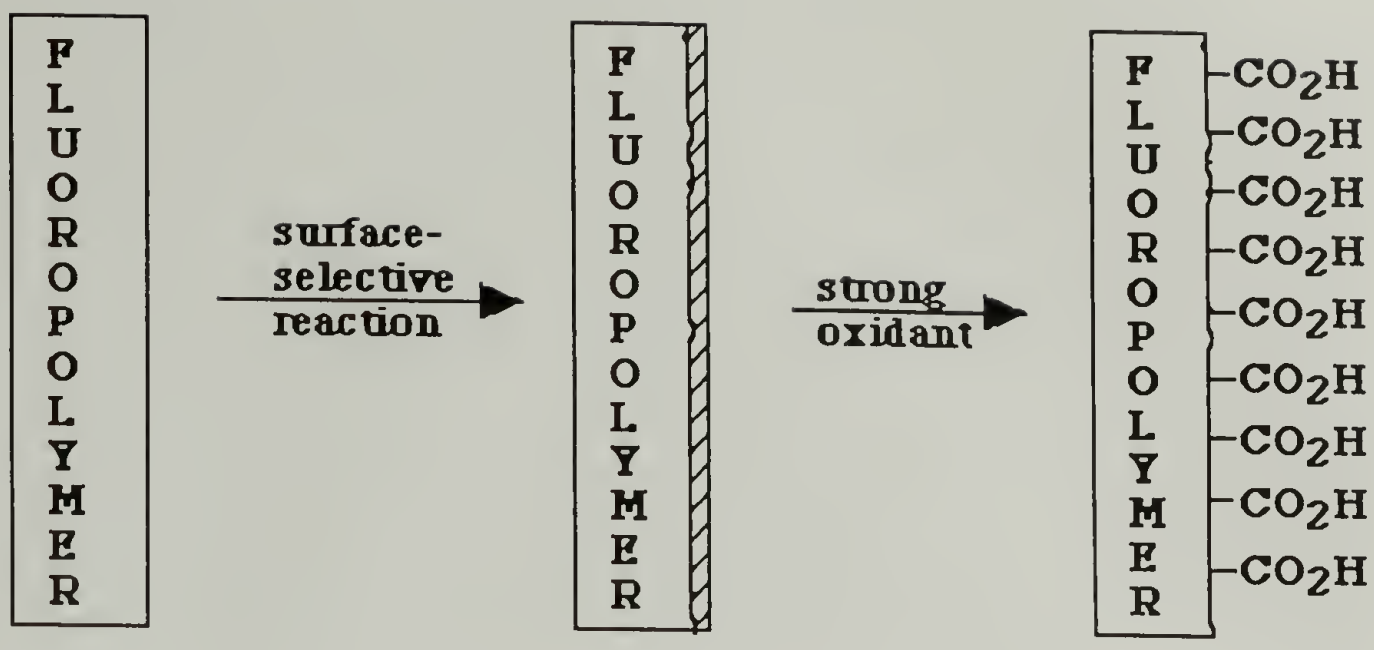


Scheme 1.1 Strategy Employed for Introduction of Carboxylic Acid Functionality to the Fluoropolymer Film Surface.

## Experimental

All reactions were carried out under nitrogen and solutions were degassed by sparging with nitrogen unless otherwise noted.

### Materials and Methods

**Poly(vinylidene fluoride)** ($PVF_2$) film (5 mil, Pennwalt Kynar) was obtained from Westlake Plastics and extracted in refluxing dichloromethane for 30 minutes, rinsed in fresh dichloromethane and dried (50 °C, 0.05 mm) to constant mass. Film samples were stored under vacuum.

**Poly(chlorotrifluoroethylene)** (PCTFE) film (5 mil, Aclar 33C) was provided by Allied and extracted in refluxing dichloromethane for 30 minutes, rinsed in fresh dichloromethane and dried (50 °C, 0.05 mm) to constant mass. Film samples were stored under vacuum.

**Poly(tetrafluoroethylene-co-hexafluoropropylene)** (FEP) film (5 mil, duPont) was extracted in refluxing dichloromethane for 30 minutes, rinsed in fresh dichloromethane and dried (50 °C, 0.05 mm,) to constant mass. Film samples were stored under vacuum.

**House Distilled Water** was redistilled using a Gilmont still.

**Tetrahydrofuran** (THF) (Aldrich, 99.9% anhydrous) was distilled from sodium benzophenone dianion.

**Heptane** (Aldrich) was distilled from calcium hydride.

**Thallous Ethoxide** (Aldrich) was filtered before use.

**Ethanol** (Absolute, 200° Pharmco) was distilled from magnesium/carbon tetrachloride.

**Pyridine** (Aldrich) was vacuum distilled from calcium hydride.

**pH Buffered Solutions** were prepared according to a published procedure.[22]

**Standardization of *n*-Butyllithium.**[23] 1 mmol of 1,3-diphenylacetone *p*-tosylhydrazone (Aldrich) was dissolved in 10 ml of THF in a 50 ml Erlenmeyer flask which was equipped with a stirring bar and purged with nitrogen. The solution was cooled to 0 °C and *n*-butyllithium (Aldrich, 1.6 M) was added dropwise via a 1 ml syringe until an orange color, indicative of the dianion, was present.

**Sodium Naphthalide** was prepared by reacting 5 g (40 mmol) naphthalene (Aldrich) dissolved in 250 ml THF with ~1.7 g (74 mmol) sodium pieces under nitrogen. The dark green solution was stirred for 3 h and stored under positive nitrogen pressure.

**Dehydrofluorination of $PVF_2$ ($PVF_2$-CH=CF).**[24,25] 20 ml of 8 M sodium hydroxide (Fisher) solution was added to a nitrogen-purged Schlenk tube containing a $PVF_2$ film sample which was then equilibrated for 30 minutes at 40 °C. 3 ml of a 0.03 M aqueous tetra-*n*-butylammonium bromide (Aldrich) solution, which had been equilibrated for 30 minutes at 40 °C, was added to the tube via cannula. After 3 minutes, the solution

was removed and the film sample was washed with water (10 x 20 ml), methanol (Fisher) (5 x 20 ml), and then dichloromethane (Fisher) (3 x 20 ml) and dried (>48 h, 0.05 mm, 50 °C). [I6,7,16,20,28,31,38,48,70,92,94,102,132,144; II18,21,43,62][26]

**Reaction of PCTFE with *n*-BuLi (PCTFE-Bu).** To a nitrogen-purged Schlenk tube equipped with a magnetic stirring bar, 15 ml of heptane and 3 mmol of *n*-butyllithium were added by cannula and stirred at -78 °C for 15 minutes. 15 ml of THF, equilibrated at -78 °C, was added to the tube and the solution was stirred for an additional 30 minutes at -78 °C. The solution was added by cannula to a nitrogen-purged Schlenk tube containing a PCTFE film sample equilibrated at -78 °C. The solution was removed after 1 h and the film sample was washed with methanol (20 ml, -78 °C), methanol (4 x 20 ml, room temperature), water (5 x 20 ml), and then dichloromethane (5 x 20 ml) and dried (>24 h, 0.05 mm). [II91,110,111]

**Reduction of FEP (FEP-C).**[27] 5 ml of THF was added by cannula to a nitrogen-purged Schlenk tube containing an FEP film sample which was equilibrated at -78 °C for 30 minutes. 15 ml of sodium naphthalide solution equilibrated to -78 °C was added by cannula to the Schlenk tube. After 1 h the solution was removed and the film sample was rinsed with THF (5 x 20 ml), water (5 x 20 ml), and then THF (2 x 20 ml), and dried (>24 h, 0.05 mm, 50 °C). The same procedure was followed for the reaction at 0 °C for 15 min. [II37,50,70,83,103,104]

**Oxidation of $PVF_2$-CH=CF with Potassium Permanganate/Acetone**

An eliminated $PVF_2$ ($PVF_2$-CH=CF) film sample was immersed in 400 ml of a 0.5 M solution of potassium permanganate (Fisher) dissolved in acetone (Aldrich) in an open vessel. After 30 minutes, 200 ml of water was added. The films were removed from the reagent and washed with water (3 x 100 ml), 0.5 M aqueous sodium bisulfate (3 x 100 ml), water (3 x 100 ml), 10% v/v aqueous sulfuric acid (100 ml), water (10 x 20 ml), methanol (5 x 20 ml) and then methylene chloride (3 x 20 ml) and dried (>24 h, 50 °C, 0.05 mm). [I28,33,38,42,44]

**Oxidation of Modified Film Samples ($PVF_2$-$CO_2H$, FEP-$CO_2H$, PCTFE-$CO_2H$)** The modified film sample was treated with a solution of 0.5 g potassium chlorate (Alfa) in 25 ml of sulfuric acid (Fisher, 98%) (0.16 M) for 2 hours at room temperature in an open vessel. After 2 h, the solution was removed and the film sample was washed with water (10 x 20 ml), methanol (5 x 20 ml), and then dichloromethane (3 x 20 ml), and dried (>24 h, 50 °C, 0.05 mm). [I142, II4,16,33-37-39,90]

**Labeling of Surface Carboxylic Acids with Thallium ($PVF_2$-$CO_2Tl$, FEP-$CO_2Tl$, PCTFE-$CO_2Tl$)** An oxidized film sample was exposed to neat thallous ethoxide at room temperature in a nitrogen-purged glove bag for 30 s. The film sample was washed with distilled ethanol (3 x 20 ml) and dried (>24 h, 50 °C, 0.05 mm). [II61,68,117,118; 112; 50,71,83,103]

**Reduction of Surface Carboxylic Acids ($PVF_2$-$CH_2OH$, FEP-$CH_2OH$, PCTFE-$CH_2OH$)** 20 ml of a 1.0 M solution of borane•THF (Aldrich, HPLC) was added via cannula to a nitrogen-purged Schlenk tube containing an oxidized film sample. After 1 h (at room temperature), the solution was removed and the film was washed with THF (5 x 20 ml), water (5 x 20 ml), and then methanol (5 x 20 ml), and dried (>24 h, 50 °C, 0.05 mm). [II68,117,118,126; 84,103,104; 109,111]

**Reaction of Surface Alcohols with Trichloroacetyl Chloride ($PVF_2$-$CH_2O$-$COCCl_3$, FEP-$CH_2O$-$COCCl_3$, PCTFE-$CH_2O$-$COCCl_3$)** 19 ml of THF, 0.5 ml of trichloroacetyl chloride, (Aldrich) and then 1 ml of pyridine were added to a nitrogen-purged Schlenk tube containing an alcohol-functionalized film sample. The solution was removed after 12 h at room temperature and the film sample was washed with THF (3 x 20 ml), methanol (6 x 20 ml), and then dichloromethane (3 x 20 ml), and dried (>24 h, 50 °C, 0.05 mm). [II68,117,118; 110,111; 84,103,104]; [II118,126; 104; 111]

**Contact Angle Titration Curves** were prepared by measuring the contact angles of pH buffered aqueous solutions between pH 1 and pH 13 on a fluoropolymer film

substrate: carboxylic acid-functionalized, alcohol-functionalized, or unmodified. The data reported is an average of at least 5 contact angle measurements made at different locations on the fluoropolymer film sample. [II43,66,69,94-97]

## Analytical Techniques

**Attenuated Total Reflectance Infrared** (ATR IR) spectra were taken under nitrogen using an IBM 32 FTIR spectrometer and a 45° germanium internal reflection element.

**Dynamic Advancing and Receding Contact Angle** ($\theta_A/\theta_R$) measurements were made using a Ramé-Hart telescopic goniometer and a Gilmont syringe with a 25-gauge flat tipped needle. Advancing ($\theta_A$) and receding ($\theta_R$) contact angles were measured using as the probe fluid either redistilled water or buffered aqueous solutions where noted. Contact angles reported are an average of at least five measurements taken at different locations on the film sample.

**Gravimetric Analysis** was performed on a Cahn 29 electrobalance containing a polonium source.

**pH** was checked using a Fisher 825MP pH meter which was calibrated with standard buffer solutions of pH 4, 7 and 11 (Fisher) before use.

**Scanning Electron Micrographs** (SEM) were recorded on a JEOL 60 SEM at magnifications of 20,000× and 100,000×. A thin gold layer (~200 Å) was sputter coated onto the film sample before analysis.

**Ultraviolet-visible** (UV-vis) spectra were taken on a Perkin Elmer λ3A spectrophotometer with an extracted unmodified film sample in the reference beam.

**X-ray Photoelectron Spectra** (XPS) were taken on a Perkin Elmer-Physical Electronics 5100 spectrometer using Mg Kα excitation (300W, 15 kV). The pressure in

the analysis chamber was ~$10^{-8}$ mm during data acquisition. Samples were analyzed at a 15° takeoff angle (between the film surface and the detector) at a pass energy of 89.45 eV and 71.55 eV for ~12 minutes for survey and $C_{1s}$ region spectra, respectively. The sensitivity factors used were $C_{1s}$ 0.210, $F_{1s}$ 1.00, $O_{1s}$ 0.628, $Cl_{2p}$ 0.557, $Tl_{4f}$ 6.150. Binding energies reported are not corrected for charging.

## Results and Discussion

Polymer surface modification involves the introduction of a versatile functional group or reactive handle which can be further modified to introduce additional functionality to the polymer surface. The surface can be defined as that part of the polymer that interacts or reacts with the solution or reagents. The mobility of the surface groups of an organic material is affected both by reaction temperature and solvent. The initial reaction defines the surface of subsequent reactions in terms of roughness, thickness, and chemical heterogeneity, assuming that the bulk polymer is inert to subsequent reaction conditions. On the one hand, a thinly modified layer which intersects the unmodified bulk polymer at a sharp interface produces a smooth surface upon subsequent reaction. On the other hand, a diffuse and pitted surface produces a rough surface upon subsequent reaction. Reactions of the former type have been reported for all three fluoropolymers studied $PVF_2$,[24,25,28] FEP,[27] and PCTFE.[4,5] In this work, the sharpness/diffuseness at the modified - unmodified polymer interface defines the topography of the polymer surface of subsequent reactions because reagents are chosen that react with the reactive handle only, and not the bulk fluoropolymer.

$PVF_2$: Elimination

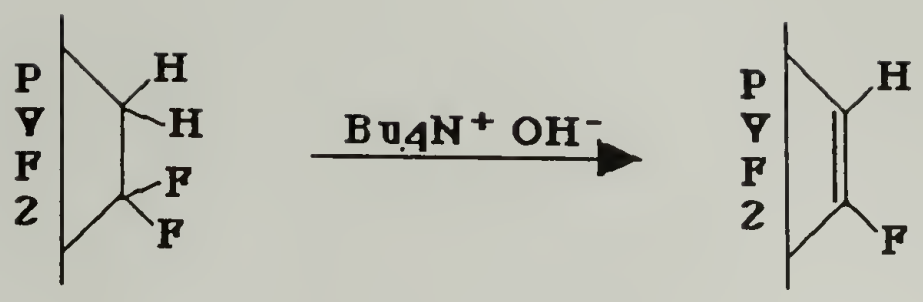


Scheme 1.2 Elimination of Poly(vinylidene fluoride) Film.

Poly(vinylidene fluoride) film is dehydrofluorinated when exposed to base. When exposed to sodium hydroxide alone, no reaction on $PVF_2$ occurs; however, with the addition of a small amount of tetrabutylammonium bromide, a thin eliminated layer forms. The tetrabutylammonium ion acts as a phase transfer catalyst, transporting hydroxide across the aqueous/organic interface. The reaction at room temperature is autoinhibitive; hydroxide accesses vinylidene fluoride repeat units within the top ~10 Å,[24] forming an eliminated layer to this depth. By increasing the reaction temperature, the modified depth of the dehydrofluorinated layer increases; at 40 °C, the elimination reaction is also autoinhibitive with a depth of reaction of ~50 Å whereas at 80 °C, the reaction continues to greater depths with time. As time and temperature are increased, side reactions occur which introduce polar functionality, such as hydroxyl and ketone, to the modified layer.[25] Table 1.1 summarizes the reaction conditions employed to study the dehydrofluorinated film. The $PVF_2$ film sample which was eliminated at 40 °C for 3 minutes with tetrabutylammonium hydroxide was used for further reaction. Other reagents, such as 1,8-diazabicyclo[5.4.0]undec-7-ene (DBU) in heptane react with $PVF_2$ to produce an eliminated layer, without side reactions, but which is pitted.[29]

Table 1.1 Summary of Dehydrofluorination Reaction Conditions Tested for $PVF_2$.

| Technique | $PVF_2$ | $PVF_2$-E<br>40 °C; 3 min | $PVF_2$-E<br>80 °C; 3 min | $PVF_2$-E<br>80 °C; 20 min |
|---|---|---|---|---|
| XPS | $C_1F_1$ | $C_8F_5O_1$ | $C_{11}F_3O_2$ | $C_{10}F_1O_3$ |
| $\theta_A/\theta_R$ | 86°/65° | 79°/38° | 76°/30° | 73°/9° |
| UV-vis | 0 | $\lambda$ =440 nm<br>A = 0.08 - 0.09 | $\lambda$ = 430 nm<br>A = 0.156 | $\lambda$ = 390 nm<br>A = 0.168 |
| ATR IR | 0 | no change | 1616 $cm^{-1}$ | 1641 $cm^{-1}$ |
| gravimetric analysis (thickness) | 0 | ~50 Å | ~130 Å | |

## $PVF_2$-CH=CF: Oxidation

The carbon-carbon double bonds, introduced in the surface-selective chemical reaction of $PVF_2$ and tetrabutylammonium hydroxide, were the reactive handle for further chemical modification. Two oxidants were used in the oxidation reaction, potassium permanganate dissolved in acetone and potassium chlorate dissolved in sulfuric acid.

The reaction of a fluoroolefin and potassium permanganate in acetone was described by Burdon and Tatlow.[30] Manganese dioxide precipitates as the fluoroolefin is oxidized to carboxylic acid. Sodium bisulfate solubilizes $MnO_2$ by hydrolysis to $Mn(OH)_4$. A brown precipitate, likely $MnO_2$, was observed on $PVF_2$-CH=CF film samples which were exposed to potassium permanganate/acetone oxidation. The precipitate readily dissolved in aqueous sodium bisulfate. No precipitate was observed on the control, $PVF_2$ film sample, exposed to similar oxidation conditions. No change by XPS ($C_{26}F_{24}$), contact angle (86°/70°), UV-vis and ATR IR was observed for the control

film sample. Table 1.2 summarizes the oxidation conditions used. The eliminated product was not completely removed by this oxidation reaction based on XPS atomic composition data; reaction of $PVF_2$-CH=CF with potassium permanganate/acetone was not pursued further.

Table 1.2 Oxidation of Eliminated $PVF_2$-CH=CF Using Potassium Permanganate Dissolved in Acetone.

| Technique | 0.2 M $KMnO_4$ | 0.5 M $KMnO_4$ | 1.0 M $KMnO_4$ |
|---|---|---|---|
| XPS | $C_{14}F_{10}O_2$ | $C_{27}F_{22}O_2$ | $C_{28}F_{20}O_2$ |
| $\theta_A/\theta_R$ | 74°/26° | 79°/37° | 79°/37° |
| UV-vis | A = 0 | A = 0 | A = 0 |
| ATR IR | 1653 $cm^{-1}$ insignificant | 1653 $cm^{-1}$ insignificant | 1653 $cm^{-1}$ insignificant |

$PVF_2$-CH=CF, when exposed to potassium chlorate/sulfuric acid, was oxidized to $PVF_2$-$CO_2H$; the fluoroolefin was oxidatively removed either completely or partially according to the concentration of reagent. Conversion was determined by XPS atomic composition and UV-vis data. Evidence of unsaturation by either of these techniques indicates incomplete conversion. The strength of the oxidant was largely dependent upon the concentration of sulfuric acid employed. Concentrated sulfuric acid oxidizes potassium chlorate to potassium perchlorate.[31] Potassium perchlorate, a stronger oxidant than potassium chlorate, oxidized the fluoroolefin more completely. Tables 1.3 (a) and (b) summarize the XPS, $\theta_A/\theta_R$, and UV-vis data for the oxidation of $PVF_2$-CH=CF with potassium chlorate/sulfuric acid according to concentration of potassium chlorate and dilution of sulfuric acid. No additional information was discerned from ATR IR

spectroscopy. The control sample ($PVF_2$) was inert to the oxidation solution as indicated by XPS ($C_{27}F_{23}$), contact angle (87°/67°), UV-vis and ATR IR which showed no changes. 0.16 M potassium chlorate dissolved in neat sulfuric acid was used in all subsequent oxidations.[32] The deep red solution of potassium chlorate/sulfuric acid released fumes (chlorine gas) during the oxidation and became yellow after several hours. Unlike permanganate oxidation, no precipitate formed on the films during oxidation with potassium chlorate/sulfuric acid.

Table 1.3 Oxidation of Eliminated $PVF_2$-CH=CF with Potassium Chlorate (a) Dissolved in 10% v/v Sulfuric Acid / Distilled Water.

| Technique | 0.008M 1 h | 0.04 M 1 h | 0.08 M 1 h |
|---|---|---|---|
| XPS | $C_{13}F_2O_4$ | $C_{14}F_2O_4$ | $C_{11}F_2O_2$ |
| $\theta_A/\theta_R$ | 76°/30° | 74°/22° | 78°/25° |
| UV-vis | $\lambda$ = 420-440 nm; A=0.135 | $\lambda$ = 390 nm; A = 0.128 | $\lambda$ = 415-430 nm; A=0.121 |

Table 1.3 Oxidation of Eliminated $PVF_2$-CH=CF with Potassium Chlorate (b) Dissolved in Sulfuric Acid.

| Technique | 0.008 M<br>1 h | 0.04 M<br>1 h | 0.08 M<br>1 h | 0.16 M*<br>2 h | $H_2SO_4$<br>1 h |
|---|---|---|---|---|---|
| XPS | $C_{14}F_8O_3$ | $C_{18}F_{13}O_3$ | $C_{21}F_{10}O_3$ | $C_{29}F_{25}O_2$ | $C_{22}F_2O_8S_1$ |
| $\theta_A/\theta_R$ | 76°/22° | 69°/22° | 65°/22° | 75°/29° | 54°/17° |
| UV-vis | A = 0 | A = 0 | A = 0 | A = 0 | $\lambda$ = 430 nm;<br>A=0.09 |

*The eliminated sample was prepared at 40 °C for 3 min.; all other samples were prepared at 80 °C for 3 minutes.

The two step modification produees a carboxylie aeid surface-funetionalized film surfaee ($PVF_2$-$CO_2H$); the $PVF_2$ surfaee was selectively eliminated using tetrabutylammonium hydroxide at 40 °C for 3 minutes and then subsequently oxidized with 0.16 M potassium ehlorate in sulfuric acid. The polymer film, a pale brown color after dehydrofluorination, was transparent after oxidation. Figure 1.1 ineludes XPS and UV-vis spectra for the two step modifieation. The introduetion of CH=CF funetionality is expressed in terms of a broad absorbance in the UV-vis speetrum, with $\lambda_{max}$ at 440 nm, eorresponding to a eonjugated layer. By XPS, a broadened lower binding energy $C_{1s}$ photoeleetron peak results from a contribution of the *C*H=*C*F functionality. The higher binding energy $C_{1s}$ peak decreases eorrespondingly as $CF_2$ is eonverted to CH=CF with the elimination reaetion. By gravimetrie analysis, the depth of modifieation was estimated at ~50 Å.[33] Gravimetric analysis was done by eomparing the mass of the film sample (vaeuum-dried) before ($PVF_2$) and after ($PVF_2$-$CO_2H$) reaction. The depth of modifieation (t) was caleulated aeording to equation 1.1

(1.1) $$t = \frac{m}{2(l \times w)(d)}$$

where the mass lost (m) is divided by the dimensions (l and w) and the density (d) of the film sample. The mass lost is divided by a factor of two to account for reaction at both sides of the film sample. Upon oxidation, the conjugation observed by UV-vis is removed and the high binding energy $C_{1s}$ peak increases to its original intensity. The thinly eliminated layer which dominates the features of both UV-vis and XPS spectra is removed upon oxidation. The resulting spectra resemble the starting material except for the presence of an $O_{1s}$ peak at a binding energy of 536 eV. From XPS atomic composition, $C_{14}F_{13}O$, there is approximately one carboxylic acid in thirteen vinylidene fluoride repeat units in the top ~10 Å of the film surface: $(CH_2CF_2)_{13}CO_2H$. (This corresponds to complete conversion.) The contact angles, 75°/29°, reflect the increased hydrophilicity of the carboxylic acid-modified film with respect to the unmodified $PVF_2$ substrate (86°/65°). ATR IR spectra (included in Figure 1.2) indicate that absorbance in the carbon-carbon double region ~1650 $cm^{-1}$ is removed upon oxidation. (The changes observed by ATR IR are very subtle; the spectrum included is that of $PVF_2$-CH=CF eliminated at 80 °C for 20 minutes.) The film samples showed no changes by SEM indicating a relatively smooth reaction.

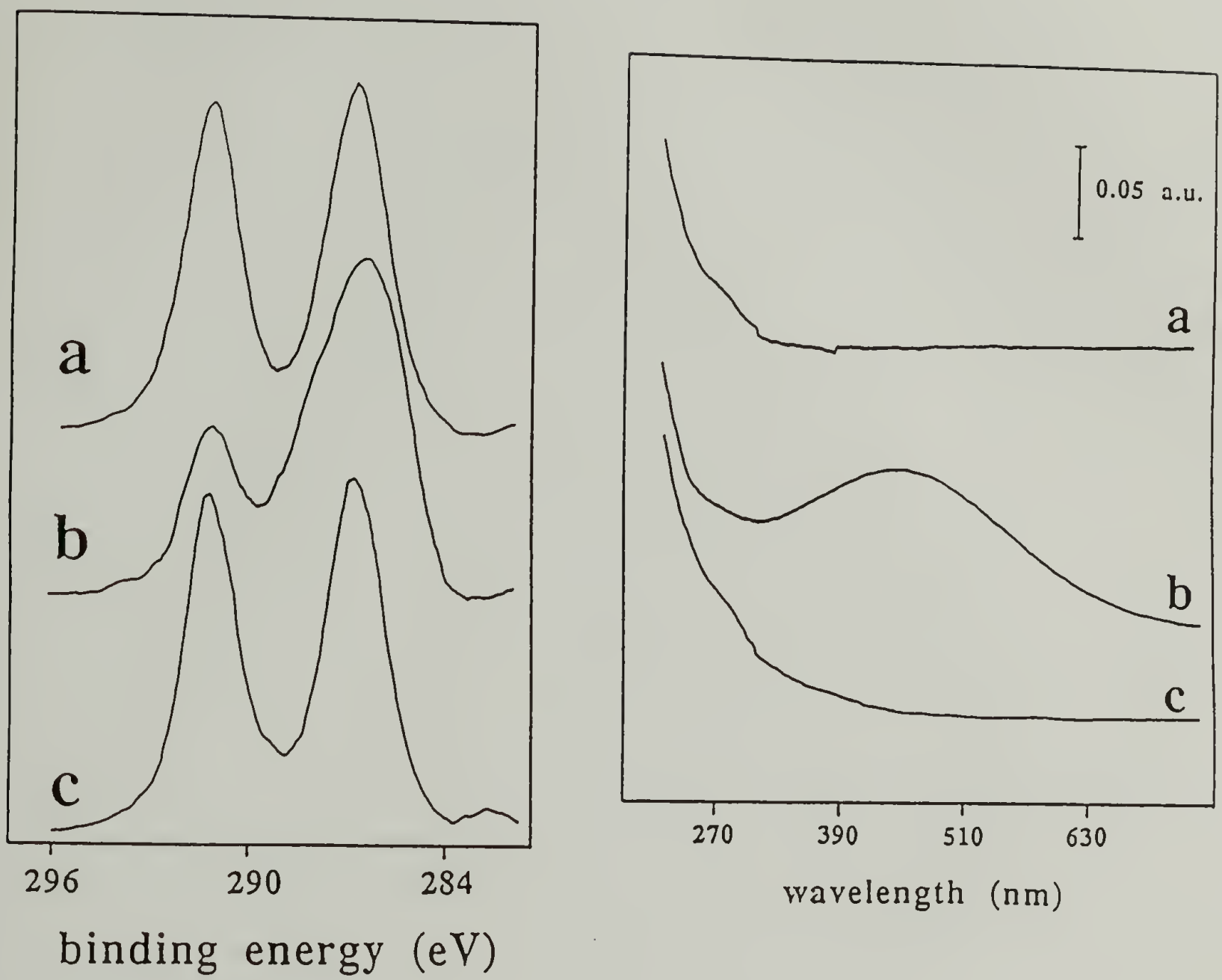


Figure 1.1 XPS ($C_{1s}$ region, 15° takeoff angle) and UV-vis Spectra of (a) $PVF_2$, (b) $PVF_2$-CH=CF, (c) $PVF_2$-$CO_2H$.

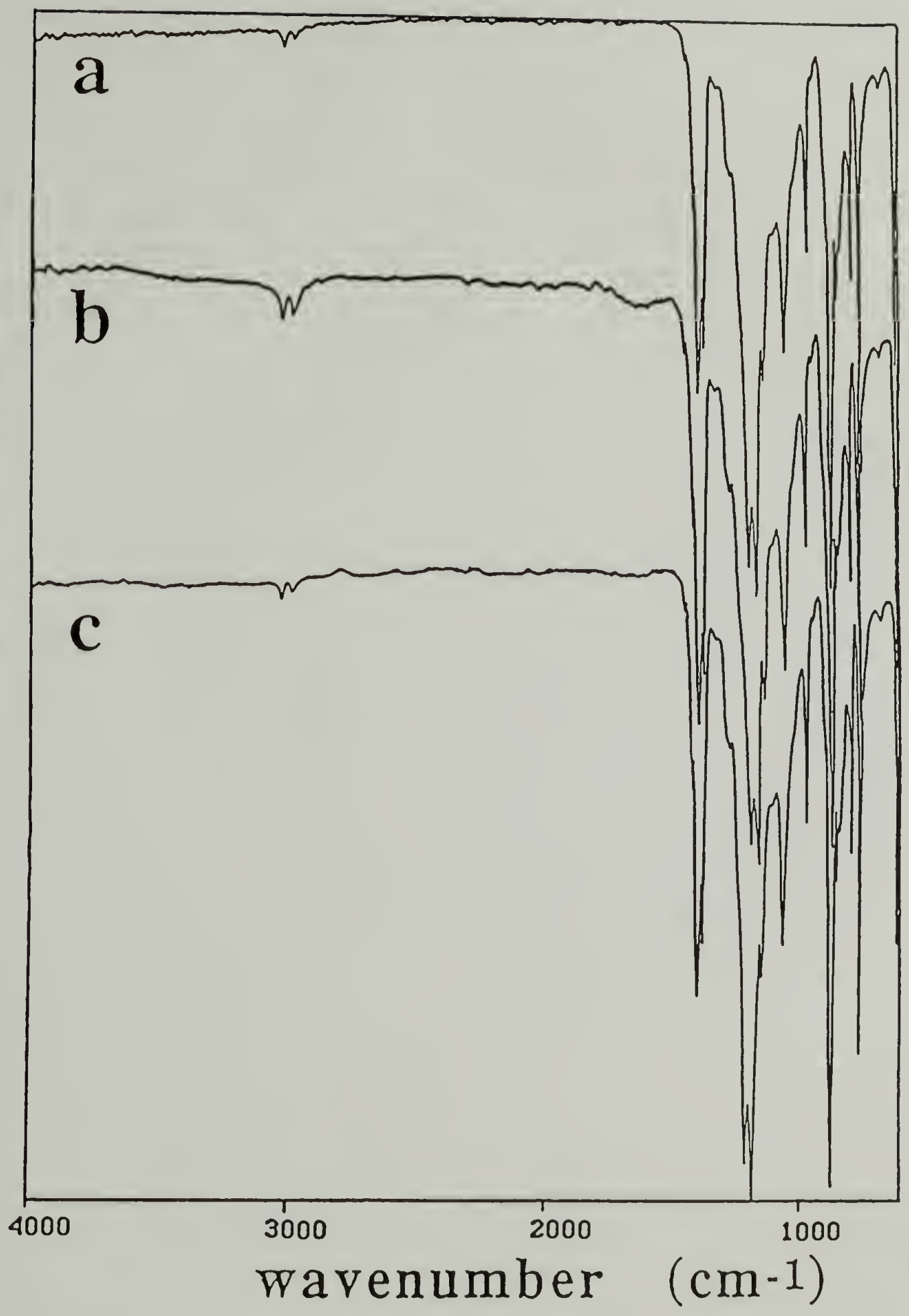


Figure 1.2 ATR IR Spectra of (a) $PVF_2$, (b) $PVF_2$-CH=CF, (c) $PVF_2$-$CO_2H$.

PCTFE: Reduction/Alkylation

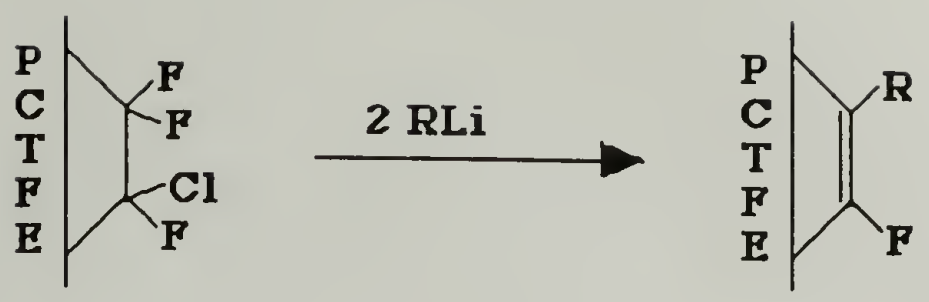


Scheme 1.3 Reduction/Alkylation of PCTFE.

Poly(chlorotrifluoroethylene) is modified by reaction with lithium reagents[4,7,34,35] where two equivalents of an alkyllithium reacts with PCTFE. Alkyllithium reacts by metal halogen exchange of chlorine for lithium; the lithiated product eliminates lithium fluoride producing a difluoroolefin. A second equivalent of alkyllithium adds to the fluoroolefin and a second lithium fluoride is eliminated, producing the alkylated and reduced product. Scheme 1.4 summarizes this mechanism for *n*-butyllithium. The reduction/alkylation of PCTFE is controlled by reaction temperature, reaction time, solvent, and alkyllithium reagent. The interaction of the solvent with PCTFE controls the depth of reaction; thinly reduced layers result from a solvent which does not "wet" PCTFE well (i.e. heptane).

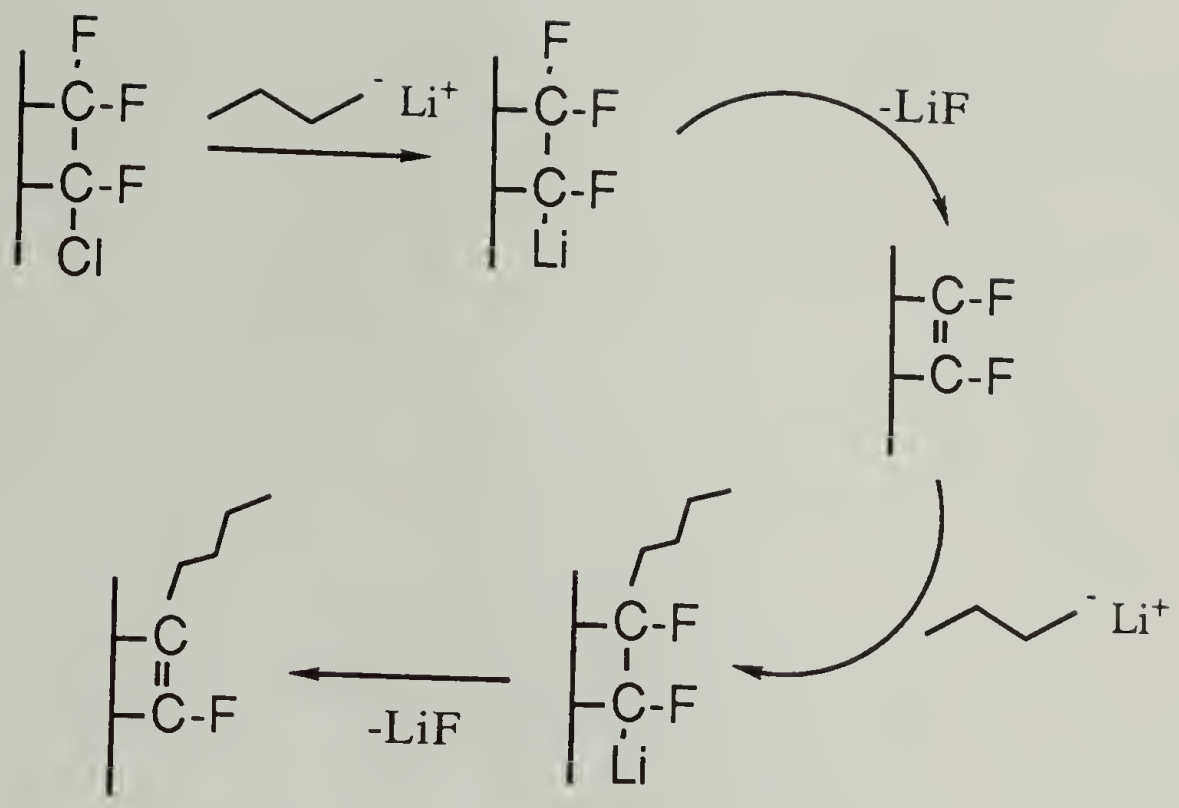


Scheme 1.4 Mechanism for the Reaction of PCTFE with 2 Equivalents of *n*-Butyllithium.

## PCTFE-Bu: Oxidation

The two step modification, reaction with *n*-butyllithium and subsequent oxidation with potassium chlorate/sulfuric acid, produces PCTFE-$CO_2H$. PCTFE was reduced/alkylated with *n*-butyllithium in 50:50, v/v heptane:THF solution at -78 °C for 1 h to produce PCTFE-Bu. The depth of modification was estimated from gravimetric analysis at ~35 Å. The thickness of the reduced layer was determined as described for $PVF_2$ (equation 1.1), by calculating the mass change observed on conversion of the starting material to the acid-functionalized film. PCTFE-Bu, when exposed to 0.16 M potassium chlorate/sulfuric acid, is oxidized to PCTFE-$CO_2H$. Carboxylic acid groups form at the PCTFE - PCTFE-Bu interface because PCTFE is inert to the oxidation conditions. The control film (PCTFE) was judged inert to oxidation conditions by XPS analysis, $C_{100}F_{208}Cl_{44}$, and $\theta_A/\theta_R$, 94°/70°. Table 1.4 summarizes XPS, $\theta_A/\theta_R$, UV-vis, and ATR IR data for the reduction/alkylation (PCTFE-Bu) and the subsequent oxidation

(PCTFE-$CO_2H$). Figure 1.3 includes XPS and UV-vis spectra and Figure 1.4 includes ATR IR spectra for the three film samples, PCTFE, PCTFE-Bu, PCTFE-$CO_2H$. By XPS analysis, the high binding energy $C_{1s}$ peak due to $CF_2$, CFCl (PCTFE) is replaced by a low binding energy $C_{1s}$ peak due to $CH_2$ and $CH_3$ (PCTFE-Bu) with a high binding energy shoulder due to C(Bu)=CF. The high binding energy $C_{1s}$ peak is regenerated with oxidation and an $O_{1s}$ peak at 534 eV is present in the photoelectron spectrum. The stoichiometry of PCTFE-$CO_2H$, $C_{13}F_{18}Cl_6O$, corresponds to one carboxylic acid in twelve chlorotrifluoroethylene repeat units, $(CF_2CFCl)_{12}CO_2H$. By UV-vis, a broad absorbance corresponding to the conjugated carbon-carbon double bond system of PCTFE-Bu is removed by oxidation to PCTFE-$CO_2H$. A similar trend is observed by ATR IR where methyl and methylene vibrations that are detected for PCTFE-Bu are removed upon oxidation to PCTFE-$CO_2H$. The contact angle data reflect the hydrophilicity of the carboxylic acid group (96°/50°) with respect to the unmodified PCTFE (104°/76°).

Table 1.4 Summary of Reduction and Oxidation Data of PCTFE: XPS, Contact Angle, UV-vis, and ATR IR Data.

| Technique | PCTFE | PCTFE-Bu | PCTFE-$CO_2H$ |
|---|---|---|---|
| XPS | $C_{100}F_{151}Cl_{54}$ | $C_{100}F_{16}O_1$ | $C_{100}F_{144}Cl_{48}O_8$ |
| $\theta_A/\theta_R$ | 104°/76° | 104°/80° | 96°/50° |
| UV-vis | A = 0 | $\lambda$ = 230-240 nm<br>A = 0.047 | A = 0 |
| ATR IR | 0 | 2961 $cm^{-1}$ $CH_3$ $\nu_{as}$<br>2936 $cm^{-1}$ $CH_2$ $\nu_{as}$<br>2876 $cm^{-1}$ $CH_3$,$CH_2$ $\nu_s$<br>1383 $cm^{-1}$ $CH_3$ $\delta_s$ | 0 |

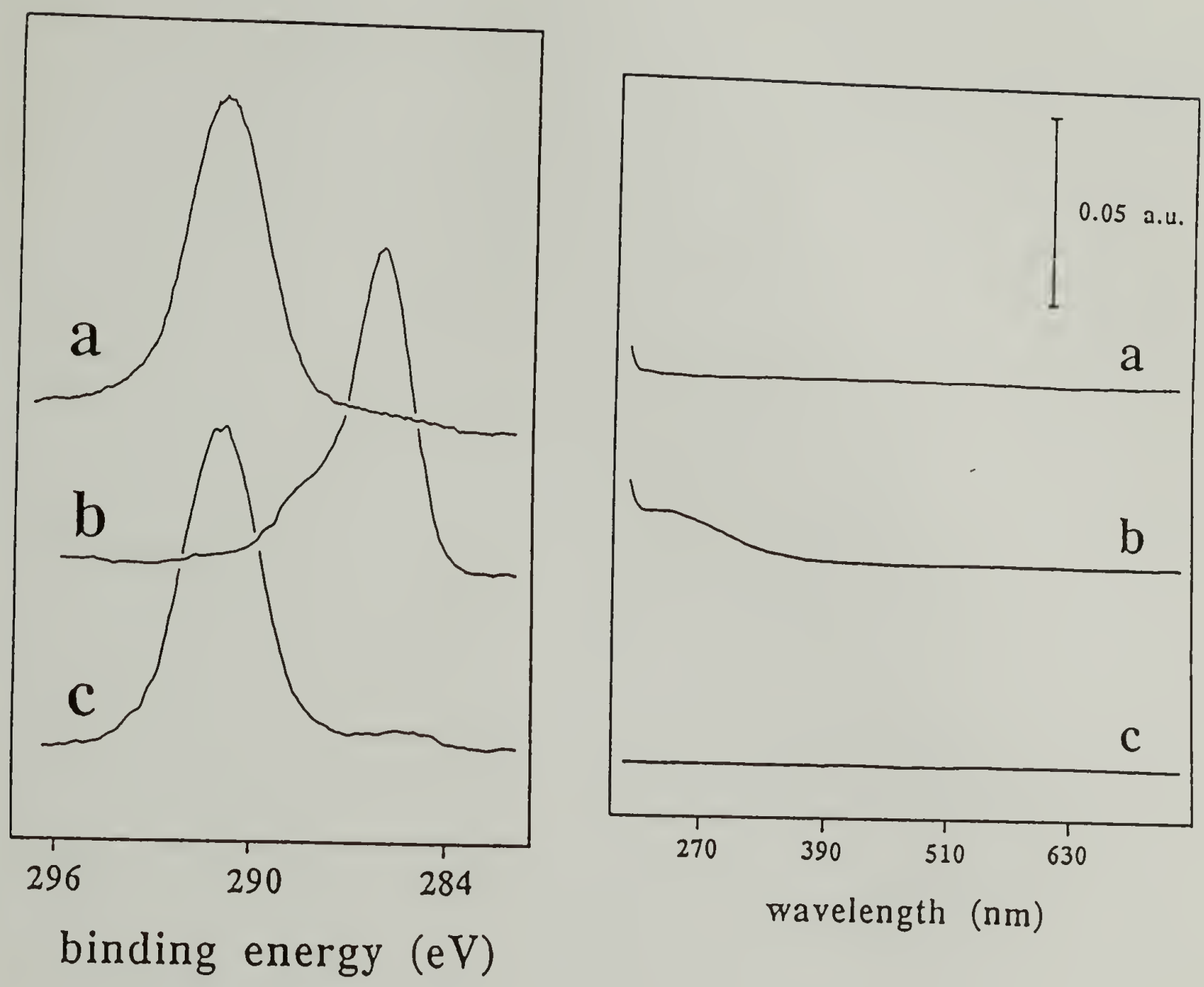


Figure 1.3 XPS ($C_{1s}$ region, 15° takeoff angle) and UV-vis Spectra of (a) PCTFE, (b) PCTFE-Bu, (c) PCTFE-$CO_2H$.

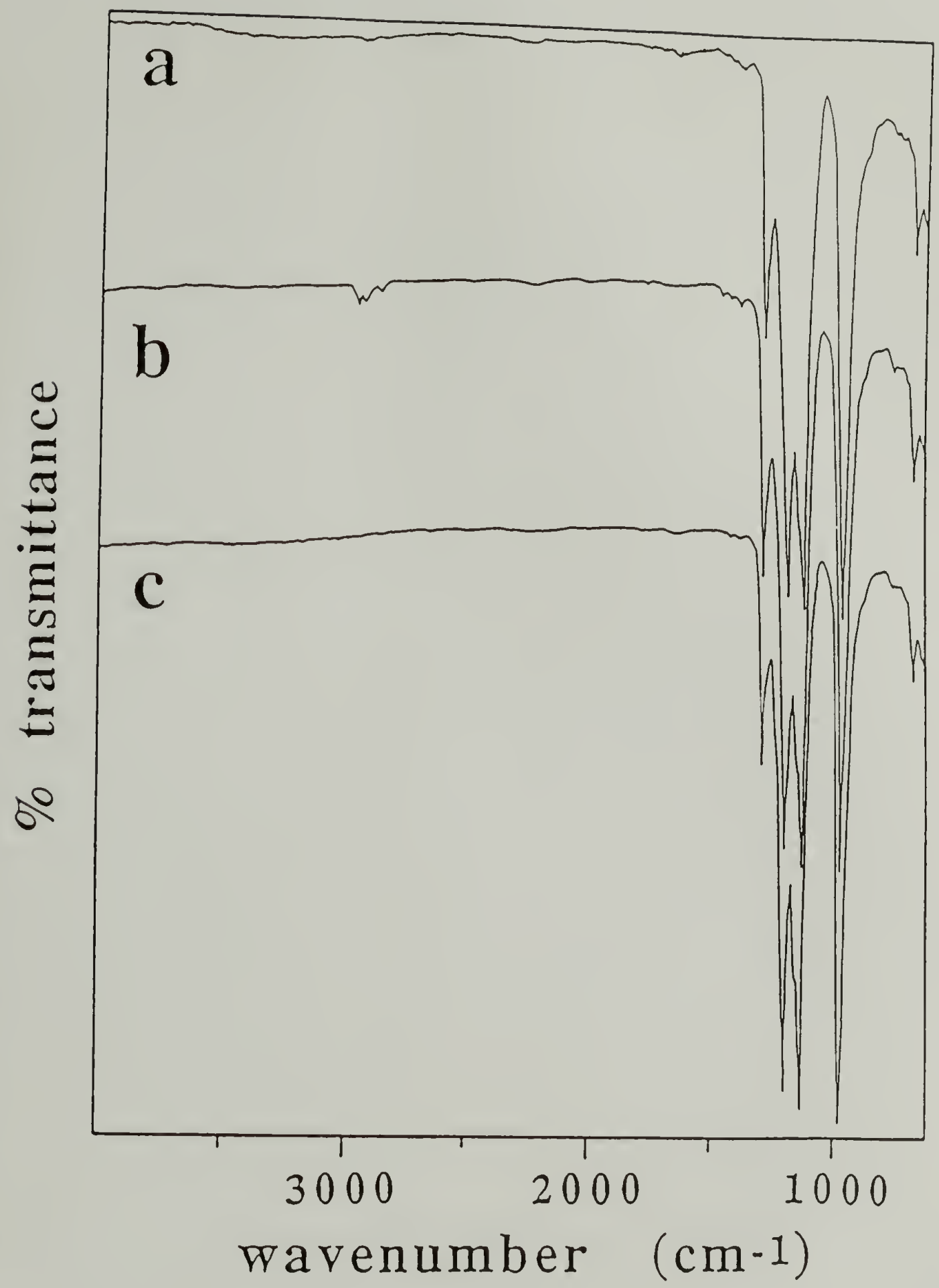


Figure 1.4 ATR IR Spectra of (a) PCTFE, (b) PCTFE-Bu, (c) PCTFE-$CO_2H$.

FEP: Reduction

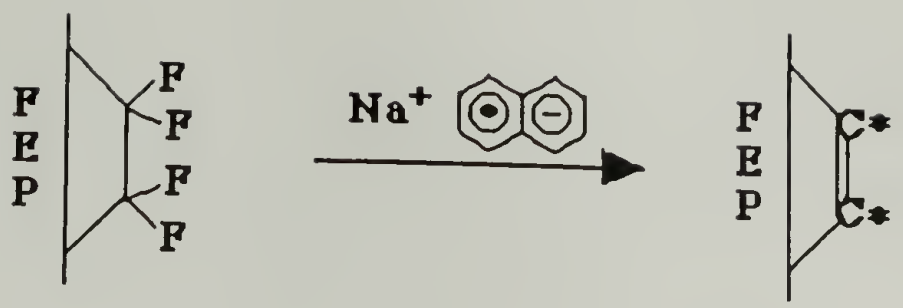


Scheme 1.5 Reduction of FEP with Sodium Naphthalide. (C* corresponds to a carbonaceous layer.)

Poly(tetrafluoroethylene-co-hexafluoropropylene) is reduced when exposed to single electron reducing agents. Both sodium naphthalide and dipotassium benzoin dianion reduce FEP to an oxidation-sensitive carbonaceous layer (FEP-C).[27,36] The reduction is complex involving diffusion of the reducing agent into the polymer film accompanied by the transport of electrons through the electronically conducting material.[6,37] At room temperature the reaction is corrosive producing a rough or diffuse FEP - FEP-C interface with a thick reduced layer. The reduction can be controlled at decreased temperatures. Reactions at -78 °C produce a modified layer where both the depth of modification and the sharpness at the FEP - FEP-C interface are controlled. Time and temperature play an important role in this reaction; as both are increased, the selectivity for the surface decreases while side reactions increase. FEP-C was produced by exposing FEP to 0.12 M sodium naphthalide for 1 h at -78 °C or for 15 minutes at 0 °C. By comparing UV-vis absorbance at 250 nm with gravimetric results, the depth of modification can be estimated. Reduction of FEP at -78 °C for 1 h produces a modified layer of ~55 Å for FEP-C whereas reduction of FEP at 0 °C for 15 minutes produces a modified layer of ~250 Å for FEP-C. The former reaction conditions were used to pursue subsequent modifications whereas the latter were

used in adsorption experiments (cf. Chapter III). Table 1.5 compares the film samples and their oxidized products by XPS, UV-vis, $\theta_A/\theta_R$, and ATR IR.

Table 1.5 FEP Reduction and Oxidation Data Summarized.

| Technique | FEP | FEP-C* (-78 °C, 1 h) | FEP-$CO_2H$ | FEP-C* (0 °C, 15 m) | FEP-$CO_2H$ |
|---|---|---|---|---|---|
| XPS | $C_{100}F_{200}$ | $C_{100}F_{15}O_7$ | $C_{100}F_{203}O_6$ | $C_{100}F_1O_{22}$ | $C_{100}F_{194}O_{11}$ |
| $\theta_A/\theta_R$ | 115°/100° | 90°/43° | 99°/47° | 69°/28° | 101°/56° |
| UV-vis | A = 0 | $\lambda$ =205 nm<br>A = 0.118 | A = 0 | $\lambda$ = 216 nm<br>A = 0.278 | A = 0 |
| ATR IR ($cm^{-1}$) | 0 | few additional peaks observed | 0 | 2959 $CH_3$ $\nu_{as}$<br>2930 $CH_2$ $\nu_{as}$<br>2870 $CH_3$,$CH_2$ $\nu_s$<br>1719 C=O $\nu$<br>1597;1458 C=C (condensed, aromatic like) | 0 |

FEP-C: Oxidation

An oxidation-sensitive layer (~55 Å) was introduced to FEP by reaction with sodium naphthalide for 1 h at -78 °C. The initial surface-selective reaction product was oxidatively removed with 0.16 M potassium chlorate/sulfuric acid producing carboxylic acid functionality at the former FEP - FEP-C interface. FEP is inert to the oxidation conditions as determined by XPS, $C_1F_2$, and $\theta_A/\theta_R$, 112°/83°. The topography of the interface produced in the initial reaction was that of the surface of FEP-$CO_2H$ and its derivatives. The films were indistinguishable by SEM, arguing for a smooth (at least to ~50 Å) interface. Figure 1.5 summarizes XPS and UV-vis data for the reduction (-78 °C, 1

h) and subsequent oxidation reactions on FEP. A broad absorbance in the UV-vis spectrum of FEP-C indicates a conjugated carbon-carbon double bond layer. The conjugation is removed upon oxidation and, based on UV-vis results alone, FEP was regenerated. By XPS analysis of the $C_{1s}$ region, the high binding energy peak of $CF_2$ decreases in intensity and another peak at lower binding energy appears as a result of the reduction reaction: $C$=C, $CH_2$, amongst other functionalities. Upon oxidation, the high binding energy $C_{1s}$ peak is regenerated. With an $O_{1s}$ peak at 533 eV, the XPS stoichiometry was $C_{16}F_{32}O$ or one carboxylic acid group per sixteen repeat units, $(CF_2CF_2)_{16}CO_2H$.[38] The contact angles of FEP-$CO_2H$ (99°/47°) reflect the increased hydrophilicity over that of FEP (115°/100°). ATR IR shows no indication of reaction for FEP film samples reduced at -78 °C, 1 h. Figure 1.6 includes spectra for the reduction at 0 °C for 15 minutes and subsequent oxidation; the reduction at 0 °C for 15 minutes indicates, by ATR IR, the introduction of methylene, methyl, carbonyl and carbon-carbon double bonds. Upon oxidation, the ATR IR spectrum of FEP-$CO_2H$ resembles that of unmodified FEP.

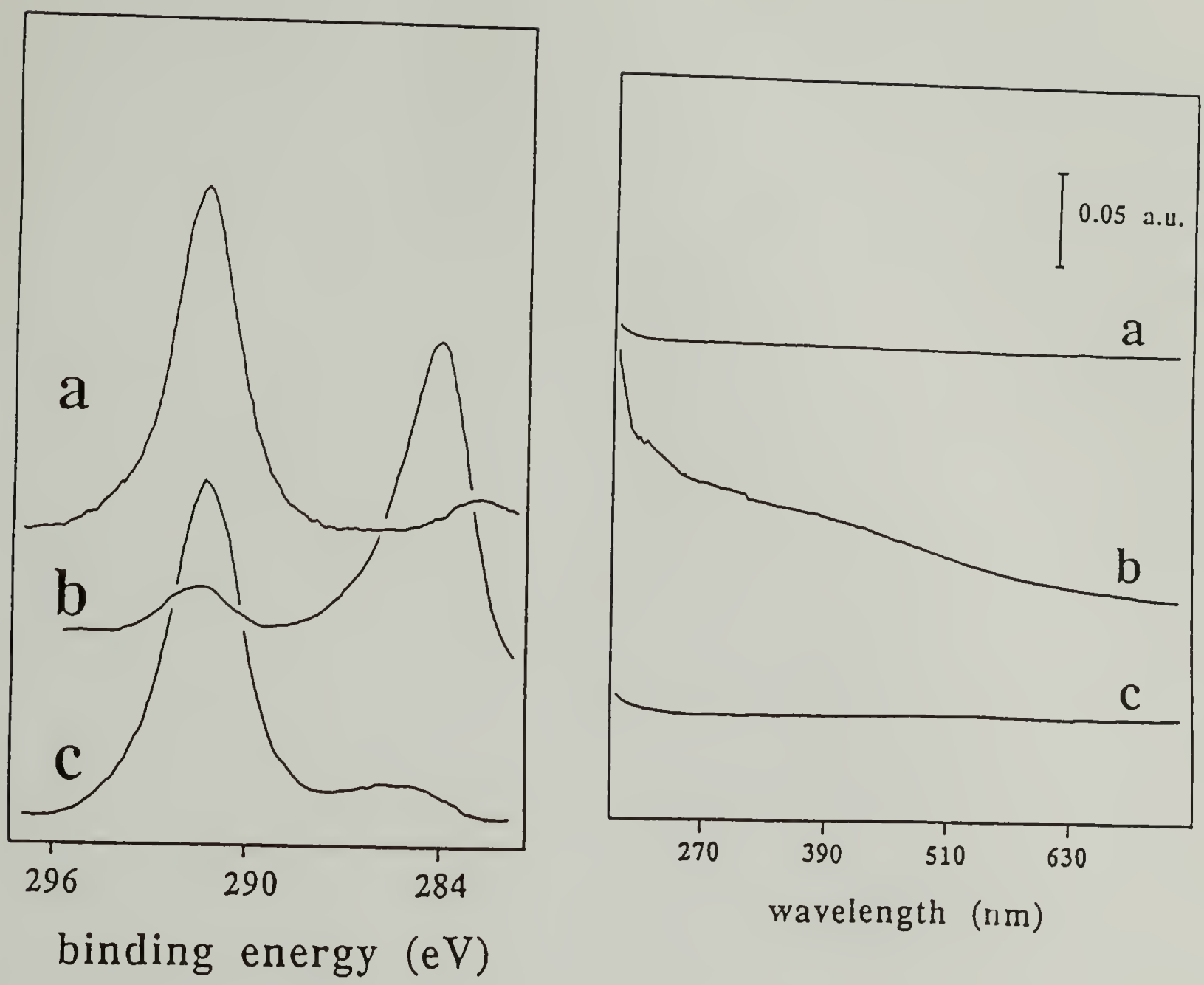


Figure 1.5 XPS ($C_{1s}$ region, 15° takeoff angle) and UV-vis Spectra of (a) FEP, (b) FEP-C, (c) FEP-$CO_2H$.

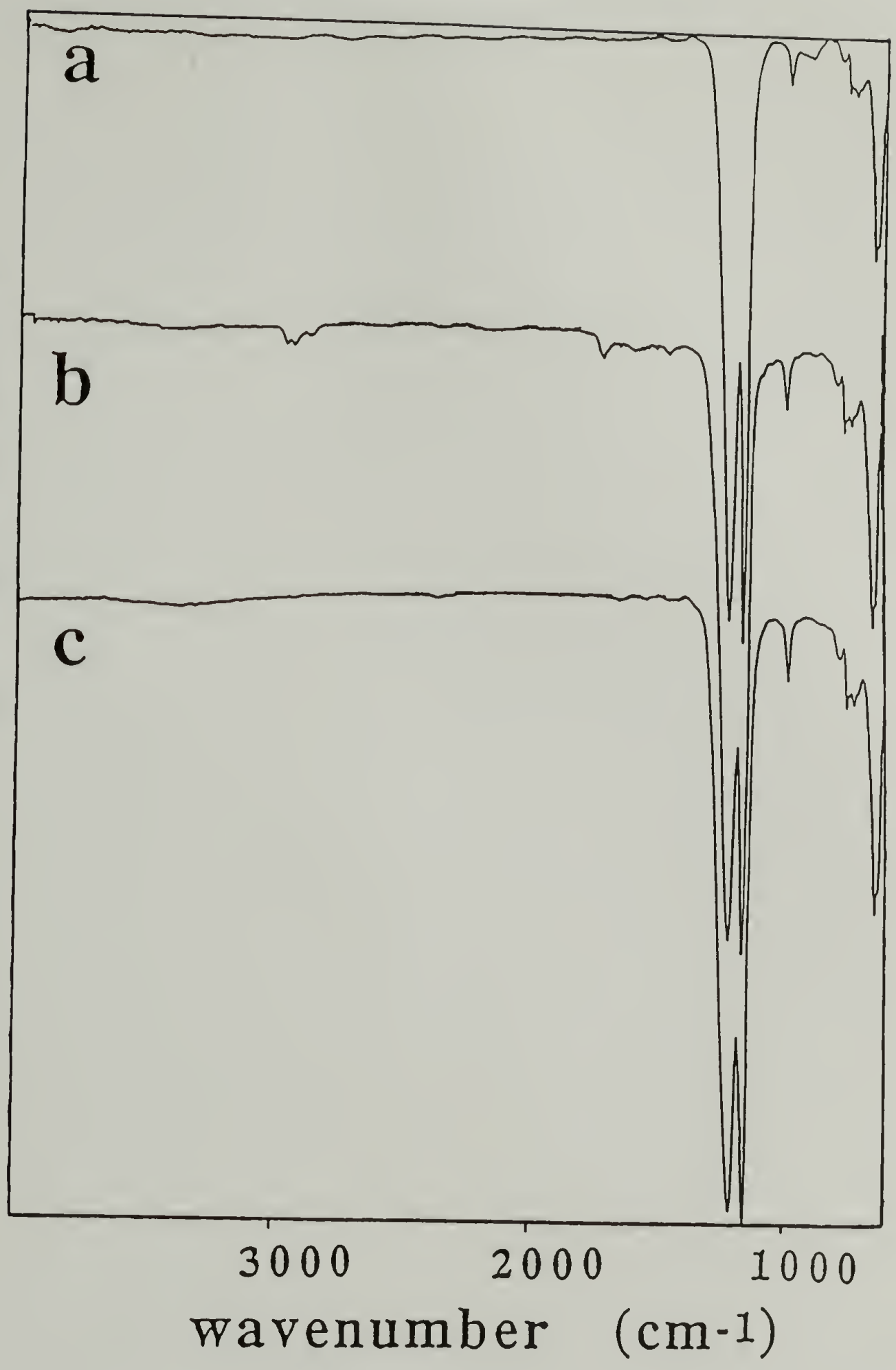


Figure 1.6 ATR IR Spectra of (a) FEP, (b) FEP-C, (c) FEP-$CO_2H$.

## Summary of Oxidation Reactions

The oxidized film samples resemble the untreated film samples in every respect except for the presence of oxygen in the 15° photoelectron spectra and the decreased contact angles. Table 1.6 compares the unmodified with the acid functionalized fluoropolymers in terms of the XPS stoichiometry of carboxylic acid groups per fluoropolymer repeat unit and their respective contact angles.

Table 1.6 Advancing ($\theta_A$) and Receding ($\theta_R$) Contact Angle Data for Modified and Unmodified Fluoropolymer Films with XPS Stoichiometry Data.

| Sample | XPS Stoichiometry | $\theta_A$ | $\theta_R$ |
|---|---|---|---|
| $PVF_2$ | $(CH_2CF_2)$ | 86° | 65° |
| $PVF_2$-$CO_2H$ | $(CH_2CF_2)_{13}CO_2H$ | 75° | 29° |
| PCTFE | $(CF_2CFCl)$ | 104° | 76° |
| PCTFE-$CO_2H$ | $(CF_2CFCl)_{12}CO_2H$ | 96° | 50° |
| FEP | $(CF_2CF_2)$ | 115° | 100° |
| FEP-$CO_2H$ | $(CF_2CF_2)_{16}CO_2H$ | 99° | 47° |

The XPS atomic composition data was determined for the top 10 Å of the film surface using a 15° takeoff angle between the plane of the film sample and detector. Clark and Thomas[39] determined that 94% of the photoelectrons detected (at 15°) originate in the top 10 Å of the film surface using poly(*p*-xylene) and a value of 14 Å for the mean free path of the $C_{1s}$ photoelectron. The XPS stoichiometries reported may be compromised by the assumptions made. For example, XPS stoichiometries were calculated assuming that the oxidized film samples were flat and homogeneous; if the surface was pitted, the

carboxylic acid groups may have been screened by fluoropolymer repeat units, thereby decreasing the number of acidic groups detected. If the carboxylic acid groups were concentrated within a thin layer, the number of acid groups reported may have been higher than what was expected because XPS sensitivity decreases exponentially with depth. These assumptions were not investigated but may account for inconsistencies in the reported data.

Labeling of Surface Carboxylic Acids with Thallium

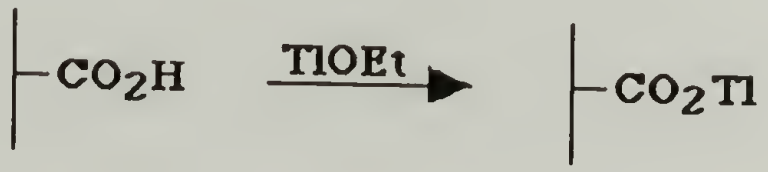


Scheme 1.6 Reaction of Surface Carboxylic Acids with Thallous Ethoxide.

The carboxylic acid functionalized surfaces were labeled with thallium by reaction with thallous ethoxide for XPS analysis. Thallous ethoxide is a suitable label because it reacts preferentially with carboxylic acids in the presence of aldehyde, ketone, or alcohol functionalities.[40] It is a useful XPS label as a result of its high sensitivity factor; in addition, thallium carboxylate is more stable to hydrolysis than other metal carboxylates.[41]

The three carboxylic acid-functionalized fluoropolymer films, $PVF_2$-$CO_2H$, PCTFE-$CO_2H$, and FEP-$CO_2H$, were labeled with thallium by reaction with thallous ethoxide producing, respectively, $PVF_2$-$CO_2Tl$, PCTFE-$CO_2Tl$, and FEP-$CO_2Tl$. Table 1.7 summarizes XPS and contact angle data for the labeled films and their controls. Unmodified $PVF_2$ and FEP were inert to the reaction conditions applied; PCTFE reacted only slightly with thallous ethoxide. Figure 1.7 shows XPS survey spectra for the thallium

carboxylated film samples. The XPS atomic concentration ratio of oxygen to thallium was expected to be 2:1 for complete labeling of carboxylic acid groups with thallium. For $PVF_2$-$CO_2Tl$, the ratio at 15° was 2.5:1 (and 2:1 at 75°); for PCTFE-$CO_2Tl$ at 15°, it was 2.7:1 (and 1.5:1 at 75°); and for FEP-$CO_2Tl$, it was 2:1 at both 15° and 75°. The 75° data indicate complete labeling for $PVF_2$-$CO_2Tl$ and FEP-$CO_2Tl$. For PCTFE-$CO_2Tl$, a slight excess of thallium was observed; this may have resulted from the slight reaction of thallous ethoxide with PCTFE as was observed for the control film sample. Reaction yields calculated from XPS atomic concentration data may be compromised by the reasons outlined above for estimates of carboxylic acid surface density.

Table 1.7 XPS and Contact Angle Data for Thallium-Labeled Surface Carboxylic Acids.

| Sample | XPS Stoichiometry 15° | XPS Stoichiometry 75° | $\theta_A/\theta_R$ |
|---|---|---|---|
| $PVF_2$-$CO_2Tl$ | $C_{100}F_{72}O_{11}Tl_4$ | $C_{100}F_{77}O_8Tl_4$ | 74°/21° |
| $PVF_2$ control | $C_{100}F_{100}$ | | 86°/62° |
| PCTFE-$CO_2Tl$ | $C_{100}F_{190}Cl_{44}O_8Tl_3$ | $C_{100}F_{188}Cl_{54}O_3Tl_2$ | 95°/53° |
| PCTFE control | $C_{100}F_{193}Cl_{44}O_{0.7}Tl_{0.4}$ | | 101°/76° |
| FEP-$CO_2Tl$ | $C_{100}F_{218}O_{12}Tl_5$ | $C_{100}F_{211}O_5Tl_{2.4}$ | 101°/59° |
| FEP control | $C_{100}F_{200}$ | | 117°/91° |

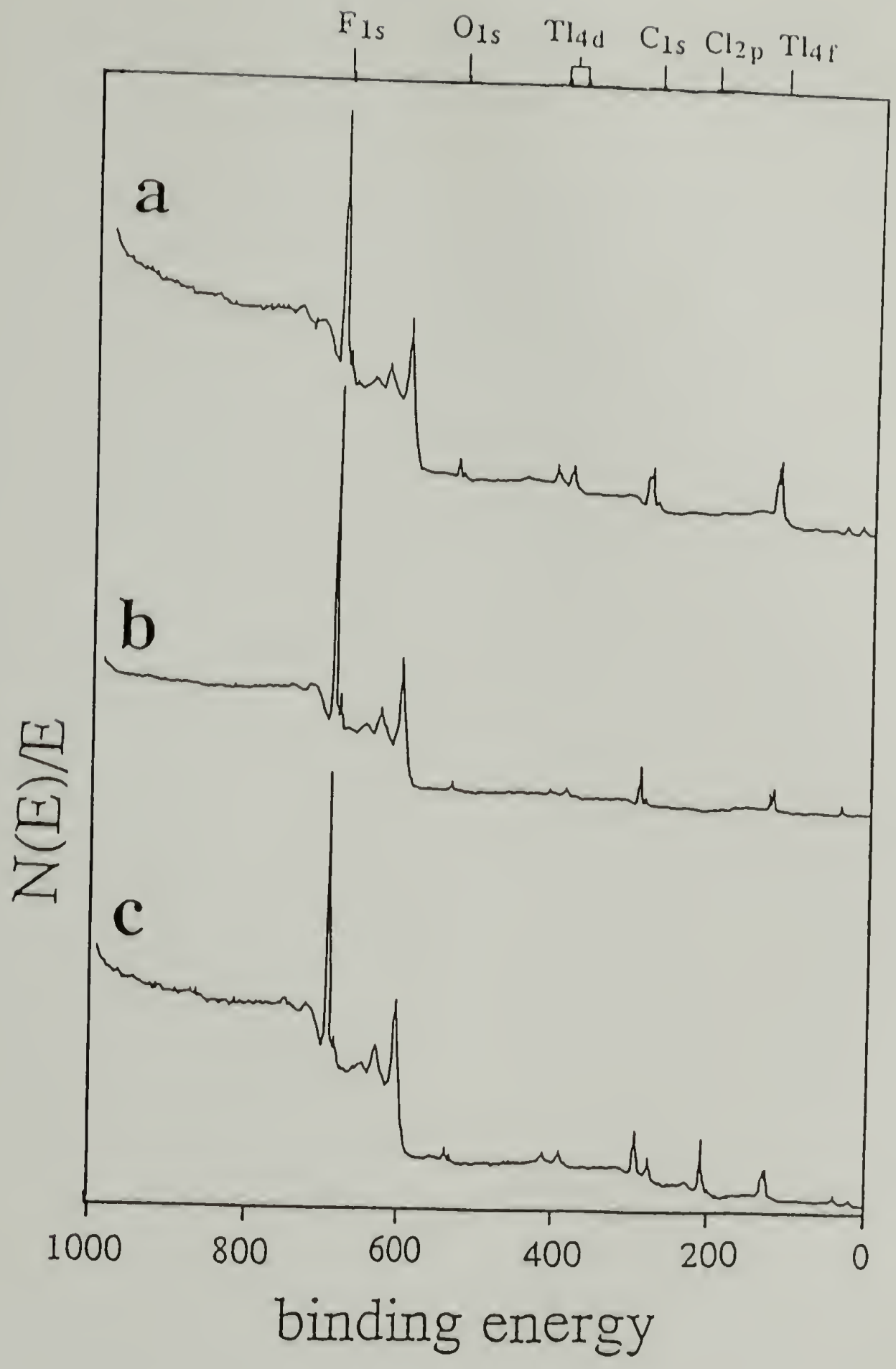


Figure 1.7 XPS (survey, 15° takeoff angle) Spectra of (a) $PVF_2$-$CO_2Tl$, (b) FEP-$CO_2Tl$, (c) PCTFE-$CO_2Tl$.

Reduction of Surface Carboxylic Acids and

Reaction of Surface Alcohols with Trichloroacetyl Chloride

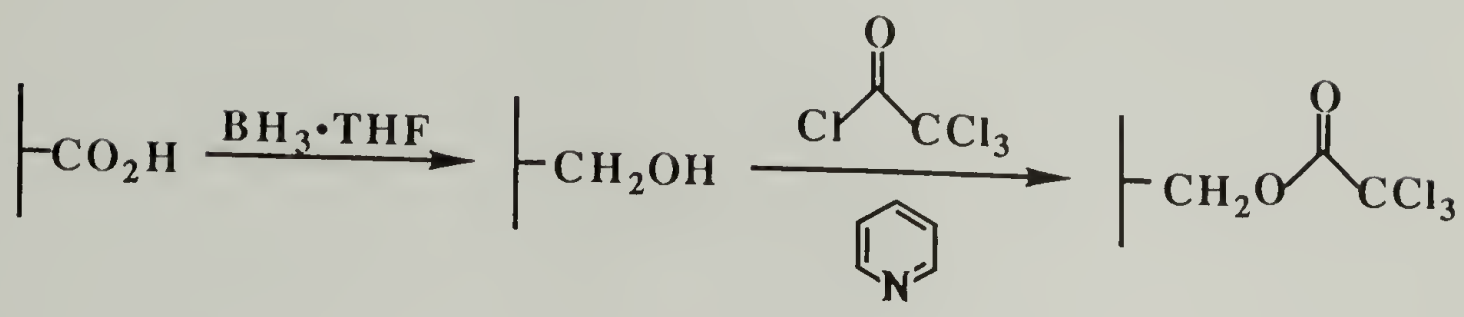


Scheme 1.7 Reduction of Surface Carboxylic Acids and Their Subsequent Reaction with Trichloroacetyl Chloride.

Carboxylic acids react selectively with borane•THF in the presence of other functional groups.[42] Carboxylic acid functionalized polymer films have been reduced with borane•THF to produce alcohol surface functionalized film samples.[43] The alcohol functionality was labeled for XPS analysis with trichloroacetyl chloride[44] producing the trichloroacetate-functionalized film sample. Table 1.8 summarizes XPS and contact angle data for these reactions; Figure 1.8 includes XPS spectra of esterified film samples. By XPS analysis, the carbon to oxygen atomic concentration ratio should double for the reduction of acid ($CO_2H$) to alcohol ($CH_2OH$). The yields (or conversions) based on XPS data were 100%, 100% and 137% respectively, for $PVF_2$-$CH_2OH$, PCTFE-$CH_2OH$, and FEP-$CH_2OH$. After esterification of the alcohols (-$CH_2OH$) with trichloroacetyl chloride, the ester surfaces (-$CH_2OCOCCl_3$) were expected to have XPS chlorine to oxygen atomic concentration ratios of 3:2. Based on XPS results the yield (conversion) of this reaction was respectively, 33%, 63%,[45] and 37% for $PVF_2$-$CH_2OCOCCl_3$, PCTFE-$CH_2OCOCCl_3$, and FEP-$CH_2OCOCCl_3$. Low yields of esterification have been previously reported for FEP-$CH_2OH$;[27] however, better yields of esterification were obtained for alcohol-functionalized films with a 3-methylene spacer, PCTFE-$(CH_2)_3OH$.[5]

Table 1.8 XPS and Contact Angle Data for the Conversion of Surface Carboxylic Acid to Surface Alcohol and then to Surface Ester: (a) $PVF_2$;

| Technique | $PVF_2$-$CO_2H$ | $PVF_2$-$CH_2OH$ | $PVF_2$-$CH_2OCOCCl_3$ | $PVF_2$ Control* |
|---|---|---|---|---|
| XPS | $C_{100}F_{87}O_{12}$ | $C_{100}F_{87}O_6$ | $C_{100}F_{93}O_8Cl_4$ | $C_{100}F_{107}$ (alcohol)<br>$C_{100}F_{106}$ (ester) |
| $\theta_A/\theta_R$ | 75°/29° | 79°/32° | 80°/49° | 86°/66° (alcohol)<br>86°/67° (ester) |

(b) PCTFE;

| Technique | PCTFE-$CO_2H$ | PCTFE-$CH_2OH$ | PCTFE-$CH_2OCOCCl_3$ | PCTFE Control* |
|---|---|---|---|---|
| XPS | $C_{100}F_{153}Cl_{48}O_8$ | $C_{100}F_{139}Cl_{40}O_4$ | $C_{100}F_{139}Cl_{47}O_5$ | $C_{100}F_{116}Cl_{51}$ (alcohol)<br>$C_{100}F_{154}Cl_{48}$ (ester) |
| $\theta_A/\theta_R$ | 96°/50° | 95°/53° | 95°/72° | 104°/73° (alcohol)<br>100°/70° (ester) |

(c) FEP.

| Technique | FEP-$CO_2H$ | FEP-$CH_2OH$ | FEP-$CH_2OCOCCl_3$ | FEP Control* |
|---|---|---|---|---|
| XPS | $C_{100}F_{194}O_{11}$ | $C_{100}F_{209}O_4$ | $C_{100}F_{209}O_9Cl_5$ | $C_{100}F_{202}$ (alcohol)<br>$C_{100}F_{196}$ (ester) |
| $\theta_A/\theta_R$ | 101°/56° | 95°/59° | 105°/79° | 114°/93° (alcohol)<br>112°/91° (ester) |

*Two control film samples were required for these reactions: (1) for the reaction with borane•THF (alcohol) and (2) for the reaction with trichloroacetyl chloride (ester).

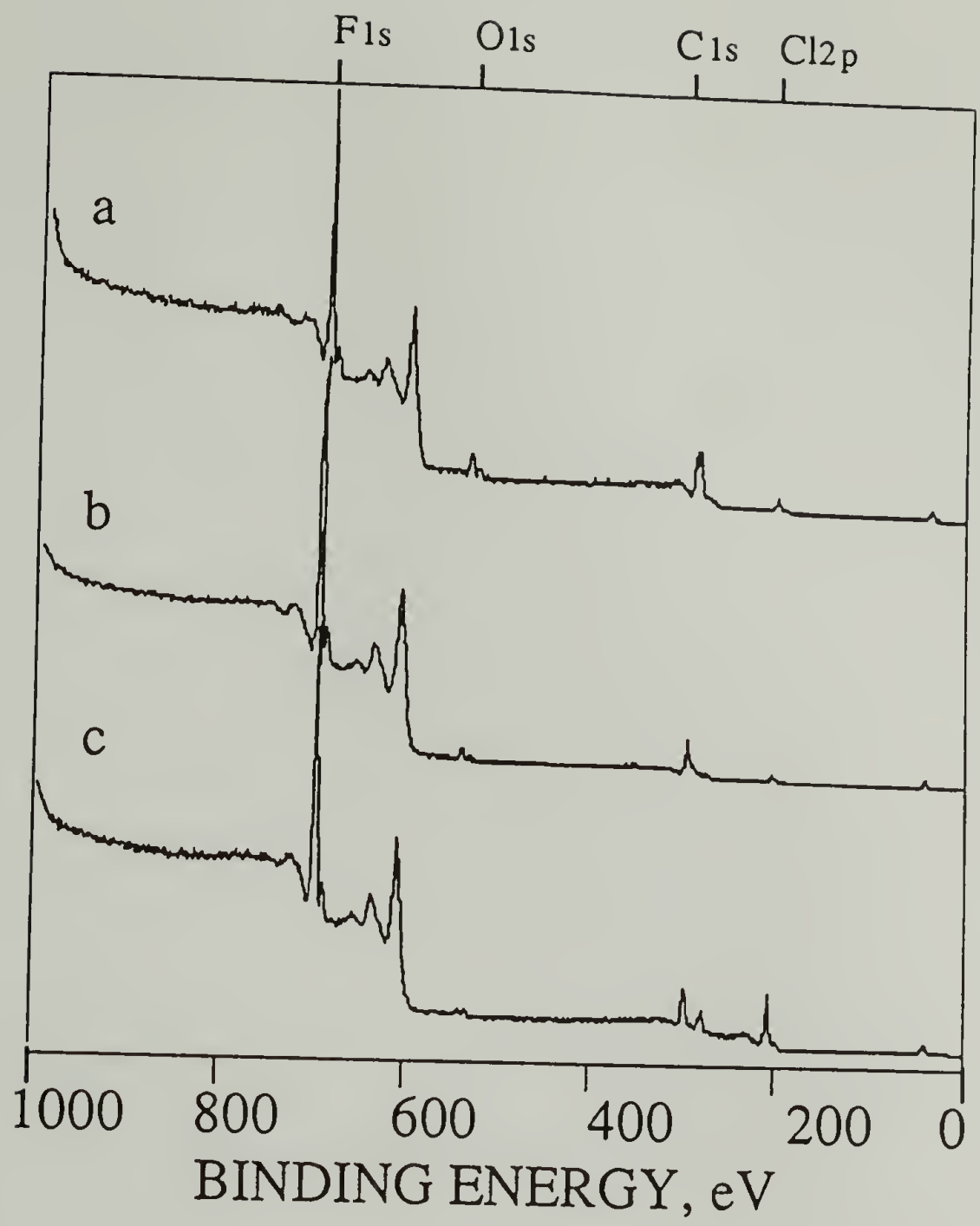


Figure 1.8 XPS (survey, 15° takeoff angle) Spectra of (a) $PVF_2$-$CH_2OCOCCl_3$, (b) FEP-$CH_2OCOCCl_3$, (c) PCTFE-$CH_2OCOCCl_3$.

## Contact Angle Titration Curves

Dynamic contact angle measurements indicate relative hydrophobicity / hydrophilicity of a surface. In contact angle measurements, several assumptions are made:[46] (1) the liquid-vapor-solid are in thermodynamic equilibrium such that $\gamma_{SV} - \gamma_{SL} = \gamma_{LV}\cos\theta$ (Young-Dupre equation); (2) the solid surface free energy is unaffected by any liquid adsorbing to it; (3) the solid surface is rigid, immobile, and non-deformable such that

surface groups neither reorient nor undergo vertical displacement; (4) the liquid maintains a constant surface tension and does not swell the solid surface. In light of these assumptions, the advancing ($\theta_A$) and receding ($\theta_R$) contact angles should be equivalent; however, true thermodynamic equilibrium is not established between the solid-liquid-vapor causing hysteresis between advancing and receding contact angles. In addition, surface roughness[47] and/or chemical heterogeneity increase the hysteresis observed. Consider a surface consisting of a hydrophobic non-wetting phase and a hydrophilic wetting phase. As water is advanced ($\theta_A$) across the surface, the hydrophobic regions hold (or pin) the drop, thereby increasing $\theta_A$ beyond $\theta_A$ for a homogeneous surface. After the surface is covered with liquid, the receding contact angle is held back by the high energy phase, such that $\theta_R$ is less than $\theta_R$ of a homogeneous surface. Consequently, $\theta_A$ represents hydrophobic regions whereas $\theta_R$ represents hydrophilic regions and the hysteresis between $\theta_A$ and $\theta_R$ increases. The hysteresis is augmented by the fact that the receding contact angle, unlike the advancing contact angle, is sensitive to a small fraction (<10%) of high energy surface coverage.[48]

Titration curves measuring contact angle with pH buffered aqueous solutions were constructed for three surface modified fluoropolymer film samples, $PVF_2$-$CO_2H$, PCTFE-$CO_2H$, and FEP-$CO_2H$. As described by Holmes Farley *et al.*,[13] it is assumed that (1) only surface groups in direct contact with the probe fluid affect the surface free energy (i.e. van der Waals forces only, no long range interactions); (2) the surface does not reconstruct on changing pH; and (3) the change in pH does not affect non-ionizable groups. The titration curves are included in Figures 1.9, 1.10, and 1.11 for $PVF_2$-$CO_2H$, PCTFE-$CO_2H$, and FEP-$CO_2H$, respectively; unmodified ($PVF_2$, PCTFE, FEP) and alcohol functionalized ($PVF_2$-$CH_2OH$, PCTFE-$CH_2OH$, FEP-$CH_2OH$) film samples did not show pH-dependent contact angles. The contact angle of the carboxylic acid, protonated at low pH, decreased as pH was increased or as the acid was deprotonated to

carboxylate. The carboxylate is more hydrophilic than the carboxylic acid, accounting for this decrease.

The $pK_a$ was calculated from the contact angle titration curves to be between 5 and 10 for all three carboxylic acid-functionalized surfaces. A similar result was obtained for carboxylic acid-functionalized polyethylene (PE-$CO_2H$).[13] Unlike acetic acid ($pK_a$ 4.75)[49] and polyacrylic acid[50], the surface carboxylic acid had a range of values for $pK_a$ which was significantly higher than that observed for carboxylic acids dissolved in solution. Several explanations have been put forward:[15,17] (1) a heterogeneous acid functionalized surface produces a range of $pK_a$ values; (2) solvation of a carboxylate anion is relatively poor at the organic-water interface with respect to that in a homogeneous solution where solvation is less hindered; (3) Coulomb interaction between carboxylate ions causes the ions to be excluded from the low polarity interfacial region; (4) the surface area that the functional group occupies at the interface determines its affect on wetting; if the carboxylate group occupies a greater area when wet than the carboxylic acid group, the decrease in contact angle may result from the "area" change. Although it is difficult to discern between these possible explanations for the increased and broad range of $pK_a$ values calculated, the carboxylate was more hydrophilic than the carboxylic acid, resulting in a decreased contact angle with increased pH. The receding contact angles were more representative of the hydrophilic nature and thus decreased more substantially than the advancing contact angles with increased pH.

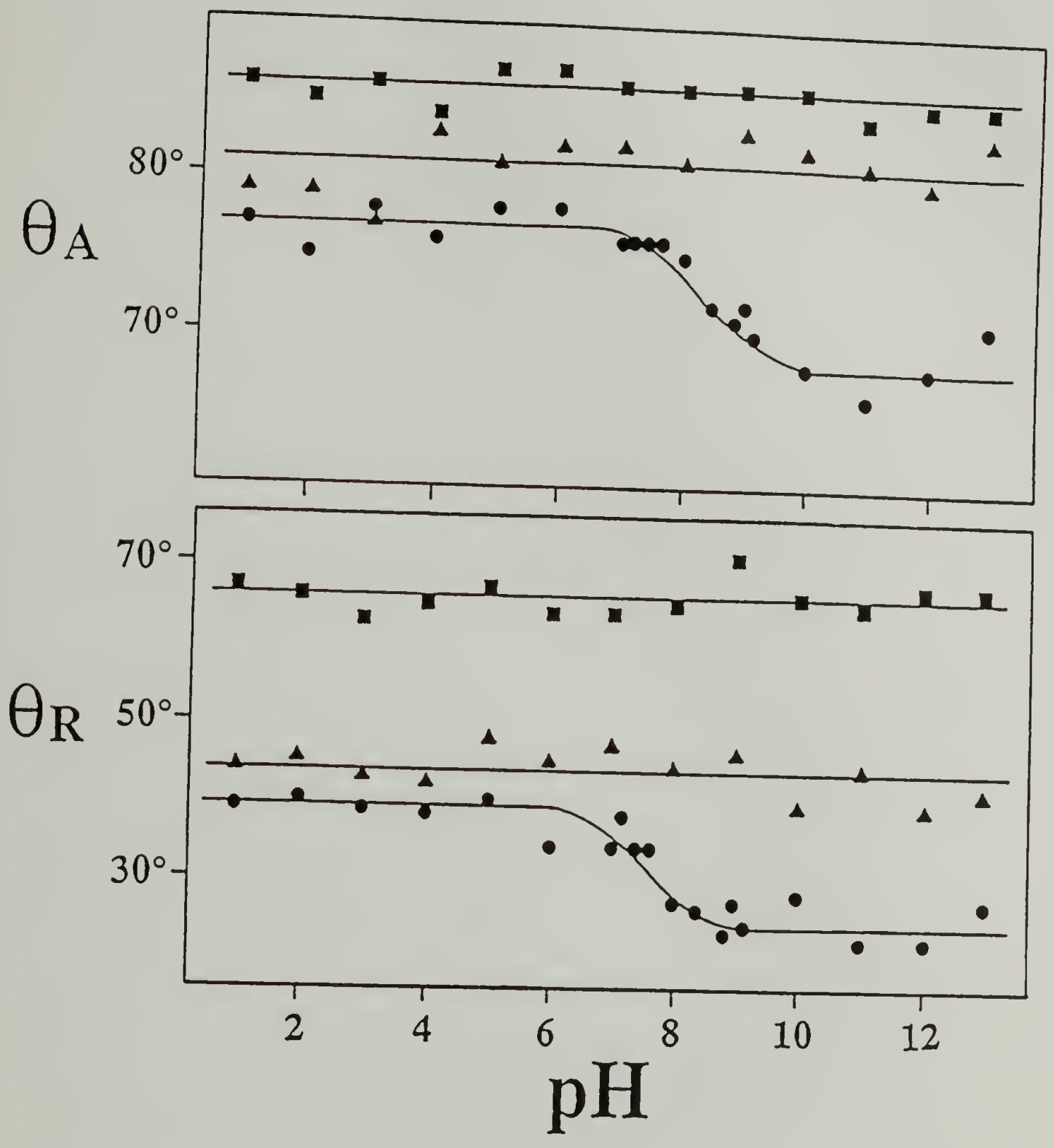


Figure 1.9 Dependence of Contact Angle ($\theta_A/\theta_R$) on pH Buffered Aqueous Solutions: (■) $PVF_2$, (▲) $PVF_2$-$CH_2OH$, (●) $PVF_2$-$CO_2H$.

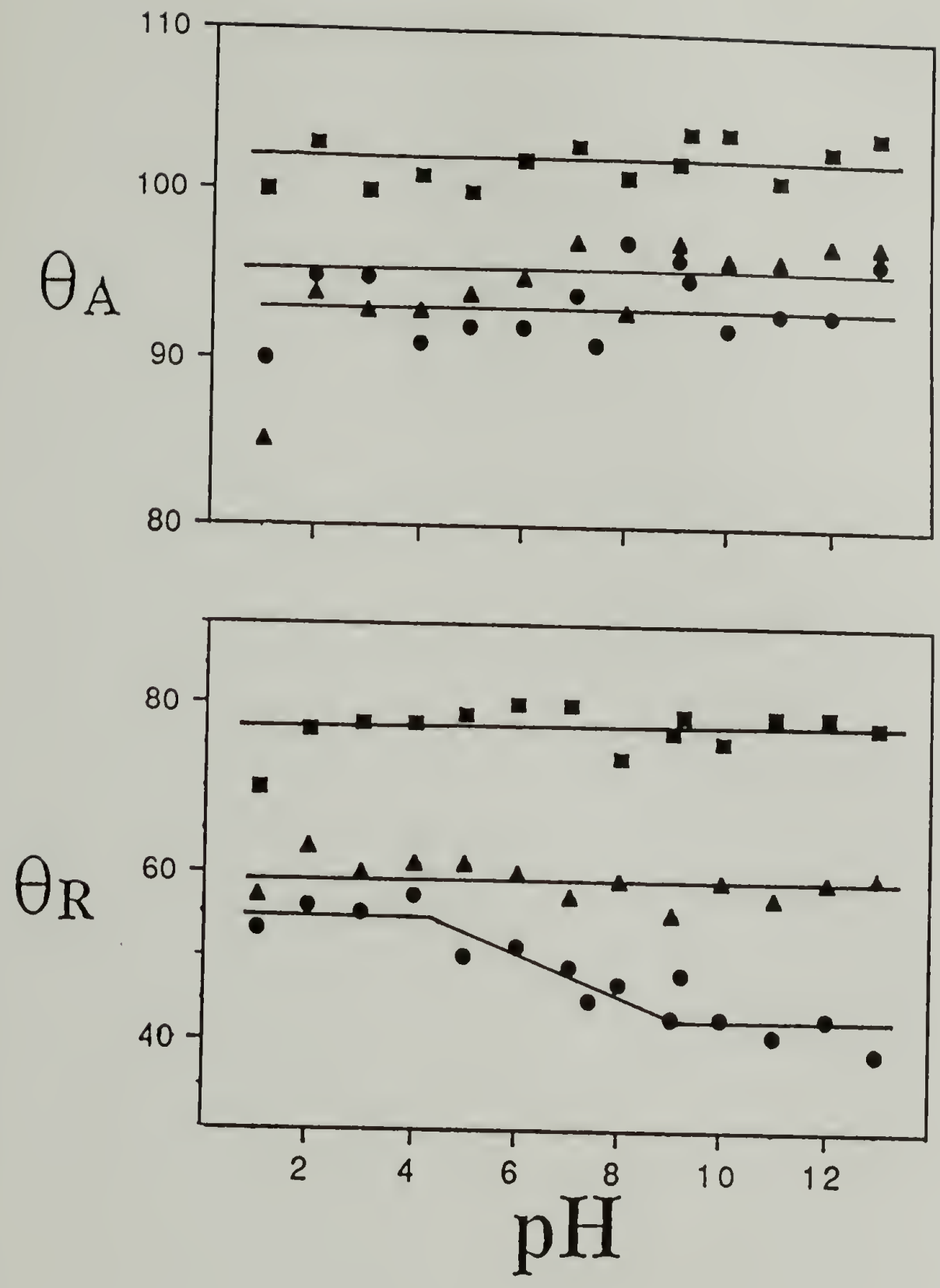


Figure 1.10 Dependence of Contact Angle ($\theta_A/\theta_R$) on pH Buffered Aqueous Solutions: (■) PCTFE, (▲) PCTFE-$CH_2OH$, (●) PCTFE-$CO_2H$.

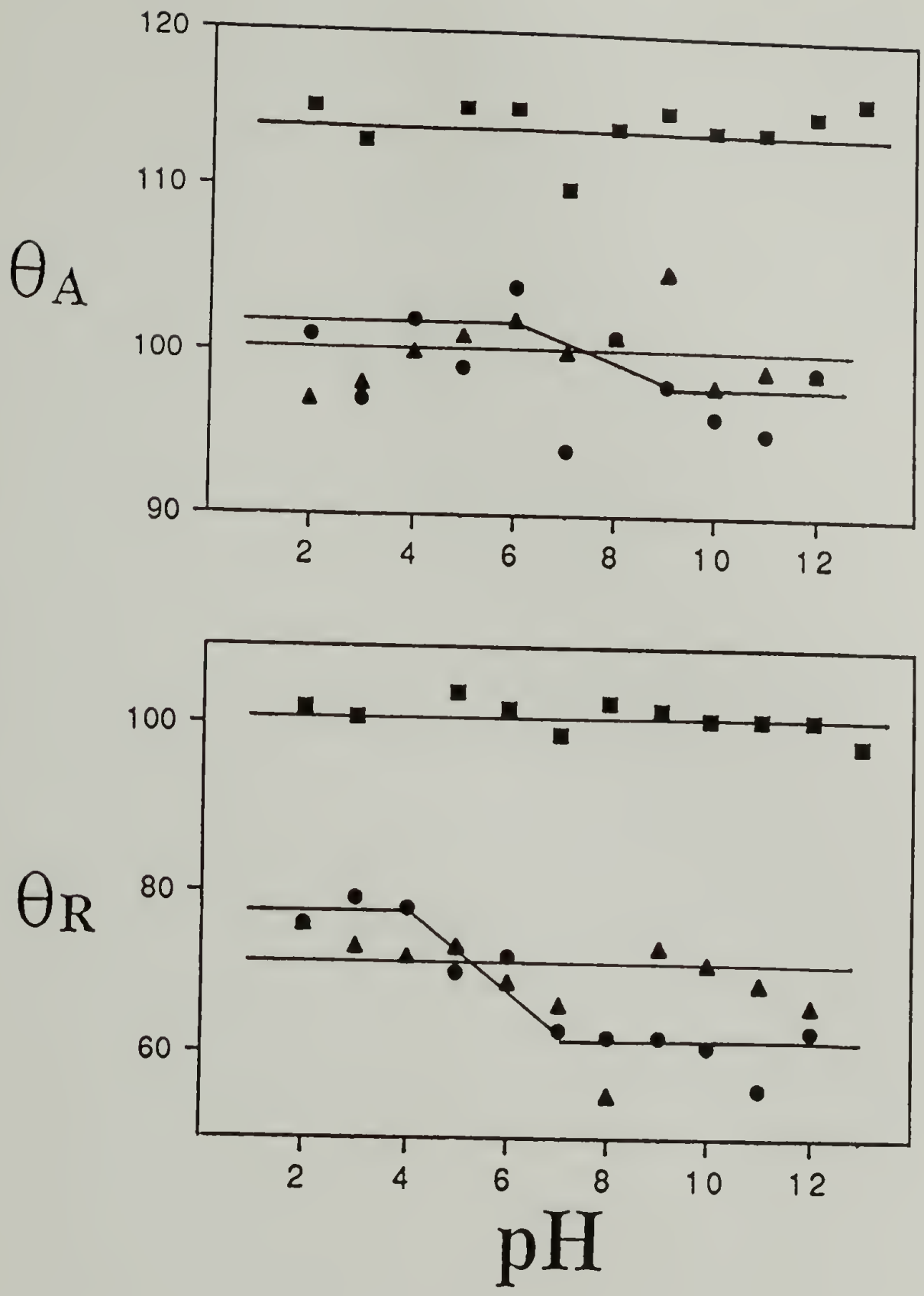


Figure 1.11 Dependence of Contact Angle ($\theta_A/\theta_R$) on pH Buffered Aqueous Solutions: (■) FEP, (▲) FEP-$CH_2OH$, (●) FEP-$CO_2H$.

## Conclusions

A surface selective technique was developed to introduce carboxylic acid functionality to fluoropolymer film samples. The method involves a two step procedure where unsaturation introduced in the first synthetic step is oxidatively removed in the second step. This technique was applied to three fluoropolymer film samples which reflects its versatility and simplicity. The carboxylic acid-functionalized film samples, $PVF_2$-$CO_2H$, PCTFE-$CO_2H$, and FEP-$CO_2H$, have less than monolayer surface coverage of carboxylic acid groups, with only 1 acid group per 12 -16 fluoropolymer repeat units. The density of carboxylic acid groups and the topography of the acid functionalized film sample depend upon the initial reaction which introduces the reactive handle for further modification. Conditions were used to control both depth of reaction and roughness of the resultant film sample. The low percentage of carboxylic acid groups was apparent in the relatively high contact angles reported. The carboxylic acid group, despite its low concentration, showed pH-dependent contact angles: $PVF_2$-$CO_2H$ (77°/39° decreases to 68°/25°); PCTFE-$CO_2H$ (93°/55° decreases to 93°/43°); and FEP-$CO_2H$ (101°/78° decreases to 97°/61°). PCTFE-$(CH_2)_3CO_2H$ in which 80% of the repeat units are functionalized shows pH dependent contact angles of 56°/0° at low pH and 30°/0° at high pH.[21] The carboxylic acid group was chemically modified by reaction with (1) thallous ethoxide to produce thallium carboxylate and (2) borane•THF to produce primary alcohol which was then reacted with trichloroacetyl chloride to produce trichloroacetate. FEP and FEP-$CO_2H$ were used in adsorption studies as described in Chapters II and III, respectively.

## References


1. Dwight, D. *Chemtech* **1982**, *March*, 166.

2. Ward, W.J.; McCarthy, T.J. in *Encyclopedia of Polymer Science and Engineering*, 2nd ed.; (Mark, H.F.; Bikales, N.M.; Overberger, C.G.; Menges, G.; Kroschwitz, J.I., Eds.); Wiley: New York, 1989, supplement, p. 674.

3. Allmer, K.; Feiring, K.A. *Macromolecules* **1991**, *24*, 5487.

4. Dias, A.J.; McCarthy, T.J. *Macromolecules* **1987**, *20*, 2068.

5. Lee, K.-W.; McCarthy, T.J. *Macromolecules* **1988**, *21*, 2318.

6. Costello, C.A.; McCarthy, T.J. *Macromolecules* **1987**, *20*, 2819.

7. Dias, A.J.; McCarthy, T.J. *Macromolecules* **1985**, *18*, 1826.

8. Rasmussen, J.R.; Stedronsky, E.R.; Whitesides, G.M. *J. Am. Chem. Soc.* **1977**, *99*, 4736.

9. Rasmussen, J.R.; Bergbreiter, D.E.; Whitesides, G.M. *J. Am. Chem. Soc.* **1977**, *99*, 4746.

10. Shoichet, M.S.; McCarthy, T.J. *Macromolecules* **1991**, *24*, 982.

11. This general strategy was outlined in Iyengar, D.R.; McCarthy, T.J. *Macromolecules* **1990**, *23*, 4344.

12. Baszkin, A.; Terminassian-Seraga, L. *Polymer* **1974**, *15*, 759.

13. Holmes, Farley, S.R.; Reamey, R.H.; McCarthy, T.J.; Deutch, J.; Whitesides, G.M. *Langmuir* **1985**, *1*, 725.

14. Holmes Farley, S.R.; Whitesides, G.M. *Langmuir* **1986**, *2*, 266.

15. Holmes Farley, S.R.; Whitesides, G.M. *Langmuir* **1987**, *3*, 62.

16. Homes Farley, S.R.; Reamey, R.H.; Nuzzo, R.; McCarthy, T.J.; Whitesides, G.M. *Langmuir* **1987**, *3*, 799.

17. Holmes Farley, S.R.; Bain, C.D.; Whitesides, G.M. *Langmuir* **1988**, *4*, 921.

18. Wilson, M.D.; Whitesides, G.M. *J. Am. Chem. Soc.* **1988**, *110*, 8718.

19. Wilson, M.D.; Ferguson, G.S.; Whitesides, G.M. *J. Am. Chem. Soc.* **1990**, *112*, 1244.

20. For example see: Briggs, D.; Brewis, D.M.; Konieczo, M.B. *J. Mater. Sci.* **1976**, *11*, 1270.

21. Bee, T.G.; McCarthy, T.J. *Macromolecules* **1992**, *25*, 2093.

22. Kolthoff, J. M.; Sandel, E. B.; Meehan, E. J.; Bruckenstein, S. *Quantitative Chemical Analysis*, 4th ed. The MacMillan Co.: Toronto, 1969, p. 1163.

23. Lipton, M.F.; Sorensen, C.M.; Sadler, A.C.; Shapiro, R.H. *J. Organometallic Chem.* **1980**, *186*, 155.

24. Dias, A.J.; McCarthy, T.J. *Macromolecules* **1984**, *17*, 2529.

25. Brennan, J.V.; McCarthy, T.J. *Polym. Prepr. (Am. Chem. Soc., Div. Polym. Chem.)* **1988**, *29* (2), 338.

26. Notebook references are included in the text of this dissertation in square brackets; roman numerals indicate the book whereas arabic numerals indicate the page.

27. Bening, R.C.; McCarthy, T.J. *Macromolecules* **1990**, *23* , 2648.

28. Brennan, J.V.; McCarthy, T.J. *Polym. Prepr. (Am. Chem. Soc., Div. Polym. Chem.)* **1989**, *30* (2), 152.

29. For more information on dehydrofluorinating reagents see Brennan, J.V. Ph.D. dissertation, University of Massachusetts, 1991.

30. Burdon, J.; Tatlow, J.C. *J. Appl. Chem.* **1958**, *8*, 293.

31. Lenher, V.; Stone, H.W.; Skinner, H.H. *J. Am. Chem. Soc.* **1922**, *44*, 143.

32. Oxidation with potasssium chlorate/sulfuric acid has been used by others, for example see Gagnon, D.R.; McCarthy, T.J. *J. Appl. Polym. Sci.* **1984**, *29*, 4335.

33. Other ways to calculate the depth of modification are illustrated in reference 26.

34. Danielson, N.D.; Taylor, R.T.; Huth, J.A.; Siergiej, R.W.; Galloway, J.G. Paperman, J.B. *Ind. Eng. Chem. Prod. Res. Dev.* **1983**, *22*, 303.

35. Kolb, B.U.; Patton, P.A.; McCarthy, T.J. *Macromolecules* **1990**, *23*, 366.

36. Dwight, D.W.; Riggs, W.M. *J. Colloid Interface Sci.* **1974**, *47*, 650.

37. Costello, C.A.; McCarthy, T.J. *Macromolecules* **1984**, *17*, 2940.

38. In these calculations the presence of ~8% $CF_2CF(CF_3)$ units has been ignored. Although the perfluoropropylene groups do not affect the C:F:O XPS ratio, if taken into account, the ratio of carboxylic acid groups to repeat units would be slightly higher.

39. Clark, D.T.; Thomas, H.R. *J. Polym. Sci., Polym. Chem. Ed.* **1977**, *15*, 2843.

40. Batich, C.D.; Wendt, R.C. in *Photon, Electron and Ion Probes of Polymer Structure and Properties* (Dwight, D.W.; Fabish, T.J.; Thomas, H.R., Eds.) American Chemical Society: Washington, D.C. 1981, (ACS Symposium Series 162), p. 221.

41. McKillop, A.; Bromley, D.; Taylor, E.C. *J. Org. Chem.* **1968**, *34*, 1172.

42. Yoon, N.M.; Pak, C.S.; Brown, H.C.; Krishnamurthy, S.; Stocky, T.P. *J. Org. Chem.* **1973**, *38*, 2786.

43. Nuzzo, R.G.; Smolinsky, G. *Macromolecules* **1984**, *17*, 1013.

44. Reilley, C.N.; Everhart, D.S.; Ho, F.F.-L. in *Applied Electron Spectroscopy for Chemical Analysis* (Windawi, H.; Ho, F.F.-L., Eds.) John Wiley & Sons: New York, 1982, ch. 6.

45. The calculation for the yield of PCTFE-$CH_2OCOCCl_3$ was complicated by the presence of chlorine in the bulk polymer. The alcohol functionalized film, $(CF_2CFCl)_{48}(CH_2OH)_4$ was converted to the esterified film, $(CF_2CFCl)_{46}(CH_2OCOCCl_3)_{2.5}$. The yield of the labeling reaction was determined from the ratio of ester groups to alcohol groups, 2.5/4.0.

46. Andrade, J.D.; Smith, L.M.; Gregonis, D.E. in *Surface and Interfacial Aspects of Biomedical Polymers: Surface Chemistry and Physics* (Andrade, J.D., Ed.); Plenum Press: New York, 1985, vol. 1, chap. 7.

47. Morra, M.; Occhiello, E.; Garbassi, F. *Langmuir* **1989**, *5*, 872.

48. Johnson, R.E., Jr.; Dettre, R.H. in *Surface and Colloid Science* (Matijevic, E., Ed.) Wiley-Interscience: New York; **1969**, *2*, 85.

49. Lide, D.R., Ed. *Handbook of Chemistry and Physics*, 72nd ed.; CRC Press: Boca Raton, 1991-1992, p. VIII-39.

50. Nemec, J.W.; Bauer, W., Jr. in *Encyclopedia of Polymer Science and Engineering*, 2nd ed. (Mark, H.F.; Bikales, N.M.; Overberger, C.G.; Menges, G.; Kroschwitz, J.I., Eds.); John Wiley and Sons: New York, 1985, p. 285.

# CHAPTER II

# SURFACE MODIFICATION OF POLY(TETRAFLUOROETHYLENE-CO-HEXAFLUOROPROPYLENE) FILM BY ADSORPTION OF POLY(L-LYSINE) FROM AQUEOUS SOLUTION

## Overview

Polymer surface modification can be accomplished by a number of techniques including both chemical reaction which was described in Chapter I and adsorption which is the subject of this chapter. The adsorption of poly(L-lysine) (PLL) to poly(tetrafluoroethylene-co-hexafluoropropylene) (FEP) was studied in an attempt to determine the important driving forces for adsorption and as a surface modification technique. PLL adsorbed to the FEP - water interface, thereby decreasing its high interfacial free energy. Adsorption of neutral PLL to neutral FEP is dependent upon PLL solution conformation. Adsorption of PLL-ammonium to FEP-carboxylate is discussed in Chapter III. The solvent-substrate and segment-solvent interactions are discussed in an attempt to explain adsorption results. The properties of the FEP-PLL film sample are compared to those of FEP in terms of wettability, chemical reactivity, adhesion, and biological cell adhesion and growth. Several techniques were used to characterize the surface modifications described herein; most of the useful information was determined from x-ray photoelectron spectroscopy, ultraviolet-visible spectrophotometry, contact angle analysis, and attenuated total reflectance infrared spectroscopy.

## Introduction

Poly(L-lysine) (PLL) has been used in several applications including those of drug delivery[1-5] and biological activity.[6-11] For example, an insulin - PLL complex demonstrates slow-release properties producing significant blood sugar lowering for up to 12 h.[12] PLL can also be used as a polymer carrier for diagnostic or therapeutic agents which are site-specifically conjugated to a targeting antibody.[13,14] In addition, bacteriophage activity can be rendered inactive by ε- and α-PLL.[15] Studies on the antimicrobial activity of ε-PLL suggest that the adsorption of ε-PLL to the bacterial cell surface plays an important role in its antibacterial activity.[16]

PLL enhances the surface properties of a number of materials on which it is coated, rendering them useful for new applications or improving their performance. For example, PLL coated on poly(ethylene terephthalate) film,[17] poly(sulfone),[18] or polyacrolein microspheres,[19] shows improved cell growth and immobilization.[20] Polak *et al.*[21] found that higher molecular weight PLL (350k) provides greater adhesive strength at low concentration, 0.05-0.1%, forming a ~5 μm layer of free amino groups on glass slides which can be used for immunocytochemical staining. In addition, PLL-coated colloidal gold particles are useful as a probe in electron microscopy for the detection of anionic cellular components (e.g. red blood cell membranes).[22] PLL-coated poly(acrylamide) beads have been used for gel filtration of human blood platelets.[23]

## PLL Solution Properties

PLL serves as an important model for protein conformational analysis[24] because it can adopt the 3 major conformations, random coil, α-helix, and β-form, observed in polypeptides and proteins. PLL at pH 7 is a highly charged molecule with a random coil-like or disordered conformation. At pH 11 and 60 °C, PLL transforms to an uncharged

antiparallel β-sheet, an entropy driven process where the decreased order of the water structure overcomes the increased order of the peptide backbone. The process is endothermic and is favored by hydrophobic bond formation. At room temperature and at pH 11, the α-helix conformation is favored. The hydrophobic bond stabilizes the α-helix as well, though not as strongly as it does the β-sheet.[25] Protonated PLL has a $pK_a$ of 10.5. The transition from random coil to α-helix can be accomplished by raising the pH of an aqueous solution to pH 11 or by dissolving the polypeptide in methanol[26], ethanol, isopropanol, or dimethylformamide. The heats of formation of the α-helix in the latter 3 solvents were determined by calorimetry to be -6.8 kJ/mol, -16.0 kJ/mol, and 10.5 kJ/mol respectively.[27] Poly(L-lysine) is synthesized by the N-carboxyanhydride (NCA) technique.[28,29] The PLL used in this study was the product of base initiated (sodium hydroxide or triethylamine) polymerization of lysine N-carboxyanhydride which was subsequently deprotected.

The solution conformations and their transitions have been studied with various spectroscopic techniques (circular dichroism (CD), electron spin resonance (ESR), ultraviolet-visible (UV-vis), infrared (IR), electron microscopy (EM), resonance Raman), potentiometry and calorimetry. In an ESR study[30] of the pH induced α-helical conformational transition, the spin label on PLL was shown to be in a more restricted environment when PLL was deprotonated. For high molecular weight polymer, both side chain - side chain interactions and segmental mobility of the backbone decreased due to deprotonation and α-helix formation. For low molecular weight (~3k) PLL, which was previously shown not to form the α-helix at high pH, the side chain - side chain interactions decreased only due to deprotonation. Dark field electron micrographs of α-helical PLL indicated that the helix has a pitch of 0.54 ± 0.01 nm, a pitch angle of 25.6° ± 1.5°, and 3.6 residues per turn.[31]

Using resonance Raman spectroscopy, the conformation of the polypeptide was determined by the line position of the amide I band: an absorption at 1670 $cm^{-1}$ indicates

β-structure while one at 1645 $cm^{-1}$ represents the α-helix conformation. An absorption between these two values, at 1660 $cm^{-1}$ is indicative of the random coil structure.[32] In a study using vibrational circular dichroism and infrared absorption, the amide I peak assignment was correlated with PLL structure. Table 2.1 summarizes these results.[33]

Table 2.1 Assignment of PLL Conformation Based on Circular Dichroism and Infrared: PLL Concentration = 3-5% wt.

| Solvent | pH | Conformation* | Amide I ($cm^{-1}$) |
|---|---|---|---|
| $D_2O$ | 7.3 | rc | 1660(sh*), 1646 |
| $D_2O$ NaOD | 10.5 | unordered | 1642, 1610(sh*) |
| $D_2O$ NaOD | 11.5 | α-h, rc, β-s | 1681, 1636(sh*), 1610 |
| $D_2O$ NaOD heat | 11.5 | anti-// β-s | 1681, 1610 |
| $CH_3OH$-$H_2O$ 96:4 | | rh α-h | 1651 |
| $CD_3OD$-$D_2O$ 96:4 | | rh α-h | 1642 |

*rc = random coil; α-h = α-helix; β-s = β-sheet; anti-// β-s = antiparallel β-sheet; rh = right-handed; sh = shoulder.

The conformations of PLL are best distinguished by circular dichroism (CD)[34] which measures the difference in absorbance of left and right circularly polarized light by a chirooptical substance. Distinct positive and negative absorption bands of the CD spectrum are associated with different conformations. Table 2.2 summarizes the important transitions used to determine PLL conformation. PLL was also studied by UV-vis spectrophotometry which, in conjunction with other techniques, can elucidate polypeptide conformation.[35]

Table 2.2 Absorption Bands Used to Identify the Conformation of PLL.

| Conformation | Absorption (nm) | Transition |
|---|---|---|
| α-helix | -222 | n-π* |
| | -208-210 | |
| | +191 | π-π* (stronger) |
| β-form | -216-218 | |
| | +195 | (stronger) |
| random coil | -198 | |
| | +220 | (weak) |
| | +235 | (weaker) |

PLL was characterized by x-ray photoelectron spectroscopy (XPS)[36] where the $C_{1s}$ binding energy peak of PLL•HBr powder was curve fit to account for three carbon types of -NHC(O)CH($(CH_2)_3CH_2NH_2$.HBr)-: (i) (C-H) at 285.0 eV, (ii) (C-N) at 286.4 eV, and (iii) (C=O) at 288.1 eV where an internal hydrocarbon reference of 285.0 eV was used. The $N_{1s}$ peak was curve fit to account for the the backbone amide nitrogen (at 401.5 eV), accounting for 55%, and the pendant amine nitrogen (at 399.5 eV), accounting for 45%, of the total peak signal. The expected atomic concentration of poly(lysine) hydrobromide, $C_{60}N_{20}O_{10}Br_{10}Cl_0$, differed from that of the observed, $C_{68}N_{15}O_{9.7}Br_{6.7}Cl_{1.4}$, indicating that adsorbate had interacted with the ammonium halide moiety.

## Adsorption of Poly(L-lysine)

PLL has been used in numerous adsorption studies where its solution properties are used to control adsorption behavior. A series of adsorption experiments investigating the interaction between PLL and sulfonated polystyrene latices (PSS) was studied by gel electrophoresis, microcalorimetry, and flocculation.[37] Furusawa *et al.* found that PLL's

solution conformation was retained, at least partially, upon adsorption; the random coil adsorbed as such whereas the α-helix seemed to unfold partly upon adsorption. They reported that neutral α-helix PLL (pH 11) seemed to adsorb vertically and to interact laterally with other α-helix PLL whereas charged random coil PLL (pH 4) interacted directly with the adsorbate surface ($-SO_3^-$). The electrophoretic mobility of negatively charged polystyrene (PSS) particles coated with positively charged PLL was further studied as a function of KBr ionic strength.[38] At low ionic strength, both low and high molecular weight PLL adsorbed in an extended flat conformation. As ionic strength increased, ($>10^{-4}$ M KBr) high molecular weight PLL formed loops and tails causing charge reversal and increased mobility for PSS-PLL. At higher ionic strengths, ($>10^{-2}$ M KBr), the electrostatic repulsion between chain segments decreased as a result of electrolyte screening; PLL loop formation enhanced further adsorption to PSS particles which then showed decreased mobility. At higher ionic strengths, the electrostatic interaction between PLL and PSS decreased; however, PLL did not desorb because, in addition to the ionic interaction, a hydrophobic interaction existed which enhanced adsorption.

Ellipsometry and XPS were used to characterize the adsorption of PLL to silicon wafers, the surfaces of which had been modified with either poly(vinyl chloride) (PVC), methacrylic acid/methacrylate copolymer (PMA), or poly(ethylene oxide) (PEO).[39] PLL adsorption increased with concentration (20 g/m$^3$ to 1000 g/m$^3$) and PLL was found most abundant on PMA followed by PVC and then PEO. PLL adsorbed to PMA as a result of a strong electrostatic interaction.

In the adsorption to mica, the ionic strength, pH, and molecular weight of PLL were varied.[40] PLL adsorbed to the negatively charged mica surface as a result of mutual electrostatic attraction; loop and tail formation were suppressed due to electrostatic repulsion between chain segments. Increasing the electrolyte (NaCl) concentration resulted in lower PLL adsorption presumably due to competition between sodium and ammonium ions. By increasing the solution pH, more PLL adsorbed because it had adopted the more

compact, neutral, α-helix conformation where repulsion between segments was reduced. The surface concentration of PLL was inversely proportional to molecular weight at both pH 5.6 and pH 11.2; there was twice as much coverage at the higher pH. The adsorption of random coil PLL at 0.1 M salt concentration was calculated based on hexagonal packing of "hard-sphere" molecules.

In this study, polymer surface modification was accomplished by the adsorption of poly(L-lysine) (PLL) from an aqueous solution to an FEP film sample.[41] PLL has been adsorbed to other substrates where the effects of electrostatic interactions, pH, salt concentration, and molecular weight were investigated. In this study, the adsorption of PLL to FEP was controlled by choice of solvent, pH of the aqueous solution, PLL solution conformation, and molecular weight. The high interfacial free energy between organic (FEP) and aqueous (PLL solution) phases acts as a driving force for adsorption. The sharp interface defined between the solid polymer film and the aqueous polymer solution ensured that the interaction between PLL and FEP was limited to the surface of the polymer film. By unfolding from the α-helix, PLL regains, at least partially, the conformational entropy which is lost upon adsorption.

FEP is a good substrate on which to study adsorption of PLL because it is a low surface free energy polymer with a high water contact angle and is spectroscopically distinct from PLL. FEP is chemically homogeneous, smooth (to at least 50 Å by SEM), and is neither swollen nor penetrated by the aqueous solution. FEP is a chemically inert, hydrophobic polymer; adsorption of poly(L-lysine) from an aqueous solution dramatically changes the surface properties of the solid FEP film samples. The samples were studied in terms of hydrophilicity, chemical reactivity, and adhesive nature.

## Experimental

All solutions were sparged with nitrogen and transferred by Schlenk technique unless specified otherwise. All materials were used as received unless specified otherwise.

### Materials and Methods

**Poly(tetrafluoroethylene-co-hexafluoropropylene)** (FEP, 5 mil) was obtained from duPont and extracted with refluxing dichloromethane for 1 h; the polymer film was rinsed in fresh dichloromethane and then dried (0.02 mm, >24 h) to constant mass. The polymer film samples were stored under vacuum.

**Poly(L-lysine)** (PLL) was purchased as the hydrobromide salt from Sigma where it was characterized by low angle laser light scattering, size exclusion chromatography, and solution viscosity. The molecular weights used are abbreviated in the text as indicated in Table 2.3. A 1 mg/ml stock solution was prepared and stored refrigerated under positive nitrogen pressure.

Table 2.3 Molecular Weight Description of Poly(L-lysine) Samples.

| Mv | DP | Mw | DP | PDI | Mw (abbreviated) |
|---|---|---|---|---|---|
| 3800 | 18 | | | | 4k |
| 22,400 | 107 | 19,500 | 93 | 1.15 | 20k |
| 50,000 | 239 | 44,120 | 211 | 1.13 | 50k |
| 64,800 | 310 | 59,000 | 282 | 1.15 | 60k |
| 100,500 | 481 | 90,300 | 432 | 1.11 | 100k |
| 421,800 | 2018 | 334,800 | 1602 | 1.26 | 400k |
| 560,000 | 2679 | 502,500 | 2404 | 1.11 | 500k |

**House Distilled Water** was redistilled from a Gilmont still apparatus before use.

**Adsorption of PLL to FEP at pH 7.** A known volume (e.g. 2 ml) of the 1 mg/ml PLL stock solution was added by cannula to a nitrogen-purged Schlenk tube containing an FEP film sample. The PLL solution was diluted with redistilled water to 20 ml (concentration = 0.1 mg/ml) and was also added by cannula. The solution in the Schlenk tube was agitated in a 25 °C water bath. After the specified time of interaction (24 h, for example), the PLL solution was removed by cannula and the film was rinsed with redistilled water (3 x 20 ml). The samples were dried before analysis (0.05 mm, > 24 h). [III7-13,21-23,57,89,126]

**pH 11 Buffer** was prepared according to a published procedure.[42] 50 ml of 0.05 M $NaHCO_3$ (Fisher) solution and 22.7 ml of 0.1 M NaOH (Fisher) solution were diluted to 100 ml with redistilled water.

**Adsorption of PLL to FEP at pH 11** (FEP-PLL). The procedure outlined for adsorption at pH 7 was followed; however, the PLL solution was diluted with pH 11 buffer to the appropriate concentration in the nitrogen-purged Schlenk tube containing an FEP film sample. The work up procedure differed by using redistilled water (1 x 20 ml), pH 11 buffer solution (2 x 20 ml), followed by redistilled water (2 x 20 ml). [III72,80-82,86-87,90,96]

**Adsorption of PLL to FEP from Isopropanol/Water (82:18, v/v).** The procedure outlined for adsorption at pH 7 was followed with some changes. A 1 mg/ml 500k PLL stock solution was prepared by dissolving PLL first in redistilled water and then diluting the solution with isopropanol (iPrOH) (Fisher) to a 82:18, v/v ratio of isopropanol:water. A known volume of this stock solution was diluted to 20 ml with a solution of similar make up to the desired concentration, 0.1 mg/ml or 0.5 mg/ml, in the nitrogen-purged Schlenk tube containing FEP. The work up procedure differed by using a solution of isopropanol:water (82:18, v/v) (3 x 20 ml). [III88-89]

**Adsorption of PLL to FEP from Methanol/Water (96:4, v/v).** The procedure outlined for adsorption from iPrOH/$H_2O$ was followed where methanol (MeOH) (Fisher) was used instead of isopropanol, and the ratio of MeOH/$H_2O$ was 96:4, v/v. The work up procedure differed by using a solution of methanol:water (96:4, v/v) (3 x 20 ml). [III88-89]

**Solvent Stability of the Adsorbed Layer** was assessed by immersing an FEP-PLL film sample in a solvent for a specified length of time. The FEP-PLL film sample was prepared by adsorbing 20 ml of a 0.5 mg/ml solution of 20k PLL at pH 11 for 6 h to FEP. [III75-78]

**3,5-Dinitrobenzoyl Chloride** (3,5-DNBC) (Aldrich, 98+%) was used as received and stored in the glove box.

**Tetrahydrofuran** (THF) (Aldrich, anhydrous, 99.9%) was distilled from sodium benzophenone (Aldrich).

**Pyridine** (Aldrich) was distilled from calcium hydride (Aldrich).

**Reaction of FEP-PLL with 3,5-Dinitrobenzoyl Chloride.** 20 ml of a 0.2 M solution of 3,5-dinitrobenzoyl chloride in THF was added by cannula to a nitrogen-purged Schlenk tube containing an FEP-PLL film sample. 1 ml of pyridine was added by syringe to the Schlenk tube and the solution was agitated for ~1 min. After 24 h, the solution was removed and the product film sample was washed with THF (3 x 20 ml), methanol (6 x 20 ml), THF (Soxhlet extract, 36 h), and dried (0.05 mm, >48 h). The FEP-PLL film sample was prepared by adsorbing 20 ml of a 0.1 mg/ml solution of 20k PLL to FEP at pH 11 for 24 h; the work up procedure outlined above was followed. [III86-87,100-105,118,132-4,139,142-6]

**Peel Tests** were performed on FEP and FEP-PLL film samples; the latter was prepared by adsorbing 20 ml of a 0.1 mg/ml solution of 20k PLL to an FEP film sample at pH 11 for 24 h and worked up as described above. Three 3M adhesive tapes were used: (1) 3M #850, a polyester backed acrylic adhesive, (2) 3M #750, an acetate backed acrylic

adhesive, and (3) 3M #5413, a kapton backed silicone adhesive. The adhesive tapes were applied to both film samples, FEP and FEP-PLL, concurrently and with even pressure using a roller; 100 strokes were applied before measurement. [III110-116]

**HeLa Cells** were grown in RPMI growth medium (Sigma) and provided by Dr. Rich McCarron and Prof. Bruce Jacobson. HeLa cells are human cervical carcinoma cells.

**Adhesion of HeLa Cells** was studied under the optical microscope. The number of HeLa cells reported are an average of 4 measurements made at different locations on the film sample within a grid area. A polymer film sample was equilibrated in a Petri dish containing RPMI growth medium for 30 minutes. $10^6$ HeLa cells were added and the number of cells that initially adhered to the film sample was counted under the optical microscope. The film sample was rinsed in growth medium for ~5 minutes before immersing it in fresh growth medium in a clean Petri dish. The number of cells that adhered to the film sample was recounted in a similar fashion, accounting for the final number of cells adhering to the film sample. The FEP-PLL film sample was prepared by adsorbing 20 ml of a 0.1 mg/ml solution of 20k PLL to FEP at pH 11 for 24 h; the work up procedure outlined above was followed. [III120-124, IV15-17]

**Growth of HeLa Cells.** The number of cells attached to the film sample was counted under the optical microscope and averaged over 4 different locations on the film sample. The growth medium was changed daily by sterile technique after the cells were counted. The Petri dishes containing cells and film samples were stored at 37 °C when not being counted.

**Endothelial Cells** were provided by Dr. Donna Beer and Prof. Bruce Jacobson. The endothelial cells studied were those from the aorta of a cow. The endothelial cells were grown on gelatin and then broken up and spun down with trypsin (~5 min, 37 °C). The cells were mixed with serum, spun down and then rediluted with serum.

**Growth of Endothelial Cells.** The procedure outlined for HeLa cell growth was followed; however, fresh serum was added every 3 days rather than changing the medium daily.

## Analytical Techniques

**Attenuated Total Reflectance Infrared** (ATR IR) spectra were recorded under nitrogen with an IBM 32 FTIR spectrometer and a 45° germanium internal reflection element.

**Circular Dichroism** (CD) spectra were acquired on a JASCO J-40A CD spectrometer. The film was held between 2 quartz plates and placed perpendicular to the light source; it was rotated by 90° in the same plane to ensure that the signal did not result from stresses within the film. CD spectra were an average of 10 scans.

**Dynamic Advancing and Receding Contact Angles** ($\theta_A/\theta_R$) were measured using a Ramé-Hart telescopic goniometer and a Gilmont syringe (25 gauge, flat tipped needle) with redistilled water as the probe fluid. The tangent normal to the drop at the drop-surface intersection was the angle measured as water was added ($\theta_A$) and removed ($\theta_R$) from the drop. Contact angles reported are the average of at least 5 measurements taken on different locations of the polymer film sample.

**Optical Microscopy** was done on a Nikon 802798 at 200 and 100 magnifications for HeLa and endothelial cells, respectively.

**Peel Tests** (180°) were conducted on an Instron at a peel rate of 1 cm/min. The polymer film was held stationary by the upper clamp while the tape was peeled from the film by moving the lower clamp assembly. A 2 kg load cell was used on the Instron which had been previously calibrated with a 200 g weight. (See Figure 2.1 for experimental set up.)

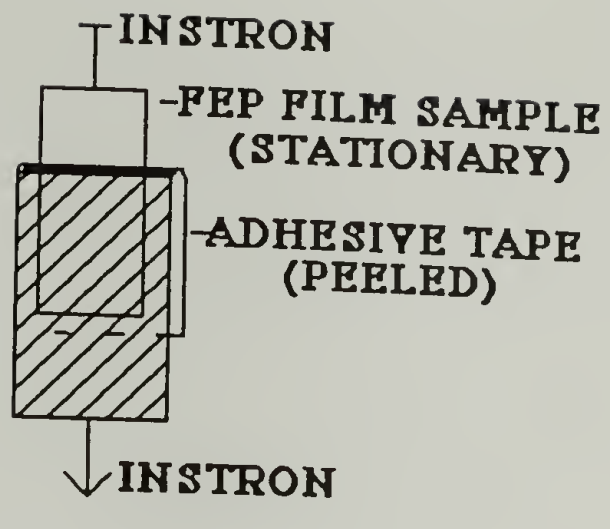


Figure 2.1 Experimental Set up for Peel Test Study.

**The pH** was checked with a Fisher 825MP pH meter that was calibrated with pH 4, pH 7 and pH 11 standard solutions (Fisher).

**Scanning Electron Micrographs** (SEM) were obtained on a JEOL 100CX at magnifications to $10^5$.

**Ultraviolet-visible** (UV-vis) spectra were recorded on a Perkin Elmer $\lambda 2$ spectrophotometer with an unreacted film sample in the reference beam.

**The Shaker Water Bath** was a Precision #25 which agitated the samples at 25 °C (120 speed).

**X-ray Photoelectron Spectra** (XPS) were recorded on a Perkin Elmer Physical Electronics 5100 spectrometer using Mg K$\alpha$ excitation at 400 W and 15 kV. Spectra were acquired at a 15° takeoff angle (between the film plane and the detector) for less than 12 minutes. A pass energy of 89.45 eV was used for survey scans whereas one of 35.75 eV was used for multiplex analysis in a chamber evacuated to less than $3.0 \times 10^{-8}$ Torr. Atomic sensitivity factors used to calculate atomic composition were $F_{1s}$, 1.000; $C_{1s}$, 0.202; $O_{1s}$, 0.540; $N_{1s}$, 0.340; and $Si_{2p}$, 0.225. The binding energies reported are not corrected for charging.

## Results and Discussion

The adsorption of PLL to FEP can be controlled by the choice of solvent, pH of the aqueous solution, PLL solution conformation, PLL molecular weight, and surface carboxylation of FEP. The latter is discussed in Chapter III. In order to discern the important driving forces for adsorption, several parameters were varied: (1) pH of the aqueous solution, (2) time of FEP and PLL interaction, (3) PLL solution concentration, (4) PLL molecular weight, and (5) solvent system. The temperature was held constant (25 °C) to avoid PLL forming the insoluble β-sheet at pH 11 and the salt concentration was not independently varied. The adsorbed FEP-PLL film samples were characterized by x-ray photoelectron spectroscopy (XPS), contact angle ($\theta_A/\theta_R$), attenuated total reflectance infrared spectroscopy (ATR IR), ultraviolet-visible spectrophotometry (UV-vis), circular dichroism spectroscopy (CD), and scanning electron microscopy (SEM). Most of the information was provided by XPS and contact angle. Figure 2.2 summarizes the adsorption experiments reported; dynamic advancing and receding contact angles are included for each surface studied.

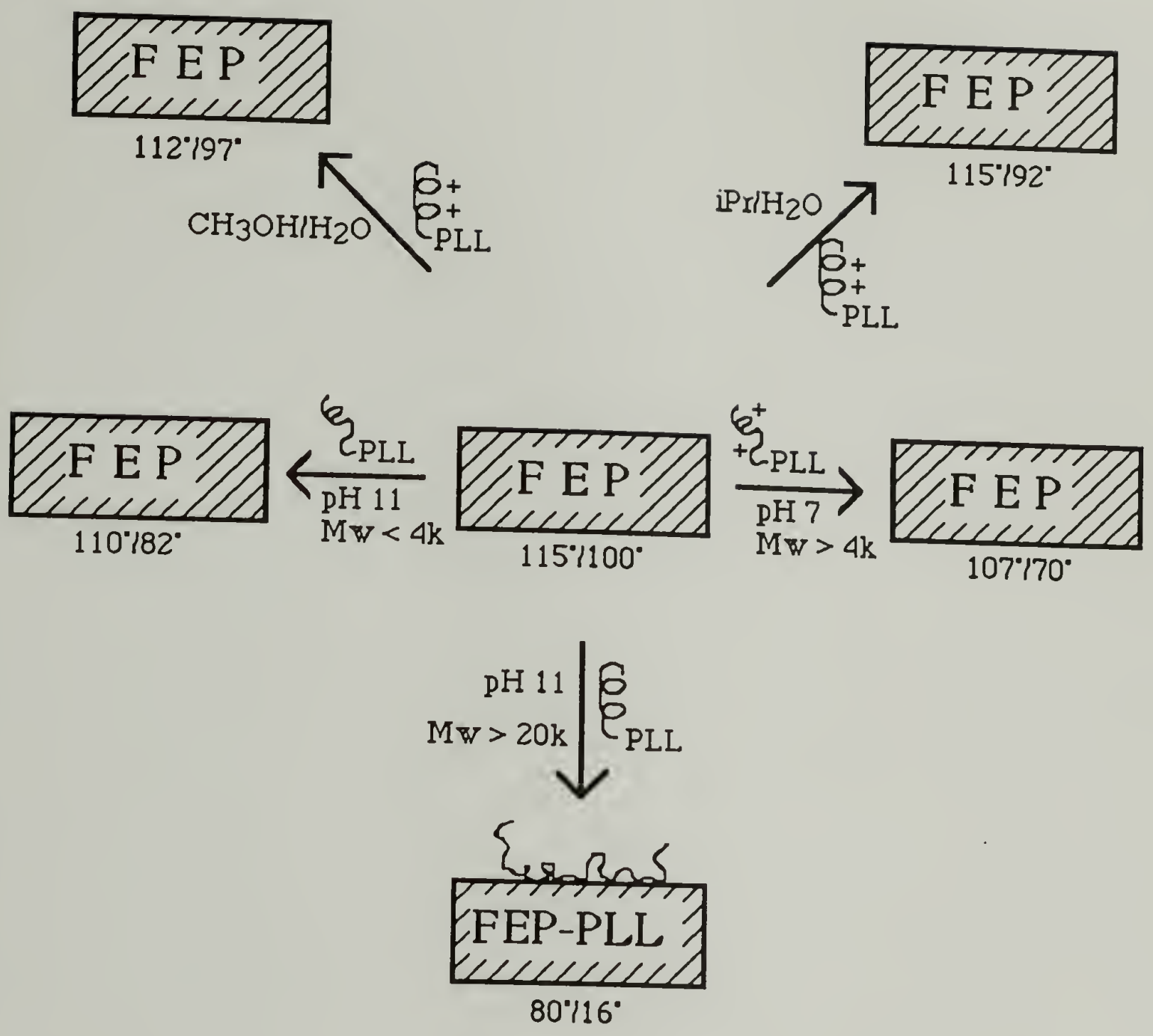


Figure 2.2 Summary of Conditions Used to Control the Adsorption of PLL to FEP with Contact Angle Data.

## FEP + PLL: pH 7 vs. pH 11

The conformation of PLL in solution was found to have a significant effect on its adsorption to FEP. PLL dissolved in doubly distilled water has a pH 7 value. Since a buffered solution was not used, charge repulsion between chain segments was not screened. The XPS and $\theta_A/\theta_R$ results for the interaction of PLL and FEP at pH 7 are expressed in Table 2.4. Little or no PLL adsorbs to FEP from a pH 7 solution in which it is highly charged and in the random coil conformation. The amount adsorbed was not

affected by time of interaction, PLL molecular weight or PLL concentration. The XPS data presented in this Chapter represents the composition of the outer ~10 Å of the film sample.[43] The XPS atomic compositions are presented in ratios of $N_{1s}/F_{1s}$ and $C_{1s}PLL/C_{1s}FEP$. The $N_{1s}$ and $C_{1s}PLL$ peak areas are representative of PLL whereas those of $F_{1s}$ and $C_{1s}FEP$ are representative of FEP of the FEP-PLL adsorbed film sample. In XPS, the electron escape energy decays exponentially with depth; these calculations assume that the electron escape energies of $F_{1s}$ and $C_{1s}$ of FEP are not decreased by any adsorbed PLL. UV-vis and ATR IR spectra taken of these film samples were indistinguishable from those of unmodified FEP.

Table 2.4 Interaction of FEP with PLL (0.1 and 1.0 mg/ml) at pH 7 for 72 h Unless Otherwise Noted.

| Sample\Technique | $\theta_A/\theta_R$ | $N_{1s}/F_{1s}$ | $C_{1s}PLL/C_{1s}FEP$ |
|---|---|---|---|
| 4k, 0.1 mg/ml | 104°/58° | 0.007 | 0.231 |
| 20k, 0.1 mg/ml (7 days) | 109°/66° | 0.007 | 0.120 |
| 60k, 0.1 mg/ml | 112°/82° | 0.001 | 0.05 |
| 400k, 0.1 mg/ml (7 days) | 107°/70° | 0.012 | 0.114 |
| 20k, 1.0 mg/ml | 116°/88° | 0.018 | 0 |
| 400k, 1.0 mg/ml | 112°/76° | 0 | 0 |
| $H_2O$ (Control) | 119°/94° | 0 | 0 |

XPS and contact angle results indicate that little or no PLL adsorbs to FEP from the pH 7 solution where it is charged and in the random coil conformation. A non-specific interaction between trace FEP oxygen and PLL may account for the minimal adsorption

observed. Silicone grease that is used on vacuum lines is likely the source of silicon contamination that was observed on some samples. Both the $O_{1s}$ and $C_{1s}$ peak areas are enlarged by silicone contamination. For this reason, the $O_{1s}/F_{1s}$ ratio was not used to compare the amount of PLL adsorbed; the $C_{1s}PLL/C_{1s}FEP$ ratio occasionally indicates that more PLL has adsorbed than does the $N_{1s}/F_{1s}$ ratio. Because silicone contamination does not affect the $N_{1s}/F_{1s}$ XPS atomic composition ratio, $N_{1s}/F_{1s}$ is representative of the relative amount adsorbed and is used in the figures of both this Chapter and those of Chapter III.

PLL adsorbs to FEP from a pH 11 solution in which it is neutral and in the rod-like $\alpha$-helix conformation. Unlike the pH 7 solution, the pH 11 solution was buffered (0.05 M sodium bicarbonate). The adsorption of PLL to FEP at pH 11 was studied by XPS and $\theta_A/\theta_R$. The effects of time of interaction, PLL concentration, and PLL molecular weight on the amount of PLL adsorbed to FEP were assessed. Figure 2.3 shows representative XPS spectra of FEP-PLL prepared by adsorbing PLL to FEP from pH 11 (a) and pH 7 (b) solutions. As was mentioned previously, PLL was evident by XPS peaks of $N_{1s}$ (403 eV) and $O_{1s}$ (536 eV) and low binding energy (LBE) $C_{1s}$ whereas FEP by XPS peaks of $F_{1s}$ and high binding energy $C_{1s}$. A comparison of the amount of PLL adsorbed to FEP was done using XPS $N_{1s}/F_{1s}$ and $C_{1s}PLL/C_{1s}FEP$ ratios. The XPS data is best summarized graphically with the $N_{1s}/F_{1s}$ XPS atomic concentration ratio representing the relative amount of PLL adsorbed to FEP.

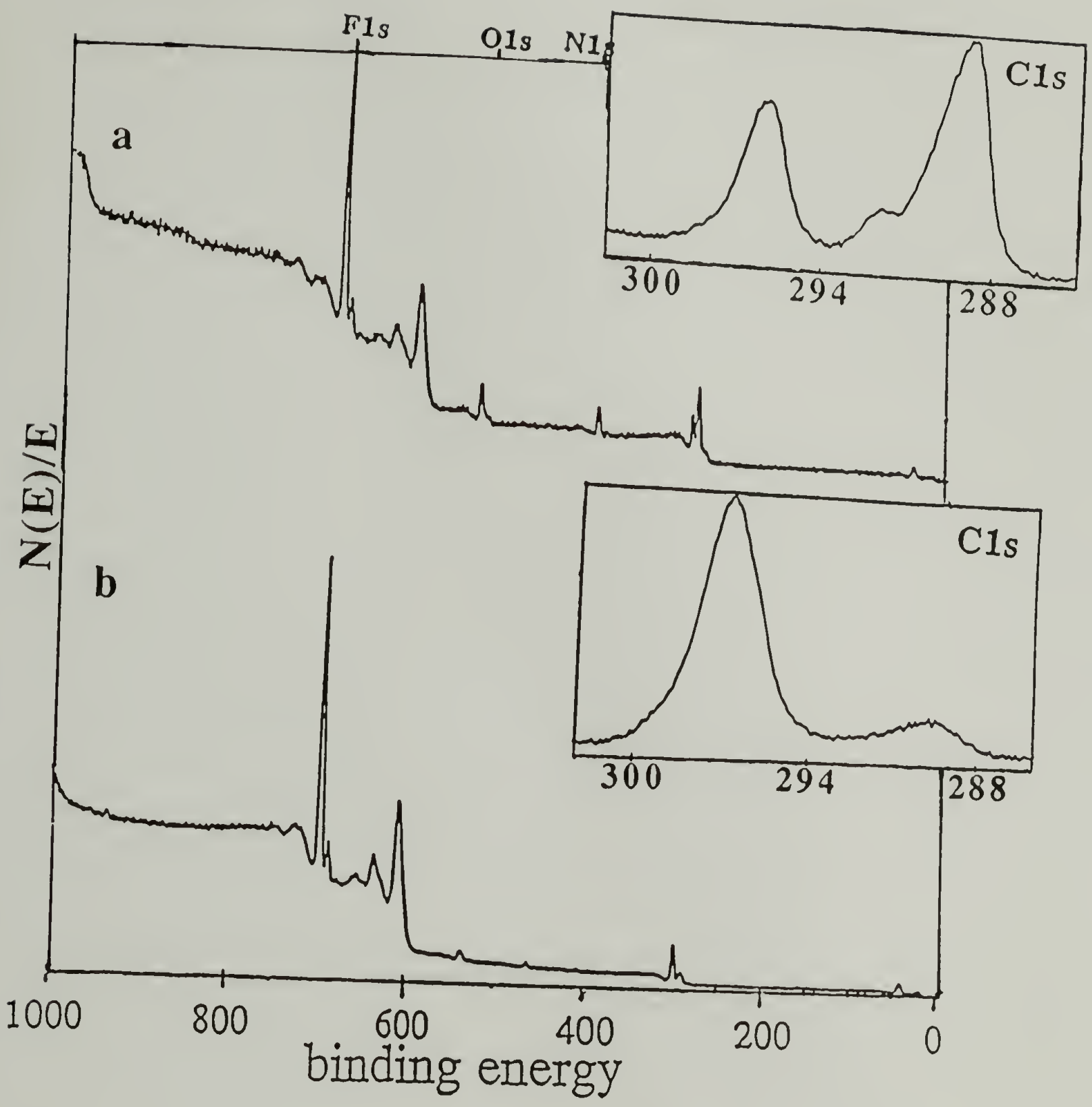


Figure 2.3 XPS Survey and $C_{1s}$ (15° takeoff angle) Spectra of (a) FEP-PLL (pH 11) and (b) FEP + PLL (pH 7).

The effect of time of interaction (Figure 2.4, Table 2.5) was first assessed in order to determine the time at which a plateau in adsorbed amount was reached; concentration

was held constant at 0.1 mg/ml and molecular weight at either 400k or 20k. Further studies on the effect of PLL molecular weight and concentration were done at 72 h.

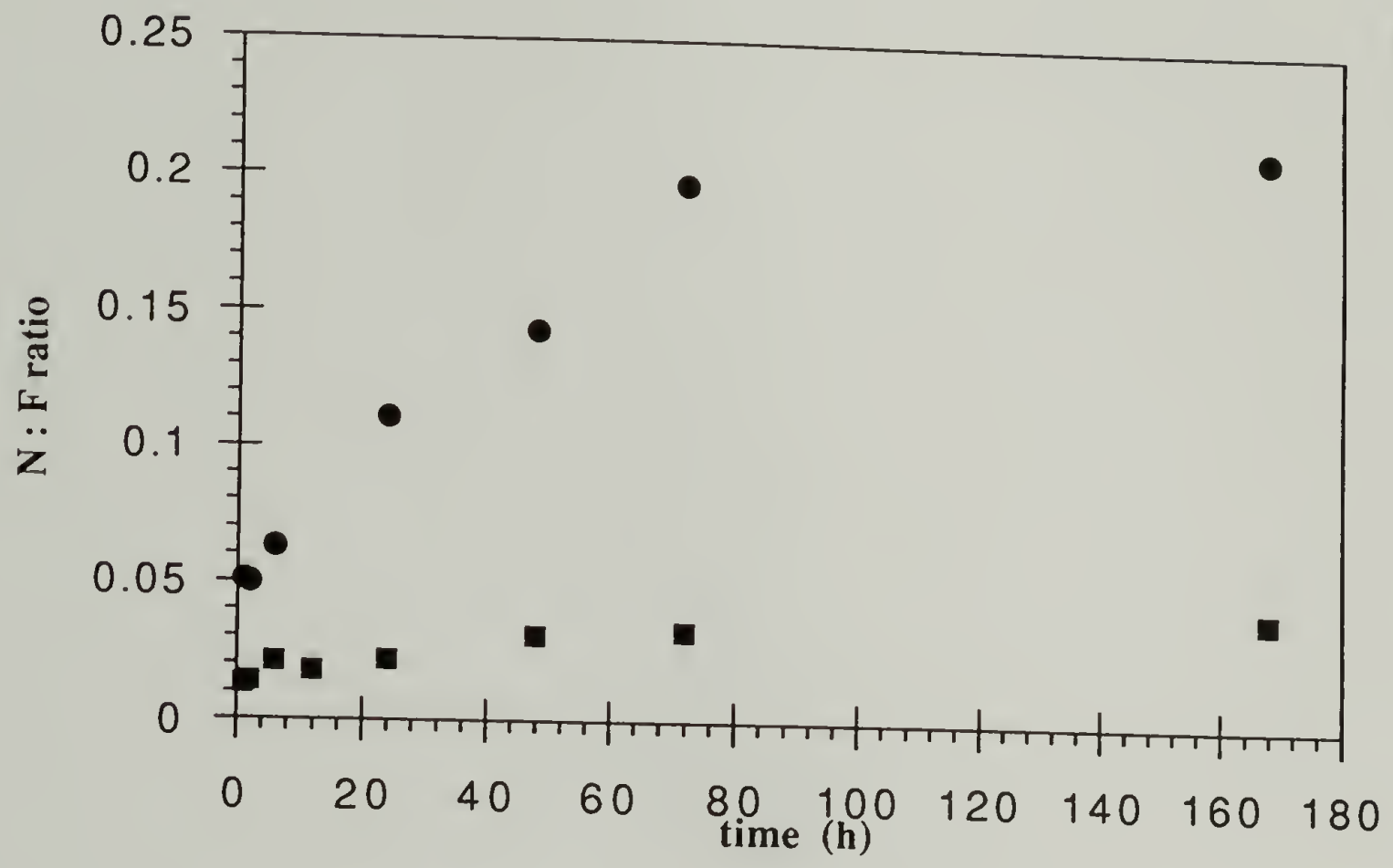


Figure 2.4 Adsorbance of PLL to FEP as a Function of Time for PLL (●) 400k and (■) 20k at pH 11.

Table 2.5 XPS Data Describing the Effect of Time on the Adsorption of PLL to FEP:
(a) 20k, 0.1 mg/ml; [III72,80]

| Time (h) | $C_{1s}$ PLL/$C_{1s}$ FEP | $N_{1s}/F_{1s}$ | C : F : O : N |
|---|---|---|---|
| 1 | 0.13 | 0.013 | 100 : 156 : 5 : 2 |
| 2 | 0.18 | 0.014 | 100 : 148 : 4 : 2 |
| 6 | 0.27 | 0.021 | 100 : 139 : 5 : 3 |
| 12 | 0.24 | 0.018 | 100 : 136 : 5 : 2 |
| 24 | 0.39 | 0.022 | 100 : 134 : 8 : 4 |
| 48 | 0.47 | 0.031 | 100: 125 : 9 : 4 |
| 72 | 0.55 | 0.033 | 100 : 117 : 9 : 4 |
| 168 | 0.49 | 0.040 | 100 : 111 : 8 : 4 |

(b) 400k, 0.1 mg/ml. [III81, 86-87]

| Time (h) | $C_{1s}$ PLL/$C_{1s}$ FEP | $N_{1s}/F_{1s}$ | C : F : O : N |
|---|---|---|---|
| 1 | 0.65 | 0.051 | 100 : 109 : 8 : 5 |
| 2 | 1.00 | 0.050 | 100 : 93 : 9 : 5 |
| 6 | 0.76 | 0.063 | 100 : 101 : 7 : 6 |
| 24 | 1.19 | 0.110 | 100 : 85 : 8 : 9 |
| 48 | 1.90 | 0.143 | 100 : 71 : 10 : 10 |
| 72 | 1.91 | 0.197 | 100 : 65 : 10 : 13 |
| 168 | 2.62 | 0.211 | 100 : 47 : 13 : 14 |

The amount of PLL that adsorbed to FEP increased over time reaching a plateau level by 72 h. The shape of the curve is more rounded and the time to reach a plateau level

is longer than what is normally observed for high affinity systems involving a neutral, monodisperse polymer adsorbing to a neutral substrate. The rounded adsorption curve and extended time to reach a plateau level may result from polydispersity effects.[44] Since PLL is not monodisperse, PLL segments of different molecular weights likely compete for surface sights, with the large molecules adsorbing preferentially over the smaller ones. Papenhuijzen *et al.* argued that the rounded curve may result from the slow establishment of equilibrium in the system.[45] Polydispersity and "equilibrium" effects may affect the adsorbance of PLL to FEP. At the plateau level, adsorption of PLL to FEP was time-independent.

The effect of PLL concentration over time was next assessed using 400k polymer dissolved in pH 11 buffer solution. At pH 11, high molecular weight (400k) PLL spontaneously forms the β-sheet at room temperature,[33] precipitating out of solution.[46] In these experiments, high molecular weight PLL in the α-helix conformation was observed to be stable in solution for 7 days at concentrations less than 1 mg/ml. Figure 2.5 plots the $N_{1s}/F_{1s}$ XPS ratio for PLL adsorbed to FEP using PLL solution concentrations of 0.001, 0.01 and 0.1 mg/ml. (See also Table 2.6 (a) 0.01 mg/ml and (b) 0.001 mg/ml and Table 2.5 (b) 0.1 mg/ml for more information.) An increased amount of PLL adsorbs to FEP at higher concentrations, indicating that PLL adsorption to FEP is concentration-dependent. The rounded curves and concentration-dependent adsorption indicate that the FEP surface interacts weakly with PLL segments.

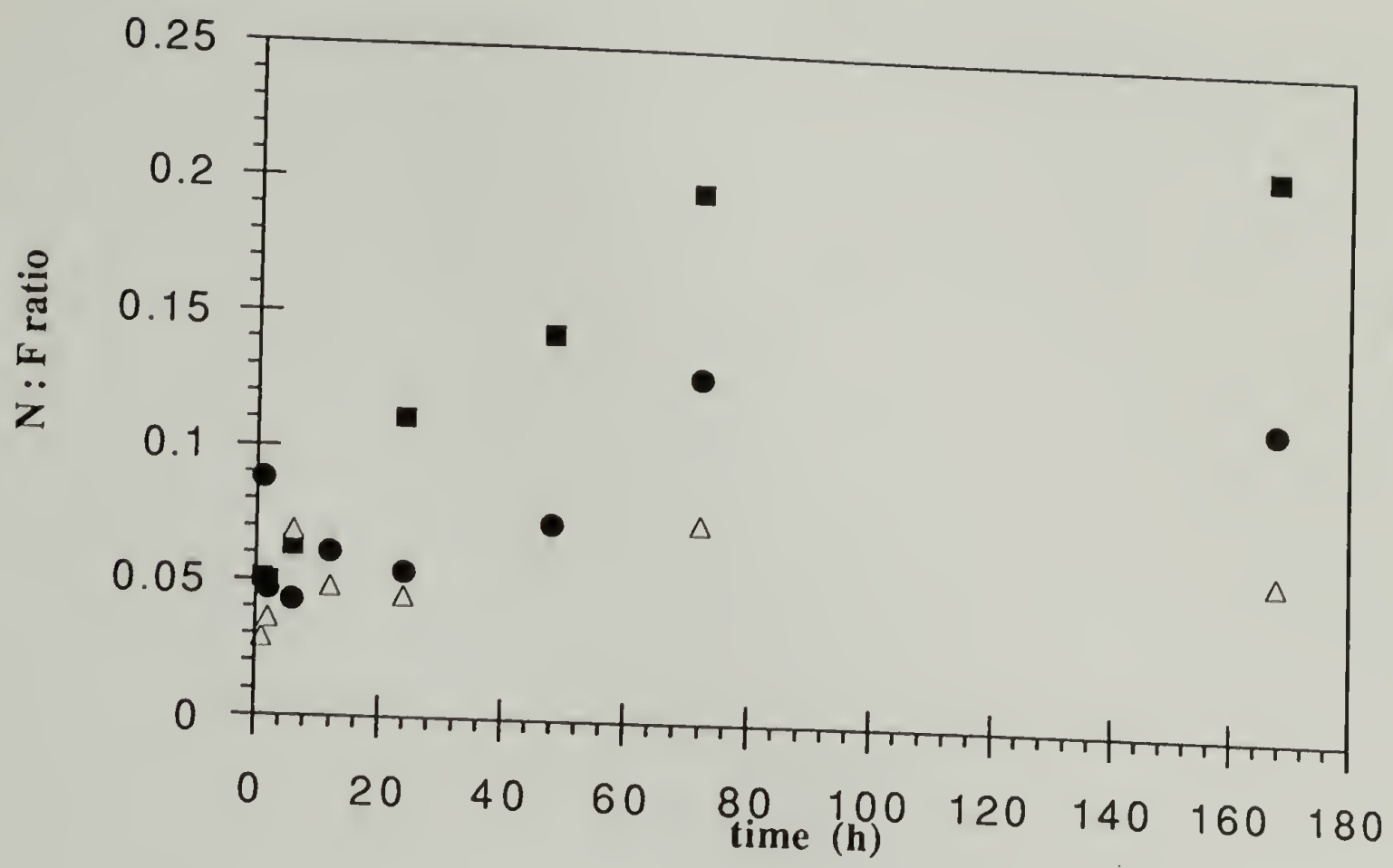


Figure 2.5 Effect of Concentration and Time on the Adsorbed Layer Thickness (PLL, 400k) at (■) 0.1 mg/ml, (●) 0.01 mg/ml, and (△) 0.001 mg/ml.

Table 2.6 Adsorption of 400k PLL to FEP at pH 11 at [III90, 96]
(a) PLL concentration of 0.01 mg/ml;

| Time (h) | $C_{1s}$ PLL/$C_{1s}$ FEP | $N_{1s}/F_{1s}$ | C : F : O : N |
|---|---|---|---|
| 1 | *1.348 | 0.088 | 100 : 94 : 17 : 8 |
| 2 | *0.740 | 0.047 | 100 : 120 : 13 : 6 |
| 6 | 0.627 | 0.043 | 100 : 113 : 10 : 5 |
| 12 | 1.264 | 0.061 | 100 : 105 : 15 : 7 |
| 24 | 0.763 | 0.054 | 100 : 117 : 10 : 6 |
| 48 | 0.993 | 0.073 | 100 : 92 : 10 : 7 |
| 72 | 1.751 | 0.128 | 100 : 70 : 14 : 9 |
| 168 | 1.657 | 0.116 | 100 : 74 : 12 : 9 |

(b) PLL concentration of 0.001 mg/ml.

| Time (h) | $C_{1s}$ PLL/$C_{1s}$ FEP | $N_{1s}/F_{1s}$ | C : F : O : N : Si |
|---|---|---|---|
| 1 | 0.538 | 0.029 | 100 : 147 : 12 : 5 |
| 2 | 0.594 | 0.036 | 100 : 146 : 10 : 5 |
| 6 | 1.299 | 0.069 | 100 : 108 ; 16 : 8 |
| 12 | 0.784 | 0.048 | 100 : 128 : 13 : 6 |
| 24 | 0.802 | 0.045 | 100 : 128 : 13 : 6 |
| 72 | 1.110 | 0.074 | 100 : 86 : 14 : 6 |
| 168 | 1.125 | 0.059 | 100 : 110 : 20 : 6 |

*Unusual silicon contamination was observed on these samples, likely skewing the $C_{1s}$PLL/$C_{1s}$FEP ratio high.

The effect of PLL molecular weight on the amount adsorbed to FEP was studied while concentration (0.1 mg/ml) and time of interaction (72 h) were held constant. Figure 2.6 and Table 2.7 summarize the XPS and contact angle data. The PLL adsorbed layer thickness (i.e. $N_{1s}/F_{1s}$ ratio) increased with PLL molecular weight, indicating that adsorption of neutral PLL to neutral FEP was molecular weight-dependent. Molecular weight-dependence is commonly observed in adsorption experiments involving a neutral polymer and a neutral substrate; such dependence is indicative of a weak adsorbent-adsorbate interaction.[47] In a system where the interactions between segment and substrate are weak, the entropy of the system dominates the interaction. Higher molecular weight polymers can form loops and tails more readily than lower molecular weight polymers. Molecular weight-dependent adsorption is often observed for near-theta or theta solvents. Although PLL dissolves readily in water at pH 7, its solubility in water decreases as it is deprotonated; pH 11 buffer is likely a near-theta solvent for PLL. Low molecular weight PLL (4k) does not adsorb to FEP from a pH 11 solution. Low molecular weight PLL is unable to form the α-helix at pH 11[30] which likely affects its ability to adsorb to FEP. The contact angle data reflect the trends observed in the XPS spectra. That the receding contact angle ($\theta_R$) decreases more substantially than the advancing contact angle ($\theta_A$), indicates a heterogeneous surface of low PLL concentration.

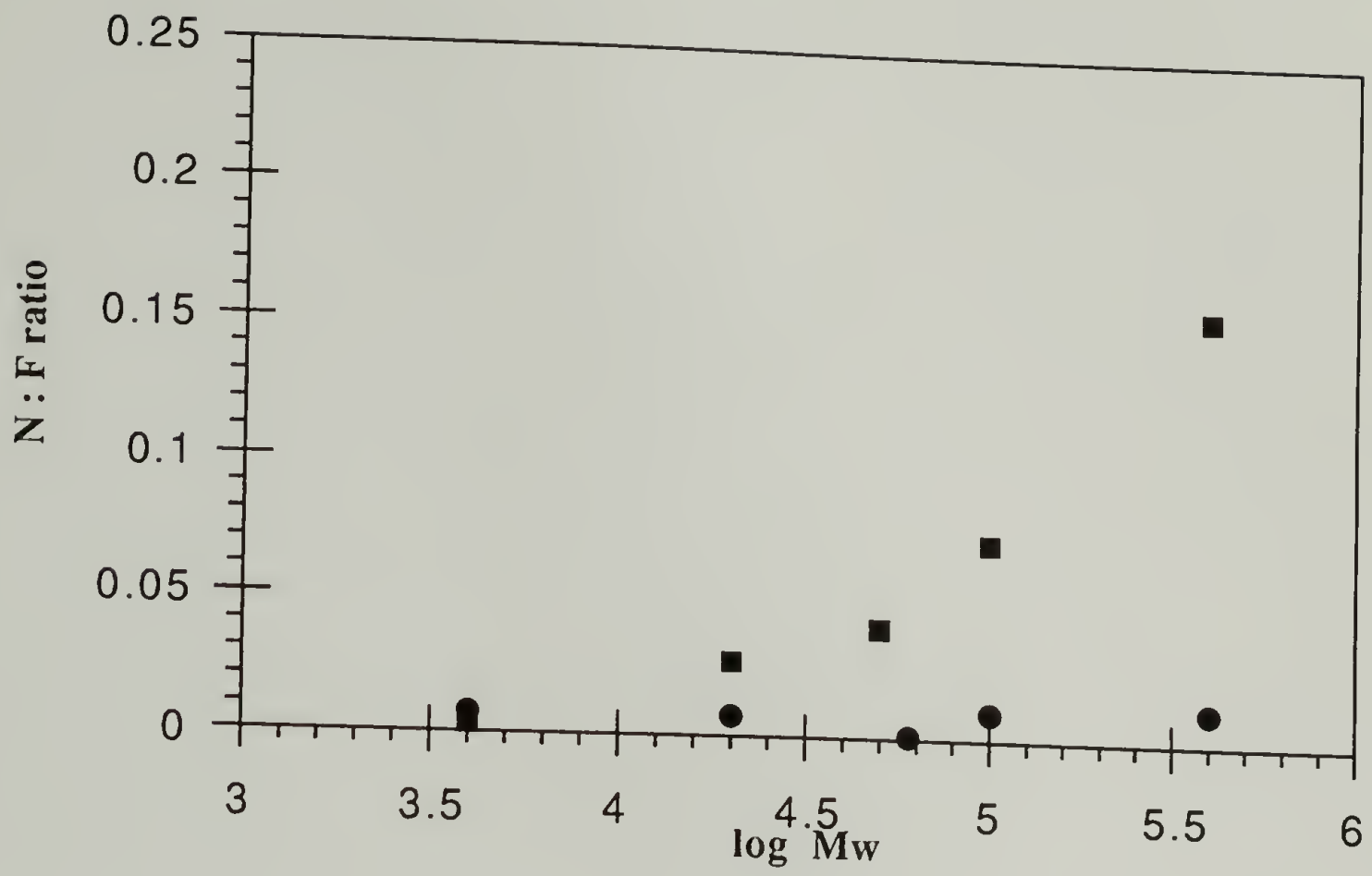


Figure 2.6 Effect of Molecular Weight of PLL on the Adsorbed Layer Thickness at (■) pH 11 and (●) pH 7.

Table 2.7 Effect of PLL Molecular Weight on Adsorption to FEP: XPS and Contact Angle Data. [III82]

| Mw | $C_{1s}$ PLL / FEP | $N_{1s}/F_{1s}$ | C : F : O : N | $\theta_A/\theta_R$ |
|---|---|---|---|---|
| 4k | 0.12 | 0.003 | 100 : 209 : 6 : 1 | 110°/82° |
| 20k | 0.55 | 0.027 | 100 : 116 : 9 : 3 | 107°/22° |
| 50k | 0.55 | 0.040 | 100 : 150 : 8 : 7 | 104°/19° |
| 100k | 0.87 | 0.072 | 100 : 139 : 9 :10 | 96°/15° |
| 400k | 1.91 | 0.156 | 100 : 67 : 10 :10 | 80°/16° |

An attempt to discern the adsorbed layer conformation was made. XPS is not useful in either determining the conformation or differentiating the morphology -- discrete islands vs. smooth monolayer -- of the adsorbed layer. However, the adsorbed layer thickness was calculated from the XPS $C_{1s}$ PLL and $C_{1s}$ FEP data;[48] the thickest PLL layer observed was ~5.5 Å for 400k PLL.[43] Unfortunately, high resolution SEM did not furnish any details on the adsorbed layer morphology because the FEP and FEP-PLL film samples could not be distinguished at the resolution of SEM (to ~50 Å). The adsorbed layer conformation can be inferred from ATR IR spectra of FEP-PLL films. ATR IR spectra of FEP-PLL film samples show characteristic amide I and amide II vibrational bands for both α-helix and random coil PLL.[49] In Figure 2.7, the ATR IR spectra of FEP and FEP-PLL are compared: the amide I peaks, 1649 $cm^{-1}$(α-helix), 1657 $cm^{-1}$(random coil) and amide II peak, 1547 $cm^{-1}$(α-helix) indicate that PLL at least partially unfolded from the α-helix upon adsorption. ATR IR was of limited utility because only high molecular weight PLL samples gave a signal intensity useful for analysis. The CD spectra of FEP-PLL indicated that the surface conformation of PLL was predominantly disordered.[50]

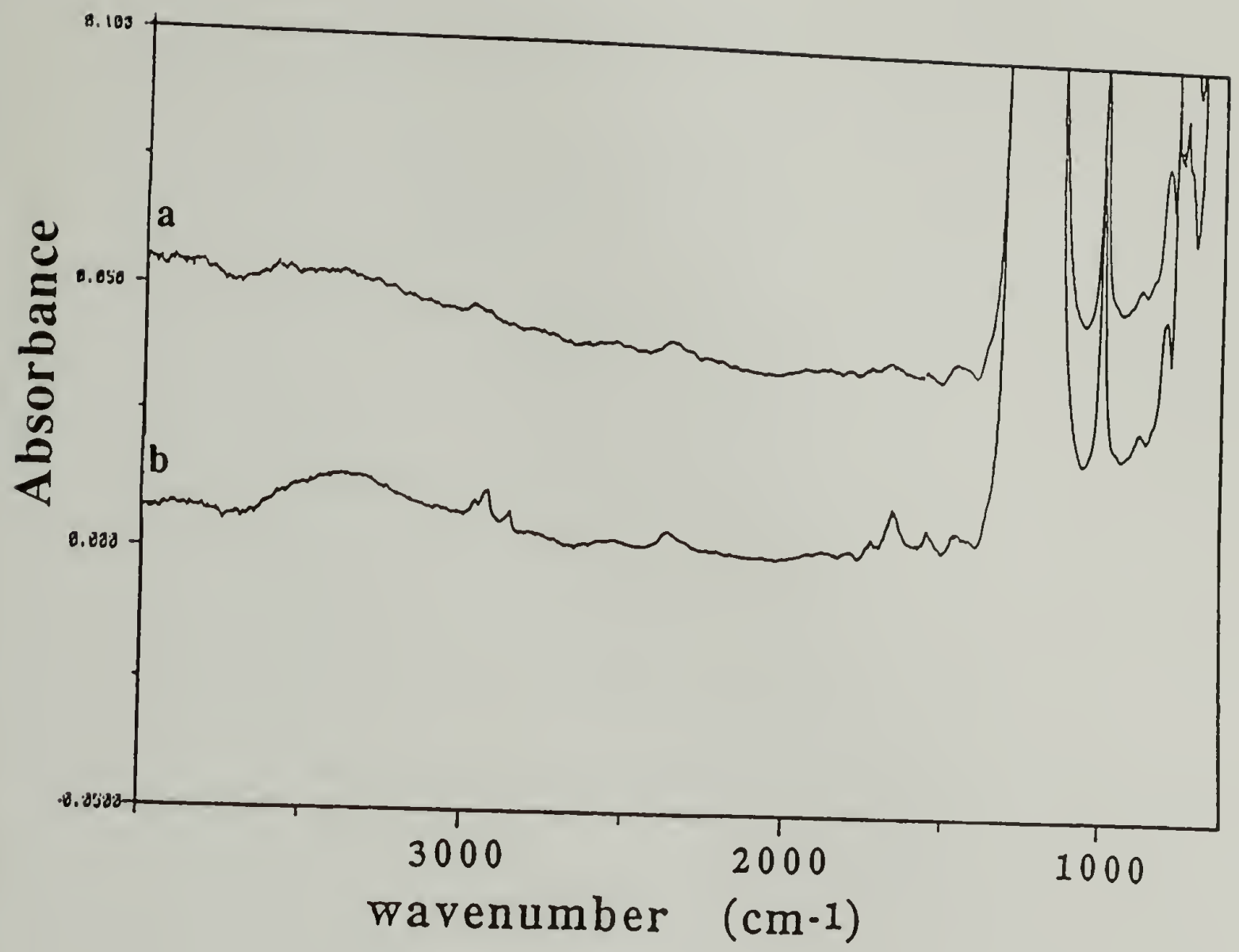


Figure 2.7 ATR IR Spectra of (a) FEP and (b) FEP-PLL (400k; pH 11).

The driving forces for PLL adsorption to FEP are complex. Adsorption of PLL to FEP at pH 11 occurs as a result of both (1) the high interfacial free energy between aqueous PLL and organic FEP and (2) at least partial unfolding of the α-helix. By adsorbing at the FEP-water interface, PLL lowers the interfacial free energy; by unfolding from the α-helix conformation, PLL regains some conformational entropy. PLL adsorption to FEP is concomitant with the release of water molecules from the interface which is entropically favorable. The segment-substrate interaction was enhanced at pH 11,

with respect to pH 7, whereas the solvent-segment interaction was decreased. In a similar study, Panitz[51] found that PLL adsorbed to tungsten at high pH but not at neutral pH. PLL did not adsorb to FEP from the pH 7 solution where it is highly charged and disordered. The high interfacial free energy at the FEP-water interface was an insufficient driving force for adsorption. At pH 7, PLL is already "unfolded" and cannot further unfold upon adsorption.

Neutral PLL interacts more favorably with FEP than highly charged PLL; α-helix PLL interacts hydrophobically with FEP whereas the charged random coil PLL does not. Due to its high charge density, PLL at pH 7 interacts more favorably with the polar aqueous environment. Neutral PLL at pH 11 adsorbs to FEP only from the α-helix solution conformation. 4k molecular weight PLL does not adsorb to FEP from a pH 11 solution; the inability of low molecular weight PLL to form the α-helix conformation renders its adsorption to FEP unfavorable. Alternatively, it could be argued that 4k PLL does not adsorb to FEP from a pH 11 solution because polymer adsorption was molecular weight dependent.

In a recent study by Bonekamp,[52] the adsorptions of P(L)L and P(DL)L were compared at the polystyrene sulfonate (PSS) - water interface. The configuration of the polymer did not affect the amount of poly(lysine) adsorbed at pH 11; however, the solution conformation dictated the adsorbed conformation. When adsorbed from a high solution concentration, P(L)L extended both along the interface in trains and from the interface in tails where the α-helix conformation existed. Based on this argument, it is likely that partial unfolding of the α-helix occurred upon adsorption. Conversely, at low poly(lysine) concentration, α-helix formation is unlikely to persist after adsorption due to spreading of the polymer at the interface.

## FEP + PLL: $MeOH/H_2O$ or $iPrOH/H_2O$ [III88-9]

Given that PLL adsorbs to FEP from the α-helix and not from the random coil conformation, the effect of PLL solution conformation on adsorption was further investigated. High molecular weight PLL was dissolved in one of two aqueous/alcohol solutions in which PLL is known to form a charged α-helix.[53] The solutions used were methanol/water (96:4, v/v) and isopropanol/water (82:18, v/v). From XPS and contact angle analysis, (Table 2.9), it is evident that PLL did not adsorb to FEP from either solution. The interaction of 500k PLL with FEP was investigated over a broad time range, 1 - 192 h, and at two concentrations, 0.5 mg/ml and 0.1 mg/ml. Adsorption was not observed regardless of concentration or time of interaction.

Table 2.8 Interaction of PLL (0.1 mg/ml, 24 h) with FEP from Aqueous Alcohol Solutions: XPS and Contact Angle Data.

| Sample | $C_{1s}$ PLL/$C_{1s}$ FEP | $N_{1s}/F_{1s}$ | $\theta_A/\theta_R$ |
|---|---|---|---|
| PLL ($MeOH/H_2O$) | 0 | 0 | 112°/97° |
| PLL ($iPrOH/H_2O$) | 0 | 0 | 115°/92° |

PLL did not adsorb from the α-helix conformation to FEP from either the $MeOH/H_2O$ or $iPrOH/H_2O$ solutions. Both aqueous/alcohol solutions wet the FEP film sample better than water exhibiting contact angles on FEP of 75°/70° (methanol/water) and 48°/40° (isopropanol/water) which are both significantly lower than that of water, 115°/100°. This underlines the importance of the high interfacial free energy as a driving force for adsorption in the FEP-PLL system (pH 11). PLL did not adsorb to FEP from aqueous alcohol solutions because the interfacial free energy was reduced, diminishing its

effect as a driving force for adsorption. Alternatively, PLL may not have adsorbed to FEP from either aqueous alcohol solutions because adsorption would involve that of a charged molecule to a neutral substrate. The electrostatic effect opposes the accumulation of a charged polyelectrolyte.[54]

## Properties of FEP-PLL

### Wettability

FEP-PLL, unlike FEP, has diverse surface properties, such as wettability, chemical reactivity, and adhesion. The FEP-PLL film sample shows improved wetting: the water contact angle of FEP, 115°/100°, decreases with PLL (400k) adsorption to 80°/16° for FEP-PLL. The large hysteresis between advancing and receding contact angles reflects the small percentage of PLL surface coverage on FEP. Typically, the advancing contact angle is indicative of the hydrophobic (FEP) and the receding contact angle of the hydrophilic (PLL) constituents on a chemically heterogeneous surface.[55] A low percentage of hydrophilic moieties affects the receding more than the advancing contact angle.[56] The water contact angle for FEP + PLL (400k) adsorbed from pH 7 solution is 107°/70°. The relatively high receding contact angle indicates that an insignificant amount of PLL adsorbs to FEP at pH 7 with respect to that at pH 11.

### Solvent Stability of the Adsorbed Layer

The stability of the adsorbed FEP-PLL film sample to different solvents was assessed by immersing the film sample in a particular solvent for a specified length of time. The FEP-PLL film sample was prepared by adsorbing 20 ml of a 0.5 mg/ml solution of 20k PLL at pH 11 for 6 h to FEP. The solvents that were used are described in Table 2.10

along with the XPS data. To test irreversible adsorption, the adsorbent solution is replaced with pure solvent. When the PLL solution was replaced with pure pH 11 buffered solution (3rd entry); the adsorbed amount changed insignificantly indicating irreversible adsorption. PLL adsorbed from pH 11 was not displaced by water; however, recall that PLL did not adsorb from water (pH 7). Water was unable to displace PLL because it was energetically more favorable for PLL than water to be at the FEP surface. Methylene chloride and ethanol[57] wet FEP better than water yet were unable to displace PLL from FEP; this may have resulted, in part, from PLL's insolubility in these solvents. The FEP-PLL adsorbed layer was stable to different work-up conditions: water, pH 11, ethanol, and methylene chloride. The segment-substrate interaction was greater than that of the solvent-substrate. Although none of the solvents used in this study were able to displace PLL from FEP, a solvent with both a higher affinity for FEP and capable of dissolving PLL, may be able to displace PLL.

Table 2.9 Stability of the Adsorbed FEP-PLL Film Sample to Different Solvents.

| Solvent | $C_{1s}PLL/C_{1s}FEP$ | $N_{1s}/F_{1s}$ | C : F : O : N |
|---|---|---|---|
| none | 0.295 | 0.019 | 100 : 152 : 10 : 3 |
| $ddH_2O$ (3 x 20 ml) | 0.350 | 0.016 | 100 : 122 : 8 : 2 |
| pH 11 (3 x 20 ml) | 0.274 | 0.017 | 100 : 124 : 6 : 2 |
| $ddH_2O$; 24 h; still | 0.291 | 0.035 | 100 : 118 : 7 : 4 |
| $ddH_2O$; 24 h; shake | 0.378 | 0.023 | 100 : 110 : 8 : 3 |
| $C_2H_5OH$; 42 h | 0.192 | 0.020 | 100 : 129 : 5 : 3 |
| $CH_2Cl_2$ (3 x 20 ml) | 0.209 | 0.021 | 100 : 125 : 9 : 3 |

Chemical Reactivity of FEP-PLL

To investigate whether the adsorbed PLL layer on FEP could be used for further chemical modification, the chemical reactivity of the ε-amine functional group of PLL was studied. Several reagents were tried including 5-dimethylamino-1-naphthalene-sulfonyl chloride (dansyl chloride),[58] trichloroacetyl chloride, and fluorescein isothiocyanate;[59] however, the best results were achieved with 3,5-dinitrobenzoyl chloride (Scheme 2.1).

FEP-PLL + 3,5-Dinitrobenzoyl Chloride

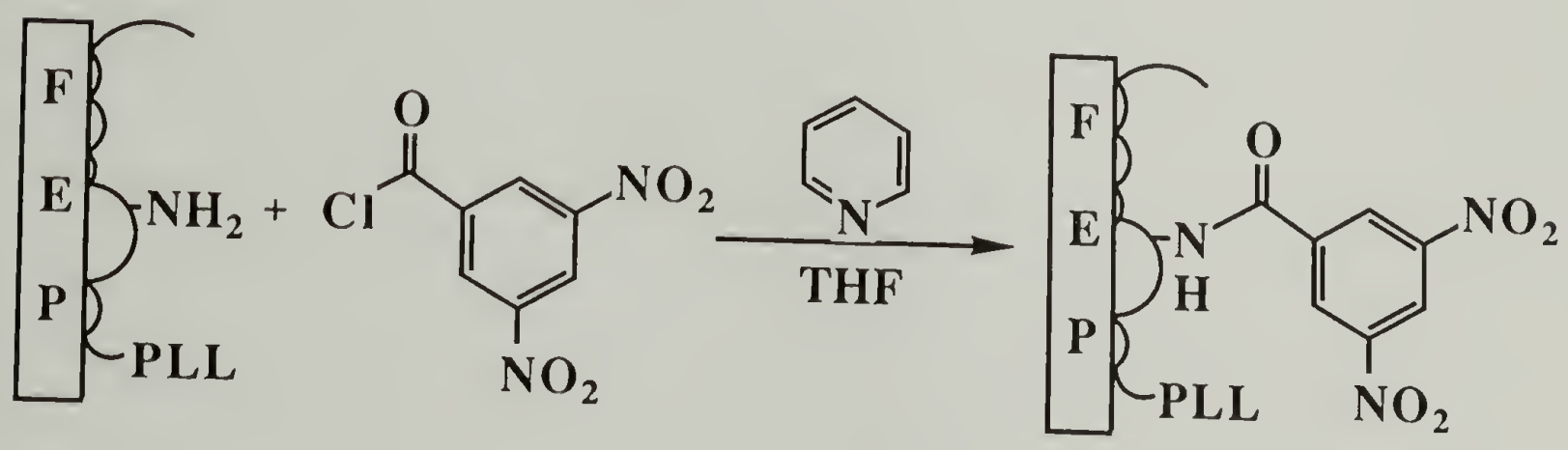


Scheme 2.1 Reaction of FEP-PLL with 3,5-Dinitrobenzoyl Chloride.

The pendant ε-amine group of PLL on FEP-PLL reacts with the 3,5-dinitrobenzoyl chloride to form FEP-PLL-3,5-dinitrobenzamide (FEP-PLL-3,5-DNBA). The reaction between amine and acid chloride required pyridine catalysis.[60] Because THF swelled FEP, the product was exposed to a prolonged work up procedure to remove any reagent that may have diffused into the polymer film sample. FEP-PLL was prepared by adsorbing 20 ml of a 0.1 mg/ml solution of 20k PLL to FEP at pH 11 for 24 h. In Table 2.11, XPS, UV-vis and contact angle data are summarized for FEP-PLL-3,5-DNBA. The XPS survey, $C_{1s}$, and $N_{1s}$ spectra are included in Figure 2.8. The UV-vis spectrum is shown in Figure 2.9.

Table 2.10 XPS, UV-vis, and Contact Angle Data for the Reaction between FEP-PLL and 3,5-Dinitrobenzoyl Chloride.

| Sample | $C_{1s}$PLL/FEP | $N_{1s}/F_{1s}$ | $NO_2/NH_2$ | UV-vis A (210 nm) | $\theta_A/\theta_R$ |
|---|---|---|---|---|---|
| FEP-PLL (pH 11) | 1.09 | 0.037 | 0.67 | 0.018 | 110°/52° |
| FEP + PLL (pH 7) | 0.04 | 0.007 | * | 0.005 | 115°/81° |
| FEP | 0 | 0 | 0 | 0 | 118°/99° |

*too low for accurate measurement

The chemical reactivity of FEP is enhanced by PLL adsorption because FEP is inert to the reaction conditions whereas PLL reacts with 3,5-DNBC. Adsorbed PLL serves as a reactive handle on FEP for further chemical reaction. (This concept was introduced in Chapter I with carboxylic acid functionalized film samples.) XPS provided quantitative information. The aromatic carbons of 3,5-DNBA contribute to the low binding energy $C_{1s}$ peak, thereby increasing the $C_{1s}$PLL/$C_{1s}$FEP ratio from 0.39 (Table 2.5) to 1.09. The $NO_2$ functionality of 3,5-DNBA contributes to the $N_{1s}$ peak area, increasing the $N_{1s}/F_{1s}$ ratio from 0.022 (Table 2.5) to 0.037 by reaction of PLL with 3,5-DNBC. By comparing the XPS $N_{1s}$ peak area ratio of $NO_2$ (3,5-DNBA) to that of $NH_2$ (PLL), the yield of the labeling reaction was determined as 67%. The yield (ratio) lends insight into the adsorbed PLL conformation in which ~1/3 of the pendant ε-amine groups of PLL groups were unable to access the acid chloride for reaction. These amine groups were possibly involved in either hydrogen-bonding or hydrophobic interactions with FEP which made them inaccessible for reaction with 3,5-DNBC. This reaction was an interesting technique to understand the adsorbed conformation.

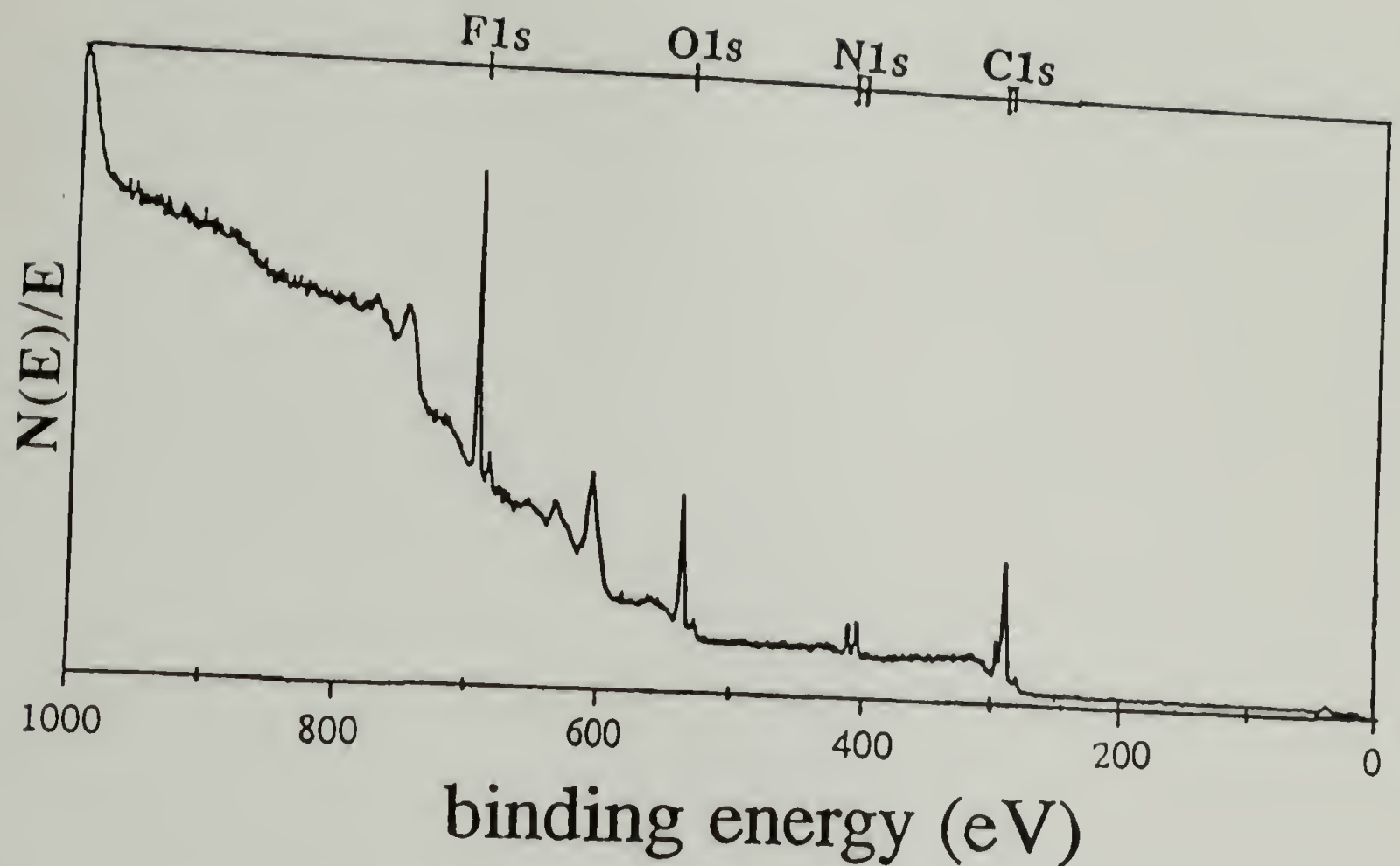


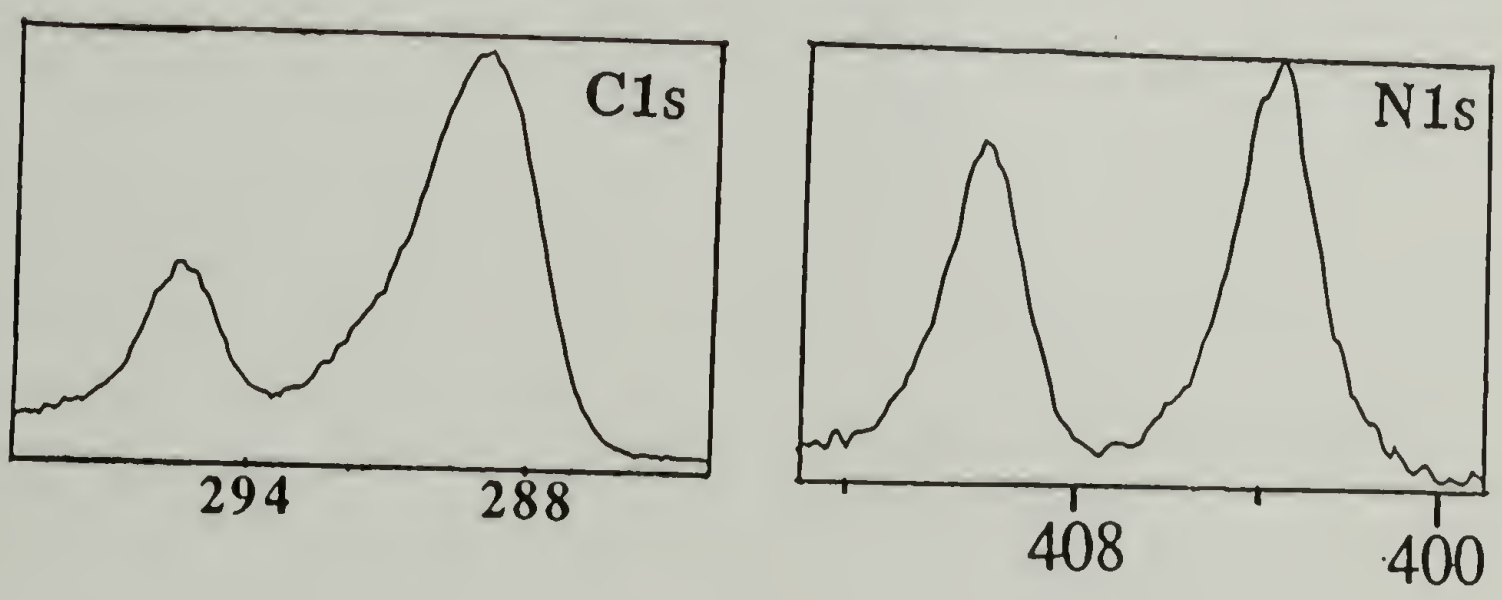


Figure 2.8 XPS Survey, $C_{1s}$, and $N_{1s}$ (15° takeoff angle) Spectra of FEP-PLL-3,5-Dinitrobenzamide.

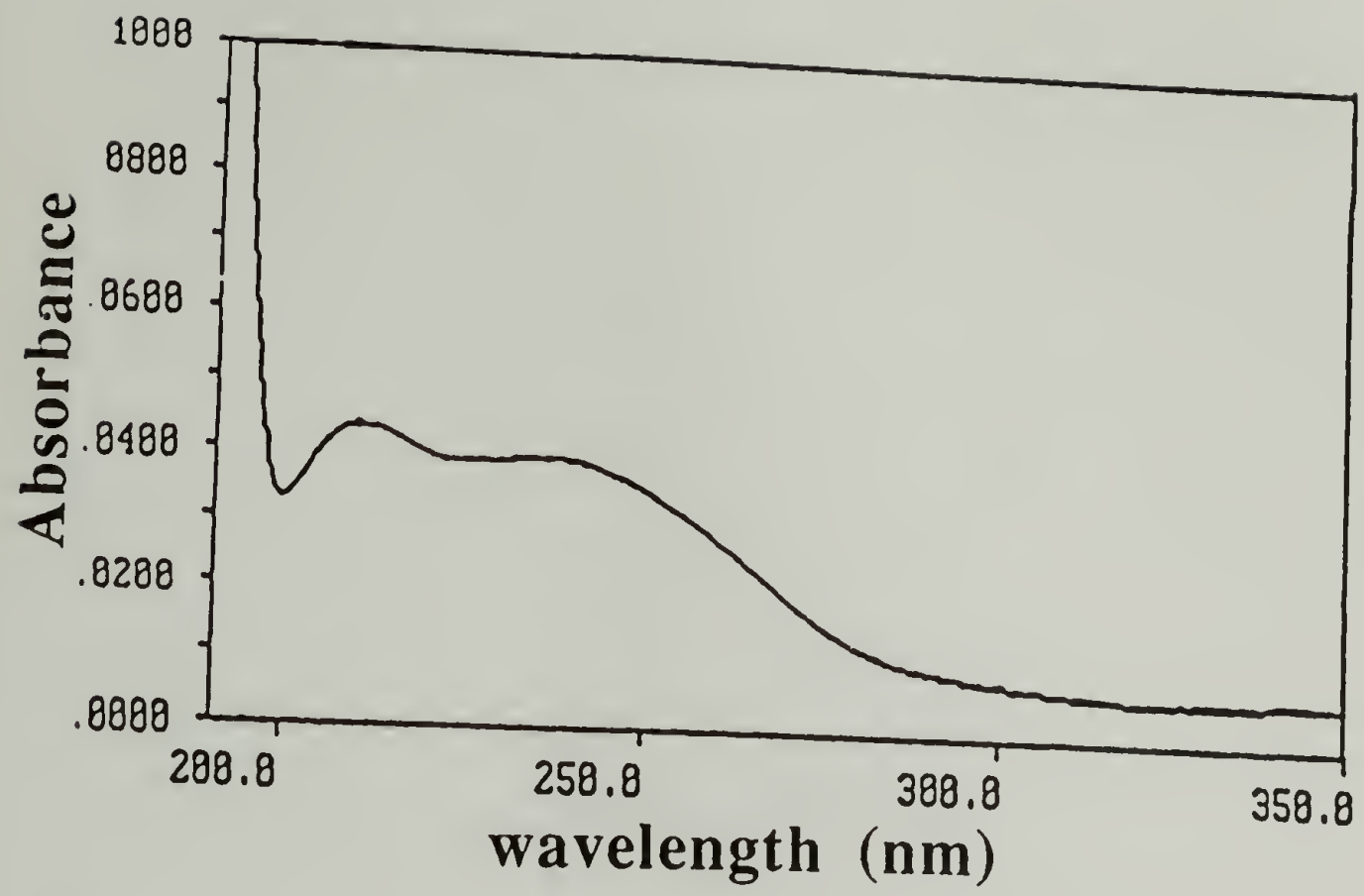


Figure 2.9 UV-vis Spectrum of FEP-PLL-3,5-Dinitrobenzamide.

The contact angle and UV-vis absorption data reflect the trends observed by XPS. By the reaction of FEP-PLL with 3,5-DNBC, the UV absorption at 210 nm increased due to the introduction of an additional carbonyl group. The contact angle increased from 107°/22° for FEP-PLL (Table 2.7) to 110°/52° for FEP-PLL-3,5-DNBA. The receding contact angle of FEP-PLL-3,5-DNBA increased as a result of the decreased hydrophilicity of the aromatic functionality.

Adhesion

The 180° peel test was used to determine whether surface modification improved the adhesion of FEP, a low surface free energy polymer which shows poor adhesion. (See Figure 2.1 for experimental set up.) Several adhesives were used in the peel test study in an attempt to discern whether the adhesive strength of FEP improved with PLL adsorption. FEP-PLL was prepared by adsorbing 20 ml of a 0.1 mg/ml solution of 20k PLL to an FEP

film sample at pH 11 for 24 h. The best results were obtained with two pressure sensitive acrylic adhesive tapes, 3M #850 and 3M #750. Since the adhesive bond that formed resulted from contact adhesion, special care was taken to apply constant pressure to all polymer film - adhesive interfaces. Table 2.12 summarizes peel test, XPS, and contact angle data for FEP-PLL and FEP film samples after peeling either 3M #850 or 3M #750. The chart recording results of the peel tests are included in Figures 2.10 and 2.11. (In these figures are included the chart recordings of peeled FEP-$CO_2H$ and FEP-$CO_2H$-PLL which are discussed in Chapter III.) The XPS results for the peeled film samples are included in Figure 2.12.

Table 2.11 FEP-PLL Peel Test Study: Peel Strength, XPS, and $\theta_A/\theta_R$ Data.

| Sample (Film-Adhesive Tape Peeled) | Peel Force (g/cm) | XPS **not** peeled | XPS peeled | XPS peeled* $C_{1s}$LBE/FEP; $N_{1s}/F_{1s}$ | $\theta_A/\theta_R$ **not** peeled | $\theta_A/\theta_R$ peeled |
|---|---|---|---|---|---|---|
| FEP-850 | 6 ± 2 | $C_{100}F_{200}$ | $C_{103}F_{200}$ | 0; n/a | 115°/102° | 110°/99° |
| FEP-PLL-850 | 57 ± 3 | $C_{171}F_{200}O_{15}N_7$ | $C_{101}F_{200}$ | 0; 0 | 107°/22° | 116°/100° |
| FEP-750 | 19 ± 3 | $C_{100}F_{200}$ | $C_{102}F_{200}$ | 0; n/a | 115°/102° | 117°/99° |
| FEP-PLL-750 | 51 ± 4 | $C_{171}F_{200}O_{15}N_7$ | $C_{100}F_{200}O_{0.6}$ | 0; 0 | 107°/22° | 114°/98° |

*$C_{1s}$ LBE = low binding energy peak in the $C_{1s}$ region which includes PLL and acrylic adhesive tape; n/a = not applicable.

Adsorption of PLL to FEP (FEP-PLL) increased the adhesive strength of an FEP - tape laminate by approximately an order of magnitude. A relatively insignificant peel force was required to remove either adhesive from FEP; it is well established that adhesion to

FEP and PTFE is usually poor.[61] An adhesive bond depends on interfacial molecular contact or wetting where both chemical bonds and van der Waals attractions are important.[62] In general, adhesion increases with roughness and/or polarity of the surface. FEP and FEP-PLL film samples are identical and smooth by SEM analysis yet different by XPS and contact angle analysis. The polar functionality of PLL introduced with its adsorption to FEP likely accounts for the increased peel strength observed. In a polar interface, dipole-dipole and/or hydrogen bond formation strengthen the adhesive bond. PLL provides a locus for adhesive-adherend interaction as a result of polar (and possibly "roughness") interactions. A roughened interface acts as a diffuse interface where an adhesive can penetrate into the "crevices" of the adherend. The FEP-PLL film sample withstood greater loads than the FEP film sample before failing. After peeling the FEP-PLL film sample the PLL layer was removed indicating failure at the FEP-PLL interface; XPS and contact angle analysis indicate that FEP was regenerated after peeling.

Another pressure sensitive adhesive tape, 3M #5413 (a silicone adhesive), was used in this study; unfortunately, FEP and FEP-PLL film samples could not be distinguished by peeling this adhesive because the adhesive failed cohesively. From the data in Table 2.13, XPS and contact angle measurements indicate the presence of the adhesive on the film samples; an increase in oxygen and silicon concentrations was observed. The FEP-PLL interface did not fail as evidenced by the presence of nitrogen in the 75° XPS data. The contact angle of FEP decreased sightly after peeling indicating that the silicone functionality was more hydrophilic than FEP; in contrast, the contact angle of FEP-PLL increased after peeling indicating that the silicone adhesive was more hydrophobic than PLL. In a separate attempt to distinguish film samples by the peel test, EPON 828 was spin-coated on the polymer film samples; however, adhesion was either too low to measure or the adhesive did not evenly wet the sample.

Table 2.12 FEP-PLL Peel Test Study Using 3M #5413: Peel Strength, XPS, and $\theta_A/\theta_R$ Data.

| Sample | Peel Force (g/cm) | XPS peeled | *$C_{1s}$lbe/FEP | $\theta_A/\theta_R$ peeled |
|---|---|---|---|---|
| FEP-3M #5413 | 44 | $C_{100}F_{107}O_{27}Si_{21}$ (15°)<br>$C_{100}F_{139}O_{17}Si_8$ (75°) | 0.43<br>0.16 | 110°/91° |
| FEP-PLL-3M #5413 | 57 | $C_{100}F_{94}O_{54}Si_{34}$ (15°)<br>$C_{100}F_{116}O_{35}Si_{16}N_3$ (75°) | 1.19<br>0.49 | 106°/80° |

*$C_{1s}$ lbe is the low binding energy carbon peak which includes PLL and the adhesive.

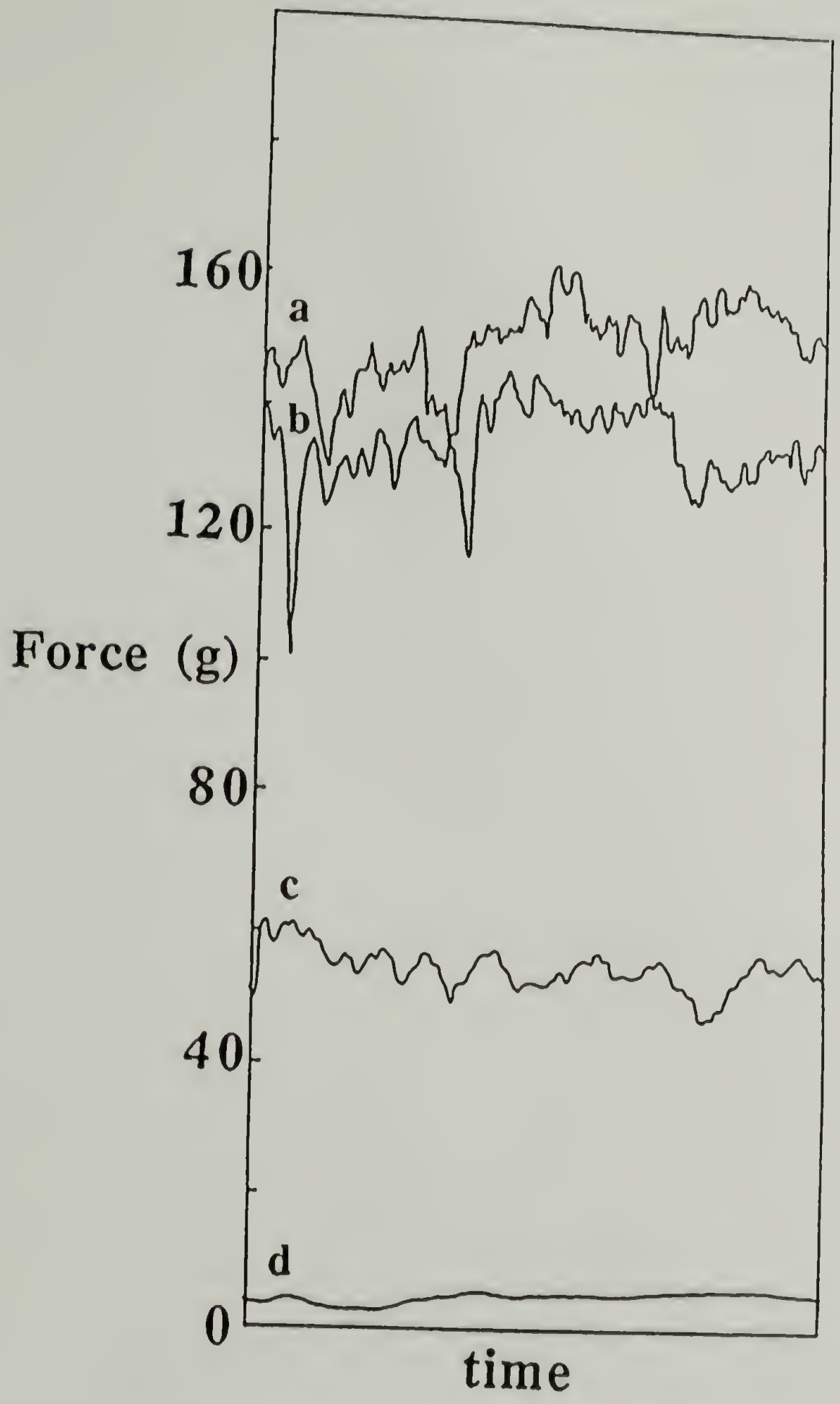


Figure 2.10 Chart Recordings of Peel Test Study for Films Peeled from 3M #850: (a) FEP-$CO_2H$-PLL, (b) FEP-$CO_2H$, (c) FEP-PLL, (d) FEP.

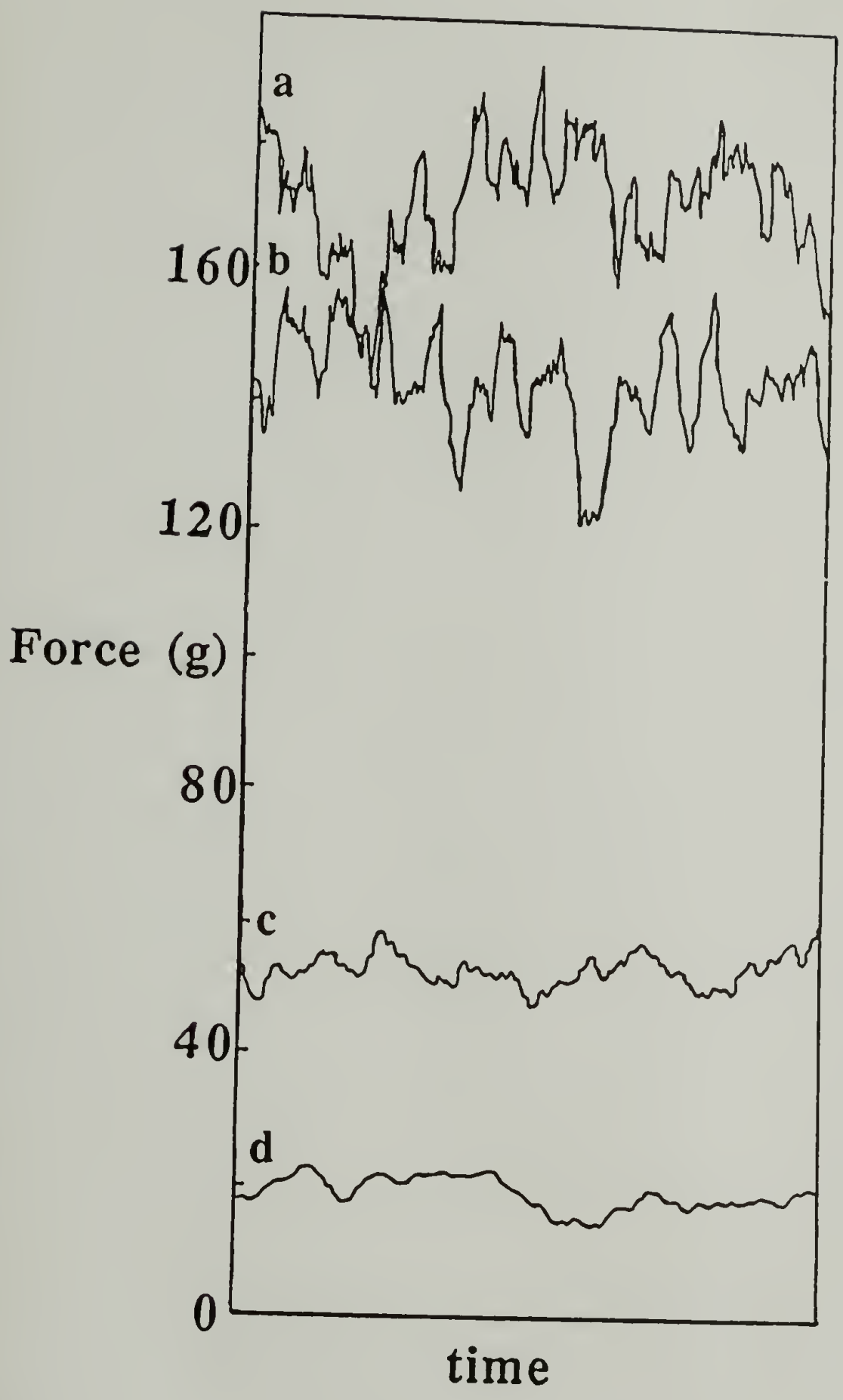


Figure 2.11 Chart Recordings of Peel Test Study for Films Peeled from 3M #750: (a) FEP-$CO_2H$, (b) FEP-$CO_2H$-PLL, (c) FEP-PLL, (d) FEP.

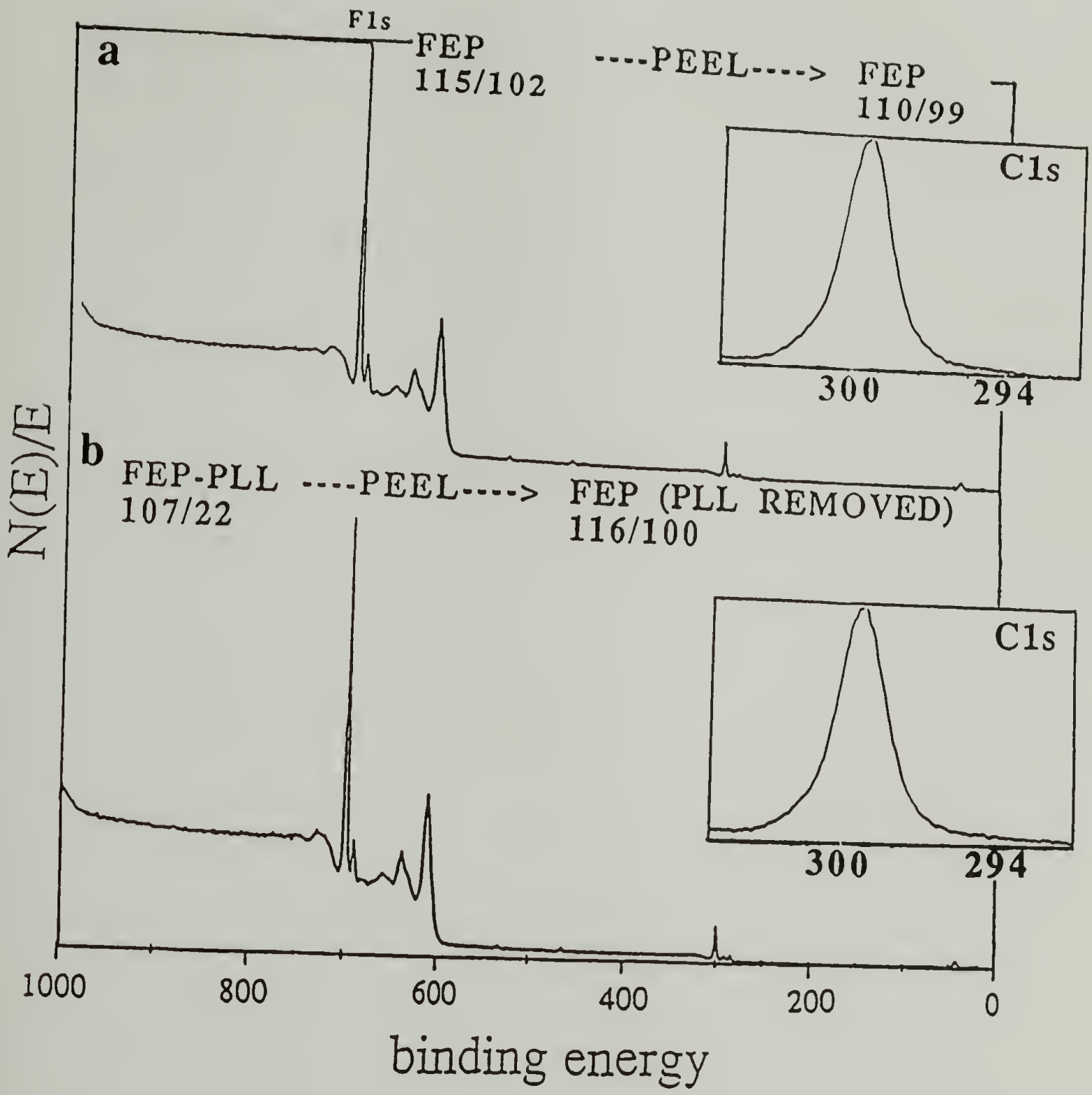


Figure 2.12 XPS Survey and $C_{1s}$ (15° takeoff angle) Spectra for Peeled Film Samples: (a) FEP and (b) FEP-PLL.

Adhesion and Growth of Biological Cells

The adhesion and growth of biological cells study was used both as a technique to distinguish between the surface modified film samples and to determine whether cell growth on FEP improved with PLL adsorption. The adhesion of HeLa cells to FEP and

FEP-PLL film samples was compared. FEP-PLL was prepared by adsorbing 20 ml of a 0.1 mg/ml solution of 20k PLL to FEP at pH 11 for 24 h. Table 2.14 summarizes the HeLa cell adhesion test results. Although HeLa cells adhered to both film samples initially, they adhered more strongly to FEP-PLL than to FEP after rinsing; an interaction between positively charged PLL and negatively charged HeLa cell membrane may have improved the adhesion observed on FEP-PLL.[63]

Table 2.13 Adhesion of HeLa Cells to FEP and FEP-PLL Film Samples.

| Film Sample | Initial # HeLa Cells | Final # HeLa Cells | % HeLa Cells Adhered |
|---|---|---|---|
| FEP | 350 | 40 | 11 |
| FEP-PLL | 700 | 400 | 57 |

FEP and FEP-PLL film samples were also distinguished by HeLa and endothelial cell growth. (See Figures 3.11 - 3.14 in Chapter III for growth curves and photographs.) Neither HeLa cells nor endothelial cells grew on the unmodified FEP film sample; however, on the FEP-PLL film sample, a monolayer of cells was observed after 3 and 6 days for HeLa and endothelial cells, respectively. Cell growth was a useful technique to distinguish between unmodified and modified FEP film samples.

## Conclusions

The adsorption of PLL from solution to the FEP-water interface is described as physisorption because no specific interaction drives the adsorption. Rather, adsorption results from thermodynamic properties of the system. The adsorption of PLL to an FEP film sample was controlled both by segment - solvent interactions and the solution -

substrate interfacial free energy. PLL adsorbs at the FEP-water interface concomitant with the liberation of water molecules from the interface and likely partial unfolding of the PLL α-helix. No distinct conformation was observed by CD spectroscopy. By adsorbing, PLL decreases the unfavorably high interfacial free energy between water and FEP; by partially unfolding from the α-helix upon adsorption, PLL regains some of the conformational entropy it loses upon adsorption. Although PLL likely unfolds (partially) from the α-helix, it is inconclusive whether this unfolding is responsible for or merely a result of PLL adsorption.

Charged PLL does not adsorb to FEP from an aqueous solution; although a high interfacial free energy between substrate and solution is established, PLL is already "unfolded" in a random coil or disordered conformation and cannot further unfold upon adsorption. Charged, α-helical PLL does not adsorb to FEP from an aqueous alcohol solution because the interfacial free energy between solution and substrate is substantially decreased with respect to that of water. More simply, charged PLL may not have adsorbed to FEP due to an electrostatic barrier which prevents the adsorption of a polyelectrolyte to a neutral substrate. In addition, PLL may have adsorbed to FEP from the neutral α-helix conformation as a result of its decreased solubility in the pH 11 solution with respect to that in water. Neutral, low molecular weight, PLL does not adsorb to FEP at pH 11 due to either its inability to form the α-helix conformation or its inability to overcome losses of translational and conformational entropies with enthalpic gain.

The properties of the adsorbed FEP-PLL film sample were studied to determine whether surface modification affected the properties of FEP and to distinguish between unmodified and modified FEP film samples. The adsorption of PLL to FEP improved its wettability, chemical reactivity, adhesion, and ability to support biological cell adhesion and growth. The 67% yield obtained for the labeling reaction with 3,5-dinitrobenzoyl chloride provided further insight into the adsorbed PLL conformation; the α-helix partially unfolded upon adsorption.

## References


1. Rha, C.; Rodriguez-Sanchez, D. *Eur. Pat. Appl. EP 152,898* **1984**. [CA 104:18670u]

2. Hommel, M.; Sun, A.M.F.; Goosen, M.F.A. *Eur. Pat. Appl. EP 167690* **1984**. [CA 104:174704]

3. Shen, S.; Kibat, P.G.; Chow, M.B.; Langer, R.S. *Polym. Prepr. (Am. Chem. Soc., Div. Polym. Chem.)* **1989**, *30 (1)*, 478.

4. Ryser, H.J.P.; Shen, W.C.; Morad, N. *Polym. Prepr. (Am. Chem. Soc., Div. Polym. Chem.)* **1986**, *27*, 15.

5. Arnold, L.J., Jr. *Methods Enzymol.* **1985**, *112*, 270.

6. Weiler, J.M. *Immunopharmacology* **1983**, *6*, 245.

7. Hardebo, J.E. *J. Kaahrstroem Acta Physiol. Scand.* **1985**, *125*, 495.

8. Antohi, S.; Brumfeld, V. *Rev. Roum. Morphol., Embryol. Physiol., Physiol.* **1984**, *21*, 213.

9. Crabb, H.J.; Jackson, R.C. *J. Membr. Biol.* **1986**, *91*, 85.

10. Young, P.R.; Vacante, D.A.; Snyder, W.R. *J. Am. Chem. Soc.* **1982**, *104*, 7287.

11. Lundblad, R.L.; Robert, H.R. *Thromb. Res.* **1982**, *25*, 319.

12. Losse, G.; Raddatz, H.; Naumann, W. *J. Kossowicz Pharmazie* **1988**, *43*, 105.

13. Shih, L.B.; Primus, F.J.; Goldenberg, M.D. *PCT Int. Appl. WO 8705031* **1987**. [CA 108:68965x]

14. Kurami, M.; Shirakami, Y.; Takahashi, K.; Ueda, N. *Eur. Pat. Appl. EP 233,619* **1987**. [CA 108:34189g]

15. Shima, S.; Fukuhara, Y.; Sukai, H. *Agric. Biol. Chem.* **1982**, *46*, 1917.

16. Shima, S.; Matsuoka, H.; Iwamoto, T.; Sakai, H. *J. Antibiot.* **1984**, *37*, 1449.

17. Asako, S.; Hirai, Y.; Okita, K.; Matsubara, H.; Niwa, S.; Takashina, M. *Jpn Kokai Tokkyo Koho* JP63196282[88,196,282] **1987**. [CA 110:113245s]

18. Asako, S.; Hirai, Y.; Okita, K.; Matsubara, H.; Niwa, S.; Takashira, M. *Jpn Kokai Tokkyo Koho* JP 63,198,978 [88,198,978] **1987**. [CA 110:113252s]

19. Lazar, A.; Silverstein, L.; Margel, S.; Mizrahi, A. *Dev. Biol. Stand.* **1985**, *60*, 457.

20. Sepulveda, C.A.; Schlager, S.I. *Methods Enzymol.* **1983**, *93*, 260.

21. Huang, W.M.; Gibson, S.J.; Facer, P.; Gu, J.; Polak, J.M. *Histochemistry* **1983**, *77*, 275.

22. Skutelsku, E.; Roth, J. *J. Histochem. Cytochem.* **1986**, *34*, 693.

23. Walz, D.A.; Penner, J.; Barnhart, M.I. *Scanning Electron Microsc.* **1984**, *(1)*, 303.

24. Greenfield, N.; Fasman, G.D. *Biochemistry* **1969**, *8*, 4108.

25. Cosani, A.; Terbojevich, M.; Romanin-Jacur, L.; Peggion, E. in *Peptides, Polypeptides and Proteins* (Blout, E.R.; Bovey, F.A.; Goodman, M.; Lotan, N., Eds.); John Wiley and Sons: New York, 1974, p. 166.

26. Satoh, M.; Matsumoto, N.; Komiyama, J.; Iijima, T. *Polym. Comm.* **1987**, *28*, 71.

27. Tanaka, S.; Fukagawa, O.; Baba, Y.; Kagemoto, A.; Fujishiro, R. *Netsu Sokutei* **1982**, *9*, 2.

28. Pease, J.P.; Tsang, W.-G.; Magee, A.S.; Konopacki, D.B. *Macromol. Synth.* **1989**, *11*, in press.

29. Mobashery, S.; Johnston, M. *J. Org. Chem.* **1985**, *50*, 2200.

30. Skinner, J.F.; Calkins, H.H.; Liles, W.C, Jr.; Kaplan, L.J. *Biopolymers* **1982**, *21*, 833.

31. Andrews, D.W.; Ottensmeyer, F.P. *Ultramicroscopy* **1982**, *9*, 337.

32. Yu, T.J.; Peticolas, W.L. in *Peptides, Polypeptides, and Proteins* (Blout, E.R.; Bovey, F.A.; Goodman, M.; Lotan, N., Eds.); John Wiley and Sons: New York, 1974, p. 370.

33. Yasui, S.C.; Keiderling, T.A. *J. Am. Chem. Soc.* **1986**, *108*, 5576.

34. Yang, J.T. *Abs. Pap. (Am. Chem. Soc.)* **1982**, *183*, 147.

35. Rosenhack, K.; Doty, P. *Biochemistry* **1961**, *47*, 1775.

36. Bomben, K.D.; Dev, S.B. *Anal. Chem.* **1988**, *60*, 1393.

37. Furusawa, K.; Kanesaka, M.; Yamashita, S. *J. Colloid Interface Sci.* **1984**, *99*, 341.

38. Bonekamp, B.C.; Alvarez, R.H.; De Las Nieves, F.J.; Bijsterbosch, B.H. *J. Colloid Interface Sci.* **1987**, *118*, 366.

39. Golander, C.-G.; Kiss, E. *J. Colloid Interface Sci.* **1988**, *121*, 240.

40. Davies, R.J.; Dix, L.R.; Toprakcioglu, C. *J. Colloid Interface Sci.* **1989**, *129*, 145.

41. Shoichet, M.S.; McCarthy, T.J. *Macromolecules* **1991**, *24*, 1441.

42. Kolthoff, I.M.; Sandel, E.B.; Meehan, E.J.; Bruckenstein, S. *Quantitative Chemical Analysis*, 4th ed.; MacMillan: Toronto, 1969, p. 1163.

43. This value is calculated using 14 Å as the mean free path of $C_{1s}$ electrons ejected by Mg Kα irradiation. This value was measured in poly(*p*-xylene): Clark, D.T.; Thomas, H.R. *J. Polym. Sci., Polym. Chem. Ed.* **1977**, *15*, 2843.

44. Cohen Stuart, M.A.; Scheutjens, J.M.H.M.; Fleer, G.J. *J. Polym. Sci.: Polym. Phys. Ed.* **1980**, *18*, 559.

45. Papenhuijzen, J.; Fleer, G.J.; Bijsterosch, B.H. *J. Colloid Interface Sci.* **1985**, *104*, 530.

46. Pederson, D.; Gabriel, D.; Hermans, J., Jr. *Biopolymers* **1971**, *10*, 2133.

47. Fleer, G.J.; Lyklema, J. in *Adsorption from Solution at the Solid/Liquid Interface* (Parfitt, G.D.; Rochester, C.H., Eds.); Academic Press: New York, 1983, p. 153.

48. Andrade, J. D. in *Surface and Interfacial Aspects of Biomedical Polymers: Surface Chemistry and Physics* (Andrade, J. D., Ed.); Plenum: New York, 1985, vol. 1, p. 184.

49. The peak assignments used in this report are based on a simple model proposed by Miyazawa, T. in *Poly(α-amino acids): Protein Models for Conformational Studies* (Fasman, G. D., Ed.); Marcel Dekker: New York, 1967, p. 90.

50. CD spectroscopy was of limited utility because PLL, adsorbed from both pH 7 and pH 11 solutions, showed a disordered conformation by comparison with PLL solution CD spectra. Although FEP-PLL adsorbed at pH 11 showed the least disordered conformation, few conclusions could be drawn from the data.

51. Panitz, J.A. *Ultramicroscopy* **1983**, *11*, 161.

52. Bonekamp, B.C. *Colloids Surfaces* **1989**, *41*, 267.

53. Epand, R. F.; Scheraga, H. A. *Biopolymers* **1968**, *6*, 1383.

54. Cohen Stuart, M.A.; Fleer, G.J.; Lyklema, J.; Norde, W.; Scheutjens, J.M.H.M. *Adv. Colloid Interface Sci.* **1991**, *34*, 477.

55. Andrade, J. D.; Smith, L. M.; Gregonis, D. E. in *Surface and Interfacial Aspects of Biomedical Polymers: Surface Chemistry and Physics* (Andrade, J. D., Ed.); Plenum: New York, 1985, vol. 1, pp. 276-7.

56. Johnson, R.E., Jr.; Dettre, R.H. *J. Phys. Chem.* **1964**, *68*, 1744.

57. Dann, J.R. *J. Colloid Interface Sci.* **1970**, *32*, 302.

58. Holmes Farley, S.R.; Whitesides, G.M. *Langmuir* **1986**, *2*, 266.

59. Rasmussen, J.R.; Bergbreiter, D.E.; Whitesides, G.M. *J. Am. Chem. Soc.* **1977**, *19*, 4746.

60. Fersht, A.R.; Jencks, W.P. *J. Am. Chem. Soc.* **1970**, *92*, 5432.

61. Eagland, D. *Chemtech* **1990**, *April*, 248.

62. Wu, S. *Polymer Interface and Adhesion* Marcel Dekker: New York, **1982**, pp. 337, 359.

63. HeLa cells have been shown to grow more efficiently on positively charged microcarriers: Jacobson, B.S.; Ryan, U.S. *Tissue and Cell* **1982**, *14*, 69.

# CHAPTER III

# ADSORPTION OF PLL TO SURFACE CARBOXYLIC ACID-FUNCTIONALIZED POLY(TETRAFLUOROETHYLENE-CO-HEXAFLUOROPROPYLENE) FILM

## Overview

Polymer surface modification can be accomplished by several techniques including plasma irradiation,[1] chemical reaction, or adsorption. Chapter I elucidated several ways to chemically modify polymer film samples where both the depth of modification and the chemical nature of the film were controlled. Chapter II discussed some of the important parameters involved in the adsorption of a neutral polymer to a neutral substrate and how such a technique was useful for surface modification. In this chapter, these two methods of surface modification are combined in the study of poly(L-lysine) adsorption to surface-carboxylated poly(tetrafluoroethylene-co-hexafluoropropylene) (FEP-$CO_2H$) film samples. The adsorption of charged PLL to an FEP-$CO_2H$ film sample involves an electrostatic interaction which likely includes both a hydrogen-bonding and an ionic attraction. The chapter begins with an overview of polyelectrolyte adsorption and then examines the important driving forces for PLL adsorption. The properties of the adsorbed FEP-$CO_2H$-PLL film sample are compared to those of FEP-$CO_2H$ and FEP in terms of wettability, chemical reactivity, adhesion, and ability to support biological cell adhesion and growth.

# Introduction

## Polyelectrolyte Adsorption

Polyelectrolyte adsorption is important in several applications including those in food technology, paint production, soil stabilization, and medical science. In order to understand these applications and develop new ones, it is imperative to comprehend polyelectrolyte behavior near a surface.

Polyelectrolyte adsorption theory was developed by Van der Schee and Lyklema[2] and extended to include weakly dissociated polyelectrolytes by Evers *et al.*[3] Their theories were based on the self consistent field approaches of Scheutjens and Fleer[4] and/or Roe[5] where a lattice model is invoked to explain segment-substrate ($\chi_s$) and segment-solvent ($\chi$) interactions. Polyelectrolyte theory extends (uncharged) polymer adsorption theory to include electrostatic interactions which arise as a result of charged groups on the polymer chain. The electrostatic component affects polymer solution and adsorption conformations by segment-substrate, segment-solvent, and segment-segment interactions.

Cohen Stuart *et al.*[6] summarized the polyelectrolyte adsorption model. The multilayer Stern model is combined with that of Scheutjens and Fleer to account for all possible conformations. The energy of each segment depends upon its local environment which includes an electrostatic contribution; by summing over the energy of the segments and adding a spatial distribution, the energy of the chain is determined using a lattice model.

The theoretical results for polyelectrolyte adsorption are summarized in terms of the strength of the polyelectrolyte (weak vs. strong or extent of dissociation), ionic strength of added electrolyte, and charged nature of the substrate (oppositely or similarly charged or neutral). At low salt concentration, a strong polyelectrolyte adsorbs to an oppositely charged substrate in a flat conformation where segment-segment repulsions inhibit loop and

tail formation and promote chain extension in the form of trains. The amount of polymer that adsorbs is low and independent of chain length, yet increases with increasing surface charge. Since surface charge is usually slightly overcompensated, charge reversal occurs with the adsorption of an oppositely charged polymer; the extent to which overcompensation occurs depends upon $\chi_s$ (segment-substrate interaction parameter). As the ionic strength increases, the adsorbed amount increases; if the surface charge is low or neutral, the increase in adsorbed amount is more substantial. An increase in salt concentration enhances adsorption by screening lateral electrostatic repulsions in the polymer layer.

For a polyelectrolyte, $\chi_s$ includes chemical and electrostatic interactions in addition to those of the segment-substrate; in other words, $\chi_s$ depends upon surface charge and ionic strength. The electrostatic interaction is positive for an attractive interaction between substrate and polyelectrolyte; however, as the salt concentration increases, the adsorption of the polyelectrolyte decreases because the salt ions compete with those of the polyelectrolyte for surface sites. The $\chi$ parameter of a polyelectrolyte is a function of segment-segment and electrostatic interactions. The electrostatic interaction is negative due to mutual repulsion between segments. Consequently, the amount of polyelectrolyte that adsorbs decreases. However, as salt concentration increases, repulsion between segments decreases due to screening and the amount adsorbed increases. The effective $\chi$ ($\chi_{eff}$) balances the two opposing effects of salt concentration on the amount adsorbed. At low salt concentration, $\chi_{eff}$ is low; the polyelectrolyte displays the same adsorption pattern observed for a neutral polymer adsorbing from a good solvent - low adsorbed amount, flat conformation, weak chain length dependence. As the salt concentration increases, $\chi_{eff}$ increases; the adsorption behavior of the polyelectrolyte is similar to that of an uncharged polymer from a theta solvent - increased adsorbed amount with molecular weight, loop and tail formation. At high salt concentration and high surface charge, less polymer adsorbs

because the small ions that are attracted to the surface make it more difficult for the polymer to find a surface site for adsorption.

PLL, a positively charged polyelectrolyte, has been the subject of numerous adsorption studies; it has been adsorbed to other substrates, such as mica,[7] tungsten,[8] and sulfonated poly(styrene).[9, 10] In addition, PLL is an important model for protein conformational analysis[11] because it adopts one of three solution conformations according to temperature and pH of the aqueous solution: α-helix, β-sheet, or random coil/disordered. In this research, adsorption of PLL to FEP-$CO_2H$ is studied to determine the important driving forces for adsorption and as a surface modification technique. At pH 7, the adsorption involves the interaction between highly charged, random coil-like PLL and surface carboxylate/carboxylic acid-functionalized FEP-$CO_2H$. The interaction between PLL-ammonium and FEP-carboxylate was investigated as a possible driving force for adsorption. Recall from Chapter II, that PLL does not adsorb to unmodified FEP from a pH 7 solution. Unlike adsorption of neutral PLL to neutral FEP (Chapter II), the adsorption of cationic PLL to anionic FEP-$CO_2H$ relies upon specific electrostatic (ionic and/or hydrogen-bonding) interactions for adsorption. The important parameters for chemisorption were investigated in light of these two possible driving forces. With adsorption of PLL, the properties of FEP-$CO_2H$ changed in terms of wettability, chemical reactivity, adhesion, and biological cell adhesion and growth. The polymer film samples were characterized by attenuated total reflectance infrared spectroscopy (ATR IR), ultraviolet-visible spectrophotometry (UV-vis), contact angle ($\theta_A/\theta_R$), and quantitatively by x-ray photoelectron spectroscopy (XPS). Additional techniques were used in studying the properties of the adsorbed film samples as indicated in the text.

## Experimental

All solutions were deoxygenated by sparging with nitrogen and transferred by Schlenk technique, unless otherwise specified. All materials were used as received unless otherwise specified.

### Materials and Methods

**Poly(tetrafluoroethylene-co-hexafluoropropylene)** (FEP, 5 mil) film was obtained from duPont and extracted with methylene chloride for 1 hour; the polymer film was rinsed in fresh methylene chloride and then dried (0.05 mm, >24 h) to constant mass. The polymer film samples were stored under vacuum.

**Reduction of FEP (FEP-C)** was described in Chapter I; the FEP film sample was immersed in a 0.12 M solution of sodium naphthalide (Aldrich) in THF for 15 min at 0 °C. The film sample was rinsed according to the method outlined in Chapter I.

**Oxidation of Reduced FEP (FEP-$CO_2H$).**[12] The FEP-C film sample was immersed in a 0.16 M potassium chlorate (Alfa) in sulfuric acid (Fisher) solution for 2 h as described in Chapter I.

**Reaction of Surface Carboxylic Acids with Borane•THF (FEP-$CH_2OH$).** The FEP-$CO_2H$ film sample was immersed in a 1 M borane•THF (Aldrich) solution for 1 h as described in Chapter I.

**Tetrahydrofuran** (THF) (Aldrich, anhydrous, 99.9%) was distilled from sodium benzophenone (Aldrich).

**pH 4** solution (Fisher) was buffered with 0.05 M potassium acid phthalate.

**pH 11** buffer solution was prepared by a standard technique.[13] 50 ml of 0.05 M sodium bicarbonate (Fisher) and 22.7 ml of 0.1 M sodium hydroxide (Fisher) were diluted to 100 ml with redistilled water.

**House Distilled Water** was redistilled using a Gilmont Still apparatus.

**Poly(L-lysine)** (PLL) was purchased as the hydrobromide salt from, and characterized by, Sigma. PLL of approximate molecular weights 4k, 20k, 50k, 60k, 100k, 400k, and 500k were used and are described more fully in Table 2.3. PLL was dissolved in doubly distilled water and stored refrigerated as a 1 mg/ml stock solution.

**Adsorption of PLL to Modified FEP Film Samples from an Aqueous Solution at pH 7** (FEP-X-PLL, X = $CO_2H$ or $CH_2OH$). 20 ml of a 0.1 mg/ml PLL solution in doubly distilled water ($ddH_2O$) was added by cannula to a nitrogen-purged Schlenk tube containing an FEP film sample. The Schlenk tube was immersed in a 25 °C water bath and agitated for the specified time (1 h - 168 h). The film sample was rinsed with $ddH_2O$ (3 x 20 ml) and dried (0.05 mm, >24 h). [See Results and Discussion for notebook references.]

**Adsorption of PLL to FEP-$CO_2H$ at pH 4** (FEP-$CO_2H$-PLL). The experimental procedure outlined for adsorption at pH 7 was followed; however, 20 ml of a 0.1 mg/ml PLL solution in pH 4 buffer (Fisher) was used for the adsorption experiment. The work up procedure differed in that the film sample was rinsed in pH 4 buffer (3 x 20 ml) and $ddH_2O$ (3 x 20 ml) before it was dried (0.05 mm, >24 h). [III129, IV5]

**Adsorption of PLL to FEP-$CO_2H$ at pH 11** (FEP-$CO_2H$-PLL). The experimental procedure outlined for adsorption at pH 7 was followed; however, 20 ml of a 0.1 mg/ml PLL solution in pH 11 buffer was used for the adsorption experiment. The work up procedure differed in that the film sample was rinsed in $ddH_2O$ (1 x 20 ml), pH 11 buffer (2 x 20 ml), $ddH_2O$ (2 x 20 ml) before it was dried (0.05 mm, >24 h). [III98]

**Adsorption of PLL to FEP-$CO_2H$ from Isopropanol/Water (82:18, v/v)** (FEP-$CO_2H$-PLL). The procedure outlined for adsorption at pH 7 was followed where the PLL dissolved in an aqueous solution was replaced with one dissolved in an isopropanol (iPrOH) (Fisher) / water solution (82: 18, v/v ratio). The work up procedure

differed by using an isopropanol:water (82:18, v/v) solution (3 x 20 ml) before drying (0.05 mm, >24 h). [III135-6]

**Adsorption of PLL to FEP-$CO_2H$ from Methanol/Water (96:4, v/v)** (FEP-$CO_2H$-PLL). The procedure outlined for adsorption at pH 7 was followed where PLL was dissolved in an methanol (MeOH) (Fisher) / water solution (96: 4, v/v ratio). The work up procedure differed by using a methanol:water (96:4, v/v) solution (3 x 20 ml) before drying (0.05 mm, >24 h). [III88-89]

**Solvent Stability of the Adsorbed Layer** was assessed by immersing a FEP-$CO_2H$-PLL film sample in a solvent for a specified length of time. The FEP-$CO_2H$-PLL film sample was prepared by adsorbing 0.001 mg/ml of 400k PLL to FEP-$CO_2H$ for 24 h. [III102]

**3,5-Dinitrobenzoyl Chloride** (3,5-DNBC) (Aldrich, 98+%) was used as received and stored in the glove box.

**Pyridine** (Aldrich) was distilled from calcium hydride (Aldrich).

**Reaction of FEP-X-PLL with 3,5-Dinitrobenzoyl Chloride** (FEP-X-PLL-3,5-DNBA, X = $CO_2H$, $CH_2OH$) 20 ml of a 0.2 M 3,5-dinitrobenzoyl chloride solution in THF was added by cannula to a nitrogen-purged Schlenk tube containing an FEP-X-PLL film sample. 1 ml of pyridine was transferred to the Schlenk tube by cannula and the solution was agitated for 1 min. After 24 h, the solution was removed and the film sample was washed with THF (3 x 20 ml), methanol ($CH_3OH$) (6 x 20 ml), THF (soxhlet extract, 36 h) and then dried (0.05 mm, >24 h). PLL adsorbed film samples were prepared by adsorbing 20 ml of a 0.1 mg/ml solution of 20k PLL for 24 h at the appropriate pH. [III86-7,105,118,119,132-4,139,142-6]

**Peel Tests** were performed on FEP-$CO_2H$ and FEP-$CO_2H$-PLL film samples, the latter were prepared by adsorbing 20 ml of a 0.1 mg/ml solution of 20k PLL to an FEP-$CO_2H$ film sample at pH 7 for 24 h. Two 3M adhesive tapes were used: (1) 3M #850, a polyester backed acrylic adhesive and (2) 3M #750, an acetate backed acrylic

adhesive. The adhesive tapes were applied to both film samples, FEP-$CO_2H$ and FEP-$CO_2H$-PLL, concurrently and with even pressure using a roller; 100 strokes were applied before measurement. [III110-116]

**HeLa Cells** were grown in RPMI growth medium (Sigma) and provided by Dr. Rich McCarron and Prof. Bruce Jacobson. HeLa cells are human cervical carcinoma cells.

**Adhesion of HeLa Cells** was studied under the optical microscope. The number of HeLa cells reported is an average of 4 measurements made at different locations on the film sample within a grid area. A polymer film sample was immersed in a Petri dish containing RPMI growth medium for 30 minutes before adding $10^6$ HeLa cells. After addition of the cells, the number of cells that initially adhered to the film sample was determined by counting using an optical microscope. The film sample was rinsed in growth medium for ~5 minutes before immersing it in fresh growth medium in a clean Petri dish. The number of cells that adhered to the film sample was redetermined in a similar fashion, accounting for the final number of cells adhering to the film sample. FEP-$CO_2H$-PLL film samples were prepared by adsorbing 20 ml of a 0.1 mg/ml solution of 20k PLL to FEP-$CO_2H$ at pH 7. [III120-123]

**Growth of HeLa Cells.** The number of cells attached to the film sample was determined using an optical microscope and reported values are averages over 4 different locations on the film sample. The growth medium was changed daily by sterile technique after the cells were counted. The Petri dishes containing cells and film samples were stored at 37 °C when not being counted. [III124; IV15,17]

**Endothelial Cells** were provided by Dr. Donna Beer and Prof. Bruce Jacobson. The endothelial cells studied were those from the aorta of a cow. The endothelial cells were grown on gelatin and then broken up and spun down with trypsin (~5 min, 37 °C). The cells were mixed with serum, spun down and then rediluted with serum.

**Growth of Endothelial Cells.** The procedure outlined for HeLa cell growth was followed; however, fresh serum was added every 3 days as opposed to changing the medium daily. [IV19]

## Analytical Techniques

**Attenuated Total Internal Reflectance Infrared** (ATR IR) spectra were recorded under nitrogen with an IBM 32 FTIR spectrometer and a 45° germanium internal reflection element.

**Circular Dichroism** (CD) spectra were acquired on a JASCO J-40A CD spectrometer. The film was held between 2 quartz plates and placed perpendicular to the light source; it was rotated by 90° in the same plane to ensure that the signal did not result from stresses within the film. CD spectra are an average of 10 scans.

**Dynamic Advancing and Receding Contact Angles** ($\theta_A/\theta_R$) were measured with a Ramé-Hart telescopic goniometer and a Gilmont syringe (25 gauge flat-tipped needle) using redistilled water as the probe fluid. Contact angles reported are an average of at least 5 measurements made at different locations on the film surface. The angle between the tangent of the water droplet at the drop-surface intersection and the horizontal was measured as water was added ($\theta_A$) to and removed ($\theta_R$) from the surface.

**Optical Microscopy** was done on a Nikon 802798 at 200 and 100 magnifications for HeLa and endothelial cells, respectively.

**Peel Test** data were acquired on an Instron using a 2 kg load cell which had been calibrated with a 200 g weight. An adhesive tape was mounted identically on all film samples. The adhesive was bent back from the film at 180° and attached to the lower clamp of the Instron and the film sample was attached to the upper clamp of the Instron. The adhesive was peeled from the film at a rate of 1 cm/min. See Figure 2.1 for experimental set up.

**pH** was checked with a Fisher 825MP pH meter which was calibrated before use with standard pH 4, pH 7 and pH 11 buffer solutions (Fisher).

**Scanning Electron Micrographs** (SEM) were obtained on a JEOL 100CX at magnifications to $10^5$.

**The Shaker Water Bath** was a Precision #25 which agitated samples at 25 °C and 120 speed.

**Ultraviolet-visible** (UV-vis) spectra were recorded on a Perkin Elmer λ2 spectrophotometer with the unreacted film in the reference chamber.

**X-ray Photoelectron Spectra** (XPS) were obtained on a Perkin Elmer-Physical Electronics 5100 spectrometer; samples were acquired at a 15° takeoff angle (between the film plane and the detector) for less than 12 minutes, using Mg Kα excitation at 400 W. Pass energies of 89.45 eV and 35.75 eV were used to acquire survey and $C_{1s}$ region spectra, respectively, in a chamber evacuated to $3 \times 10^{-8}$ torr. Atomic sensitivity factors used to calculate atomic composition were: $F_{1s}$ 1.000, $C_{1s}$ 0.202, $O_{1s}$ 0.540, $N_{1s}$ 0.340, $Si_{2p}$ 0.225. The binding energies reported are not corrected for charging.

## Results and Discussion

Surface modification can be accomplished by a number of techniques including chemical reaction and adsorption. We have reported several chemical modifications of polymer film samples where both the depth and chemical functionality on the film were controlled.[14] We have also studied the adsorption of a polymer dissolved in an organic solvent to a solid (metallic[15] or polymeric[16]) substrate. In the research described in this Chapter, these two fields of interest are combined to study the adsorption of a polymer in solution, poly(L-lysine) (PLL), to a chemically modified polymer film, carboxylic acid-functionalized poly(tetrafluoroethylene-co-hexafluoropropylene) (FEP-$CO_2H$).[17] Other polymer adsorption studies in our research group depend upon specifically functionalizing

a polymer for adsorption; here the surface, rather than the segment, is specifically functionalized. The objective was to control the adsorption of PLL to FEP by chemical surface modification or by choice of solvent.

FEP is a chemically inert, hydrophobic polymer whereas poly(L-lysine) is a water soluble poly(amino acid) with interesting and well-characterized solution properties. Unlike previous adsorption studies in our research group, adsorption was studied from an aqueous solution rather than an organic solvent. The aqueous - fluoropolymer interface is sharp and well-defined because water neither swells nor penetrates the film sample.

In an attempt to understand the parameters that control PLL adsorption to FEP-$CO_2H$, several variables were studied: time of interaction, molecular weight of PLL, concentration of PLL, and surface charge density of the FEP-$CO_2H$ film sample. The latter was studied by changing either the pH of the aqueous solution, the solvent used, or the surface functionality of the FEP film substrate. Figure 3.1 summarizes the variables studied in an attempt to control PLL adsorption. Poly(tetrafluoroethylene-co-hexafluoropropylene) was carboxylic acid-functionalized by a two-step synthesis involving first reduction with sodium naphthalide in THF and then oxidation with potassium chlorate dissolved in sulfuric acid. The surface charge density of FEP-$CO_2H$ was decreased by reduction with borane•THF to FEP-$CH_2OH$. (See Chapter I for more information on chemical modification reactions.) The properties of the adsorbed FEP-$CO_2H$-PLL film substrate were related to those of FEP-$CO_2H$ and FEP in terms of wettability, chemical reactivity, peel strength, and biological cell growth and adhesion.

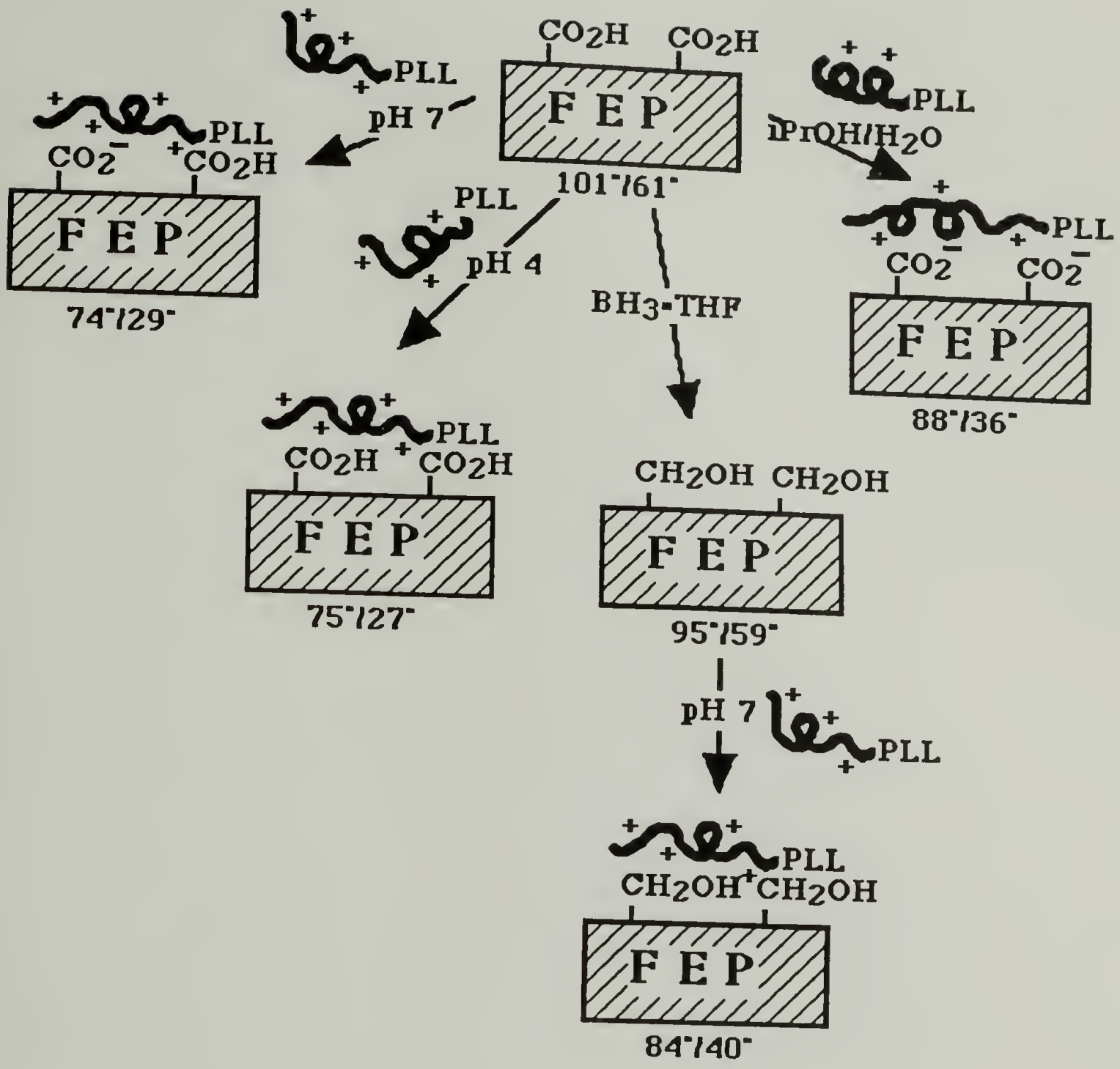


Figure 3.1 Summary of the Variables Used to Control the Adsorption of PLL to FEP-$CO_2H$ with Contact Angle Data.

## FEP-$CO_2H$-PLL: pH 7

The adsorption of PLL to the FEP-$CO_2H$ - water interface was studied from a pH 7 solution. Water has a pH 7 value when PLL is dissolved in it; this solution was not buffered with added electrolyte. When dissolved in water, the ε-amine groups of PLL are

protonated to ammonium and PLL has a random coil or disordered conformation. At pH 7, FEP-$CO_2H$ exists in both protonated (carboxylic acid) and deprotonated (carboxylate) forms, providing a mixed or heterogeneous chemically functionalized film sample. According to XPS results (Chapter I), there is one carboxylic acid group in eight FEP repeat units or $(CF_2CF_2)_8CO_2H$. As shown in the contact angle titration curve, Figure 1.11, the percentage of carboxylic acids that are deprotonated to carboxylates, at pH 7, is difficult to ascertain but can be estimated at ~50%. PLL adsorbs to FEP-$CO_2H$ at pH 7 as a result of specific interactions. The attraction between PLL-ammonium and FEP-carboxylate/carboxylic acid results in adsorption. Recall from Chapter II that PLL adsorbs to FEP at pH 11 by a non-specific interaction (physisorption) and not at pH 7.

The adsorption of PLL to FEP-$CO_2H$ at pH 7 was investigated in terms of time of interaction, PLL molecular weight and PLL concentration. The adsorption was quantified by XPS analysis where $N_{1s}$ (404 eV), $O_{1s}$ (536 eV),[18] and low binding energy $C_{1s}$ (288 eV) peaks represent PLL while $F_{1s}$ (693 eV) and high binding energy $C_{1s}$ (296 eV) peaks represent FEP-$CO_2H$. Figure 3.2 includes typical photoelectron spectra for FEP-$CO_2H$-PLL (400k) and FEP-$CO_2H$. By comparing either $C_{1s}$PLL/FEP or $N_{1s}/F_{1s}$ peak ratios, the relative amount of PLL adsorbed was determined.

The effect of time of interaction on PLL adsorption to FEP-$CO_2H$ at pH 7 was studied. Figure 3.3 (Tables 3.1 and 3.2) show that the adsorption of both 20k and 400k PLL to FEP-$CO_2H$ (i.e. $N_{1s}/F_{1s}$ ratio) is time-independent; the adsorbed amount reaches a plateau level within the first hour of interaction. Although not quantitative, the contact angles reflect the hydrophilic nature of the polymer surface. The large hysteresis between advancing and receding contact angles reflects the heterogeneous nature of the surface where a low percentage of hydrophilic groups causes a greater decrease in the receding than the advancing contact angle.

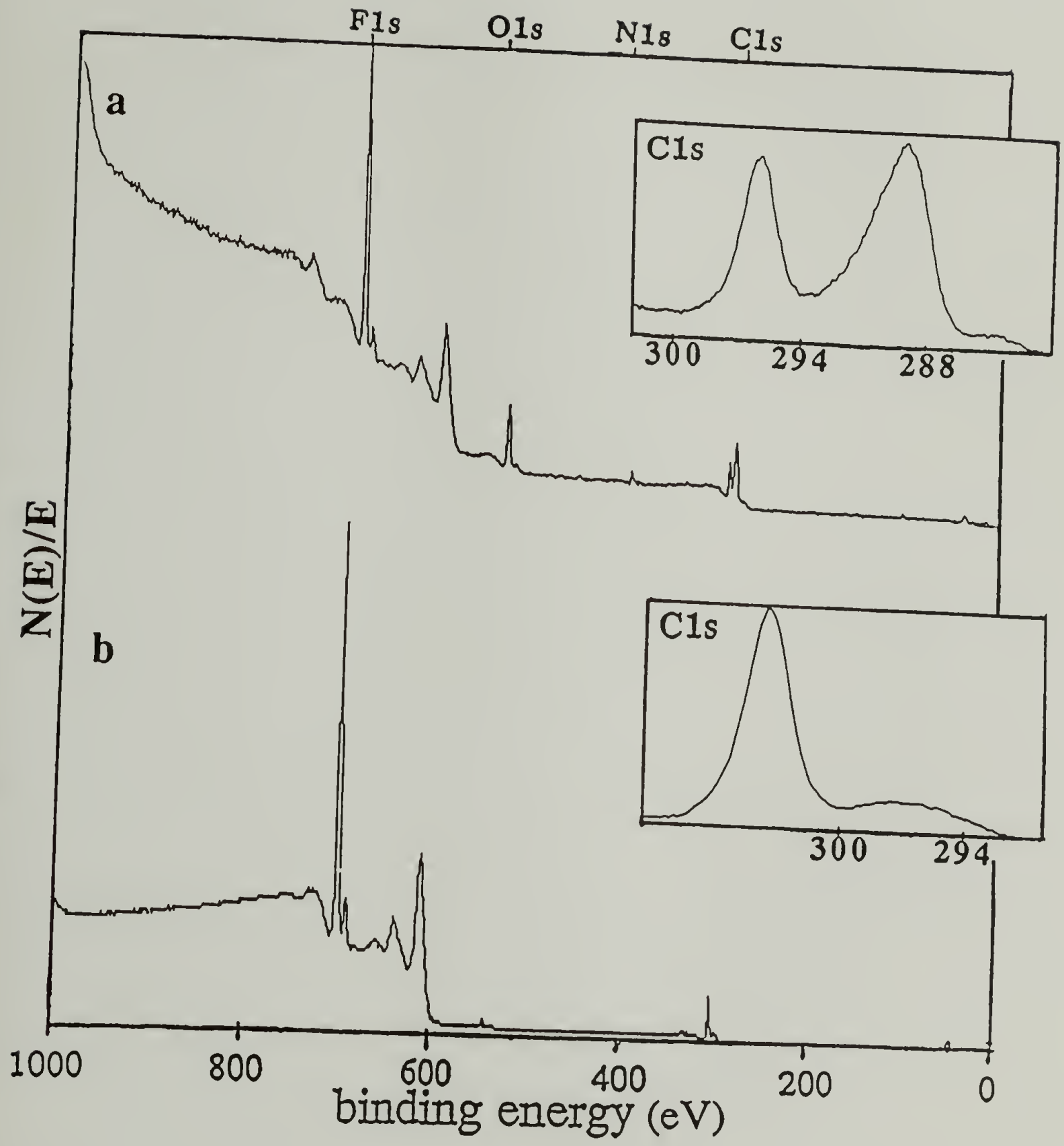


Figure 3.2 XPS Survey and $C_{1s}$ (15° takeoff angle) Spectra of (a) FEP-$CO_2H$-PLL (400k, pH 7) and (b) FEP-$CO_2H$.

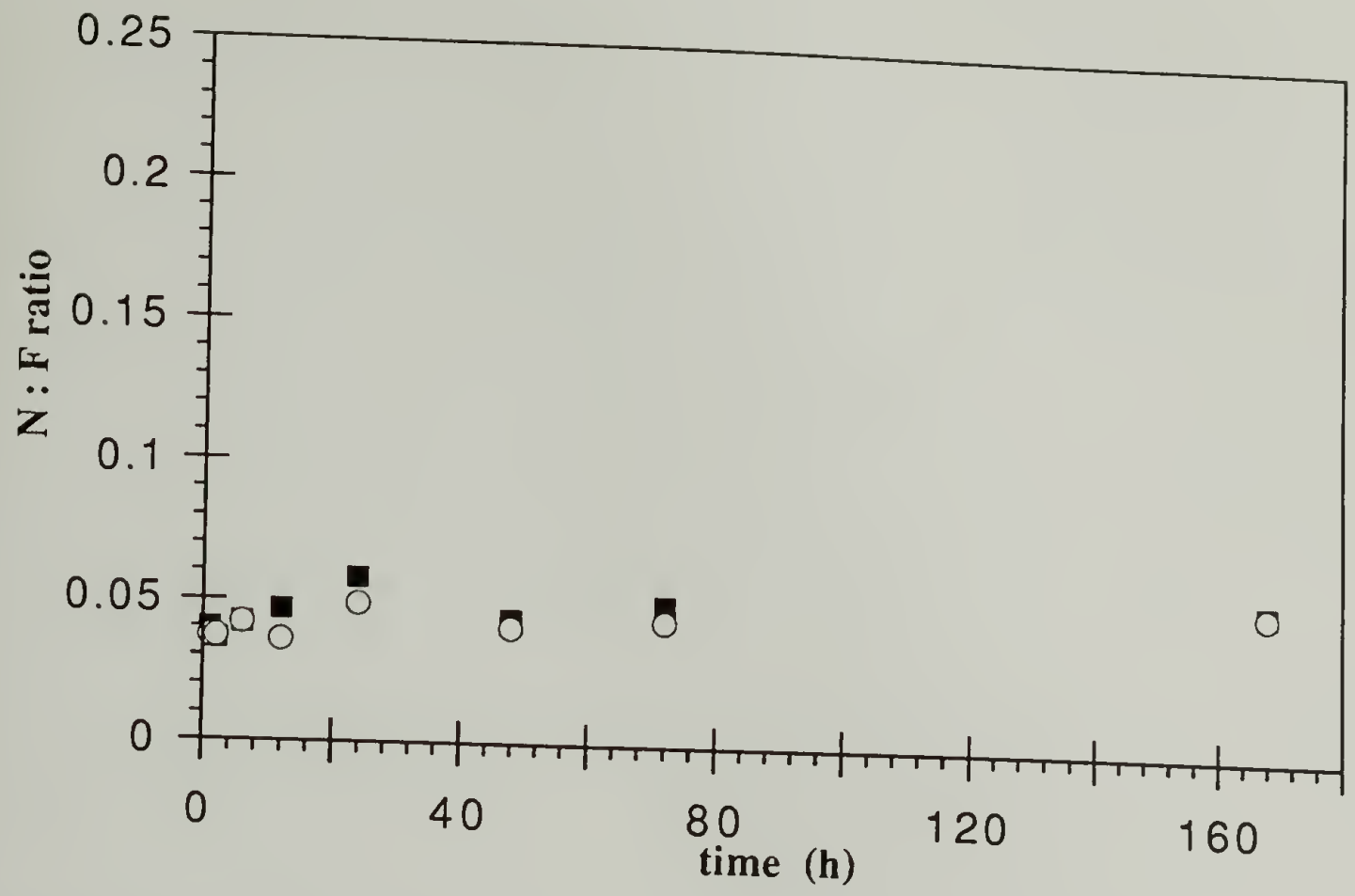


Figure 3.3 Effect of Time of Interaction on the Adsorbed Layer Thickness of FEP-$CO_2H$-PLL at pH 7 for PLL (■) 400k and (○) 20k.

Table 3.1 Effect of Time of Interaction for PLL (400k, 0.1 mg/ml) Adsorption to FEP-$CO_2H$ at pH 7: XPS and Contact Angle Data. [III92]

| Time (h) | $C_{1s}$ PLL/FEP | $N_{1s}/F_{1s}$ | *C : F : O : N | $\theta_A/\theta_R$ |
|---|---|---|---|---|
| 1 | 0.724 | 0.041 | 100 : 99 : 15 : 4 | 85°/35° |
| 2 | 0.522 | 0.036 | 100 : 108 : 14 : 4 | 83°/33° |
| 6 | 0.681 | 0.042 | 100 : 103 : 14 : 5 | 80°/25° |
| 12 | 1.140 | 0.047 | 100 : 85 : 16 : 4 | 78°/27° |
| 24 | 1.657 | 0.058 | 100 : 79 : 17 : 5 | 78°/29° |
| 48 | 0.720 | 0.044 | 100 : 99 : 16 : 4 | 72°/30° |
| 72 | 0.798 | 0.050 | 100 : 94 : 12 : 5 | 67°/21° |
| 168 | 1.017 | 0.053 | 100 : 88 : 16 : 5 | 73°/27° |

Table 3.2 Effect of Time of Interaction for PLL (20k, 0.1 mg/ml) Adsorption to FEP-$CO_2H$ at pH 7: XPS and Contact Angle Data. [III93]

| Time (h) | $C_{1s}$ PLL/FEP | N1s/F1s | *C : F : O : N | $\theta_A/\theta_R$ |
|---|---|---|---|---|
| 1 | 0.599 | 0.037 | 100 : 108 : 11 : 4 | 82°/38° |
| 2 | 0.608 | 0.037 | 100 : 106 : 14 : 4 | 90°/44° |
| 6 | 0.760 | 0.042 | 100 : 100 : 15 : 4 | 81°/39° |
| 12 | 0.766 | 0.036 | 100 : 99 : 15 : 4 | 82°/37° |
| 24 | 0.985 | 0.049 | 100 : 91 : 19 : 5 | 77°/29° |
| 48 | 1.027 | 0.041 | 100 : 89 : 17 : 4 | 77°/34° |
| 72 | 0.710 | 0.044 | 100 : 102 : 15 : 5 | 74°/29° |
| 168 | 0.864 | 0.052 | 100 : 94 : 18 : 5 | 78°/38° |

*Slight silicon contamination was occasionally observed on samples; silicone grease used on vacuum manifold is the source of this contamination and may increase PLL's $C_{1s}$ and $O_{1s}$ peak areas.

The effect of PLL concentration on its adsorption to FEP-$CO_2H$ was studied. Figure 3.4 and Table 3.3 show XPS and $\theta_A/\theta_R$ data for 400k PLL adsorbed to FEP-$CO_2H$ for 6 h. As was observed by Bonekamp and Lyklema[19] for PLL adsorption to silica and polystyrene sulfonate, a high affinity isotherm was observed for poly(L-lysine) adsorption to FEP-$CO_2H$.

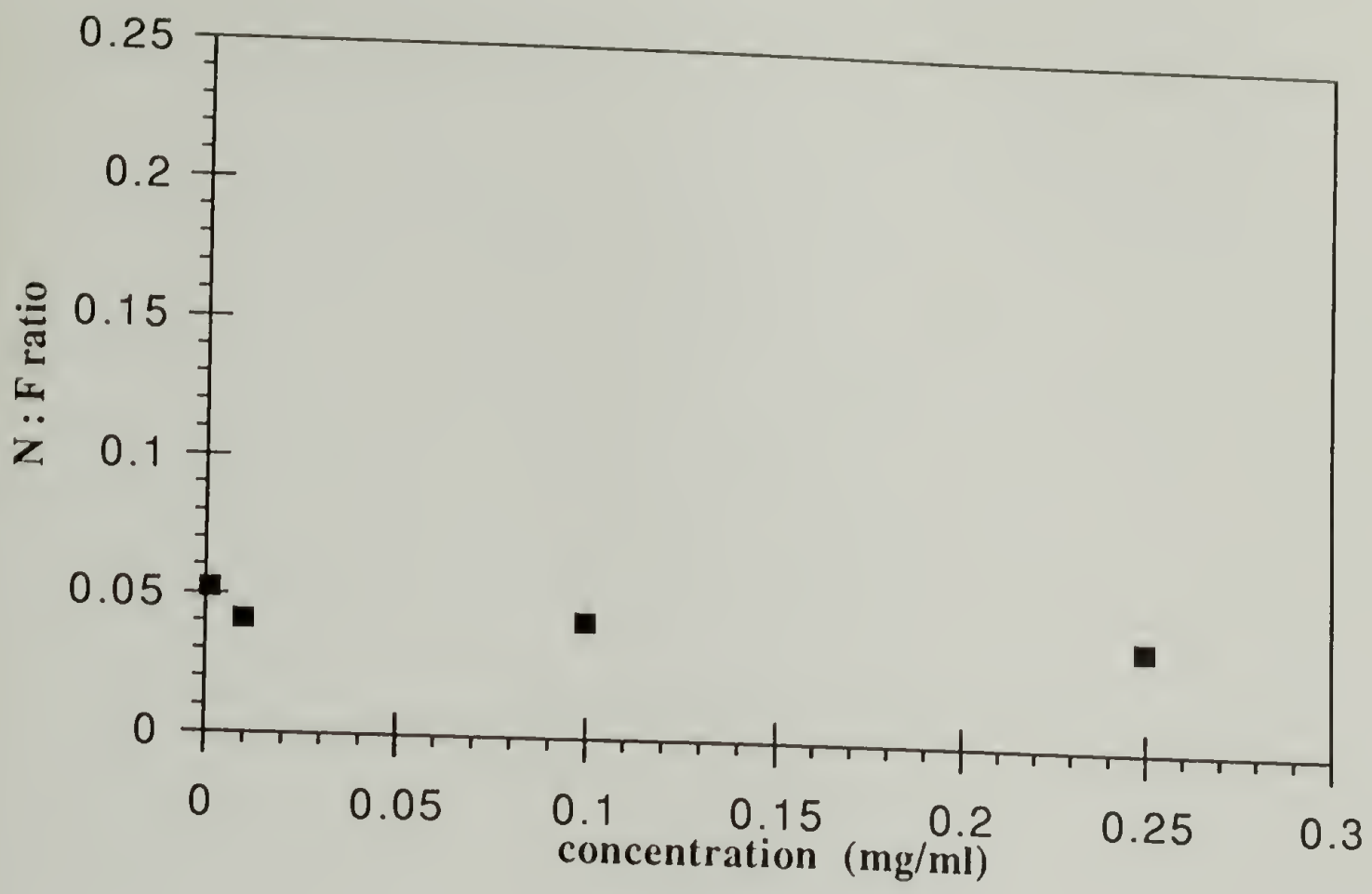


Figure 3.4 Effect of PLL (400k) Concentration on the Adsorbed Layer Thickness of FEP-$CO_2H$-PLL at pH 7.

Table 3.3 Effect of PLL (400k, 6 h) Concentration on the Adsorbed Layer Thickness of FEP-$CO_2H$-PLL (pH 7): XPS and Contact Angle Data. [III95]

| Concentration (mg/ml) | $C_{1s}$ PLL/FEP | N1s/F1s | C : F : O : N | $\theta_A/\theta_R$ |
|---|---|---|---|---|
| 0.001 | 0.834 | 0.052 | 100 : 91 : 15 : 5 | 75°/31° |
| 0.010 | 0.588 | 0.041 | 100 : 110 : 12 : 4 | 84°/44° |
| 0.100 | 0.681 | 0.042 | 100 : 103 : 14 : 5 | 80°/25° |
| 0.250 | 0.592 | 0.037 | 100 : 108 : 12 : 4 | 89°/47° |

The effect of PLL molecular weight on the amount adsorbed was studied. Figure 3.5 and Table 3.4 describe XPS and contact angle data for 0.1 mg/ml PLL adsorbed to FEP-$CO_2H$ at pH 7 for 24 h. As expected from both theoretical considerations[6] and previous experimental work,[9,10] the amount adsorbed is independent of molecular weight. The contact angles reflect the hydrophilic nature of the polymer film surfaces.

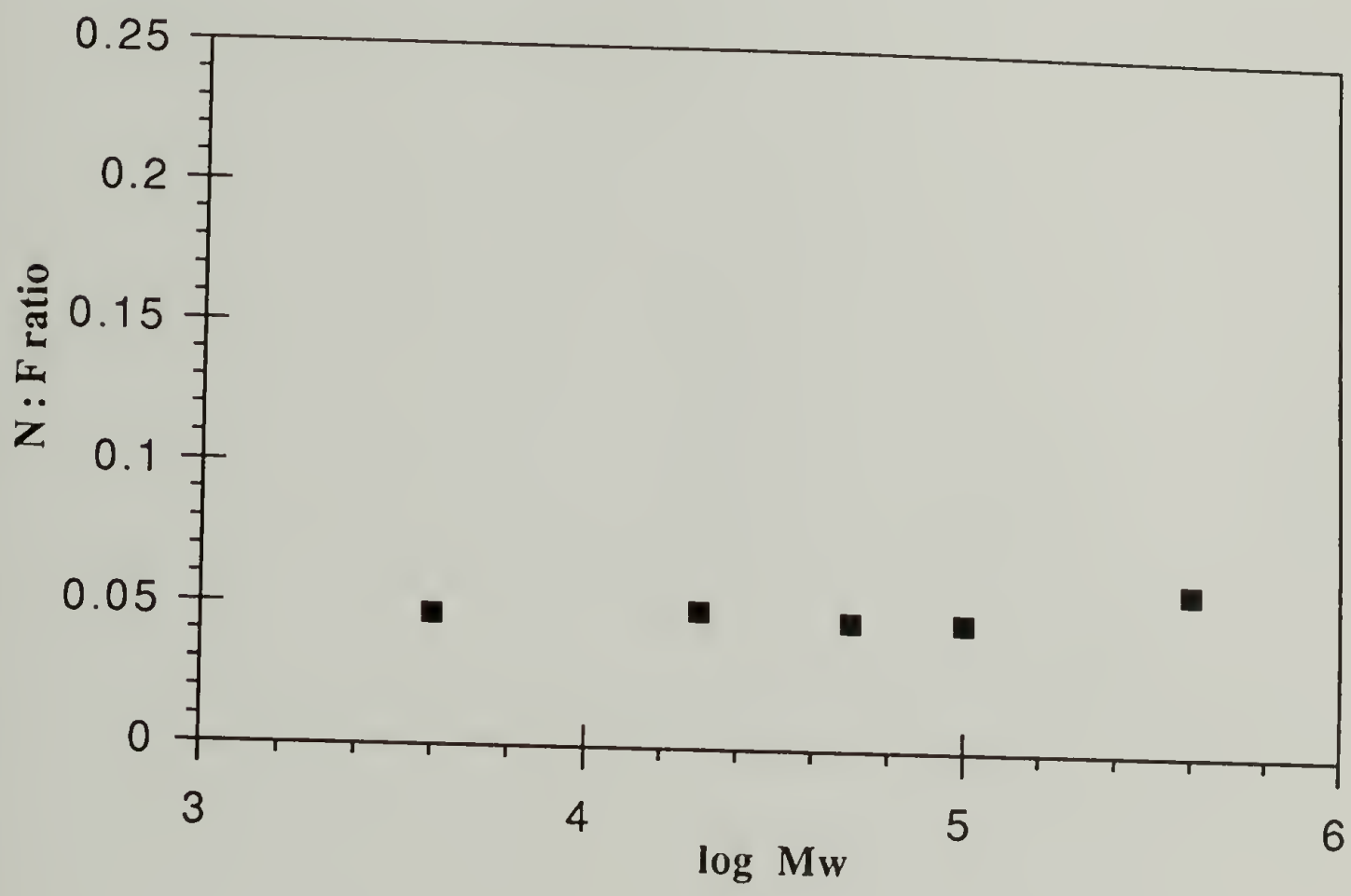


Figure 3.5 Effect of PLL Molecular Weight (0.1 mg/ml) on the Adsorbed Layer Thickness of FEP-$CO_2H$-PLL at pH 7.

Table 3.4 Effect of PLL (0.1 mg/ml, 24 h) Molecular Weight on the Amount Adsorbed to FEP-$CO_2H$ at pH 7: XPS and Contact Angle Data. [III94]

| Molecular Weight | $C_{1s}$ PLL/FEP | $N_{1s}/F_{1s}$ | C : F : O : N | $\theta_A/\theta_R$ |
|---|---|---|---|---|
| 4k | 0.971 | 0.047 | 100 : 105 : 18 : 5 | 81°/29° |
| 20k | 0.985 | 0.049 | 100 : 91 : 19 : 5 | 77°/29° |
| 50k | 0.883 | 0.046 | 100 : 110 : 17 : 5 | 77°/30° |
| 100k | 1.215 | 0.046 | 100 : 97 : 18 : 4 | 81°/32° |
| 400k | 1.657 | 0.058 | 100 : 79 : 17 : 5 | 78°/29° |

It is interesting to note that more 20k PLL adsorbs to FEP-$CO_2H$ at pH 7 ($N_{1s}/F_{1s}$ = 0.049) than to FEP at pH 11 ($N_{1s}/F_{1s}$ = 0.027). Conversely, more 400k PLL adsorbs to FEP (pH 11; $N_{1s}/F_{1s}$ = 0.156) than to FEP-$CO_2H$ (pH 7; $N_{1s}/F_{1s}$ = 0.058). At pH 7, PLL adsorption to FEP-$CO_2H$ is molecular weight-independent and involves specific electrostatic interactions. At pH 11, PLL adsorption to FEP is molecular weight-dependent and involves non-specific, weak interactions. In the FEP-PLL (pH 11) system, adsorption results from a balance of enthalpic gain and entropic loss; less PLL adsorbs at lower molecular weights because the entropic loss is greater with respect to the enthalpic gain than that of higher molecular weight PLL. More 20k PLL adsorbs to FEP-$CO_2H$ than to FEP because $\chi_s$ is enhanced by the electrostatic interaction at low molecular weight. At high molecular weight, loop and tail formation of the neutral and more compact ($\alpha$-helical) PLL enhance further adsorption. At ph 7, adsorption to FEP-$CO_2H$ is limited by lateral and segmental repulsions of PLL.

The driving forces for adsorption of PLL to FEP-$CO_2H$ are complicated by the heterogeneous nature of the polymer film surface which consists of both hydrophilic (carboxylate anions, carboxylic acid groups) and hydrophobic (FEP) regions. Polymer

adsorption to a heterogeneous surface where one component of the polymer has a particular affinity to one component of the surface has been discussed theoretically by Balazs *et al.*[20] Considering that adsorption of PLL to FEP at pH 7 does not occur without surface modification to FEP-$CO_2H$, the specific interaction between PLL-$NH_3^+$ and FEP-$CO_2^-$/H is the most important driving force for adsorption. It should be noted, however, that the hydrophilic groups account for only one in eight FEP repeat units: $(CF_2CF_2)_8CO_2H$. (Recall from Chapter I that FEP-$CO_2H$ used in the adsorption study was prepared by reducing FEP at 0 °C, 15 min followed by subsequent oxidation.) According to Balazs *et al.*, the ammonium groups which interact with the carboxylic acid functionality force adjacent ammonium groups above the hydrophobic regions. In addition, the PLL adsorbed conformation is likely extended across the FEP-$CO_2H$ surface as a result of (1) electrostatic repulsion between PLL ammonium groups and (2) attractive interactions between oppositely charged polyelectrolyte and surface groups. PLL likely adsorbs in a flat conformation where loops and tails are inhibited by electrostatic repulsion; because no salt was added, the segment-segment repulsions were not screened. In addition, lateral repulsion between PLL ammonium groups limit polymer adsorption.[21] The amount of PLL that adsorbed is low and independent of time, concentration and molecular weight.

At least two interactions drive the adsorption of PLL to FEP-$CO_2H$ at pH 7: (1) an ionic interaction between FEP-carboxylate and PLL-ammonium and (2) a hydrogen-bonding interaction between FEP-carboxylic acid and PLL backbone. In an attempt to better understand these two possible driving forces for adsorption they were studied in more detail.

## FEP-$CO_2H$-PLL: pH 4

The adsorption of PLL to FEP-$CO_2H$ was repeated in a pH 4 buffered solution to further investigate the importance of the hydrogen-bonding interaction as a possible driving force for adsorption. The ionic interaction between FEP-$CO_2H$ and PLL-$NH_3^+$ is minimized at pH 4 because both the ammonium groups of PLL and the carboxylic acid groups of FEP-$CO_2H$ are protonated (cf. Figure 1.11). Unlike the adsorption at pH 7 where both hydrogen bonding and ionic interactions are likely driving forces, that at pH 4 relies mostly on the former. Figure 3.6 compares the data of FEP-$CO_2H$-PLL adsorbed at pH 4 with that at pH 7 (24 h) while Table 3.5 summarizes the results obtained after 24 h and 72 h. The receding contact angles are slightly lower at pH 4 than at pH 7 because, as indicated by XPS data, more PLL adsorbed at the lower pH.

The amount of PLL adsorbed at pH 4 increased with molecular weight whereas that at pH 7 was independent of molecular weight. At pH 4, PLL adsorption to FEP-$CO_2H$ involves that of a charged polymer to a neutral surface. Thus the amount adsorbed is independent of surface charge density and likely a function of hydrogen bonding interactions. Unlike the pH 7 solution, that of pH 4 is buffered (0.05 M potassium acid phthalate). The presence of added electrolyte in the adsorption experiment affects the results. As was indicated by Bonekamp and Lyklema,[19] salt ions reduce lateral repulsion between chain segments by screening segment-segment interactions. The added salt enhances loop and tail formation which allows more polymer to adsorb. (At pH 7, PLL extends across the surface inhibiting further adsorption due to lateral repulsion.) The hydrogen bonding interaction between PLL and FEP-$CO_2H$ is an essential driving force for adsorption at pH 4 and likely an important one at pH 7.

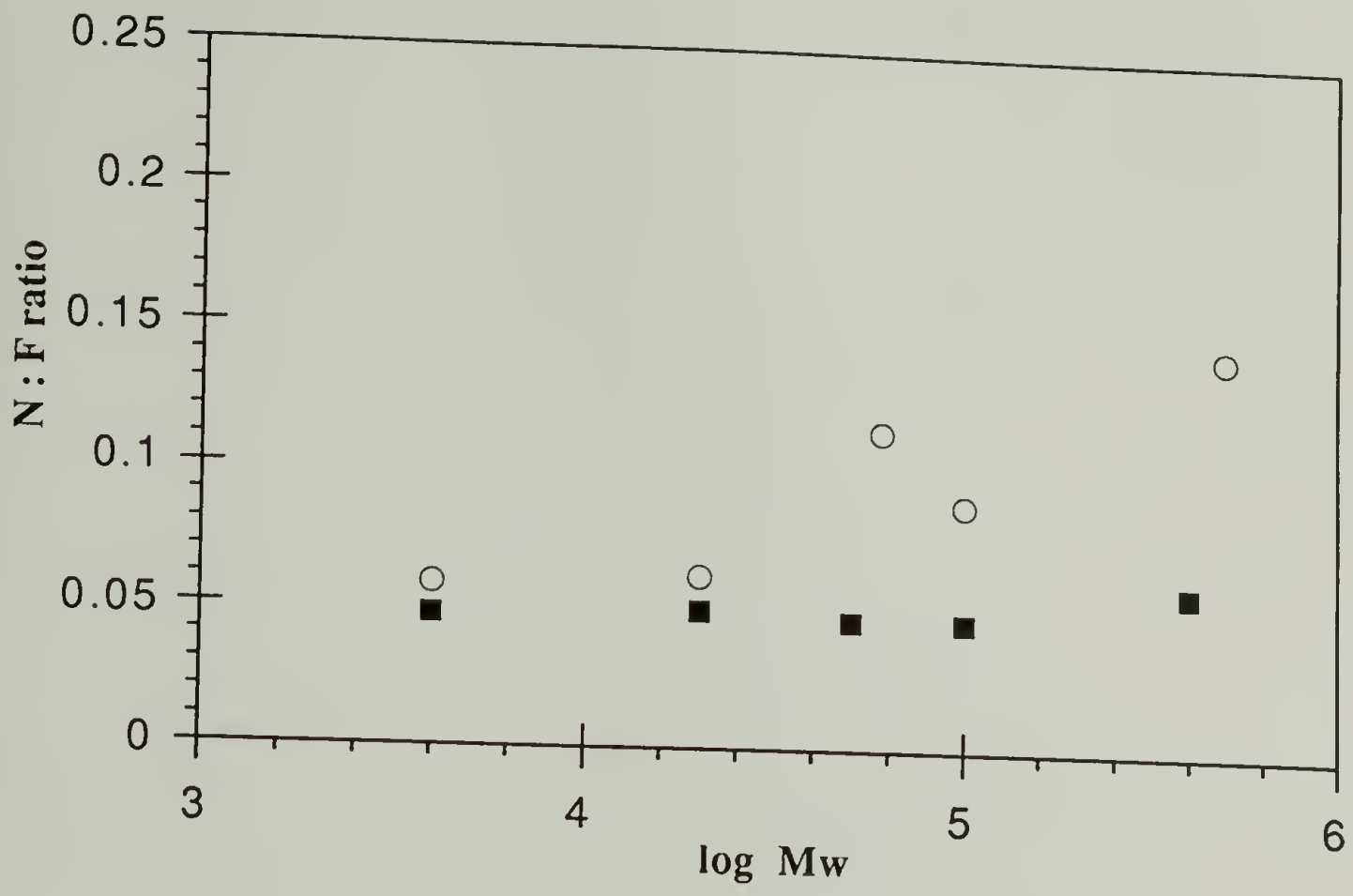


Figure 3.6 Comparison of the Adsorbed Layer Thickness of FEP-$CO_2H$-PLL at (O) pH 4 and (■) pH 7 in Terms of Molecular Weight (0.1 mg/ml).

Table 3.5 Adsorption of PLL (0.1 mg/ml) to FEP-$CO_2H$ from pH 4 Solution for 24 h and 72 h: XPS and Contact Angle Data.

| Molecular Weight | $C_{1s}$ PLL/FEP 24 h | $N_{1s}/F_{1s}$ 24 h | $\theta_A/\theta_R$ 24 h | $C_{1s}$ PLL/FEP 72 h | $N_{1s}/F_{1s}$ 72 h | $\theta_A/\theta_R$ 72 h |
|---|---|---|---|---|---|---|
| 4k | 1.02 | 0.058 | 87°/27° | 1.08 | 0.045 | 85°/39° |
| 20k | 1.15 | 0.061 | 84°/23° | 1.64 | 0.063 | 75°/27° |
| 60k | 1.57 | 0.114 | 73°/18° | 1.91 | 0.115 | 75°/24° |
| 100k | 1.35 | 0.088 | 84°/21° | 1.92 | 0.088 | 73°/20° |
| 500k | 2.71 | 0.144 | 73°/22° | 1.43 | 0.092 | 74°/25° |

FEP-$CH_2OH$-PLL: pH 7 [III130]

The surface must be oppositely charged to the polyelectrolyte for an attractive electrostatic interaction. Increasing the surface charge enhances the polyelectrolyte adsorption by providing more surface sites for interaction. Conversely, decreasing the surface charge density decreases the amount adsorbed.[22] While the surface charge density of FEP-$CO_2H$ is constant at pH 7, it limits the amount of PLL that adsorbs. The density of acidic groups is small, with a surface concentration of one per eight repeat units or $(CF_2CF_2)_8CO_2H$; at pH 7, approximately half of the groups are deprotonated. The ionic interaction between PLL-ammonium and FEP-carboxylate is sufficient for adsorption yet limited.

To determine whether the ionic interaction is an important driving force for the adsorption of PLL to FEP-$CO_2H$ at pH 7, the adsorption experiment was repeated at pH 7 with FEP-$CH_2OH$. By reducing the carboxylic acid group to the alcohol functional group, the surface charge density is decreased. (See Chapter I for more details on this reaction.) Figure 3.7 compares the amount of PLL (0.1 mg/ml, 24 h) adsorbed to FEP-$CH_2OH$ with that adsorbed to FEP-$CO_2H$; the $N_{1s}/F_{1s}$ XPS ratio is plotted against molecular weight. Table 3.6 includes XPS and contact angle adsorption data for FEP-$CH_2OH$-PLL at pH 7 for 24 h and 72 h. The amount of PLL adsorbed to FEP-$CH_2OH$ (and FEP-$CO_2H$) is independent of molecular weight. Although the differences in amount adsorbed are small, consistently less PLL adsorbed to FEP-$CH_2OH$ than to FEP-$CO_2H$ for all molecular weights studied. By reducing FEP-$CO_2H$ to FEP-$CH_2OH$, it can be argued that the ionic driving force has been either removed or decreased. In the former case, PLL would adsorb to FEP-$CH_2OH$ by a hydrogen bonding interaction. Unlike the adsorption at pH 4, the amount adsorbed does not increase with molecular weight; the added electrolyte at pH 4 likely accounts for this difference. In the latter case, the ionic interaction is important for

adsorption; less PLL adsorbs to FEP-$CH_2OH$ than to FEP-$CO_2H$ because there are fewer adsorption sites. The receding contact angles of FEP-$CH_2OH$-PLL are greater than those of FEP-$CO_2H$-PLL indicating that less PLL adsorbed to FEP-$CH_2OH$, as was observed by XPS. The ionic interaction between surface carboxylate and PLL-ammonium groups is limited by the density of surface charge groups.

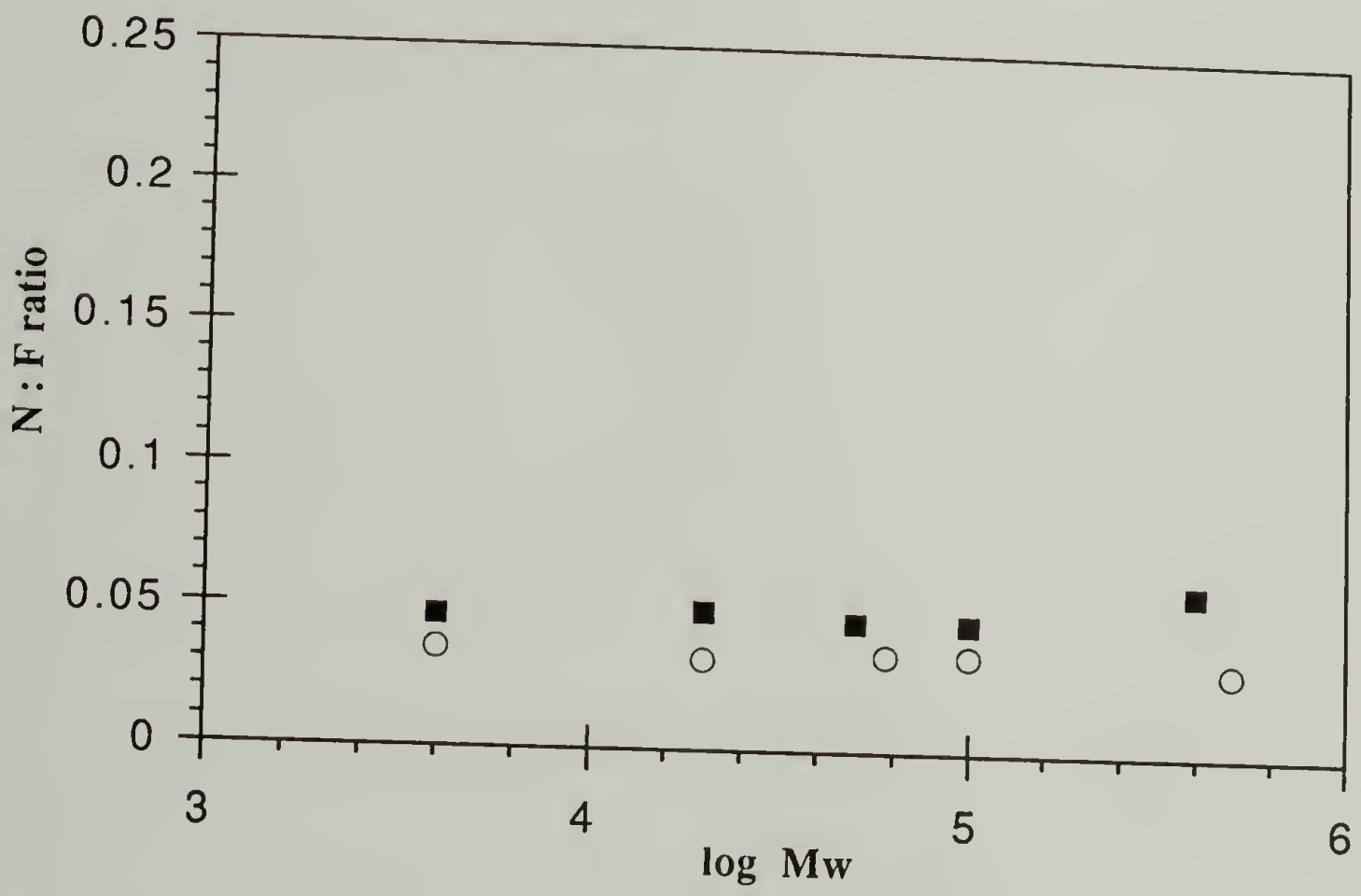


Figure 3.7 Comparison of the Adsorbed Layer Thickness of (■) FEP-$CO_2H$-PLL and (O) FEP-$CH_2OH$-PLL at pH 7 in Terms of Molecular Weight.

Table 3.6 Adsorption of PLL (0.1 mg/ml) to FEP-$CH_2OH$ at pH 7 for 24 h and 72 h: XPS and Contact Angle Data.

| Molecular Weight | $C_{1s}$PLL/FEP 24 h | $N_{1s}/F_{1s}$ 24 h | $\theta_A/\theta_R$ 24 h | $C_{1s}$PLL/FEP 72 h | $N_{1s}/F_{1s}$ 72 h | $\theta_A/\theta_R$ 72 h |
|---|---|---|---|---|---|---|
| 4k | 0.77 | 0.035 | 86°/41° | 0.69 | 0.030 | 90°/46° |
| 20k | 0.76 | 0.032 | 84°/40° | 0.62 | 0.029 | 81°/36° |
| 60k | 0.75 | 0.034 | 85°/43° | 0.39 | 0.024 | 90°/47° |
| 100k | 0.93 | 0.034 | 79°/37° | 0.69 | 0.026 | 85°/44° |
| 500k | 0.86 | 0.030 | 84°/44° | 0.66 | 0.028 | 84°/37° |

FEP-$CO_2H$-PLL: pH 11

Since the adsorbed amount of PLL decreased (relative to FEP-$CO_2H$) by reducing the surface charge density (FEP-$CH_2OH$), it was expected to increase by increasing the surface charge density. The number of surface sites was increased by exposing film samples to a pH 11 buffer solution where FEP-$CO_2H$ is deprotonated to FEP-$CO_2^-$. At pH 11, PLL is deprotonated, α-helical and consequently, unable to interact ionically with FEP-$CO_2^-$. The adsorption was not pursued in detail due to complications of the system: added salt (in the buffer solution), PLL solution conformation and its neutrality. (Regardless, PLL adsorbs to FEP-$CO_2H$ from the pH 11 solution.)

FEP-$CO_2H$-PLL: iPrOH/$H_2O$

The effect of the ionic interaction on the adsorption of PLL-ammonium to FEP-carboxylate was further studied by dissolving PLL in an aqueous alcohol solution where it forms a charged α-helix. In Figure 3.8, the $N_{1s}/F_{1s}$ XPS ratio is plotted as a function of

time; XPS and contact angle measurements are included in Table 3.7. PLL, when dissolved in either isopropanol/water (82:18, v/v) or methanol/water (96:4, v/v), adsorbs to FEP-$CO_2H$. Recall from Chapter II that PLL does not adsorb to FEP from either solution. Clearly, surface carboxylation is essential for adsorption where an ionic interaction between PLL-ammonium and FEP-carboxylate enhances adsorption. The amount of PLL adsorbed is limited by segment-segment and lateral repulsions and is independent of time of interaction.

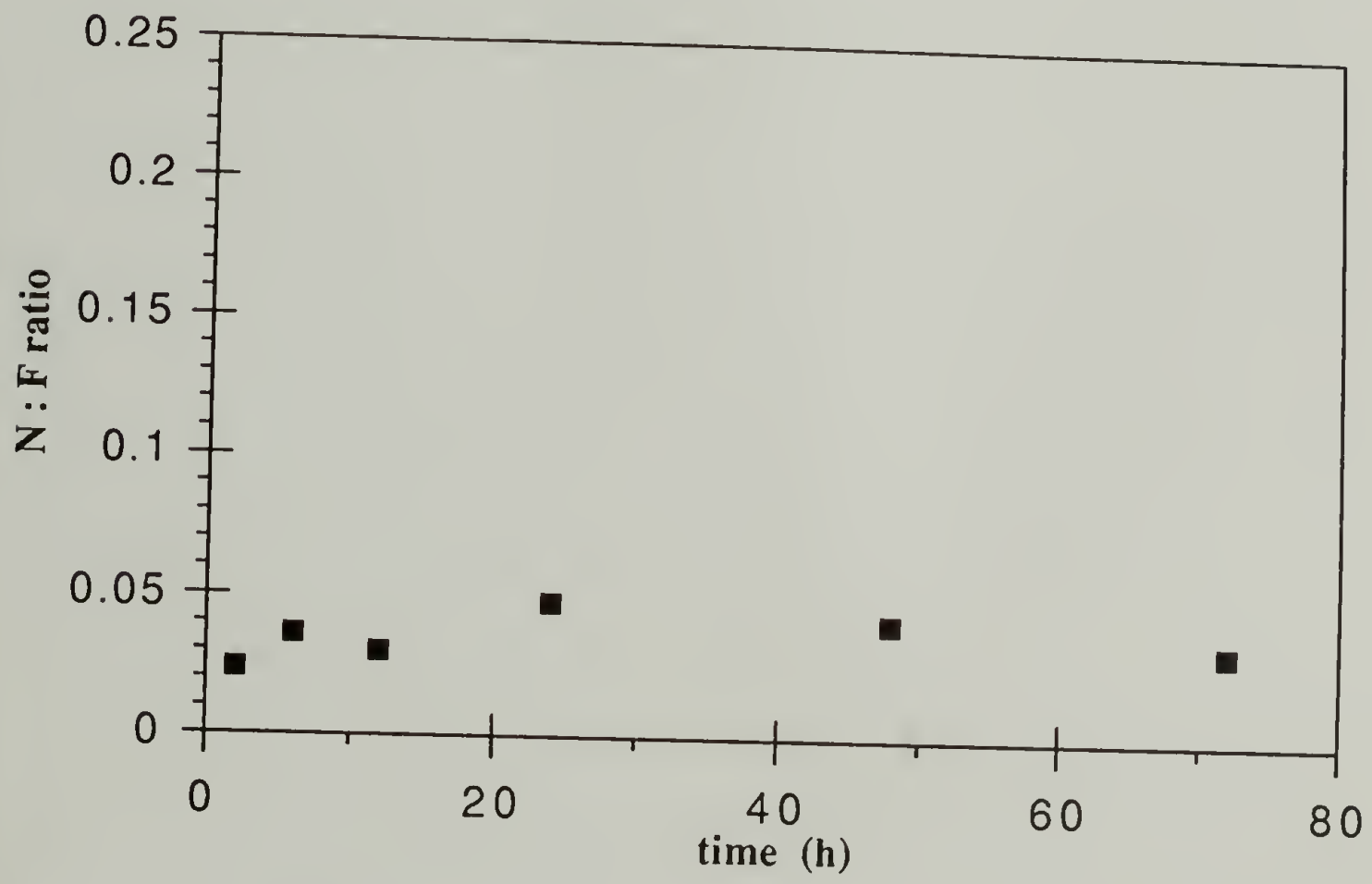


Figure 3.8 Effect of Time on the Adsorbed Layer Thickness for FEP-$CO_2H$-PLL (500k) from an Isopropanol/Water Solution.

Table 3.7 Adsorption of PLL (500k, 0.1 mg/ml) to FEP-$CO_2H$ from Isopropanol/Water: XPS and Contact Angle Data.

| Time (h) | C1s PLL/C1s FEP | N1s/F1s | $\theta_A/\theta_R$ |
|---|---|---|---|
| 2 | 0.16 | 0.024 | |
| 6 | 0.38 | 0.036 | 91°/48° |
| 12 | 0.22 | 0.030 | |
| 24 | 0.39 | 0.048 | 88°/36° |
| 48 | 0.34 | 0.042 | 89°/44° |
| 72 | 0.26 | 0.033 | |
| MeOH/$H_2O$: 24 h | 0.21 | 0.025 | 90°/35° |

Adsorption of PLL to FEP-$CO_2H$ at pH 7 is limited by the surface charge density of the polymer film substrate where both ionic and hydrogen-bonding interactions play an important role. The adsorbed PLL likely extends across the film surface in a predominantly train conformation where further adsorption is limited by charge repulsions between ε-ammonium groups. The data reported herein is consistent with the theoretical predictions of adsorption of a charged polymer to a charged surface.[3]

## Properties of FEP-$CO_2H$-PLL

The adsorption of PLL to FEP-$CO_2H$ changes the surface properties of the film sample. The properties that were investigated include wettability, solvent stability, chemical reactivity, peel strength and adhesion and growth of biological cells. The properties of film samples, FEP-$CO_2H$ and FEP-$CO_2H$-PLL, are compared and related to

those of FEP (and to FEP-PLL, where appropriate) which were discussed more fully in Chapter II.

Wettability of FEP-$CO_2H$-PLL

The wettability of a polymer film sample is determined by contact angle analysis using water as the probe fluid. Table 3.9 includes water contact angle data for the adsorption experiments described above and compares them with that of FEP (Chapter II). As is indicated in Table 3.9 (and Chapter I), the water contact angles ($\theta_A$ and $\theta_R$) of FEP decrease with surface carboxylation. Adsorption of PLL to surface-functionalized FEP film samples causes both advancing and receding contact angles to decrease. A decrease in the water contact angle corresponds to a more hydrophilic surface where water spreads on or wets the surface better. The receding contact angle decreases more substantially than the advancing contact angle because it is more sensitive to a small percentage of hydrophilic moieties on a heterogeneous surface.[23] Consequently, hysteresis between advancing and receding contact angles increases.

The "PLL-functionalized" film samples show lower contact angles than their unmodified film samples. Both $\theta_A$ and $\theta_R$ of FEP-$CO_2H$-PLL (pH 4) are lower than those of FEP-$CO_2H$-PLL (pH 7) reflecting the increased hydrophilicity of the former. Conversely, $\theta_A/\theta_R$ of FEP-$CH_2OH$-PLL are greater than those of FEP-$CO_2H$-PLL (pH 7) because less PLL adsorbed, rendering it more hydrophobic. The contact angle data reflect the trends observed by XPS.

Table 3.8 Wettability of Film Samples Compared Before and After PLL (~400k) Adsorption by Contact Angles Measurements.

| Film | Solvent | $\theta_A/\theta_R$ of Film | $\theta_A/\theta_R$ of Film-PLL |
|---|---|---|---|
| FEP | pH 7 | 115°/102° | 107°/70°* |
| FEP-$CO_2H$ | pH 4 | 101°/78° | 73°/22° |
| | pH 7 | 101°/61° | 78°/29° |
| | pH 11 | 97°/61° | 81°/35° |
| FEP-$CH_2OH$ | pH 7 | 95°/59° | 84°/44° |
| FEP-$CO_2H$ | iPr/$H_2O$ | 97°/61° | 88°/36° |
| FEP-$CO_2H$ | MeOH/$H_2O$ | 97°/61° | 90°/35° |

*Little or no adsorption observed.

Solvent Stability of FEP-$CO_2H$-PLL

FEP-$CO_2H$-PLL (400k, 0.001 mg/ml, 24 h) film samples were exposed to different work up conditions in an attempt to determine whether PLL could be displaced from FEP-$CO_2H$. The XPS data included in Table 3.9 show that neither water, methanol, nor methylene chloride displace PLL. PLL is not displaced by water, indicating possible irreversible adsorption.[24] Methanol (59°/38°) and likely methylene chloride both wet FEP-$CO_2H$ better than water (101°/61°) but were unable to displace PLL; this may have resulted, in part, from PLL's insolubility in methanol and methylene chloride. Difficulty in displacing PLL from FEP-$CO_2H$ is a result of both electrostatic attraction and hydrophobic interaction.[10] Although it was not tried, electrolyte may have displaced PLL.

Table 3.9 XPS Data for the Solvent Stability of the Adsorbed FEP-$CO_2H$-PLL Film Sample.

| Solvent | $C_{1s}$ PLL/FEP | $N_{1s}/F_{1s}$ | C : F : O : N |
|---|---|---|---|
| none | 1.059 | 0.049 | 100 : 109 : 16 |
| $H_2O$ (3 x 20 ml) | 1.794 | 0.066 | 100 : 87 : 22 : 6 |
| $H_2O$ (3 x 20 ml); $CH_3OH$ (3 x 20 ml) | 0.840 | 0.053 | 100 : 116 : 17 : 6 |
| $H_2O$ (3 x 20 ml); $CH_3OH$ (3 x 20 ml); $CH_2Cl_2$ (3 x 20 ml) | 0.942 | 0.054 | 100 : 112 : 20 : 6 |

## Chemical Reactivity of FEP-$CO_2H$-PLL

To determine whether adsorption of PLL affected the chemical reactivity of the FEP-$CO_2H$ film sample, the pendent ε-amine group of PLL was targeted for further chemical reaction. (FEP-$CO_2H$ was already shown to be more chemically reactive than FEP in Chapter I.) Several reagents were tried including trichloroacetyl chloride, 5-dimethylamino-1-naphthalene-sulfonyl chloride (dansyl chloride),[25] and fluorescein isothiocyanate;[26] however the best results were obtained with 3,5-dinitrobenzoyl chloride (3,5-DNBC) which are included below.

### FEP-$CO_2H$-PLL-3,5-Dinitrobenzamide (-3,5-DNBA)

The reaction between 3,5-dinitrobenzoyl chloride (3,5-DNBC) and the PLL-ε-amine is used to determine whether (1) adsorbed PLL can be used for further chemical modification and (2) reactivity of the primary amine is affected by the adsorbed conformation. The chemical reaction, described in Scheme 2.1, involves 3,5-

dinitrobenzoyl chloride in THF and pyridine catalysis.[27] The reaction was characterized by XPS, UV-vis, and $\theta_A/\theta_R$ analyses which are summarized in Table 3.11. (Typical XPS and UV-vis spectra were included in Figures 2.8 and 2.9, respectively.) The ATR IR spectra of FEP (control) and FEP-$CO_2H$-PLL-3,5-dinitrobenzamide are included in Figure 3.9 where the stretching frequency of the nitro group was evident at 1345 $cm^{-1}$ and 1541 $cm^{-1}$. The reaction between 3,5-dinitrobenzoyl chloride and FEP-$CO_2H$-PLL-$NH_2$ (20k, 0.1 mg/ml, 24 h) is clearly successful; the yield of the reaction is calculated from the XPS $N_{1s}$ atomic concentration ratio of $NO_2$ groups (representative of 3,5-DNBA) to $NH_2$ groups (representative of PLL). The yield is approximately 100% for PLL adsorbed from a charged, random coil-like conformation (pH 4 or pH 7). Recall from Chapter II that the yield of reaction is only ~65% for PLL adsorbed from a neutral α-helix conformation (pH 11). Likewise, PLL adsorbed to FEP-$CO_2H$ from pH 11 solution reacted in 66% yield. The reactivity of the ε-amine is affected by the conformation from which PLL adsorbed and thus its adsorbed conformation. PLL, adsorbed from the random coil-like conformation, is likely extended across the surface, exposing its amine groups to further chemical reaction. PLL, adsorbed from the α-helix conformation, likely only partially unfolds upon adsorption, inhibiting the access of some of its amine groups to 3,5-dinitrobenzoyl chloride. (These ε-amine groups may be involved in intermolecular hydrogen-bonding interactions similar to those of β-sheets.) The reaction yields of FEP-$CO_2H$-PLL pH 11 (66%) and pH 7 (100%) provide the best evidence for the hypothesis that the adsorbed conformation of PLL is different at pH 11 and pH 7.

The XPS and UV-vis data reflect the same trends in adsorbed amount. Both $C_{1s}$ PLL/FEP and $N_{1s}/F_{1s}$ ratios increased with the 3,5-DNBC reaction. The relative amount of PLL adsorbed can be compared using the UV-vis absorbance at 210 nm (corresponding to the electronic transitions of (C=O) groups). Relative to the adsorption to FEP-$CO_2H$ at pH 7, more PLL adsorbs from pH 4 solution and less adsorbs to FEP-$CH_2OH$. Both FEP-$CO_2H$ and FEP-$CH_2OH$ can react with 3,5-DNBC; however, the likelihood of this

reaction is minimized by the fact that the FEP functional groups are saturated by PLL (and likely overcompensated by PLL charged groups).[28] Contact angle data indicate the decreased hydrophilicity of the FEP-$CO_2H$-PLL-3,5-DNBA film sample with respect to that of FEP-$CO_2H$-PLL. The 3,5-dinitrobenzamide functional group is less hydrophilic than PLL, thereby increasing both advancing and receding contact angles.

Table 3.10 XPS, UV-vis, and Contact Angle Data for the Reaction between FEP-$CO_2H$-PLL and 3,5-Dinitrobenzoyl Chloride.

| Sample | *$C_{1s}$PLL/FEP | $N_{1s}/F_{1s}$ | $NO_2/NH_2$ | UV-vis A (210 nm) | $\theta_A/\theta_R$ |
|---|---|---|---|---|---|
| FEP-$CO_2H$-PLL (pH 7) | 1.28 | 0.107 | 0.98 | 0.016 | 89°/48° |
| FEP-$CO_2H$-PLL (pH 4) | 2.40 | 0.161 | 1.00 | 0.030 | 85°/34° |
| FEP-$CH_2OH$-PLL (pH 7) | 0.60 | 0.057 | 0.91 | 0.015 | 92°/56° |
| FEP-$CO_2H$-PLL (pH 11) | 4.63 | 0.373 | 0.66 | 0.044 | 81°/42° |

*The PLL $C_{1s}$ region includes the aromatic functionality of 3,5-dinitrobenzamide.

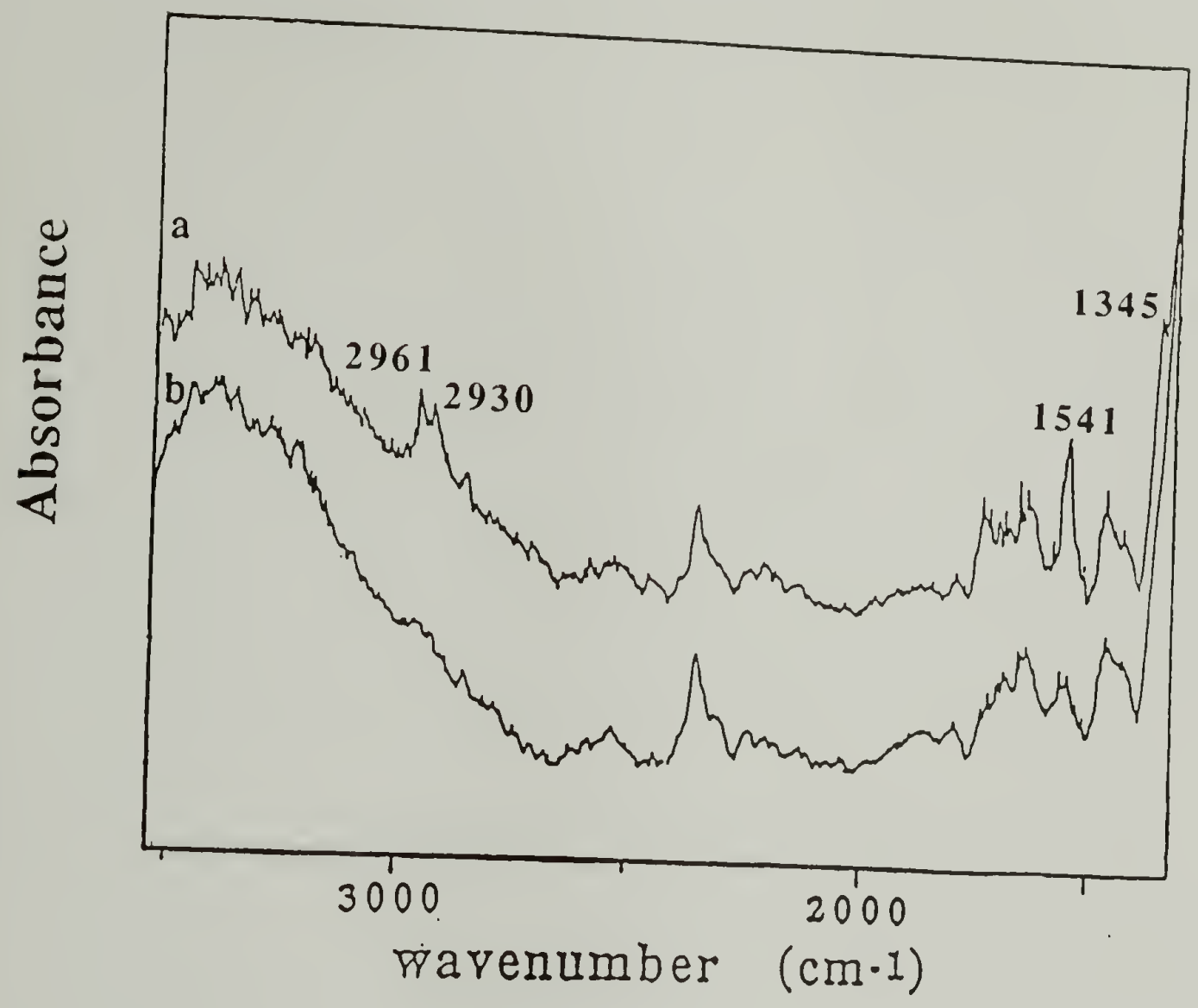


Figure 3.9 ATR IR Spectra of (a) FEP-$CO_2H$-PLL-3,5-DNBA and (b) FEP (Control).

Adhesion

Adhesion results from attractive forces between an adhesive and an adherend which include van der Waals forces, hydrogen bonds and chemical bonds.[29] For the former, intimate contact or wettability is required. The adhesive joint is enhanced by both polar interactions which contribute to the attraction of adhesive and adherend and roughness which allows greater molecular contact.

The 180° peel test is used to determine whether surface modification of FEP, to FEP-$CO_2H$ and FEP-$CO_2H$-PLL (20k, 0.1 mg/ml), improves its adhesion properties. (See Figure 2.1 for experimental set-up.) In this way, the peel test is also used as an

analytical technique to distinguish between the chemically diverse FEP film surfaces. The film samples are identical and smooth by scanning electron microscopy (to ~50 Å) yet distinct by both x-ray photoelectron spectroscopy (to ~10 Å) and contact angle analysis. The peel test data for adhesives 3M #850 and 3M #750 are included in Table 3.11 along with XPS and contact angle data of the peeled samples. Since both 3M tapes had acrylic adhesives, the trends observed were similar. A greater peel force was required to remove the adhesive from both FEP-$CO_2H$ and FEP-$CO_2H$-PLL than FEP; however, the difference between FEP-$CO_2H$ and FEP-$CO_2H$-PLL was indistinguishable. (The chart recordings of the peel tests were included in Figures 2.10 and 2.11 for 3M #850 and 3M #750, respectively.) The polar functionalities of both carboxylic acid and amino acid groups likely enhance the strength of the adhesive bond; roughness may also contribute to the improved adhesion.

Table 3.11 FEP-$CO_2H$-PLL Peel Test Study: Peel Strength, XPS, and Contact Angle Data.

| Sample (Film - Adhesive Peeled) | Peel Force (g/cm) | XPS **not** peeled | XPS peeled | peeled* $C_{1s}$LBE/FEP; $N_{1s}/F_{1s}$ | $\theta_A/\theta_R$ **not** peeled | $\theta_A/\theta_R$ peeled |
|---|---|---|---|---|---|---|
| FEP-$CO_2H$-850 | 135±5 | $C_{88}F_{200}O_{10}$ | $C_{135}F_{200}O_{15}$ | 0.28; n/a | 101°/56° | 99°/61° |
| FEP-$CO_2H$-PLL-850 | 136±8 | $C_{196}F_{200}O_{29}N_{10}Si_2$ | $C_{210}F_{200}O_{34}N_6Si_4$ | 1.35; 0.032 | 74°/29° | 86°/43° |
| FEP-$CO_2H$-750 | 160±8 | $C_{88}F_{200}O_{10}$ | $C_{198}F_{200}O_{24}$ | 0.95; n/a | 101°/56° | 110°/54° |
| FEP-$CO_2H$-PLL-750 | 141±7 | $C_{196}F_{200}O_{29}N_{10}Si_2$ | $C_{444}F_{200}O_{98}N_7$ | 7.28; 0.035 | 74°/29° | 104°/32° |

*The low binding energy (LBE) $C_{1s}$ peak includes PLL and acrylic adhesive intensities.

The XPS and contact angle data indicate the loci of failure of the two film samples. From XPS analysis (Figure 3.10, Table 3.11) the atomic concentrations of both carbon and oxygen increase after peeling, indicating cohesive failure of the adhesive. For 3M #850, the contact angle of FEP-$CO_2H$ changed insignificantly while that of FEP-$CO_2H$-PLL increased appreciably after peeling. Because the adhesive failed, the two film samples could not be distinguished by peeling data. However, XPS and contact angle data reveal more adhesive on the FEP-$CO_2H$-PLL film sample; the adhesive likely interacts more strongly with FEP-$CO_2H$-PLL making failure more prominent. The trend observed for 3M #850 was emphasized with 3M #750, where a much greater amount of adhesive was present on FEP-$CO_2H$-PLL than FEP-$CO_2H$. In this case, the advancing contact angle, responsive to the hydrophobic moieties, increased more substantially than the receding contact angle, sensitive to the hydrophilic groups. The increased polarity of PLL likely accounts for the stronger interaction observed between adhesive and FEP-$CO_2H$-PLL than FEP-$CO_2H$. From this data alone, it is difficult to determine if the FEP-$CO_2H$-PLL interface failed. (XPS data could not be obtained on the adhesive because the pressure in the vacuum chamber was too great for analysis.)

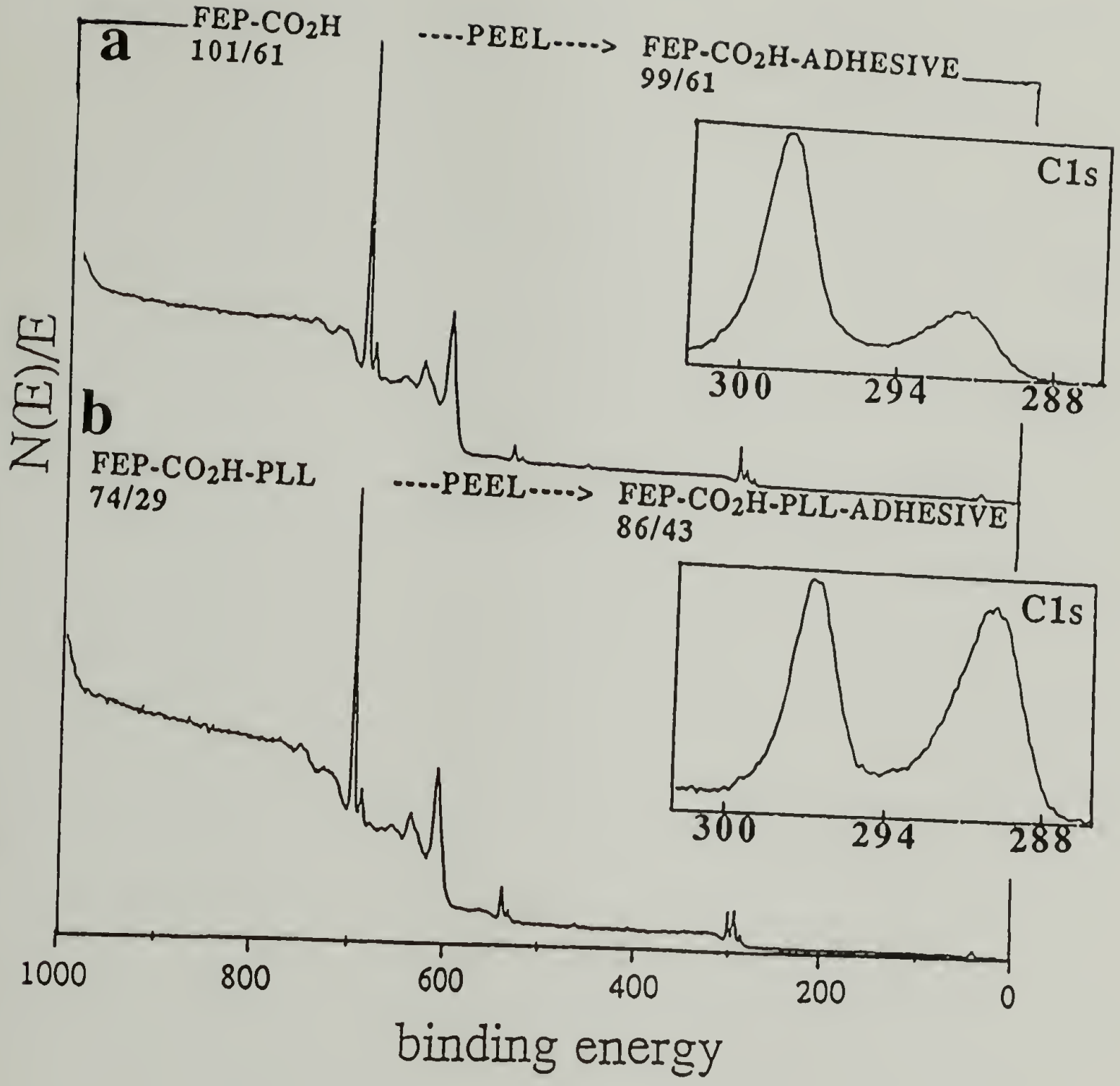


Figure 3.10 XPS Survey and $C_{1s}$ (15° takeoff angle) Spectra of Peeled Film Samples: (a) FEP-$CO_2H$ and (b) FEP-$CO_2H$-PLL.

Adhesion and Growth of Biological Cells [III120-4, IV15-17, 19]

The adhesion and growth of biological cells were used to distinguish between FEP-$CO_2H$ and FEP-$CO_2H$-PLL film samples. Previous studies on poly(ethylene terephthalate),[30] polysulfone,[31] and polyacrolein microspheres.[32] indicate that the PLL-

coated material shows improved cell growth relative to the uncoated material. HeLa cells were used in this study because they grow more efficiently on positively charged microcarriers.[33] Unlike endothelial cells which produce an extracellular matrix on which to grow, HeLa cells interact directly with the substrate.[34] As indicated in Table 3.13 HeLa cells adhered more strongly to FEP-$CO_2H$-PLL than to FEP-$CO_2H$, possibly as a result of an ionic attraction[35] between the negatively charged HeLa cell membrane and positively charged PLL and/or repulsion between HeLa cell membrane and carboxylate/carboxylic acid-functionalized FEP-$CO_2H$.

Table 3.12 Adhesion of HeLa Cells to FEP-$CO_2H$ and FEP-$CO_2H$-PLL Film Substrates.

| Film Sample | Initial # HeLa cells | Final # HeLa Cells | % HeLa Cells Adhered |
|---|---|---|---|
| FEP-$CO_2H$ | 50 | 20 | 40 |
| FEP-$CO_2H$-PLL | 450 | 250 | 56 |

The growth curves of HeLa cells on FEP-$CO_2H$ and FEP-$CO_2H$-PLL are included in Figure 3.11 with those of FEP and FEP-PLL. (Figure 3.12 includes photographs of the cells taken on the fourth day of growth on each film sample.) The modified film samples (FEP-PLL, FEP-$CO_2H$, FEP-$CO_2H$-PLL) were easily distinguished from FEP by HeLa cell growth. It was more difficult to distinguish between the modified film samples by this technique for reasons beyond the scope of this thesis dissertation.

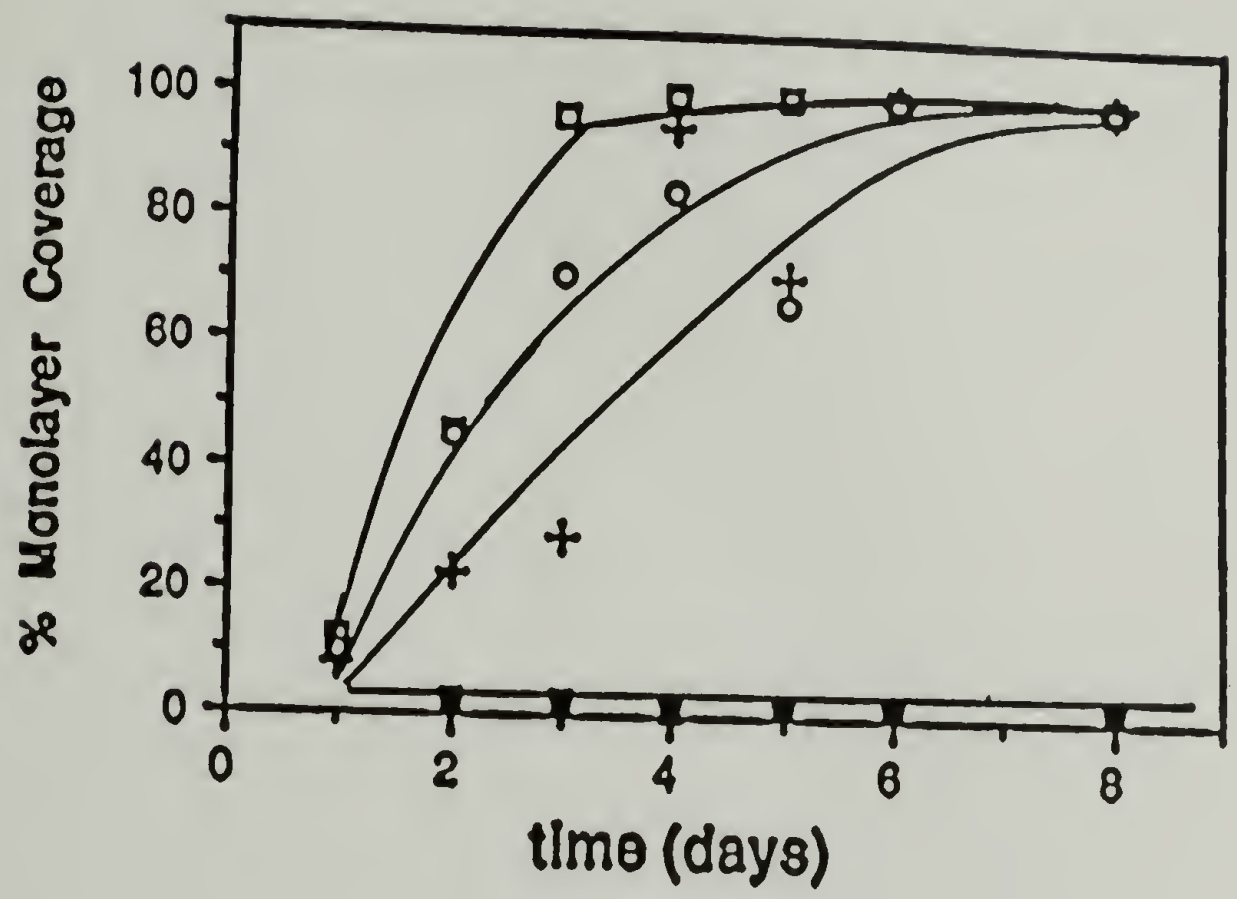


Figure 3.11 HeLa Cell Growth Curves of (■) FEP, (□) FEP-PLL, (+) FEP-$CO_2H$, and (○) FEP-$CO_2H$-PLL.

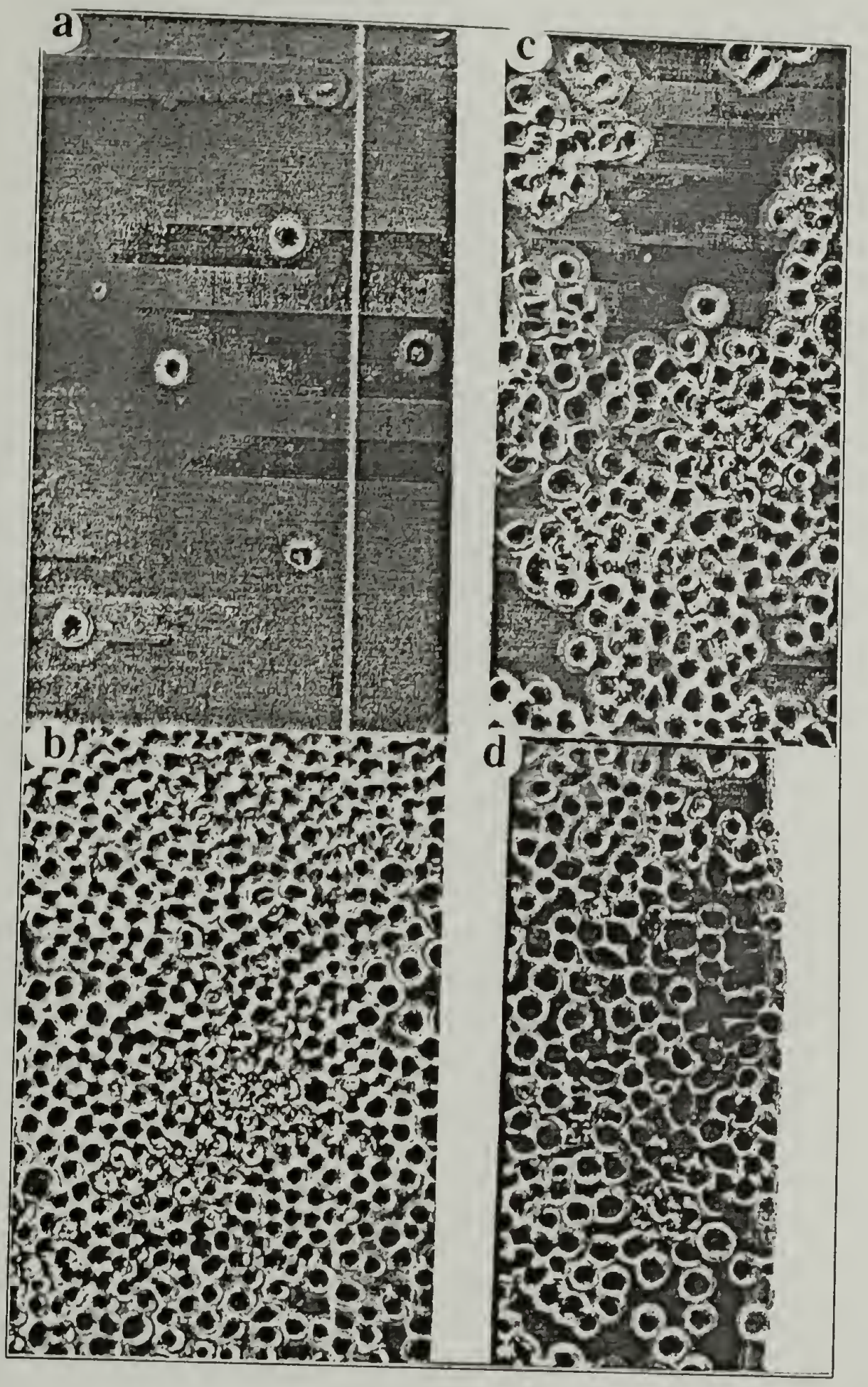


Figure 3.12 Optical Microscope Photographs on Fourth Day of HeLa Cell Growth on (a) FEP, (b) FEP-PLL, (c) FEP-$CO_2H$, (d) FEP-$CO_2H$-PLL.

In another attempt to differentiate film samples, endothelial cell growth was studied. Figures 3.13 and 3.14 include growth curves and photographs taken of the cells on the fourth day, respectively. As was observed for HeLa cells, FEP was easily distinguished from the modified FEP film samples by endothelial cell growth. However, modified film samples could not be distinguished by this technique possibly because endothelial cells do not grow directly on a surface but rather produce an extracellular matrix on which to grow. The large increase in growth observed on day 4 likely resulted from replenishing the serum the previous day.

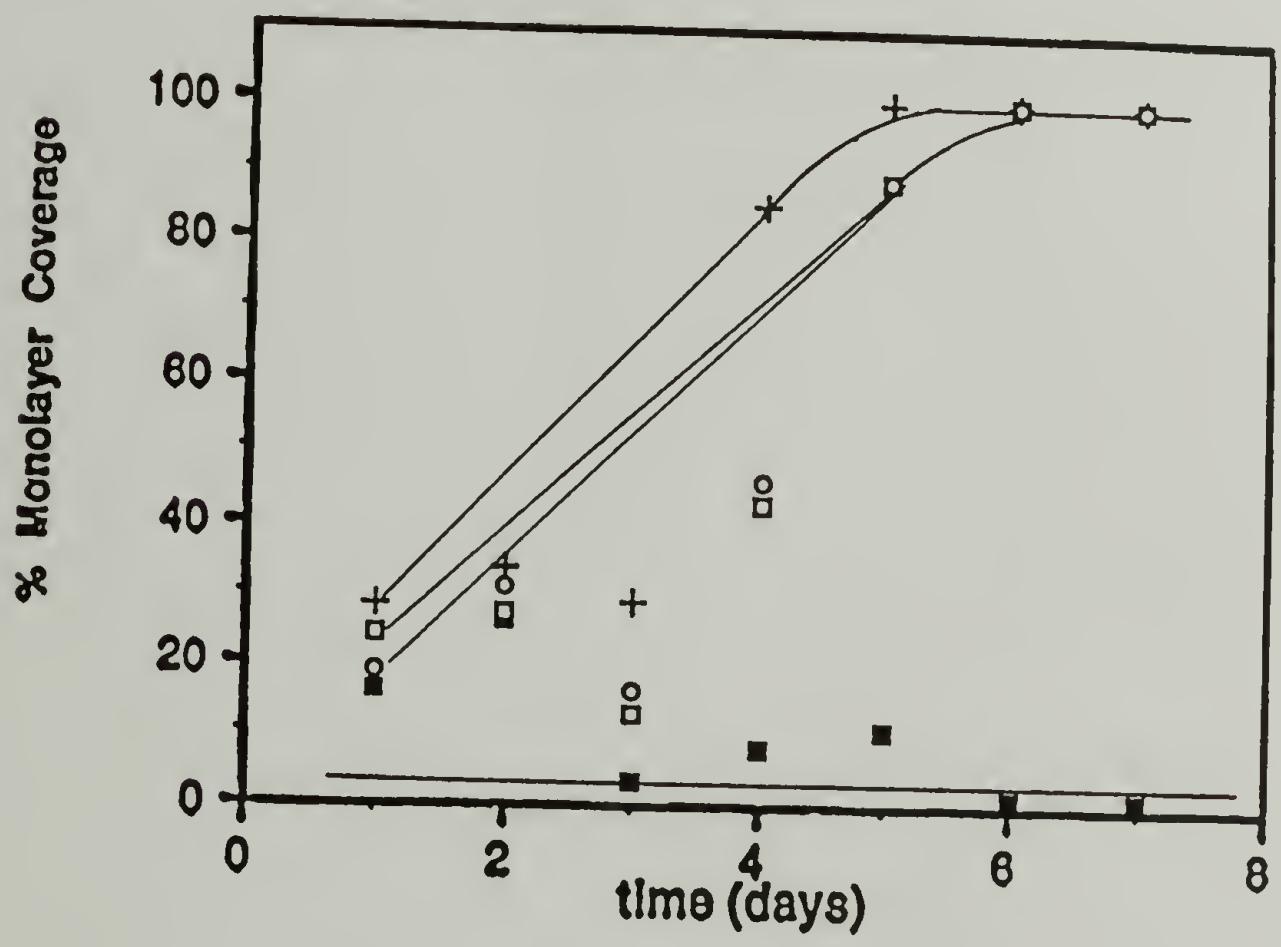


Figure 3.13 Endothelial Cell Growth Curves of (■) FEP, (□) FEP-PLL, (+) FEP-$CO_2H$, and (O) FEP-$CO_2H$-PLL.

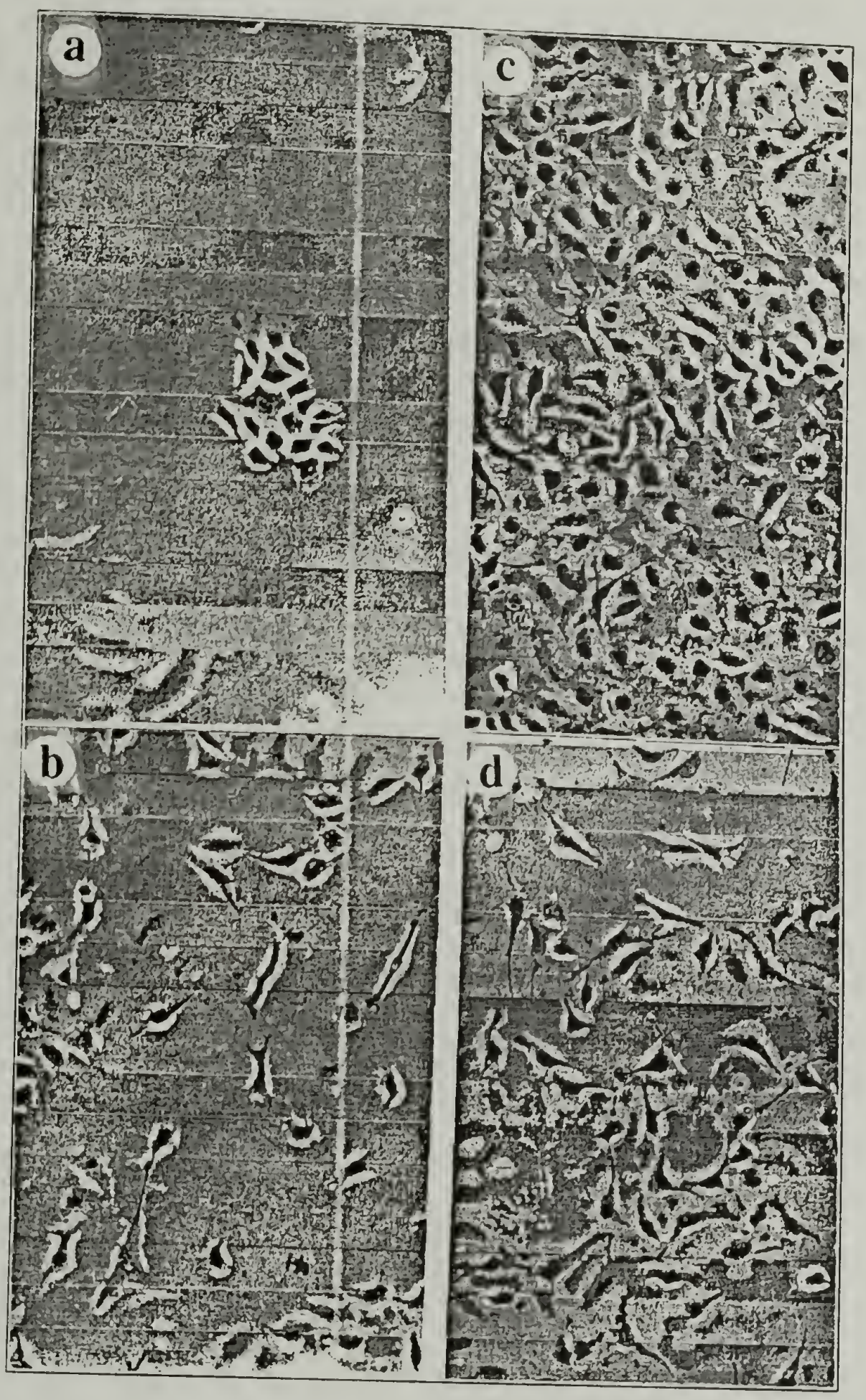


Figure 3.14 Optical Microscope Photographs Taken on Fourth Day of Endothelial Cell Growth on (a) FEP, (b) FEP-PLL, (c) FEP-$CO_2H$, (d) FEP-$CO_2H$-PLL.

## Conclusions

PLL adsorbs to FEP-$CO_2H$ (pH 7) by both an ionic attraction between PLL-ammonium and FEP-carboxylate and a hydrogen-bonding interaction between PLL backbone and FEP-carboxylic acid. At lower pH (pH 4) where both ammonium and carboxylate groups are protonated (to carboxylic acid), the amount adsorbed depends mostly upon hydrogen-bonding interactions. While the adsorption at pH 7 showed time-, concentration- and molecular weight-independence that at pH 4 showed molecular weight-dependent adsorption. The surface charge density of FEP-$CO_2H$ limited the amount adsorbed at pH 7 but not at pH 4 where the surface charges were neutralized. In addition, the electrolyte present in the pH 4 buffer solution likely screened lateral and segment-segment repulsions, enhancing loop and tail formation and thus the amount of PLL adsorbed. The effect of surface charge density on the amount adsorbed was studied by comparing the adsorption of PLL to FEP-$CH_2OH$ and FEP-$CO_2H$; less PLL adsorbed to FEP-$CH_2OH$ which had fewer surface sites available for ionic interactions as a result of its decreased surface charge density.

The FEP-$CO_2H$-PLL film samples were further characterized in terms of wettability, solvent stability, chemical reactivity, adhesion, and biological cell adhesion and growth. Adsorption of PLL to FEP-$CO_2H$ decreases its water contact angles indicating a more hydrophilic film surface. PLL was not displaced from FEP-$CO_2H$ by water indicating possible irreversible adsorption. The PLL-ε-amine reacts quantitatively with 3,5-dinitrobenzoyl chloride when adsorbed from the random coil conformation; the reaction yield is only ~65% for PLL adsorbed from the α-helix conformation. Approximately 35% of PLL-ε-amine groups (adsorbed at pH 11) are unavailable for further chemical reaction. FEP-$CO_2H$ and FEP-$CO_2H$-PLL show similar peel forces due to cohesive failure of the adhesive. From biological cell growth and adhesion studies, it was shown that PLL enhances the adhesion and growth of cells on FEP film samples.

## References


1. For examples see Ward, W. J.; McCarthy, T. J. in *Encyclopedia of Polymer Science and Engineering*, 2nd. ed.; Supplement, Wiley: New York, 1989, p. 674 and references cited therein.

2. Van der Schee, H.A.; Lyklema, J. *J. Phys. Chem.* **1984**, *88*, 6661.

3. Evers, O.A; Fleer, G.J; Scheutjens, J.M.H.M.; Lyklema, J. *J. Colloid Interface Sci.* **1985**, *111*, 446.

4. (a) Scheutjens, J.M.H.M.; Fleer, G.J. *J. Chem. Phys.* **1979**, *83*, 1619;
(b) Scheutjens, J.M.H.M.; Fleer, G.J. *J. Chem. Phys.* **1980**, *84*, 178.

5. Roe, R.J. *J. Chem. Phys.* **1974**, *60*, 4192.

6. Cohen Stuart, M.A.; Fleer, G.J.; Lyklema, J.; Norde, W.; Scheutjens, J.M.H.M. *Adv. Colloid Interface Sci.* **1991**, *34*, 477.

7. Davies, R.J.; Dix, L.R.; Toprakcioglu, C. *J. Colloid Interface Sci.* **1989**, *129*, 145.

8. Panitz, J.A. *Ultramicroscopy* **1983**, *11*, 161.

9. Furusawa, K.; Kanesaka, N.; Yamashita, S. *J. Colloid Interface Sci.* **1984**, *99*, 341.

10. Bonekamp, B.C.; Alvarez, R. H.; De Fas Nieves, F.J.; Bijsterbosch, B.H. *J. Colloid Interface Sci.* **1987**, *118*, 366.

11. Greenfield, N.; Fasman, G.D. *Biochemistry* **1969**, *8*, 4108.

12. Shoichet, M.S.; McCarthy, T.J. *Macromolecules* **1991**, *24*, 982.

13. Kolthoff, I.M.; Sandel, E.B.; Meehan, E.J.; Bruckenstein, S. *Quantitative Chemical Analysis*, 4th ed. The MacMillan Co.: Toronto, 1969, p. 1163.

14. For example see Bening, R.C.; McCarthy, T.J. *Macromolecules* **1990**, *23*, 2648.

15. Stouffer, J.M.; McCarthy, T.J. *Macromolecules* **1988**, *21*, 1204.

16. Iyengar, D.R.; Brennan, J.V.; McCarthy, T.J. *Macromolecules* **1991**, *24*, 5886.

17. Shoichet, M.S; McCarthy, T.J. in *Materials Synthesis Based on Biological Processes* (Alper, M.; Calvert, P.; Frankel, R.; Rieke, P.; Tirrell, D., Eds.); Materials Research Society Symposium Proceedings, 1990, vol. 218, Materials Research Society: Pittsburgh, 1991, p. 57.

18. A small percentage of the $O_{1s}$ peak attributed to PLL results from the carboxylic acid of FEP-$CO_2H$.

19. Bonekamp, B.C.; Lyklema, J. *J. Colloid Interface Sci.* **1986**, *113*, 67.

20. Balazs, A.C.; Gempe, M.; Zhou, Z. *Macromolecules* **1991**, *24*, 4918.

21. Blaakmeer, J.; Bohmer, M.R.; Cohen Stuart, M.A.; Fleer, G.J. *Macromolecules* **1990**, *23*, 2301.

22. Papenhuijzen, J.; Van der Schee, H.A.; Fleer, G.J. *J. Colloid Interface Sci.* **1985**, *104*, 540.

23. Johnson, R.E., Jr.; Dettre, R.H. *J. Phys. Chem.* **1964**, *68*, 1744.

24. Cohen Stuart, M.A.; Scheutjens, J.M.H.M.; Fleer, G.J. *J. Polym. Sci.: Polym. Phys. Ed.* **1980**, *18*, 559.

25. (a) Airhart, J.; Sibiga, S.; Sanders, H.; Khairallah, E.A. *Anal. Biochem.* **1973**, *53*, 132; (b) Jacobsen, C.; Jacobsen, J. *Biochem. J.* **1979**, *181*, 251.

26. van den Beld, C.M.B.; Lingeman, H.; van Ringen, G.J.; Tjaden, U.R.; van der Greef, J. *Anal. Chim. Acta* **1988**, *205*, 15.

27. Pirkle, W.H.; Hyun, M.H. *J. Org. Chem.* **1984**, *49*, 3043.

28. Cohen Stuart, M.A. *J. Phys. France* **1988**, *49*, 1001.

29. Owens, D.K.; Wendt, R.C. *J. Appl. Polym. Sci.* **1969**, *13*, 1741.

30. Asako, S.; Hirai, Y.; Okita, K.; Matsubara, H.; Niwa, S.; Takashina, M. *Jpn Kokai Tokkyo Koho* JP 63,196,282 [88,196,282] **1987**. [CA 110:113245s]

31. Asako, S.; Hirai, Y.; Okita, K.; Matsubara, H.; Niwa, S.; Takashina, M. *Jpn Kokai Tokkyo Koho* JP 63,198,978 [88,198,978] **1987**. [CA 110:113252s]

32. Lazar, A.; Silverstein, L.; Margel, S.; Mizrahi, A. *Dev. Biol. Stand.* **1985**, *60*, 457.

33. Jacobson, B.S.; Ryan, U.S. *Tissue and Cell* **1982**, *14*, 69.

34. Jacobson, B.S. *Adv. Cell Biol.* **1988**, *2*, 91.

35. Jacobson, B.S.; Branton, D. *Science*, **1977**, *195*, 302.

# CHAPTER IV

# SYNTHESIS OF POLY(ETHYLENE OXIDE) DERIVATIVES AND THEIR ADSORPTION AT AQUEOUS INTERFACES

## Overview

Poly(ethylene oxide) (PEO) and end-capped PEO are synthesized for adsorption experiments. In Chapter II, it was shown that poly(L-lysine) (PLL) adsorbs to poly(tetrafluoroethylene-co-hexafluoropropylene) (FEP) from an aqueous solution by a hydrophobic interaction (Chapter II). While the adsorption can be controlled by solvent choice, it is not an ideal system to study due to the polydispersity of PLL. To overcome polydispersity effects and to further study the hydrophobic interaction as a driving force for adsorption, monodisperse poly(ethylene oxide) (PEO) was synthesized and end-capped with hydrophobic groups. PEO was end-capped with perfluoroalkyl or alkyl (linear and branched) end groups to form PEO-R. The adsorption of PEO-R was compared to that of PEO at three aqueous interfaces: with fluoropolymer film, polystyrene latex, and air. This chapter begins with a literature review of poly(ethylene oxide) synthesis and adsorption. Synthesis of PEO, PEO-R and R groups are discussed before comparing their adsorption at aqueous interfaces.

## Introduction

PEO has interesting and distinct solution properties that make it desirable for use in several industries as either a lubricant or a surfactant. PEO is used in the pharmaceutical, detergent, and food industries because it is water soluble, nonionic, of low toxicity, biodegradable, and it decomposes to volatile products. Approximately 60% of PEO

produced is used in automotive antifreeze. Additional applications of PEO include those in adhesives, cosmetics, water treatment, flocculation, hydrodynamic drag reduction, photography, and wood products preservation.[1] PEO is soluble in a number of solvents[2] such as water (between 18 °C and ~97 °C), aqueous potassium sulfate, aqueous magnesium sulfate, alcohols, benzene, chloroform, cyclohexane, esters, dimethylformamide, and acetonitrile. PEO is insoluble in other solvents such as aliphatic hydrocarbons, ethers, and dioxane. When dissolved in water, PEO affects the structure of water; molecules organize about the PEO backbone by hydrogen bonding to the ether oxygen of the PEO repeat unit.[3]

## Synthesis

Ethylene oxide can be polymerized using cationic, anionic, or coordinate anionic initiation.[4] Cationic polymerization suffers from side reactions where dimers (dioxane) or cyclic oligomers are formed; molecular weight and polydispersity are not easily controlled.[3] Anionic polymerization, however, produces polymer of known molecular weight and narrow molecular weight distribution. Aida and Inoue[5,6] produced narrow molecular weight distribution poly(ethylene oxide) and copolymers by a living polymerization technique where the polymer molecular weight could be predicted from the molar ratio of the monomer to catalyst; ethylene oxide is polymerized by insertion into the aluminum-chlorine bond of the catalyst, 5,10,15,20-tetraphenylporphine-diethylaluminum chloride.

Work in the field of anionic polymerization of ethylene oxide has persisted for over 30 years. Gee *et al.*[7] polymerized ethylene oxide using sodium methoxide initiation in dioxane; Wojtech[8] later found that the reaction rate could be increased by the addition of alcohol. Although the alcohol solubilized the metal alkoxide through complexation and increased the separation of the ion pair, it also served as a chain transfer agent and thus destroyed the living nature of the reaction. Price *et al.*[9,10] used potassium *tert*-butoxide to initiate polymerization of ethylene oxide in the polar aprotic solvents, DMSO and HMPA.

They were able to produce polymers with molecular weights between 9,840 to 42,500 g/mole but were plagued with problems of alkoxide association and chain transfer.

Figueruelo *et al.*[11] reported further studies of ethylene oxide polymerization in HMPA using the sodium and potassium salts of diethylene glycol monomethyl ether as initiators. The living polymer chains were found to be associated (~2-fold) in solution, showing only a moderate degree of ion dissociation. At low concentrations, the reaction rate increased with increasing initiator concentration; however, at higher concentrations, the reaction rate became independent of initiator concentration due to ion pair association. Addition of sodium or potassium tetraphenylboride decreased the rate of reaction (common ion effect) demonstrating that the reaction proceeded faster for free ions than for ion pairs. The polymer anion showed reduced mobility as the chain lengthened. Figueruelo *et al.*[12] arrived at similar conclusions using the cesium salt of diethylene glycol monoethyl ether as the initiating species in HMPA at 40 °C. The polymer formed had $M_V$ ~ 7,600 - 17,100 g/mole as determined from viscometry. The same reaction in DMSO (50 °C) was complicated by chain transfer to DMSO concomitant with the formation of alcohol.[13]

Cabasso *et al.*[14] successfully polymerized ethylene oxide in either THF or DMSO with potassium naphthalide initiation; lithium naphthalide (and lithium alkoxides) are not suitable for the polymerization of ethylene oxide because the lithium-oxygen association is very strong and dissociation is lacking.[15,16] Kazanskii[17] found increased activity and decreased association, when cesium, potassium, and sodium cations were used with naphthalene.

Using carbazyl potassium and kryptofix [222] (4,7,13,16,21,24-hexaoxa-1,10-diazabicyclo[8.8.8]-hexacosane) in THF (20 °C), Deffieux *et al.*[18] claimed that they were able to predict the molecular weight of poly(ethylene oxide) based on the molar ratio of monomer to initiator. $M_n$, determined from osmometry, ranged from 67,000 to 337,000 g/mole; polydispersity data was not given. Although some ionic associations were found from viscosity data, they were found to be negligible at $3 \times 10^{-4}$ mol/l. Unfortunately,

Eisenbach *et al.*[19] were unable to repeat the work of Deffieux *et al.* and suggested that chain transfer led to the decreased molecular weights observed; for $M_n$ values calculated between 61,000 and 149,800 g/mole, $M_n$ values between 21,000 and 40,000 g/mole (by GPC) were observed. Eisenbach *et al.*[20] repeated their experiment using deuterated ethylene oxide in THF (30 °C) with carbazyl potassium initiation and kryptofix [222]. In the early stages of the polymerization, a transfer reaction occurred which lowered the $M_n$ of the polymer. From GPC analysis, it was shown that polymers were made with $M_n$ values between 31,000 and 82,000 g/mole with polydispersity indices between 1.38 and 1.54.

Reuter *et al.*[21] were able to polymerize ethylene oxide with both cumyl potassium and diphenyl methyl potassium initiators in THF (25 °C or 40 °C). The polymers produced had $M_n$ values of 2,900 - 53,200 g/mole with polydispersities of 1.10 - 1.17 as determined from GPC analysis using polystyrene standards. Cumyl potasssium was determined to be the better initiator.

In the work described in this thesis, ethylene oxide was polymerized anionically with the potassium salt of triethylene glycol monomethyl ether (TEGMEK). PEO and end-capped PEO (PEO-R) samples were prepared for use in adsorption studies where the effect of the hydrophobic end group was studied. With this in mind, the initiator that was chosen did not have a bulky hydrophobic end group that could distort adsorption results. Most of the initiators discussed above were excluded by this requisite. The initiator, TEGMEK, is similar to that used by Figueruelo *et al.*;[11] the system differs in the choice of solvent (THF). Poly(ethylene oxide)s were characterized by GPC using water as the mobile phase and with poly(ethylene oxide) standards (Polymer Labs, PolySciences).

PEO and PEO-R were synthesized (and not purchased) because the effect of the hydrophobic end group was the primary focus of adsorption experiments and because monodisperse polymers are best suited for adsorption experiments. Adsorption of polydisperse samples results in competition between polymers of different molecular weights for adsorption sites.[22] (See Chapter II for more information on polydispersity

effects.) PEO-R was prepared by reacting the terminal hydroxyl group of PEO with an alkyl or a perfluoroalkyl acid chloride in THF with pyridine catalysis; PEO-R was characterized by GPC, IR, and elemental analysis.

## Adsorption

Polymer adsorption occurs as a result of attractive forces between a surface and a polymer which cause the polymer to adhere to the surface. Polymer adsorption depends upon three important interactions: (i) polymer - solvent, (ii) solvent - substrate, and (iii) polymer - substrate. According to the Flory-Huggins polymer - solvent interaction parameter, $\chi$, the solvent can be described as either good/athermal ($\chi = 0$) or theta ($\chi = 0.5$). In a good solvent, the dissolved polymer is well solvated and in an expanded conformation ($Rg \sim M^{0.6}$) whereas in a theta solvent, the interaction between polymer and solvent is minimized such that $R_g$ of the polymer is in an unperturbed dimension ($Rg \sim M^{0.5}$). The solvent - substrate and polymer segment - substrate interactions are described by $\chi_S$ or molecular interactions at the surface. The exchange free energy, $\chi_S$, involves the attachment of polymer segments to, concomitant with the liberation of solvent molecules from, the surface. The solvent - substrate interaction can be described in terms of the solvent's ability to "wet" the substrate. Poor wetting of the substrate by the solvent results in a high interfacial free energy and can enhance adsorption. The polymer - substrate interaction can be either non-specific, as in physisorption, or specific, as in chemisorption. Physisorption typically involves the adsorption of a neutral polymer to a neutral substrate whereas chemisorption involves a specific interaction, e.g. an ionic interaction, between the polymer and the substrate.

The conformation of an adsorbed polymer is described in terms of trains, loops, and tails. Figure 4.1 describes the conformation of a polymer adsorbed to the solution - substrate interface. Trains describe those segments of the polymer which interact directly

with the substrate giving rise to a flat conformation. Tails arise at the chain's ends which, except for a few polymer segments which anchor the chain to the surface, extend from the surface into the solution. Loops also extend from the surface but have polymer segments on either side which interact directly with the surface (small trains); loops extend further than trains but not as far as tails from the surface.

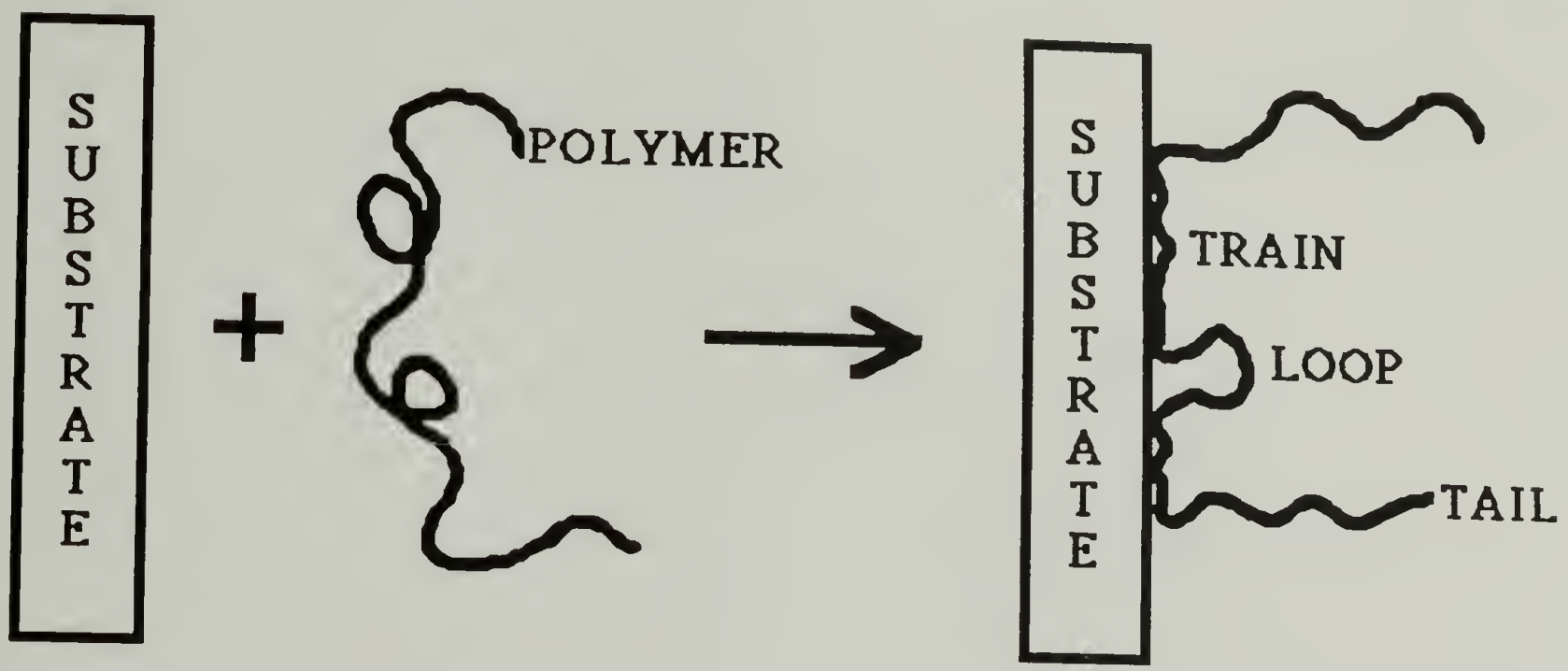


Figure 4.1 Typical Conformation of a Polymer Adsorbed to the Solution - Substrate Interface.

Adsorption is often described in terms of amount adsorbed ($\Gamma$), thickness of the adsorbed layer ($\delta_H$), and the bound fraction (p). The thickness of the adsorbed layer is largely due to tails which extend further than loops or trains into the solution. The amount adsorbed depends on the type of adsorption; for multipoint anchoring of a polymer to a substrate, both the amount adsorbed and the thickness of the adsorbed layer are limited. For adsorption experiments conducted in the dilute regime, but with an excess of polymer in solution with respect to adsorption sites, the amount adsorbed can increase as the flatter conformation of adsorbed polymer becomes more extended; this allows more polymer to

adsorb and increases the adsorbed layer thickness.[23] Most adsorption experiments are conducted in the dilute regime; in the semi-dilute regime, polymer adsorption is complicated by polymer - polymer interactions or entanglements.

Adsorption of Poly(ethylene oxide)

Poly(ethylene oxide) adsorption has been a subject of much interest and debate. Klein and Luckham[24] studied PEO adsorption to mica from a good solvent (0.1 M aqueous $KNO_3$) by measuring the force between two mica surfaces. They found that the PEO extended from the surface with a hydrodynamic thickness, $\delta_H$, of ~$3R_g$. Interestingly, the amount of PEO that adsorbed, $\Gamma = 4 \pm 1.5$ mg/m$^2$, was independent of molecular weight. (By contrast, Kawaguchi *et al.*[25] found that the adsorbed amount $\Gamma \sim M^{0.4}$ for adsorption from a good solvent.) Hair *et al.*[26] studied the adsorption of PEO-b-PS block copolymers from toluene (a good solvent for both blocks) to mica by the same technique. They found that PEO formed an anchor on mica while PS acted as a buoy. Hair *et al.* explained that an overlap of "buoy" blocks which formed a polymer brush accounted for the extended length of the PS layer beyond $R_g$.

The interaction of PEO with Aerosil silica has been the subject of many adsorption papers. Parnas *et al.*[27] found that ~0.3 mg/m$^2$ of high molecular weight PEO adsorbed to chemically modified silica from water in the plateau regime. Killmann[28] used infrared spectroscopy to study PEO adsorption to Aerosil silica from four solvents - water, carbon tetrachloride, benzene, and methanol. Kawaguchi *et al.*[29] also studied PEO adsorption to silica by infrared spectroscopy. After adsorbing PEO to silica from carbon tetrachloride (35 °C), they found that of benzene, dioxane, acetone, and methylcellosolve, only the latter displaced PEO. The amount of polymer adsorbed was determined by comparing the IR peak at 2890 cm$^{-1}$ of PEO in solution before and after (in the supernatant) adsorption. Kawaguchi *et al.* postulated that PEO's adsorption to silica was enhanced by a hydrogen

bonding interaction between the ether oxygen of the PEO backbone and the hydroxyl hydrogen on the silica. In a separate study, Kawaguchi *et al.*[30] studied the competitive adsorption of poly(styrene) (PS) and PEO at the silica/carbon tetrachloride interface at 35 °C. PEO adsorbed more strongly to silica than PS as was determined from IR frequency shift data: $\nu$(OH) shifted 375 $cm^{-1}$ for PEO vs. 94 $cm^{-1}$ for PS. In addition, PEO displaced PS previously adsorbed, demonstrating both the reversibility of PS adsorption and the superior affinity of PEO for silica. The amount adsorbed was determined from IR and UV-vis analysis.

Adsorption of PEO to the PS latex/water interface has been studied by several researchers, including Dobbie *et al.*,[31] who found that the steric stability of carboxylic acid-functionalized PS latex particles was enhanced by PEO adsorption. The steric stability of the latex was determined by its critical flocculation temperature (CFT) where an increase in CFT corresponded to increased stability of the latex. At low PEO concentration and at pH 4.65, the CFT of the PS latex increased by ~20 °C as a result of hydrogen-bonding between the carboxylic acid proton of PS-$CO_2H$ and the ether oxygen of the PEO repeat unit. At lower pH (2), the CFT increased further than was observed at pH 4.65 due to increased hydrogen bonding interactions. At higher pH (10), flocculation occurred at a much lower temperature because no steric stabilization was possible; at pH 10, the carboxylic acid was deprotonated inhibiting any hydrogen bonding interaction with PEO. Dobbie *et al.* described the adsorbed conformation: at low concentration, PEO adsorbed to the PS latex with a flattened or multipoint anchoring conformation. As the PEO concentration increased, its flattened conformation became more vertical in order to accommodate more PEO chains.

Cosgrove *et al.*[32] studied the adsorption of PEO to PS latex and later compared their results with theory. Cosgrove *et al.* found that PEO adsorbed to PS latex with a high surface charge density and only scarcely to PS latex with a low surface charge density. From a combination of techniques including $^1H$ NMR, small angle neutron scattering

(SANS), and UV-vis, they determined (using the high surface charge density PS) that ~0.65 mg/m$^2$ of PEO adsorbed to the PS latex - water interface with a hydrodynamic thickness of 19 ± 3 nm. They reported good correlation between theory and experiment by comparing the conformation[33] of the adsorbed polymer with the theoretical predictions of Scheutjens and Fleer.[34]

Cohen Stuart *et al.*[35] also compared the theoretical predictions of Scheutjens and Fleer to the hydrodynamic thickness $\delta_H$, observed by photon correlation spectroscopy (PCS), of PEO adsorbed at the PS latex - water interface. They reported good agreement between theory and experiment for the following parameters: (1) for chain length R, $\delta_H$ is a function of tails because loops and trains are effectively screened; (2) for segmental adsorption energy $\chi_S$, $\delta_H$ is independent of $\chi_S$ because $\chi_S$ affects trains and loops only; (3) for adsorbed amount $\Gamma$, $\delta_H$ is a function of $\Gamma$ because the flat conformation which exists for low $\Gamma$ changes to one of loops and tails as segment density approaches saturation (higher $\Gamma$); (4) for the diameter of free coil in solution $2R_g$, $\delta_H$ is less than $2R_g$ for short chains but $\delta_H$ is greater than $2R_g$ as tails develop. In addition, $\delta_H$ is greater for adsorption from $\theta$ -solvents ($\chi = 0.5$) than from good solvents ($\chi = 0$).

Baker and Berg[36] used PCS to compare the conformation of adsorbed PEO and PEO-PPO (poly(propylene oxide)) copolymers at the PS latex - water interface. PPO segments were expected to adsorb to the PS latex by a "hydrophobic interaction" while PEO segments were expected to extend from the surface in the tail conformation. The amount of PEO and PEO-PPO that adsorbed was determined from turbidity measurements of the tannic acid - PEO complex after adsorption. PEO homopolymer adsorbed in a flat conformation where $\delta_H \sim M^{0.35}$; this exponent, 0.35, is lower than those that were predicted, $\delta_H \sim M^{0.5}$ in a $\theta$-solvent and $\delta_H \sim M^{0.6}$ in a good solvent. The hydrodynamic radius, $\delta_H$, decreased after 24 h, indicating that the initial tail-loop-train conformation had rearranged to a loop-train conformation. Baker and Berg found that the adsorbed layer

thickness was independent of molecular weight after 24 h. From copolymer adsorption studies, they postulated that PPO lay flat while PEO extended from the surface.

Couture and van de Ven[37] compared the adsorption of PEO and PEO-PS to PS latex from water at 25 °C by PCS. They found that PEO had a thicker adsorbed layer (~20 nm) than PEO with an anchor group (i.e. PS) (~14 nm) and reasoned that PEO-PS, with only one "tail", had a lower hydrodynamic thickness than PEO because it had two "tails". The layer thickness was also found to be inversely proportional to the concentration of the PS latex suspension: 20 nm for a 0.001% PS latex suspension and 9 nm for a 0.1% PS latex suspension. The surface coverage of PEO-PS was less than 1 $mg/m^2$ whereas that of PEO was 1.25 $mg/m^2$. In light of their results, Couture and van de Ven suggested three stages for polymer adsorption kinetics. Initially polymer adsorption is diffusion controlled where the conformation of the random coil in solution changes to a flatter one on the surface. Then the adsorbed monolayer acts as an energy barrier layer to further adsorption and forces other polymers to diffuse through it to get to the surface. Finally, a few more polymers accumulate on top of the dense adsorption layer where either one end is adsorbed to the surface or the chain becomes entangled.

PEO adsorption at the air-water interface was studied by Granick *et al.*[38] who found that PEO formed an insoluble monolayer (< 1 $mg/m^2$) using the Wilhelmy Plate method. Interestingly, entropy increased with surface coverage up to 0.5 $mg/m^2$ yet decreased for higher surface coverage because water molecules formed an ordered structure around the PEO repeat unit. In addition, a slight exothermic enthalpic contribution was observed with increasing surface concentration. Granick *et al.* described the PEO monolayer as close-packed with $\Gamma = 0.45$ $mg/m^2$ (16 $Å^2$/segment) which corresponded to ~5 PEO layers. The surface pressure, $\pi$, increased with surface concentration, $\Gamma$, such that $\pi \sim \Gamma^{2.85}$. Surface pressure was defined as the amount by which the liquid's surface tension was depressed by the presence of the surface polymer film. Kawaguchi *et al.*[39] observed the same phenomenon and found that it agreed with the scaling predictions for

good solvent conditions. From surface pressure - area isotherms, the PEO monolayer was found to be stable to $\pi = 6.4$ dyn/cm which corresponds to a close-packed model for the PEO repeat unit of 16 $Å^2$/molecule. At higher pressures, the monolayer collapsed.

In the work described here, the adsorption of PEO was compared to that of alkyl end capped PEO (PEO-R) from aqueous solution. The hydrophobic interaction between PEO-R and a hydrophobic surface was investigated as a driving force for adsorption from an aqueous solution. Three interfaces were studied: (1) the fluoropolymer film - water interface, (2) the polystyrene latex (PS) - water interface, and (3) the free or air - water interface. The fluoropolymer film and PS latex - water interfaces provided possible sites for hydrophobic interactions. However, adsorption at the PS latex - water interface was complicated by surface carboxylic acid groups which stabilized it by electrostatic repulsion in the aqueous solution. Photon correlation spectroscopy provided information on the adsorbed layer thickness of PEO-(R) to PS latex. XPS and contact angle analysis were used to investigate adsorption at the fluoropolymer - water interface. Surface pressure measurements were used both to study adsorption at the air - water interface and to determine possible micelle or aggregate formation of end-capped PEO-R.[40]

Several parameters were studied in the adsorption experiments. At the fluoropolymer - water interface, the effects of PEO molecular weight, concentration, and time of interaction, on adsorption were assessed. For a given PEO molecular weight (50,000 g/mole), the effect of different alkyl end groups on adsorption at the three interfaces were studied. Both the nature, alkyl, perfluoroalkyl or branched alkyl, and the length of the end group were investigated in terms of facilitated adsorption. In addition, the effect of PEO-R concentration was studied. Five different PEO end groups were compared in terms of their adsorption to aqueous interfaces: (i) hydroxyl (PEO), (ii) nonadecafluorodecanoate (PEO-$C(O)C_9F_{19}$ or PEO-FD), (iii) stearate (PEO-$C(O)C_{17}H_{35}$ or PEO-ST), (iv) dioctylacetate (PEO-$C(O)CH(C_8H_{17})_2$ or PEO-DO), and (v) tripentylacetate (PEO-$C(O)C(C_5H_{11})_3$ or PEO-TP). Adsorption of PEO and

PEO-R to the three aqueous interfaces (fluoropolymer, PS and air) provide a good overview of some of the important adsorption parameters.

## Experimental

All reagents were used as received unless otherwise noted. All procedures were conducted under an inert, nitrogen environment except where noted and in adsorption experiments. All glassware used in the synthesis section was dried by heating under vacuum and then recharging with nitrogen; this cycle was repeated three times.

## Materials and Methods

### Synthesis

**Tetrahydrofuran** (THF) (Aldrich, 99.9% anhydrous) was distilled from sodium benzophenone (Aldrich) dianion.

**Triethylene Glycol Monomethyl Ether** (TEGME) (Aldrich, 95%) was stirred over activated alumina (~2 h) and calcium sulfate (overnight), filtered and then fractionally distilled from sodium at 10 mm (b.p. 143-144 °C). (See Figure 4.2 for Gas Chromatogram (GC) of TEGME.) 1 μl of a TEGME solution (1 ml TEGME: 5 ml THF) was injected into the capillary GC at 80 °C. After 2 minutes at 80 °C, the temperature of the column increased 10 °C/min to 200 °C at which temperature it remained for 2 minutes. As indicated in the gas chromatogram, one peak was observed indicating the purity of TEGME. [V4,64,100,114,124; VII22]

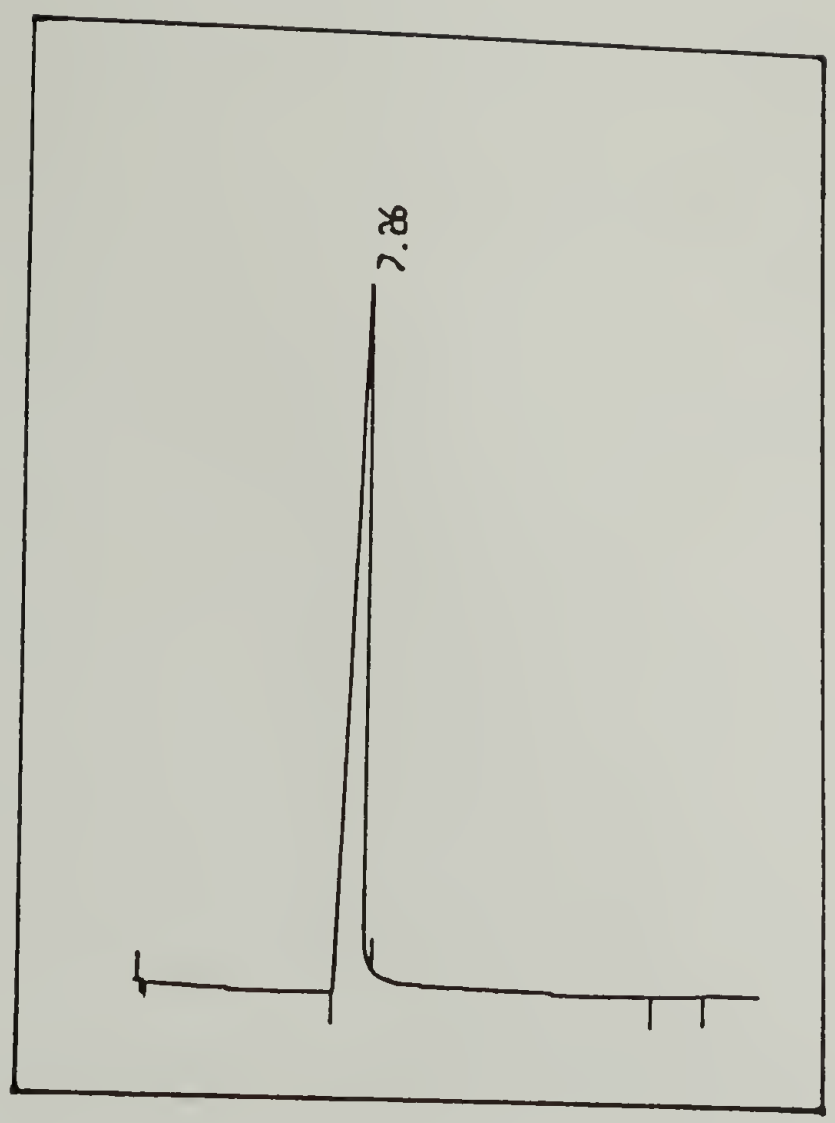


Figure 4.2 Gas Chromatogram of Triethylene Glycol Monomethyl Ether.

**Triethylene Glycol Monomethyl Ether Potassium** (TEGMEK) was prepared by reacting an excess of potassium pieces (rinsed in hexane (Aldrich) prior to use) with TEGME diluted in ~20 ml of THF in a side arm round bottom flask equipped with a glass stir bar and a teflon stopcock. The reaction proceeded for ~2 - 3 h during which time it became deep blue in color. The solution was filtered, using a Millipore 0.5 μm teflon syringe filter, into a 25 ml volumetric flask equipped with a teflon stopcock. The solution was degassed by a freeze-pump-thaw cycle to avoid bumping of the THF which was removed at reduced pressure. (This step may not be necessary but was found to be useful in the preparation of narrow molecular weight distribution PEO.) TEGMEK was redissolved in fresh THF and diluted to 25 ml. This solution was further diluted to a concentration appropriate for poly(ethylene oxide) synthesis.

**Ethylene Oxide** (EO) (Kodak) was stirred over calcium hydride (Aldrich) at 0 °C overnight in a round bottom flask equipped with a teflon coated stir bar and a teflon stopcock. The solution was degassed with three freeze-pump-thaw cycles and distilled (trap-to-trap). (EO was redistilled from calcium hydride (trap-to-trap) on occasion.)

**Poly(ethylene oxide)** (PEO) was prepared by anionic ring opening polymerization of ethylene oxide using triethylene glycol monomethyl ether potassium as the initiator (Scheme 4.1). The experimental set up consisted of a reaction flask, containing initiator, THF and a teflon-coated magnetic stir bar, and a centrifuge tube containing ethylene oxide (Figure 4.3). Both reaction flask and centrifuge tube were equipped with a teflon stopcock. ~50 - 75 ml of THF was added to the reaction flask followed by a known amount of TEGMEK (moles). Both the initiator solution and ethylene oxide were degassed with freeze-pump-thaw cycles. After refreezing both solutions and closing vacuum stopcocks, the teflon stopcocks of both the reaction flask and the ethylene oxide centrifuge tube were opened. The vacuum stopcock between reaction flask and centrifuge tube was opened. The solution in the reaction flask was allowed to warm to room temperature. When stirring could just be started, the ethylene oxide was allowed to warm to room temperature at which temperature it distilled into the reaction flask. After all ethylene oxide was transferred into the reaction flask (approximately 1 h), the reaction flask and centrifuge tube were immersed in a 40 °C oil bath. The reaction proceeded for ~40 h after which the reaction flask was purged with nitrogen. The polymerization was terminated with ~5 ml of degassed methanol (a 10% HCl solution in methanol was used on occasion); the solution was stirred for ~15 minutes. The poly(ethylene oxide) solution was slowly transferred by cannula into a beaker containing ~250 ml hexane (Aldrich) in which PEO precipitated. PEO was redissolved in THF (Aldrich) and reprecipitated in hexane twice more. PEO was dried overnight (room temperature, 0.02 mm). [V19,22,25,27,29,32,36,40,44,54,56,58, 62,67,74,78,82,85,87,89,102,106,110,120,126,132,138,147; VII24]

By way of example, a detailed synthetic procedure is included; for more information on the synthesis of PEO to other molecular weights, see notebook page references. 4.8082 g ($2.928 \times 10^{-2}$ moles) of TEGME (determined by weight) was added to a side arm flask containing ~20 ml THF to which a molar excess of potassium pieces was added under positive nitrogen. After stirring for ~2 h, the solution of TEGMEK was too thick for filtration; ~10 ml of additional THF was added and the solution stirred for an additional 1/2 h. The solution was transferred by a syringe which was equipped with a 0.5 μm Millipore filter to a nitrogen-purged 25 ml volumetric flask equipped with a teflon stopcock. The THF was removed under reduced pressure after degassing by freeze-pump-thaw to avoid bumping. Fresh THF was added to the volumetric flask to dissolve the TEGMEK ($1.171 \times 10^{-3}$ moles/ml). 2.5 ml of this solution was transferred by syringe to a clean, nitrogen-purged, 25 ml volumetric flask equipped with a teflon stopcock and brought up to volume with fresh THF ($1.288 \times 10^{-4}$ moles/ml). 1 ml of the diluted TEGMEK ($1.288 \times 10^{-4}$ moles) was added to the reaction flask containing freshly distilled THF. 10.1434 g (0.2303 moles) of ethylene oxide (determined by weight) was transferred to the centrifuge tube by cannula under nitrogen at 0 °C. Both centrifuge tube and reaction flask were degassed by freeze-pump-thaw and then refrozen; their stopcocks were opened to the vacuum simultaneously. The vacuum stopcocks were closed and then the middle vacuum stopcock between the flasks was opened while leaving the teflon stopcocks open. The solution in the reaction flask was warmed to room temperature. When stirring just started, the ethylene oxide was allowed warm to room temperature and distilled slowly into the reaction flask. The tubes were then immersed in a 40 °C oil bath. The reaction was terminated after 39 h with ~5 ml degassed methanol which was added by cannula. The polymer was precipitated in hexane, redissolved in THF and reprecipitated in hexane twice more, giving a yield of 87%. The expected degree of polymerization, based on the molar ratio of monomer to initiator, $0.2303/1.288 \times 10^{-4}$, was 1788 which corresponds to a $M_n$ of 78,760 g/mole. The observed $M_n$ was 50,160 g/mole [VII24].

Initiator Preparation:

Initiation and Propagation:

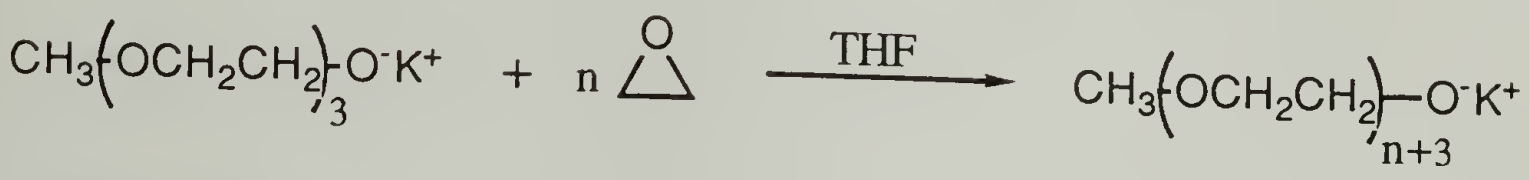

Termination:

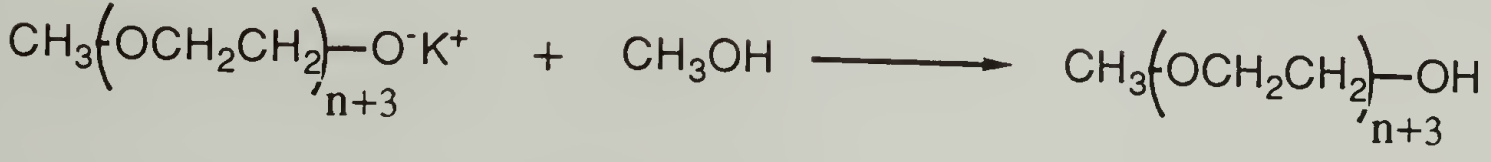

Scheme 4.1 Synthesis of Poly(ethylene oxide).

**Acetonitrile** (Aldrich, 99%) was initially dried over molecular sieves overnight and then distilled from calcium hydride at 83 °C.

**18-Crown-6** (Aldrich) was recrystallized twice from acetonitrile and dried under vacuum (0.02 mm).

**Kryptofix [222]** (4,7,13,16,21,24-hexaoxa-1,10-diazabicyclo[8.8.8]-hexacosane) was freeze-dried from benzene.

**Heptafluorobutyryl Chloride** (HFBC) (Aldrich) was degassed by three freeze-pump-thaw cycles before it was distilled (trap-to-trap).

**Benzene** (Aldrich) was distilled from calcium hydride at 80 °C.

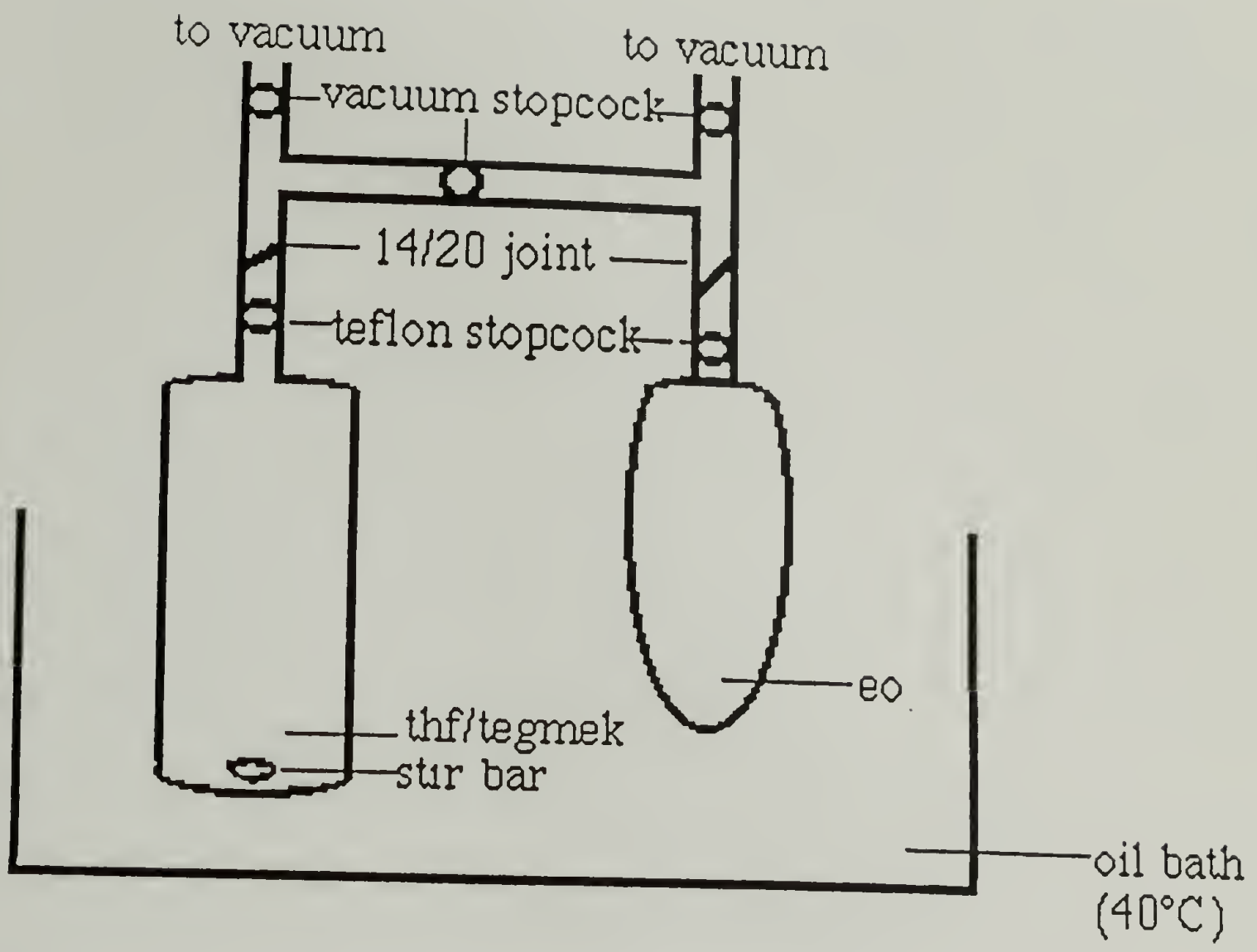


Figure 4.3 Experimental Set-up for Ethylene Oxide Polymerization.

**Nonadecafluorodecanoyl Chloride**[41] (FDC) was prepared by the reaction between phosphorous pentachloride (Aldrich) and nonadecafluorodecanoic acid (Aldrich). 13.35 g (~0.06 moles) of phosphorous pentachloride and 10 g (~0.02 moles) nonadecafluorodecanoic acid were added under nitrogen to a nitrogen-purged 3-neck round bottom flask equipped with a teflon-coated magnetic stir bar, a reflux condenser (stoppered with a septum) and two septa. The reaction flask was cooled to ~0 °C in an ice bath. ~100 ml of benzene was added by cannula to the reaction flask with stirring over a 1/2 - 1 h period. The ice bath was replaced with an oil bath, the temperature of which was increased until the solution came to a slow reflux. The solution was stirred at a slow reflux overnight under a slow nitrogen purge. The reaction flask was cooled to ~35 °C at which temperature the reaction solution separated into 2 layers and the acid chloride precipitated. The

supernatant (yellow) was transferred by cannula into a nitrogen-purged round bottom flask which was then immersed in an ice bath to recover more acid chloride. The acid chloride crystals in the 3 neck reaction flask were redissolved in fresh benzene with gentle heating and the solution was transferred by cannula into a clean, nitrogen-purged round bottom flask. Nonadecafluorodecanoyl chloride was recrystallized from benzene four times or until the crystals were white and the supernatant was clear and was stored refrigerated under nitrogen. [V128-9]

**Stearoyl Chloride** (STC) (octadecanoyl chloride) (Aldrich) was fractionally distilled (~180 °C, full vacuum). [VII26]

**Dioctylacetic Acid** was prepared according to a literature synthetic procedure.[42] Scheme 4.2 summarizes the synthetic procedure. [VII32-37]

**Diethyl Malonate** (Aldrich) was fractionally distilled (135 - 136 °C, 100 mm).

**1-Bromooctane** was fractionally distilled (94 - 97 °C, 5 mm).

**Ethanol**, absolute, was distilled from sodium (77 °C).

**Diethyl Octylmalonate** was prepared from diethyl malonate and octyl bromide. In a 1 l three - neck flask, equipped with a mechanical stirrer, reflux condenser, and dropping funnel, 68 g (1 mole) of sodium ethoxide (Aldrich) was added under nitrogen. Approximately 500 ml of ethanol was added to dissolve the sodium ethoxide; the solution was heated gently to enhance dissolution (reddish-brown color). 156 ml (1 mole) of diethyl malonate was slowly added over a 1 hour period to the reaction flask via the addition funnel; during this time the solution was heated to between 80 and 90 °C (creamy orange color). 173 ml (1 mole) of octyl bromide was added via the addition funnel over 90 min during which time the solution began to reflux (creamy yellow color). A yellow precipitate was observed. The solution was refluxed for an additional ~3 h. The flask was cooled in air and the ethanol was removed by rotary evaporation. To the remaining solution, ~300 ml of distilled water was added. The aqueous layer (lower) was separated from the ester layer (upper) in a 1 l separatory funnel. The organic layer was washed with

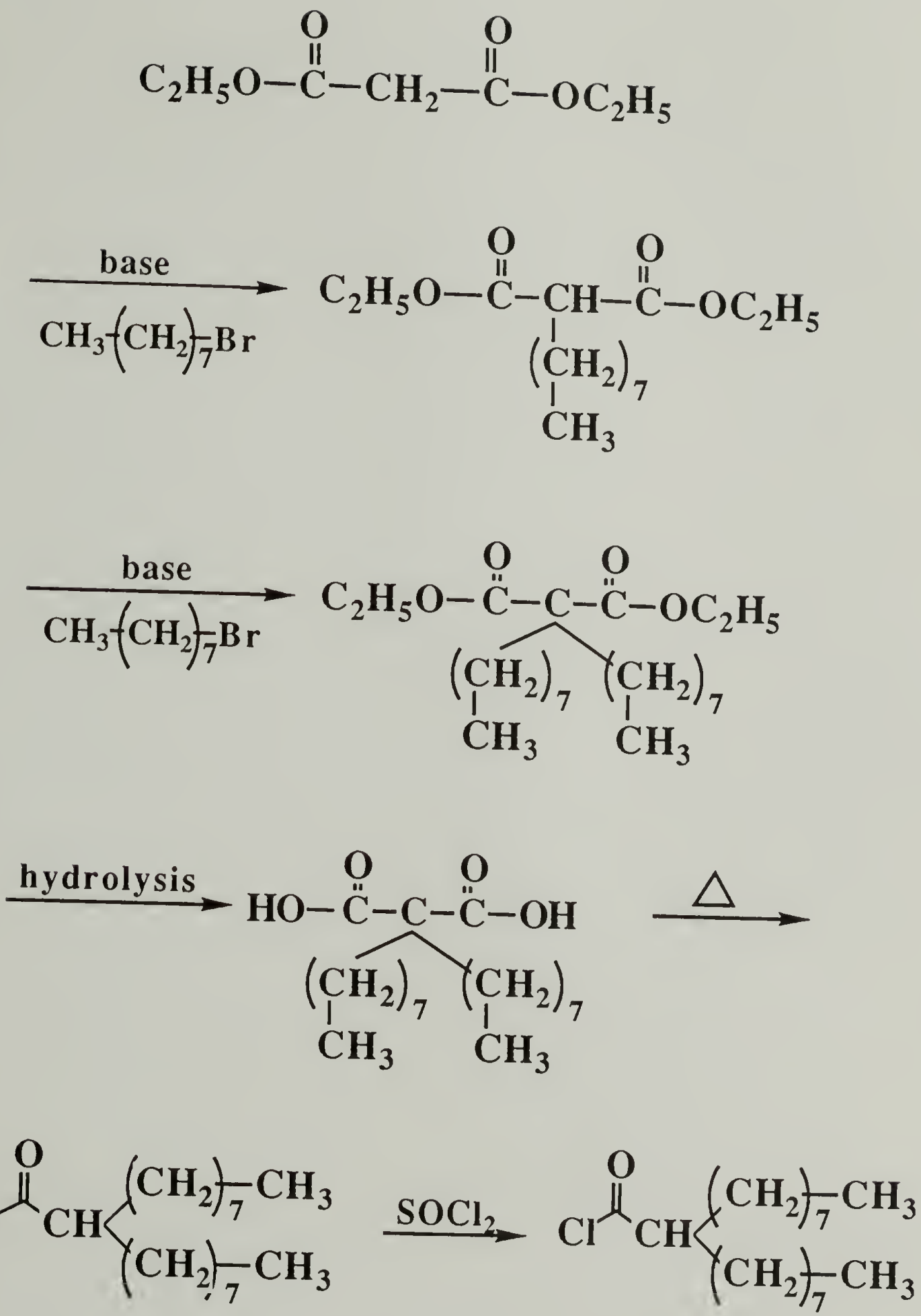


Scheme 4.2 Synthesis of Dioctylacetyl Chloride.

several ~30 ml aliquots of water and was dried by stirring over magnesium sulfate. The magnesium sulfate was removed by filtration and diethyl octylmalonate was fractionally distilled (186 - 190 °C, 20 mm) (65% isolated yield). [VII33-34]

**Diethyl Dioctylmalonate** was prepared from diethyl octylmalonate and octyl bromide. The same procedure was followed as described for the synthesis of diethyl octylmalonate; however, 44 g (0.65 moles) of sodium ethoxide was reacted with 176 g (0.65 moles) diethyl octylmalonate and 112 ml (0.65 moles) octyl bromide. Diethyl dioctylmalonate was fractionally distilled (147 °C, full vacuum) (47% isolated yield). [VII34-35]

**Dioctylacetic Acid** was prepared by hydrolyzing diethyl dioctylmalonate to dioctylmalonic acid and then decarboxylating the acid. 118 g (0.31 moles) of diethyl dioctylmalonate was placed in a 500 ml round bottom flask to which 43 g of potassium hydroxide (Fisher) in ethanol/water (80 ml:50 ml) was added by pipet. The flask was equipped with boiling chips, a magnetic stir bar and a reflux condenser. The flask was immersed in an oil bath (heated to 85 °C) and the solution was refluxed for 5 h. The ethanol was removed by rotary evaporation. (Water (~300 ml) was added in an attempt to separate the oily layer from the aqueous layer; however, an excess of water was added, inhibiting separation, thus this step should be omitted in the future.) The solution was transferred to a 500 ml round bottom flask to which 64 ml (0.93 moles) hydrochloric acid (Fisher, 12.1 N) was added. The flask was equipped with a teflon-coated magnetic stir bar and a reflux condenser. Stirring of the solution became more difficult as it thickened but was facilitated with heat and time. The solution was refluxed for 90 min during which carbon dioxide gas was emitted; the solution sounded as though it was cracking. The solution was allowed to cool to room temperature (yellow solution) and was then poured into a 1 l beaker containing ~200 ml petroleum ether (Fisher). The beaker was placed in ice for ~1 h and a white precipitate formed. The yellow solution was removed by pipet. The

white precipitate was recrystallized from petroleum ether and then dried under vacuum (70% isolated yield). [VII35-36]

**Dioctylacetyl Chloride**[43] (DOC) was prepared by reacting dioctylacetic acid with thionyl chloride (Aldrich). 61.6 g (0.22 moles) of dioctylacetic acid was placed in a 250 ml round bottom flask equipped with a magnetic stir bar. The acid was melted by immersing the flask in a 60 °C oil bath. After dissolution, 16 ml (0.22 moles) thionyl chloride (Aldrich) was added via cannula. To the round bottom flask was attached a reflux condenser, the top of which was attached via an empty trap to a bubble trap containing a 1 M sodium hydroxide (Fisher) solution. All joints were either ground glass with silicon grease or glass to tygon tubing. Figure 4.4 summarizes this experimental set up. The oil bath temperature was increased to 80 °C causing the solution to reflux. (HCl gas was emitted as observed in the bubbler.) After 1 h, the temperature was decreased slowly to 35 °C and the solution was stirred overnight. The solution (brownish) was fractionally distilled (~180 ° C, full vacuum).

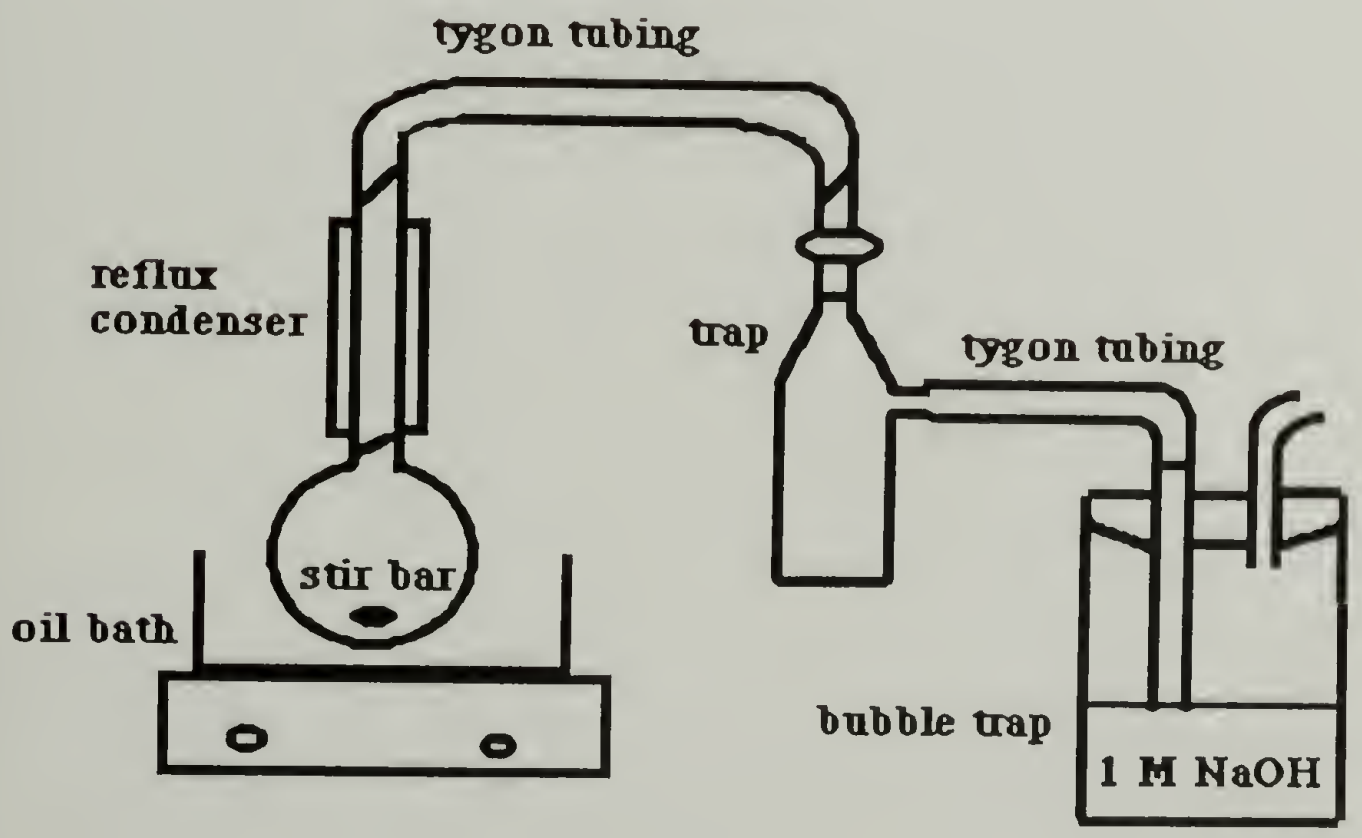


Figure 4.4 Experimental Set-up for the Acid Chloride Synthesis.

**Tripentylacetic Acid** was prepared according to a literature synthetic procedure.[44] Scheme 4.3 outlines the synthetic approach. [VII38-53, 58-61]

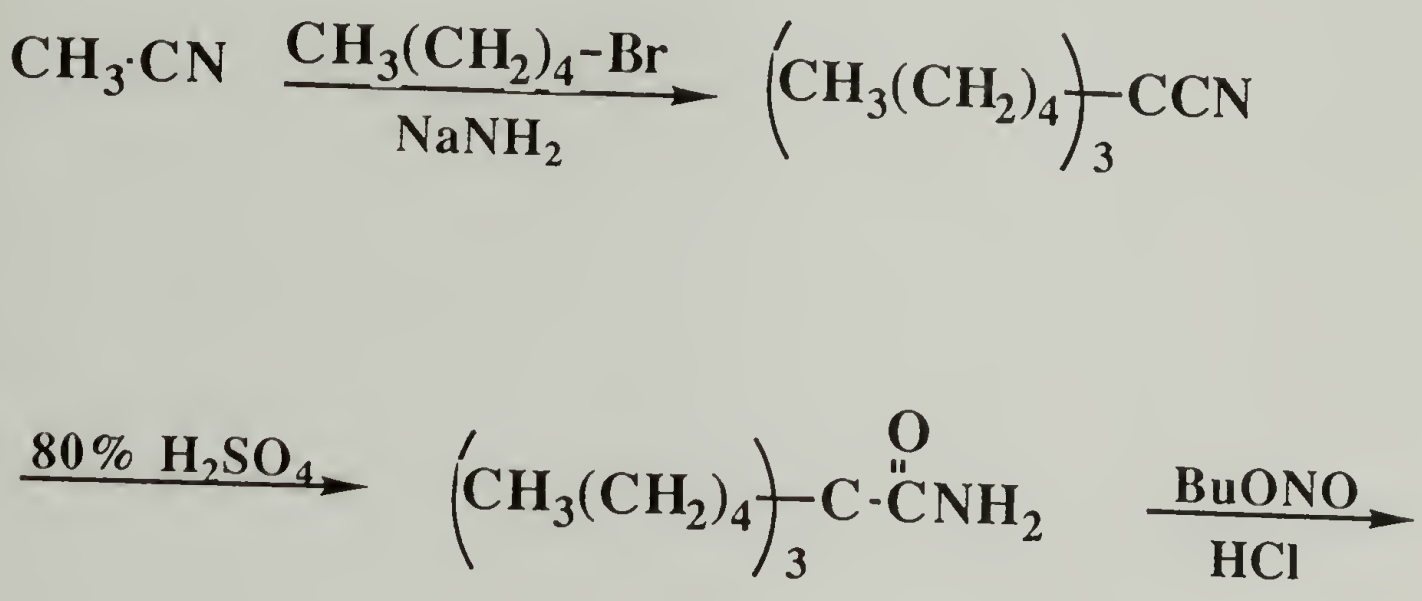


Scheme 4.3 Synthesis of Tripentylacetyl Chloride.

**Tripentylacetonitrile** [MSVII38-46] was prepared by the reaction of acetonitrile with sodamide and pentyl bromide in toluene. To a round bottom 3-neck flask equipped with a mechanical stirrer, refluxing column, and a septum was sequentially added, under nitrogen, 125 ml of toluene (Aldrich), 12.3051 g (0.25 moles) acetonitrile (Aldrich), and 102 ml (0.8 moles) pentyl bromide (Aldrich). The solution was heated gently to ~55 °C (oil bath temperature was 55 °C). 34 g of sodamide (Aldrich) was suspended in 250 ml of

toluene in a 500 ml round bottom flask equipped with a magnetic stir bar and septum under positive nitrogen. The sodamide suspension was added slowly and cautiously to the reaction pot by cannula over a 3 h period. The temperature of the reaction pot was slowly increased to ~80 °C during the addition of sodamide. The reaction pot was covered with foil during the addition and then the oil bath temperature was increased to 114 °C to effect refluxing. During addition of the sodamide, the temperature of the reaction pot increased and some effervescence was observed in addition to gas ($NH_3$) being released into the bubbler. The reaction proceeded under a slow nitrogen purge and the solution was refluxed for ~6 h. The heat was removed and the reaction pot immersed in an ice bath. The solution was poured on an ice/water mixture and then extracted. The toluene layer was creamy yellow and the water layer was somewhat discolored. The toluene layer was washed several times with water, dried with magnesium sulfate to yield a clear orange-yellow solution. The toluene was removed by rotary evaporation and the product was fractionally distilled (100-101° C, full vacuum) (35% isolated yield).

**Tripentylacetamide** [MSVII47-49] was prepared by the reaction between tripentylacetonitrile and 80% sulfuric acid in water. 22 g (0.087 moles) tripentylacetonitrile was cannulated into a 3-neck round bottom flask equipped with a mechanical stirrer, condenser, and septum. The septum was removed briefly while 70 ml (1.31 moles sulfuric acid) of 80% sulfuric acid (80/20, v/v $H_2SO4/H_2O$) was added. The septum was replaced and stirring commenced with a slow nitrogen purge. The flask was heated in a 100 °C water bath for 12 h, causing the solution to reflux. After 12 h the dark brown solution was poured into a beaker containing 100 ml of ice water. Approximately 200 - 250 ml benzene was added to extract the oily product. The benzene layer (top) was rinsed with 100 ml 10% sodium carbonate (Fisher) solution (w/v $NaCO_3/H_2O$) and then with ~100 ml water. The benzene layer, a cloudy brown color, was clarified with magnesium sulfate, filtered, and the benzene was removed by rotary evaporation. The product was a red-brown oil that

solidified at room temperature. The tripentylacetamide was distilled (135-142 °C, full vacuum) to yield a solid yellowish-white wax (85% yield).

An attempt to convert tripentylacetonitrile to tripentylacetamide using neat sulfuric acid, at ~60 °C (oil bath was 83 °C), for 8 h, failed. The product was a dark brown-black oily product that was difficult to extract and thus discarded.

**Butyl Nitrite** (Aldrich, 95%) was vacuum distilled (42 mm, 18-20 °C).[45]

**Dioxane** (Aldrich, HPLC) was dried over molecular sieves overnight.

**Tripentylacetic Acid** [MSVII51-52] was prepared by the reaction of butyl nitrite and hydrochloric acid with tripentylacetamide in dioxane. To a 1 l three-neck round bottom flask equipped with a mechanical stirrer, reflux condenser, and septum, was added 300 ml dioxane by cannula. To this was added 20 g (0.074 moles) tripentylacetamide which had been diluted with dioxane and heated to facilitate addition. HCl gas (Merriam Graves, 99.0% purity) was bubbled into the solution for 15 minutes via stainless steel tubing. 30 ml (26 g or 2.5 moles) butyl nitrite was added over a 2 h period. The solution became orange and then red with continued addition of butyl nitrite (the flask warmed as evidenced by condensation on the reflux condenser). The reaction mixture was stirred at room temperature for an additional 2 h and then at 100 °C in a water bath for an additional 2 h. The solvent was removed by rotary evaporation and the product was fractionally distilled to remove any unreacted reagent (fraction 2: 92-94 °C; fraction 3: 113 °C; fraction 4: 122 °C, full vacuum ~0.2 mm) (35% yield).

**Tripentylacetyl Chloride**[46] (TPC) [MSVII53, 58-59] was prepared by reacting tripentylacetic acid with thionyl chloride. (See Figure 4.4 for experimental set up.) To a 100 ml round bottom flask equipped with a magnetic stir bar and reflux condenser was added 8.7 g (0.0322 moles) of tripentylacetic acid. 13.43 g (0.113 moles) of thionyl chloride (Aldrich) was added by cannula. The top of the reflux condenser was attached to a gas bubble trap filled with 1 M sodium hydroxide (Fisher) solution via an empty trap to avoid sodium hydroxide being withdrawn back into the reaction pot. The solution

effervesced for ~1 h while it was heated gently to ~40 °C; the solution was cooled to room temperature and was allowed to stir overnight; the solution was heated for an additional 2 h the next morning to ensure that the reaction went to completion. The product was fractionally distilled (~0.2 mm, ~85 °C) (57% yield).

**End-Capping Poly(ethylene oxide)** was accomplished by reacting the hydroxyl end group of PEO with an alkyl (or perfluoroalkyl) acid chloride in THF with pyridine (or 4-dimethylamino-pyridine, DMAP, (Aldrich, 99+%)) catalysis. Scheme 4.4 summarizes the reaction procedure with the different end groups studied. A 250 ml side arm round bottom flask containing PEO and a magnetic stir bar was dried under vacuum and recharged with nitrogen. ~75 ml THF was added to the flask to dissolve the PEO and the flask was heated with stirring in a 40 °C oil bath. The alkyl acid chloride was added by syringe in a molar excess with respect to the PEO hydroxyl end group; pyridine was added in a molar excess with respect to the acid chloride by cannula. The solution was stirred overnight at 40 °C; the product was precipitated in hexane and redissolved in THF and reprecipitated in hexane 3 times before it was dried (0.02 mm, room temperature). The amount of reagent used is detailed for each end group: HFB = heptafluorobutyrate; FD = nonadecafluorodecanoate (or perfluorodecanoate); ST = stearate; DO = dioctylacetate; TP = tripentylacetate.

**Pyridine** (Aldrich) was vacuum distilled from calcium hydride (Aldrich) and stored in a 500 ml round bottom side arm storage flask under positive nitrogen. Immediately before it was used, pyridine was redistilled from calcium hydride (trap-to-trap).

**Poly(ethylene oxide) Heptafluorobutyrate** (PEO-HFB) (Mn ~21,500 g/mole) was prepared by reacting 0.2 ml ($1.34 \times 10^{-3}$ moles) heptafluorobutyryl chloride with 1.0028 g ($3.6 \times 10^{-5}$ moles) poly(ethylene oxide) in THF with 0.2 ml ($2.47 \times 10^{-3}$ moles) pyridine. The HFBC and pyridine were added via syringe. From elemental analysis, PEO and HFBC reacted in 96% yield to produce PEO-HFB (V143). The yield

was determined by comparing the expected and observed fluorine contents: $C_{53.14}H_{8.77}O_{35.22}F_{2.87}$ (expected) vs. $C_{51.92}H_{8.83}O_{36.50}F_{2.75}$ (observed). [V90,97,143; VII6]

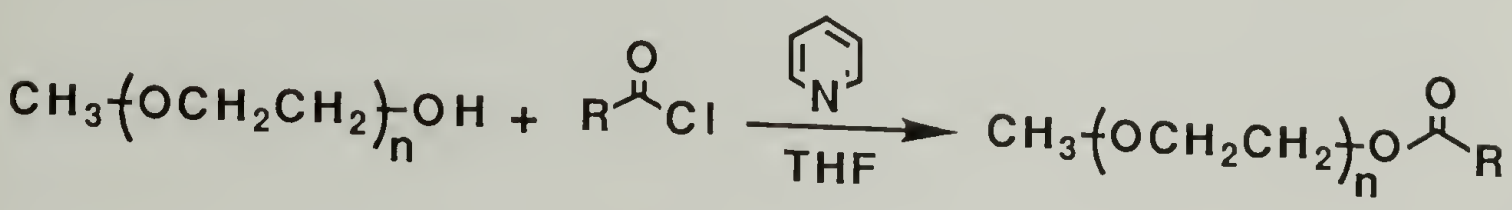


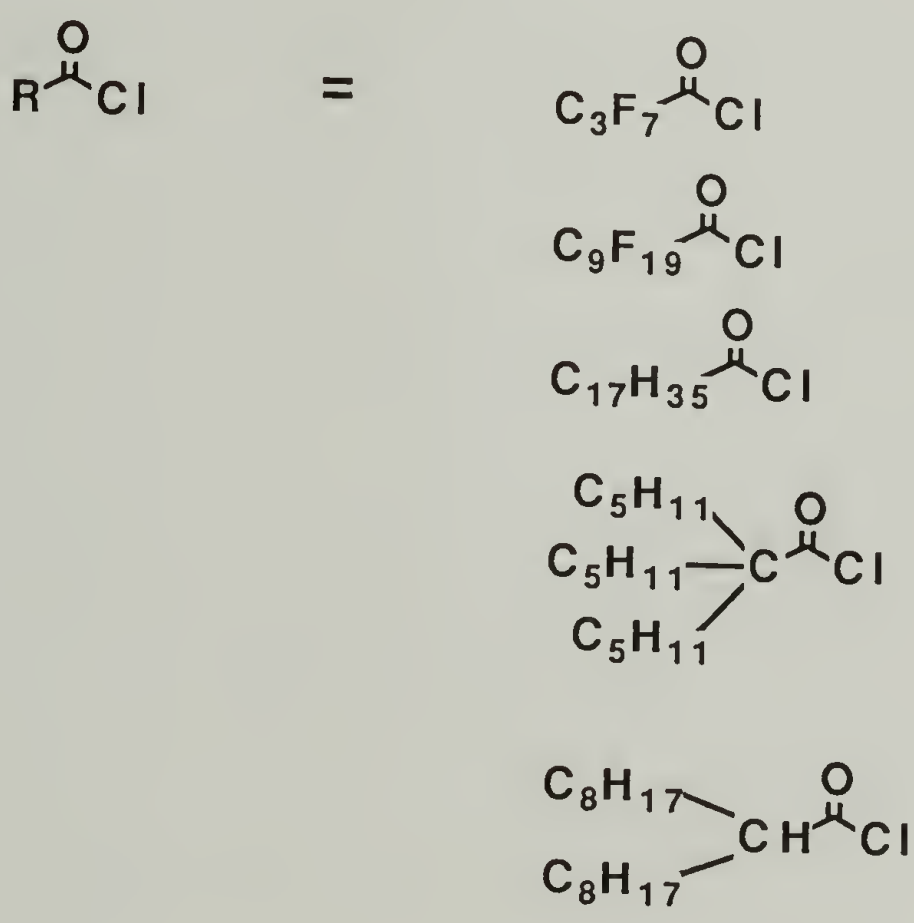


Scheme 4.4 End-Capping Reaction of Poly(ethylene oxide).

**Poly(ethylene oxide) Nonadecafluorodecanoate** (PEO-FD) (Mn ~44,000 g/mole) was prepared by reacting 0.31 g ($5.82 \times 10^{-4}$ moles) nonadecafluorodecanoyl chloride with 1.0124 g ($3.01 \times 10^{-4}$ moles) poly(ethylene oxide) in THF with 0.3 ml ($3.71 \times 10^{-3}$ moles) pyridine. FDC was dissolved in THF and added via cannula whereas pyridine was added via syringe. PEO reacted with FDC in 64% yield to produce PEO-FD

(V142). The yield was calculated by comparing the expected and observed fluorine contents determined by elemental analysis: $C_{51.37}H_{8.23}O_{33.08}F_{7.32}$ (expected) vs. $C_{51.28}H_{8.51}O_{35.56}F_{4.65}$ (observed). [V130,142, VII7, 16,54]

**Poly(ethylene oxide) Stearate** (PEO-ST) (Mn ~50,000 g/mole) was prepared by reacting 0.2 ml ($5.92 \times 10^{-4}$ moles) stearoyl chloride with 1.4 g ($2.79 \times 10^{-5}$ moles) poly(ethylene oxide) in THF with 0.6 ml ($7.42 \times 10^{-3}$ moles) pyridine. STC and pyridine were added via cannula. [VII8,26]

**Poly(ethylene oxide) Dioctylacetate** (PEO-DO) (Mn ~44,000 g/mole) was prepared by reacting 0.090 g ($2.97 \times 10^{-4}$ moles) dioctylacetyl chloride with 1.0032 g ($2 \times 10^{-5}$ moles) poly(ethylene oxide) in THF with 0.052 g ($4.11 \times 10^{-4}$ moles) DMAP. DOC was added by syringe whereas DMAP was dissolved in THF and added via cannula. [VII78]

**Poly(ethylene oxide) Tripentylacetate** (PEO-TP) (Mn ~40,000 g/mole) was prepared by reacting 0.076 g ($2.8 \times 10^{-4}$ moles) tripentylacetyl chloride with 0.9987 g ($1.99 \times 10^{-5}$ moles) poly(ethylene oxide) in THF with 0.046 g ($3.76 \times 10^{-4}$ moles) DMAP. TPC was added by syringe whereas DMAP was dissolved in THF and added by cannula. [VII72,74]

Adsorption

**Poly(tetrafluoroethylene-co-hexafluoropropylene)** (FEP, 5 mil) was obtained from duPont and extracted in refluxing dichloromethane for 1 h; the polymer film was rinsed in fresh dichloromethane and then dried (0.02 mm) to constant mass. The polymer film samples were stored under vacuum.

**Poly(chlorotrifluoroethylene)** (PCTFE, 5 mil Aclar 33C) was obtained from Allied and extracted in refluxing dichloromethane for 1 h; the polymer film samples were

rinsed in fresh dichloromethane and then dried (0.02 mm) to constant mass. The polymer film samples were stored under vacuum.

**Poly(vinylidene fluoride)** ($PVF_2$, 5 mil Pennwalt Kynar) was purchased from Westlake Plastics and extracted in refluxing dichloromethane for 1 h; the polymer film samples were rinsed in fresh dichloromethane and then dried (0.02 mm) to constant mass. The polymer film samples were stored under vacuum.

**Polystyrene Latex** (PS) (lot #10-87-17) was purchased from Interfacial Dynamics Corporation (IDC) and used without further purification. The solution provided contained 4.1% solids and was stored in the refrigerator. A working stock was prepared immediately before use by diluting 0.55 ml of the IDC solution with 3.45 ml of house distilled water redistilled using a Gilmont still. The PS latex was carboxylic acid stabilized in water where the area per charge group was 202 $Å^2$ or 14.2 Å between charge groups.

**Adsorption of Poly(ethylene oxide) (PEO) and End-Capped Poly(ethylene oxide) (PEO-R) to the Fluoropolymer - Water Interface.** A known mass of PEO or PEO-R was dissolved in 20 ml house distilled water in a glass test tube. After dissolution (30 minutes), a polymer film sample was immersed completely in the solution. The adsorption tube was immersed in a constant temperature bath (25 °C) for the duration of the adsorption experiment. The PEO (PEO-R) solution was removed by cannula and replaced with distilled water for 30 minutes. This solution was removed by cannula and the polymer film was dried (0.02 mm, 24 h).

**Adsorption of PEO and PEO-R to the Polystyrene Latex - Water Interface.** A stock solution of PEO (PEO-R) was prepared by dissolving a known amount of PEO (PEO-R) in a known amount of doubly distilled water. A known volume of the PEO (PEO-R) stock solution was diluted with doubly distilled water to a known concentration to 4 ml in a polystyrene cuvette. 28 µl of the PS latex working stock solution was added to the cuvette containing 4 ml of a PEO (or PEO-R) solution. The total area of PS latex was 20.45 $cm^2$/ml. The solution in the cuvette was sonicated for 30 minutes and

then allowed to settle for 15 minutes before making measurements on the Photon Correlation Spectrometer.

**Adsorption of PEO and PEO-R to the Air - Water Interface** was studied by measuring the surface tension of water with increasing concentrations of PEO (PEO-R) solutions. A stock solution of PEO (PEO-R) was prepared by dissolving a known amount of polymer in house distilled water which had been filtered by a Millipore Q system, providing water with a conductivity of 18.2 $M\Omega^{-1}cm^{-1}$. PEO (PEO-R) was added incrementally to 10 ml of filtered water in a glass flask, thereby increasing the concentration of PEO (PEO-R). Measurements were made in the glass flask equilibrated at 25 °C. The surface tension of the solution was measured with a Du Nuoy platinum-iridium ring. See Figure 4.5 for experimental set up.



**Constant Temperature Bath** that was used for adsorption to polymer film samples was a Haake A81.

**Contact Angle** ($\theta_A/\theta_R$) measurements were obtained on a Ramé-Hart telescopic goniometer using a Gilmont syringe with a 25 gauge flat-tipped needle. House distilled water, redistilled using a Gilmont still, was used as the probe fluid. Dynamic contact angles were determined by measuring the tangent of the drop at the intersection of the air-drop-surface while adding (advancing contact angle - $\theta_A$) and withdrawing (receding contact angle - $\theta_R$) solution to and from the drop. The values reported are an average of at least 5 measurements made at different locations on the film sample.

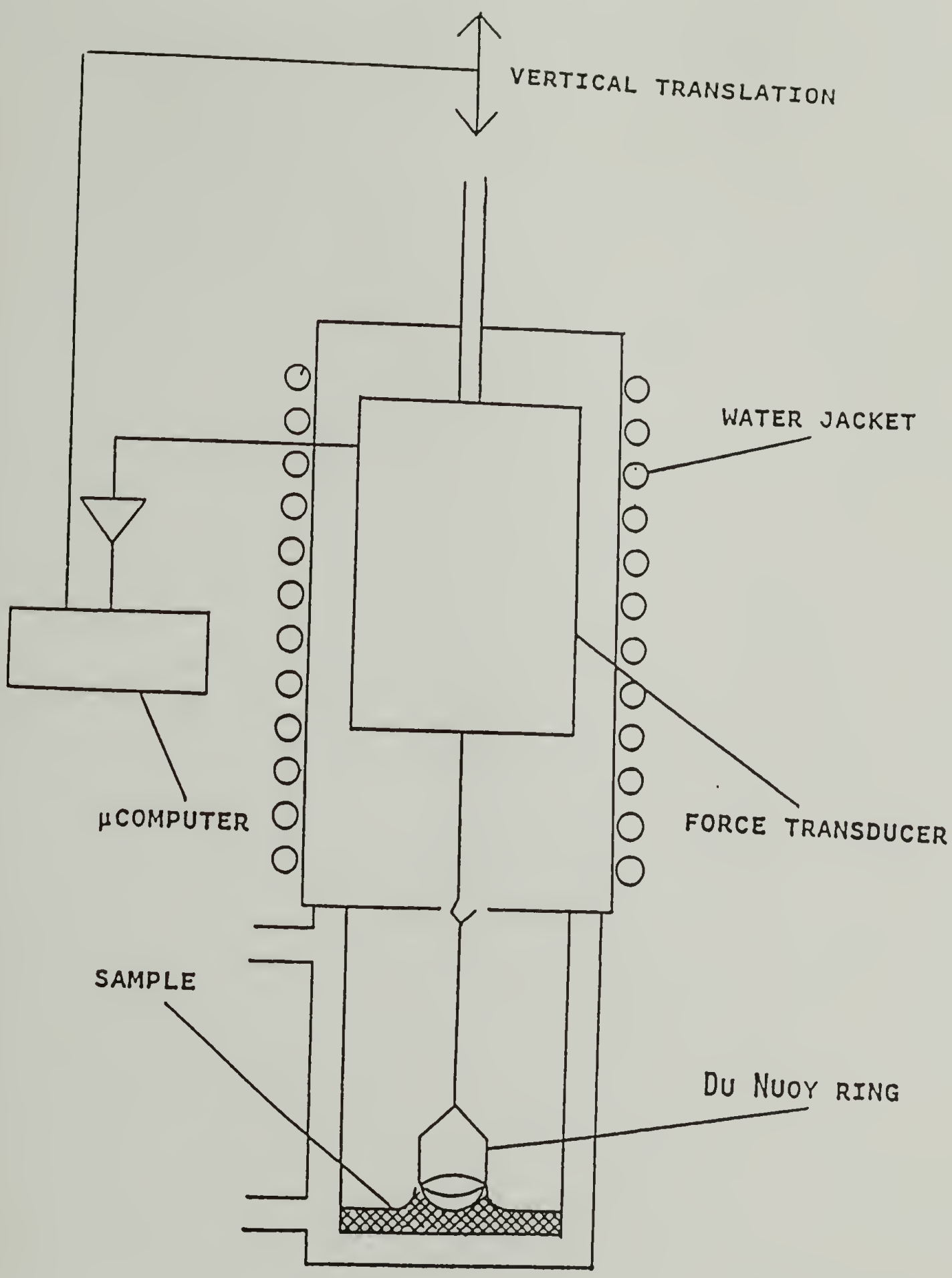


Figure 4.5 Surface Tension Apparatus.

**Captive Bubble Contact Angle** measurements were made in a glass capsule with an air bubble (Figure 4.6). The values reported are an average of at least 5 measurements made at different locations on the film sample.

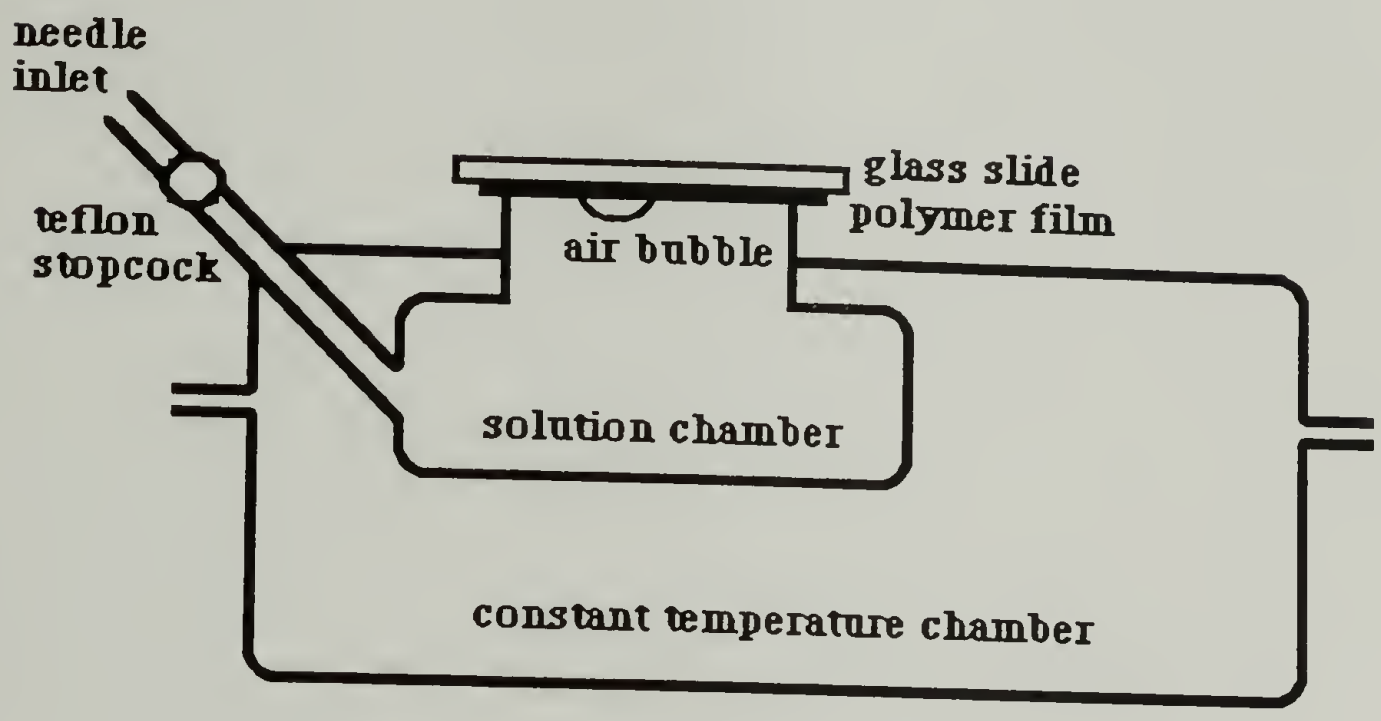


Figure 4.6 Captive Bubble Contact Angle Apparatus.

**Elemental Analysis** was provided by the Microanalysis Lab at the University of Massachusetts.

**Gas Chromatography** (GC) measurements were obtained on a Hewlett Packard 5790A series gas chromatograph; a Supelco capillary column of 0.53 mm ID packed with fused silica was used.

**Gel Permeation Chromatograms** (GPC) were obtained on an aqueous mobile phase GPC using ethylene glycol as the flow marker peak. The calibration curve was prepared with poly(ethylene oxide) standards purchased from PolySciences and Polymer Labs. Additional GPCs were obtained on a THF mobile phase GPC for comparative

purposes only; Polymer Labs styragel columns were used with a Waters differential refractometer R403.

**Infrared Spectra** (IR) were obtained under nitrogen on a IBM Nicolet 44 FT IR spectrometer by casting a film on a sodium chloride salt plate. For PEO(-R), films were cast from methanol; for "R" groups IR spectra were taken of the neat solution.

**Melting Point** (MP) measurements were made on an Electrothermal melting point apparatus.

**Proton Nuclear Magnetic Resonance** ($^1$H NMR) spectra were obtained under nitrogen on a Bruker AC80 MHz spectrometer. The deuterated solvents used included benzene and dimethylsulfoxide (both from Aldrich).

**Photon Correlation Spectroscopy** (PCS) data were obtained on a Brookehaven BI-90. 5 scans were made at 5000 cycles per scan for each measurement. The values reported are an average at least 2 separate measurements.

**Surface Tension** measurements were made on a surface tensiometer (Figure 4.5) with a platinum-iridium Du Nuoy ring (Fisher, #5430) of mean circumference 6.040 cm and with an R/r ratio of 54.107232. (R is the radius of the ring whereas r is the radius of the wire.) All values reported are an average of at least 2 measurements which were made at a constant temperature of 25 °C.

**Ultraviolet-visible** (UV-vis) spectra were obtained on a Perkin Elmer λ2. Turbidity measurements at 500 nm were attempted with an aqueous potassium iodide (Fisher) / iodine (Fisher) solution.[47] 1 g of iodine ($I_2$) and 2 g of potassium iodide (KI) were dissolved in distilled water (100 ml) in a volumetric flask. 0.25 ml of the aqueous $KI/I_2$ solution was added to 10 ml of an aqueous solution of poly(ethylene oxide). After 5 minutes the turbidity measurements were made. The reference cell contained an aqueous solution of PS latex which had been filtered by syringe through a 0.22 μm Millipore filter. The sample cell contained a PS-PEO(-R) solution which had also been filtered by syringe through a 0.22 μm Millipore filter. The filter was used to separate PS latex from PEO(-R)

dissolved in solution. $KI/I_2$ reacted with PEO(-R) to form a turbid solution. The amount of PEO(-R) adsorbed to PS latex was calculated by difference and by comparison to a calibration curve.

**X-ray Photoelectron Spectra** (XPS) were recorded on a Perkin Elmer Physical Electronics 5100 spectrometer using Mg Kα excitation (400 W, 15 kV) for less than 10 minutes. The pressure in the analysis chamber was less than ~$10^{-8}$ torr. Samples were analyzed at a 15° takeoff angle between sample and detector at pass energies of 89.45 eV and 35.75 eV for survey and $C_{1s}$ region spectra, respectively. The sensitivity factors used were $C_{1s}$ 0.202; $F_{1s}$ 1.000; $O_{1s}$ 0.540; $Si_{2p}$ 0.225. Binding energies reported are not corrected for charging.

## Results and Discussion

### Synthesis

#### PEO and PEO-R

Poly(ethylene oxide) (PEO) has been synthesized reproducibly to molecular weights as high as ~50,000 g/mole by anionic polymerization, as was shown by Reuter *et al.*[21] This success is repeated here with a different initiator. Because the PEO synthesized here was used in adsorption experiments where the effect of the end group was studied, an initiator which resembled the PEO repeat unit was chosen. Triethylene glycol monomethyl ether potassium (TEGMEK) was used to anionically initiate polymerization of ethylene oxide. The methyl group of TEGMEK was unlikely to compete with the alkyl end group (covalently attached by a separate reaction) for adsorption sites. Figueruelo *et al.*[11] used a similar initiator, diethylene glycol monomethyl ether potassium, but were unsuccessful in producing polymer with a molecular weight greater than 17,800 g/mole.

Poly(ethylene oxide) PEO was synthesized by anionic ring opening polymerization of ethylene oxide using triethylene glycol monomethyl ether potassium initiation, as described in Scheme 4.1. PEO samples, characterized on the GPC (aqueous phase) against PEO standards, are listed in Table 4.1 with molecular weight, polydispersity and yield data. (Samples marked with an asterisk (*) were used in adsorption studies.) Figure 4.7 includes two representative chromatograms. PEO of molecular weights ~5,000 to 50,000 g/mole with polydispersity indices between 1.07 and 1.17 were prepared. Difficulty in polymerizing ethylene oxide to molecular weights greater than 55,000 g/mole was observed and is evident in Table 4.1. Greater success was achieved in predicting lower (~5,000 g/mole) than higher (~25,000 to 50,000 g/mole) molecular weight PEO from the molar ratio of monomer to initiator. The molecular weight of PEO is limited by this technique.

A combination of effects likely limited PEO molecular weight. In order to prepare higher molecular weight polymers, lower ion concentrations are used; however, these show decreased activity and polymerize more slowly. Association of the ion pairs of different polymers can cause the formation of a tetramer, for example, which will also decrease the rate of polymerization. According to Kazanskii,[48] the difficulties associated with anionic polymerization of ethylene oxide result, in part, from the high negative charge localized on the terminal oxygen, $O^-$, and thus the increased strength of the ion pair (with respect to that of vinyl polymers). In addition, the terminal ion pair is solvated by the poly(ethylene oxide) chain by a process called self-solvation; the poly(ethylene oxide) chain can solvate its own ions better than crown ethers and usually better than cryptands.[49] An attempt to enhance polymerization with 18-crown-6 was unsuccessful; no polymer was isolated on three separate occasions. [V102,106,110] Humidity seemed to adversely affect polymerization; in an attempt to overcome this problem, all tygon tubing attached to nitrogen lines was replaced with stainless steel cannula. With the addition of kryptofix [222], it was difficult to assess whether polymerization was facilitated. [V147]

Table 4.1 Poly(ethylene oxide) GPC and Yield Data. [V116-119]

| Sample | $M_n$ (calc) | $M_n$ (obs) | $M_w$ | PDI | yield (%) | time of reaction (h) |
|---|---|---|---|---|---|---|
| *MSV85 | 5,815 | 7,935 | 8,465 | 1.07 | 74 | 112 |
| MSV133 | 5,083 | 6,979 | 7,819 | 1.12 | 82 | 43 |
| MSV139 | 4,625 | 4,387 | 5,021 | 1.14 | 100 | 40 |
| MSV29 | 32,190 | 26,832 | 31,292 | 1.17 | 93 | 25 |
| MSV32 | 46,980 | 27,377 | 32,454 | 1.18 | 94 | 40 |
| *MSV44 | 82,820 | 16,184 | 17,340 | 1.07 | 83 | 12 |
| MSV62 | 22,3692 | 25,823 | 29,739 | 1.15 | 85 | 24 |
| *MSV67 | 88,192 | 25,749 | 28,746 | 1.12 | 32 | 36 |
| MSV120 | 106,165 | 24,926 | 29,384 | 1.18 | 91 | 62 |
| MSV126 | 15,000 | 15,156 | 17,347 | 1.14 | 84 | 40 |
| MSV36 | 187,530 | 39,005 | 49,448 | 1.27 | 51 | 24 |
| *MSV40 | 170,157 | 52,883 | 65,757 | 1.24 | 74 | 43 |
| MSV147 | 141,740 | 48,724 | 59,476 | 1.22 | 95 | 93 |
| *MSVII24 | 78,760 | 50,160 | 59,100 | 1.17 | 87 | 39 |

*PEO samples that were used in adsorption experiments.

Poly(ethylene oxide) was end-capped by reacting the terminal hydroxyl group of PEO with an alkyl acid chloride to form an ester end group on PEO (PEO-R). The strategy for end-capping PEO is shown in Scheme 4.4 where a number of alkyl and perfluoroalkyl acid chlorides are listed as end-capping reagents: heptafluorobutyryl chloride (HFBC), nonadecafluorodecanoyl chloride (FDC), stearoyl chloride (STC), dioctylacetyl chloride

(DOC), and tripentylacetyl chloride (TPC). The reaction between primary alcohol and acid

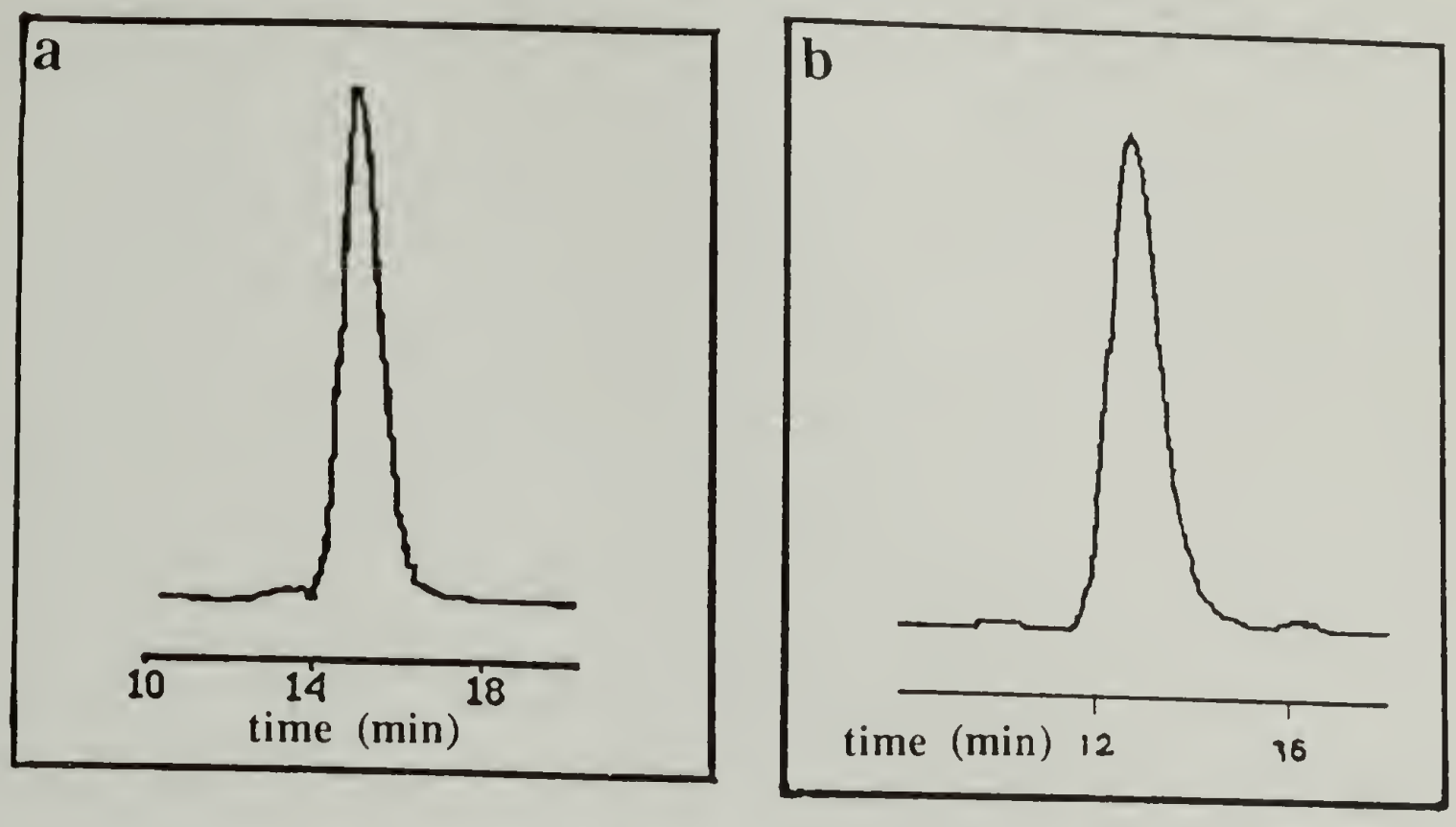


Figure 4.7 Chromatograms of Poly(ethylene oxide) Acquired on Aqueous Mobile Phase GPC (a) Mn ~7,900 g/mole, PDI 1.07; (b) Mn ~50,000 g/mole, PDI 1.17.

chloride is a standard procedure used to form esters.[50] In these reactions, pyridine (or DMAP) catalyzed the reaction by enhancing the reactivity at the carbonyl group by reacting with the acid chloride to form the pyridinium hydrochloride.[51] The pyridinium hydrochloride salt precipitated in THF; the solution was filtered before precipitating the end-capped polymer in hexane. This procedure, repeated several times, ensured that the polymer samples were not contaminated. Although in itself not proof of purity, no nitrogen was detected by XPS analysis of PEO-R films cast on glass. (Fluorine was easily detected by XPS for samples end-capped with a perfluoroalkyl group.)

PEO-R was characterized by GPC (aqueous phase) which indicated that PEO was not degraded by the end capping reaction. Table 4.2 includes GPC data and Figures 4.8

and 4.9 include representative chromatograms of PEO-R samples obtained on the aqueous and THF mobile phase GPC, respectively. (Samples marked with an asterisk (*) were used in adsorption experiments.) Apparent in these chromatograms is that PEO-ST (Figure 4.8 (c)) was not detected on the aqueous phase GPC but was easily detected by the THF-phase GPC (Figure 4.9). PEO-ST apparently adsorbed to the styragel column from water but not THF. GPC thus indicates that the labeling reaction with stearoyl chloride went to completion. Although this in itself does not indicate complete conversion, it is a good indication that the reaction was largely successful. In order to negate the hypothesis that PEO-ST was not detected on the aqueous mobile phase GPC due to micelle formation, a chromatogram was taken of a solution of PEO and PEO-ST; a peak corresponding to PEO was easily detected (Figure 4.10).

Table 4.2 GPC Data of Alkyl End-Capped Poly(ethylene oxide).

| Sample | Mn (g/mole) | Mw (g/mole) | PDI |
|---|---|---|---|
| PEO (V32) | 27,380 | 32,450 | 1.18 |
| PEO-HFB (V90) | 21,450 | 25,730 | 1.20 |
| PEO (V89) | 9,180 | 9,530 | 1.04 |
| PEO-HFB (V97) | 9,140 | 9,510 | 1.05 |
| PEO (V85) | 7,940 | 8,470 | 1.07 |
| PEO-HFB (VII6) | 7,480 | 8,300 | 1.11 |
| PEO (V139) | 4,390 | 5,020 | 1.14 |
| PEO-HFB (V143) | 3,700 | 4,270 | 1.15 |
| PEO (V120) | 24,930 | 29,380 | 1.18 |
| PEO-FD (V130) | 23,490 | 29,200 | 1.24 |
| PEO (V139) | 4,390 | 5,020 | 1.14 |
| PEO-FD (V142) | 3,370 | 3,850 | 1.14 |
| PEO (V85) | 7,940 | 8,470 | 1.07 |
| PEO-FD (VII7) | 7,180 | 8,030 | 1.12 |
| PEO (V62) | 25,820 | 29,740 | 1.15 |
| PEO-FD (VII16) | 24,650 | 28,610 | 1.16 |
| PEO (VII24) | 50,160 | 59,100 | 1.17 |
| *PEO-FD (VII54) | 43,700 | 52,355 | 1.20 |
| PEO (VII24) | 50,160 | 59,100 | 1.17 |
| *PEO-ST (VII26) | #similar | # | # |
| PEO (VII24) | 50,160 | 59,100 | 1.17 |
| *PEO-DO (VII78) | 44,320 | 53,680 | 1.21 |
| PEO (VII24) | 50,160 | 59,100 | 1.17 |
| *PEO-TP (VII62,74) | 40,311 | 51,320 | 1.27 |
| PEO (V139) | 4,390 | 5,020 | 1.14 |
| PEO-TP (VII72) | 4,590 | 5,422 | 1.18 |

#PEO-ST adsorbed to the column and could not be detected by the aqueous mobile phase GPC, but it was detected by the THF mobile phase GPC.
*PEO-R samples used in adsorption experiments.

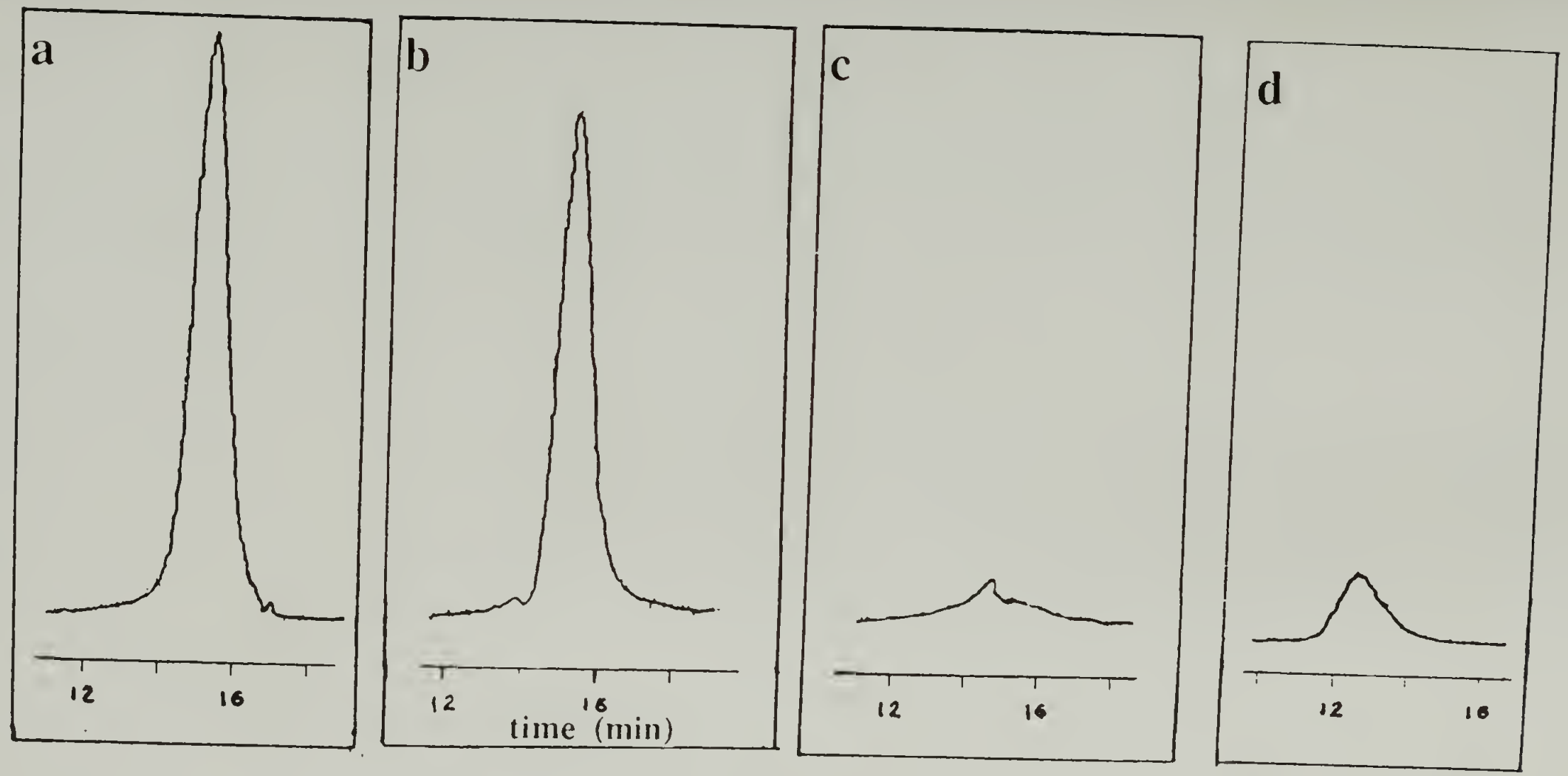


Figure 4.8 Chromatograms Acquired on Aqueous Mobile Phase GPC for (a) PEO-HFB (Mn ~7500 g/mole, PDI 1.11); (b) PEO-FD (Mn ~7200 g/mole, PDI 1.12); (c) PEO-ST (similar molecular weight and polydispersity to PEO); (d) PEO-DO (Mn ~44,320 g/mole, PDI 1.21).

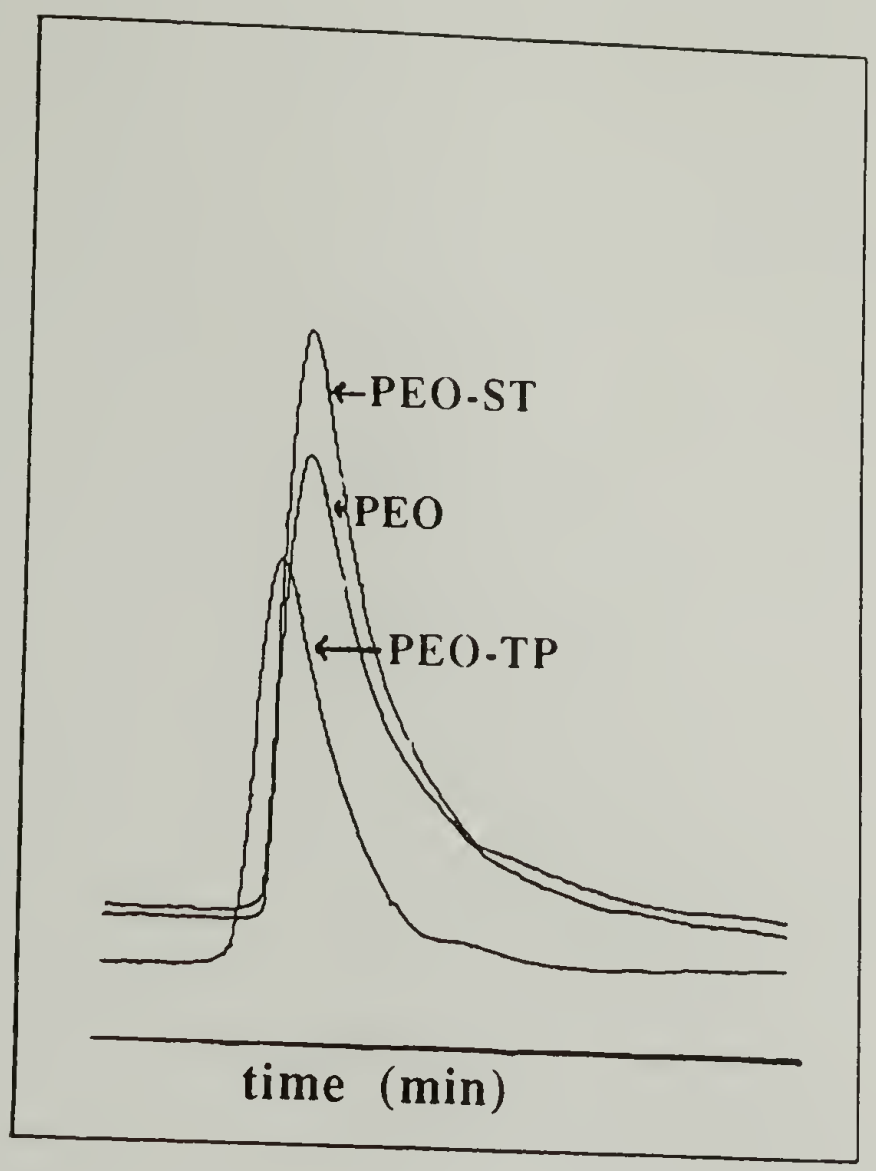


Figure 4.9 Chromatograms Acquired on THF Mobile Phase GPC Comparing PEO, PEO-ST, and PEO-TP.


Figure 4.10 Chromatogram Acquired on Aqueous Mobile Phase GPC for PEO and PEO-ST.

Characterization of PEO-R was difficult because the end group was small relative to the number of ethylene oxide repeat units. End capped poly(ethylene oxide) was characterized by infrared spectroscopy to detect the carbonyl ester. Because the end group was small relative to the ethylene oxide repeat units, low molecular weight PEO-R was used in IR measurements. It was assumed that the end-capping reaction was as successful for high as it was for low molecular weight PEO. Figure 4.11 includes some representative IR spectra for PEO and PEO-R. Although it was difficult to quantify the yield of the end-capping reaction, excess acid chloride, catalyst, and time of reaction were used in an attempt to enhance complete conversion of the hydroxyl group to the ester

group. $^{1}H$ NMR was not useful because the end group of even low molecular weight PEO was too small (relative to ethylene oxide repeat units) for detection.

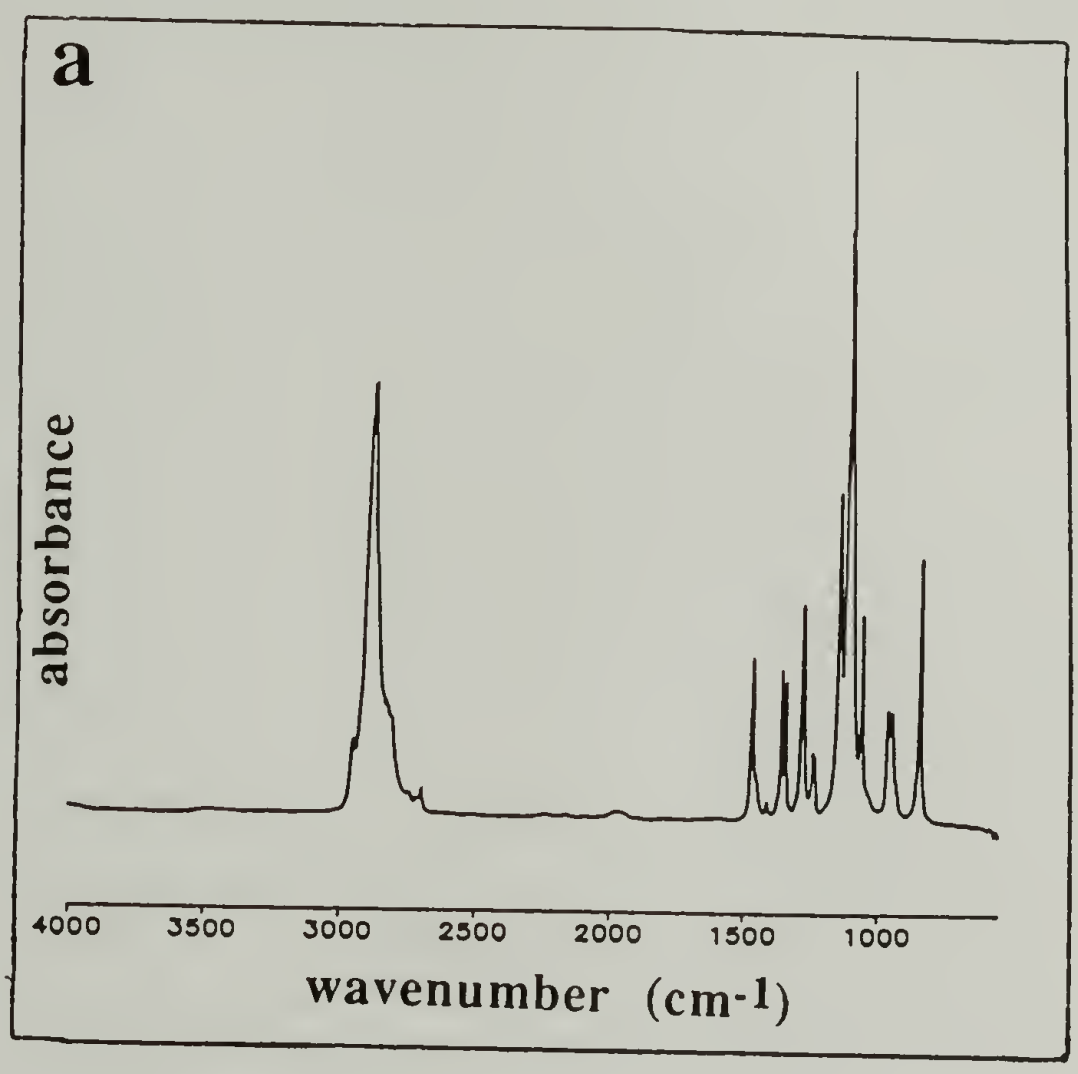


Figure 4.11 Infrared Spectra of (a) PEO; (b) PEO-HFB; (c) PEO-FD; (d) Comparison of PEO, PEO-HFB, PEO-FD; (e) PEO-TP. Continued, next page.

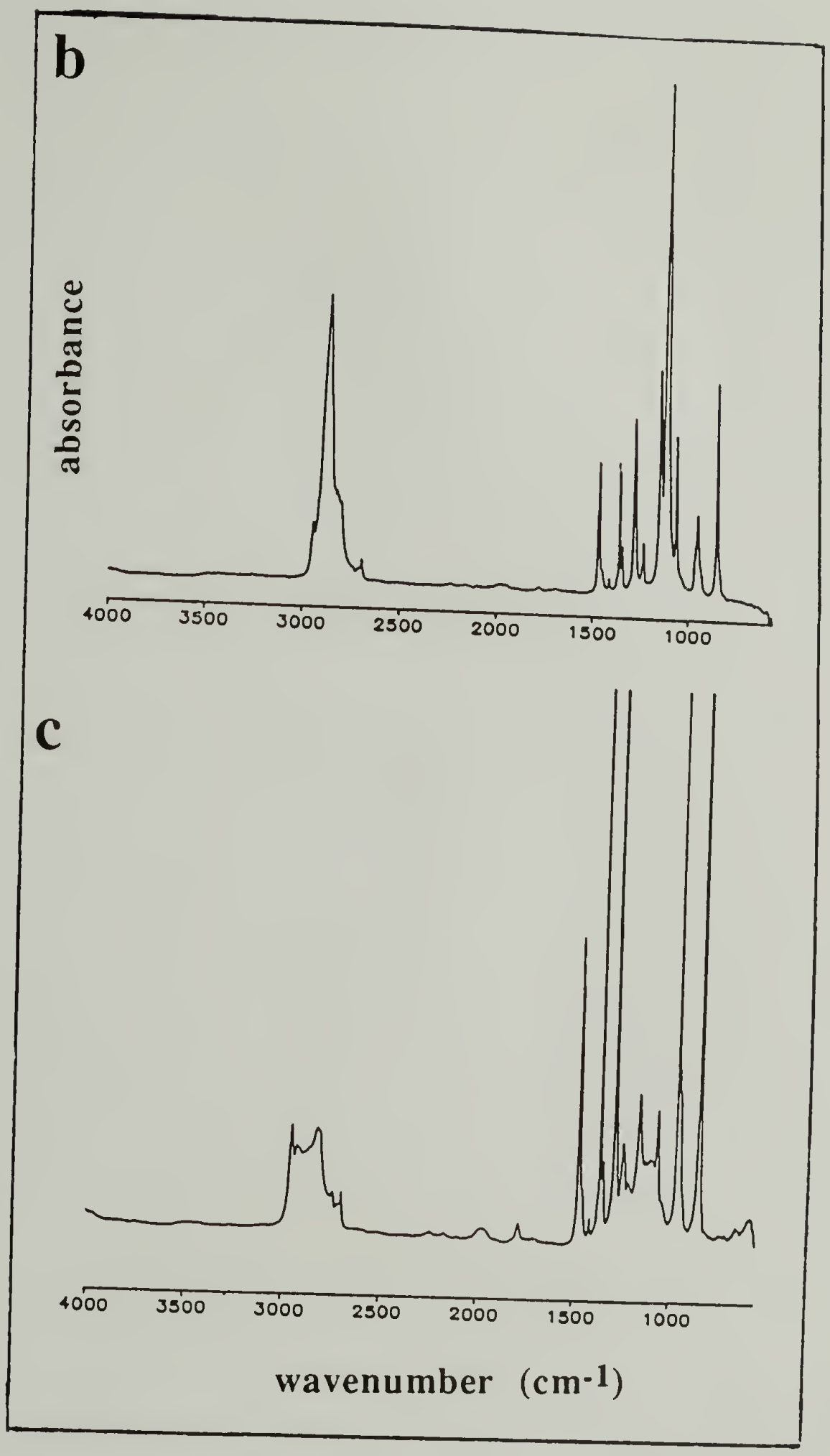


Figure 4.11 Continued.

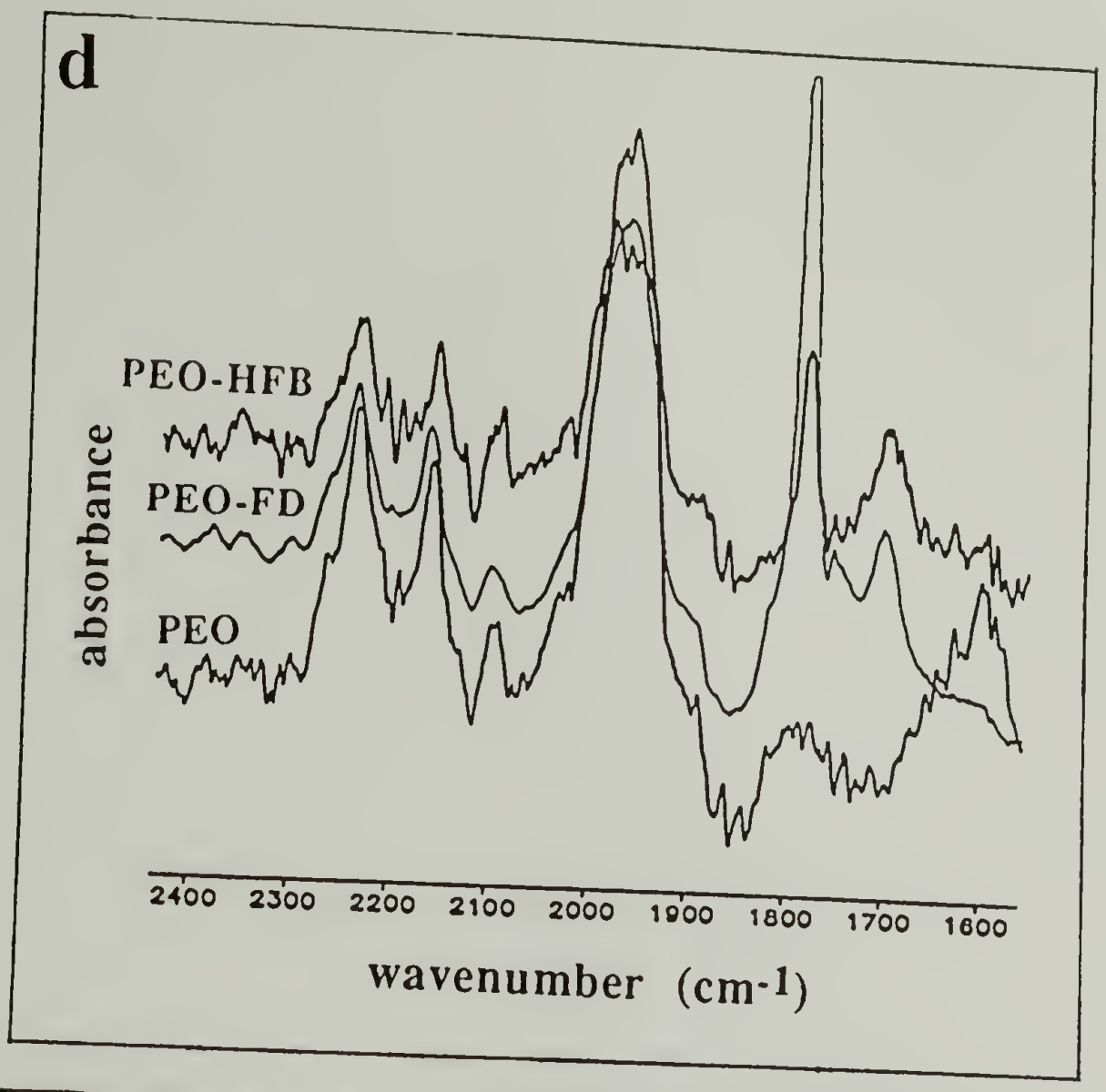


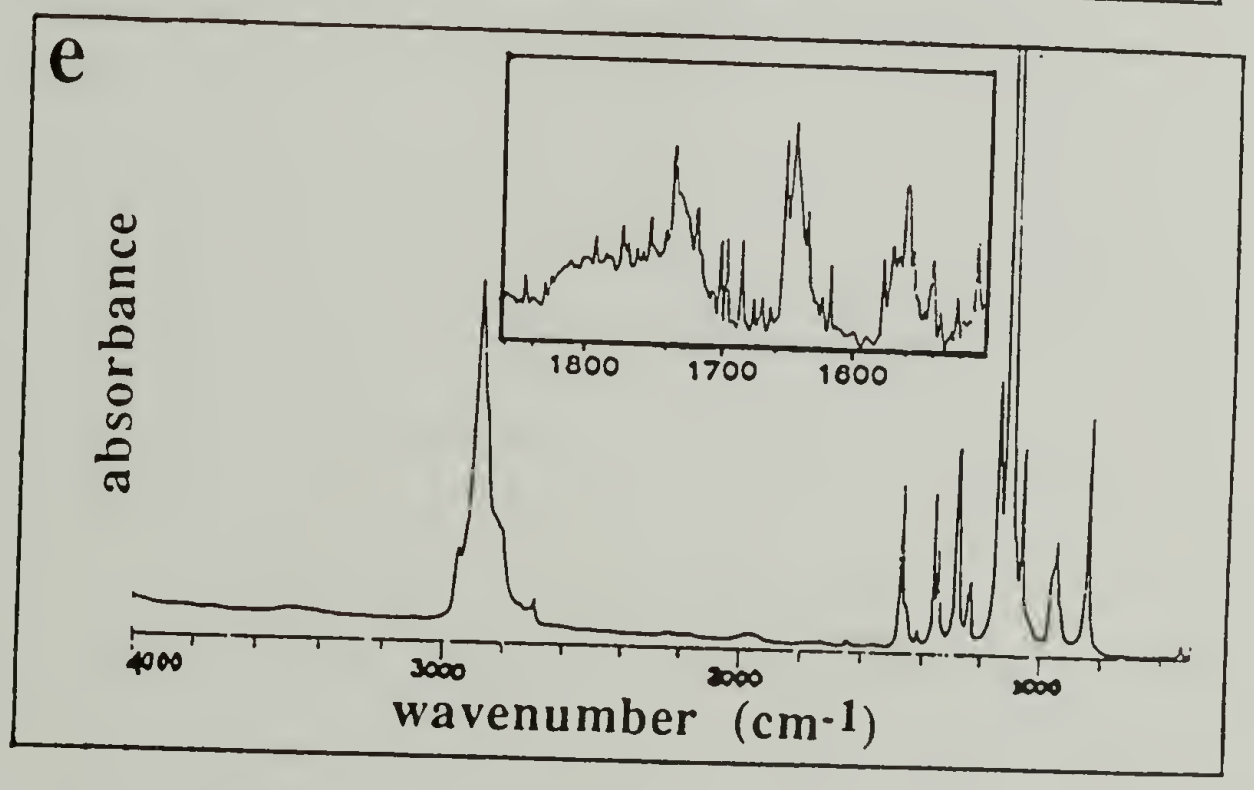


Figure 4.11 Continued.

The stability of the perfluoroester in aqueous solution was studied by infrared spectroscopy. Low molecular weight PEO-FD (MSV142) was dissolved in water to which

hydrochloric acid was added. After ~4 h, the polymer was recovered by freeze-drying. The IR spectrum, included in Figure 4.12, indicates the presence of the carbonyl ester at ~1780 $cm^{-1}$.

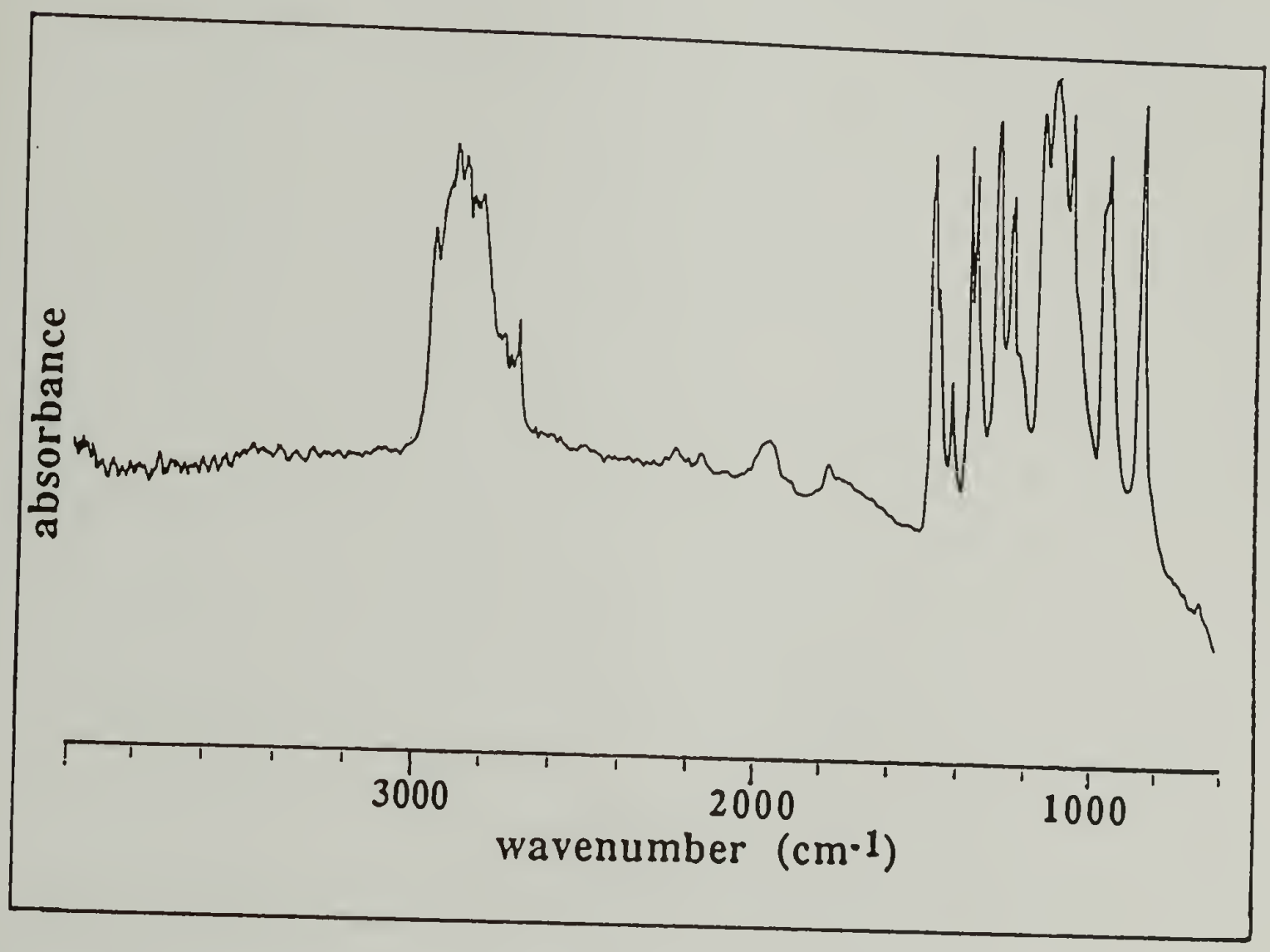


Figure 4.12 Infrared Spectrum of PEO-FD After Attempted Hydrolysis.

End Groups

Dioctylacetyl chloride[42] (DOC) and tripentylacetyl chloride[44] (TPC) were synthesized according to published procedures with some noted changes. These end groups, unlike the others, could not be purchased. DOC and TPC were synthesized for use in the end capping reaction with PEO which was described in the previous section.

Dioctylacetyl chloride was synthesized from diethyl malonate via several intermediates. The synthetic procedure used to prepare dioctylacetyl chloride is described in Scheme 4.2. These intermediates were characterized by several techniques which are listed in Table 4.3 with the expected and observed elemental analyses. The infrared, proton nuclear magnetic resonance, and gas chromatography spectra are included in Figures 4.13, 4.14, and 4.15, respectively.

Table 4.3 Elemental Analysis Results and Additional Techniques Used in Dioctylacetyl Chloride Synthesis.

| Sample | Expected (wt %) C : H : O : Cl | Observed (wt %) C : H : O : Cl | Additional Analyses |
|---|---|---|---|
| diethyl octylmalonate | 66.20 : 10.29 : 23.51 | 66.47 : 10.37 : 23.16 | $^1$H NMR; IR; GC |
| diethyl dioctylmalonate | 71.83 : 11.53 : 16.64 | 71.95 : 11.66 : 16.39 | $^1$H NMR; IR; GC |
| dioctylacetic acid | 76.00 : 12.76 : 11.24 | 76.06 : 11.08 : 12.86 | IR; MP (37 - 39 °C) (lit. 38 °C)[42] |
| dioctylacetyl chloride | 71.37 : 11.65 : 5.28 : 11.70 | 72.22 : 11.22 : 6.18 : 10.38 | IR |

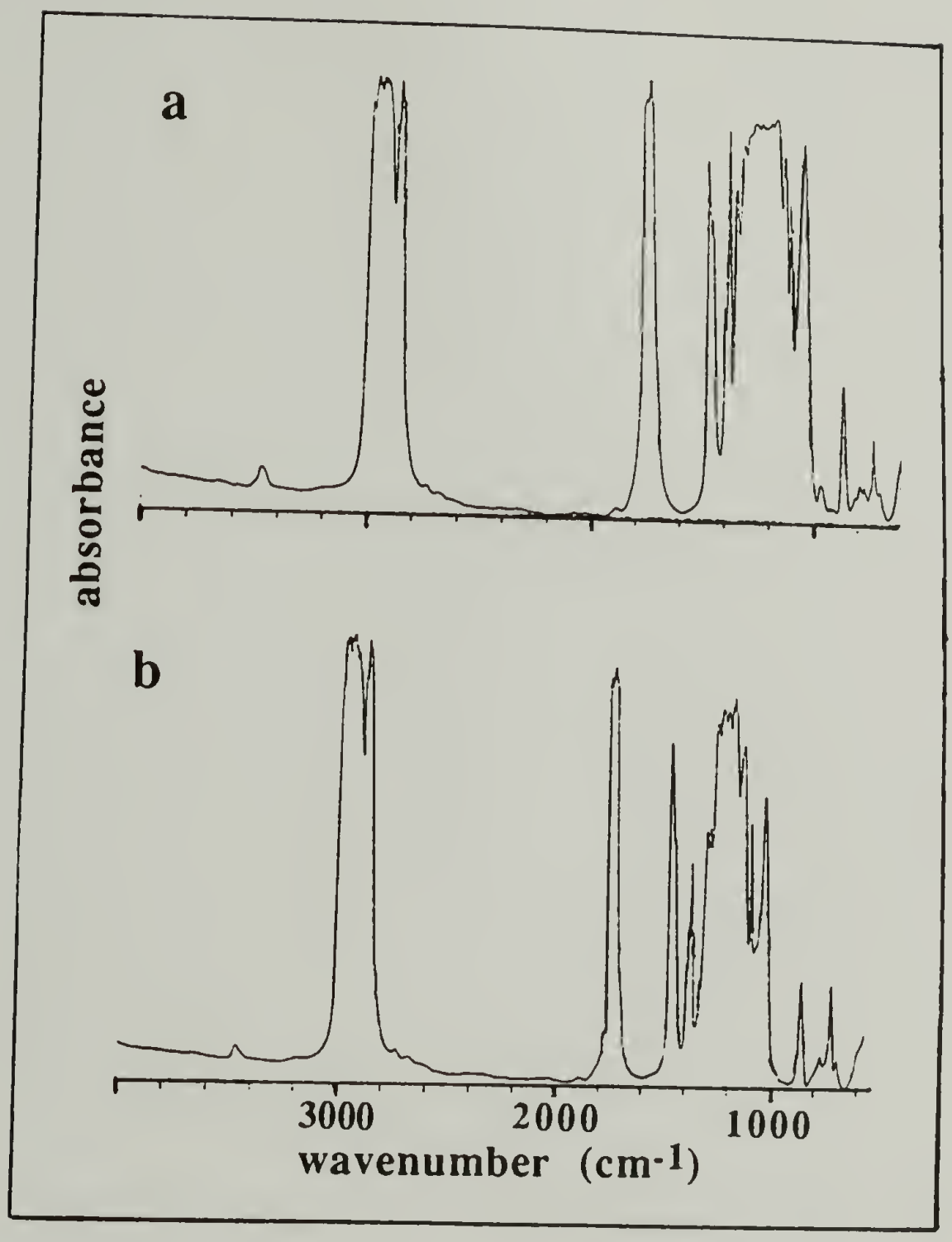


Figure 4.13 Infrared Spectra of (a) Diethyl Octylmalonate, (b) Diethyl Dioctylmalonate, (c) Dioctylacetic Acid, (d) Dioctylacetyl Chloride. Continued, next page.

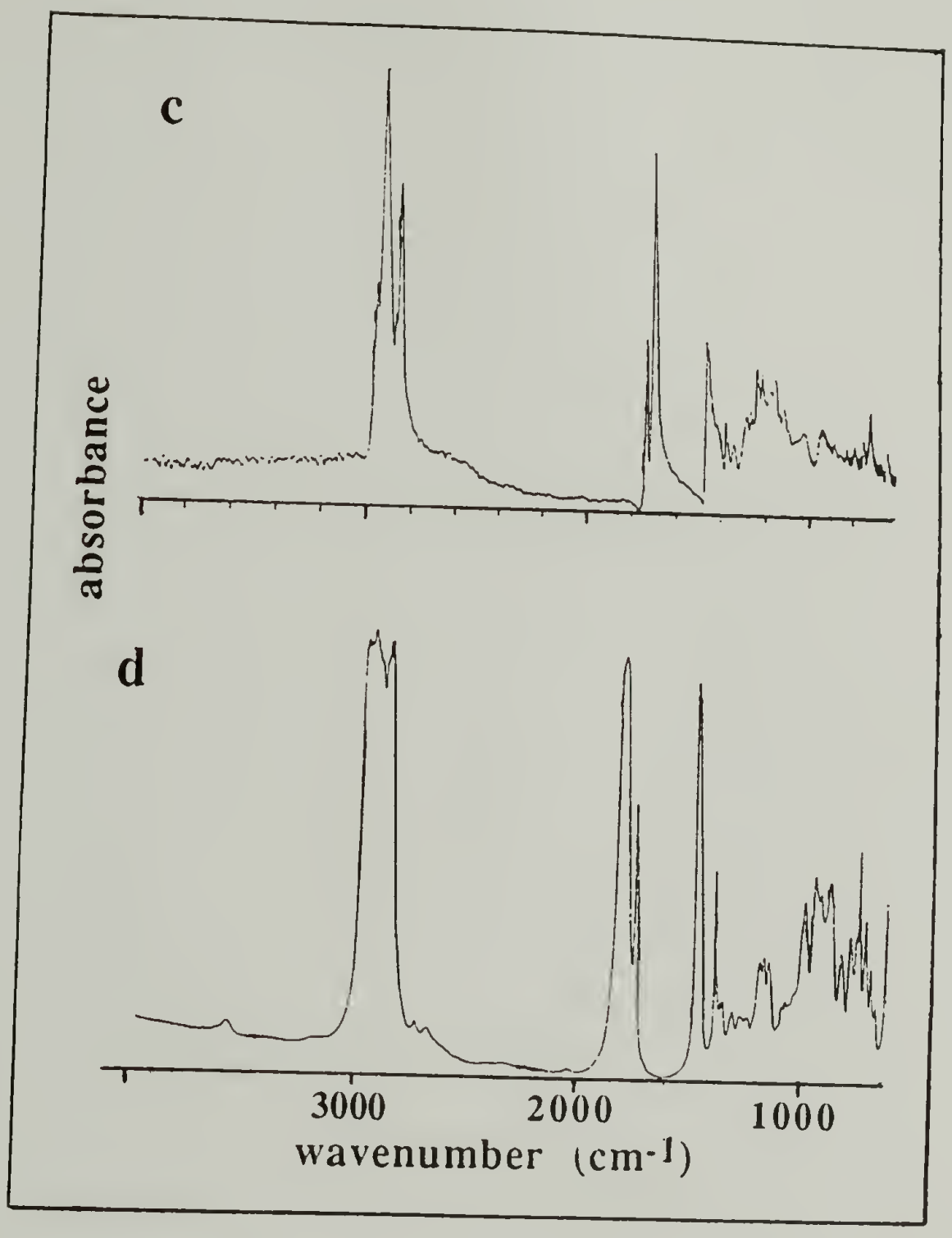


Figure 4.13 Continued.

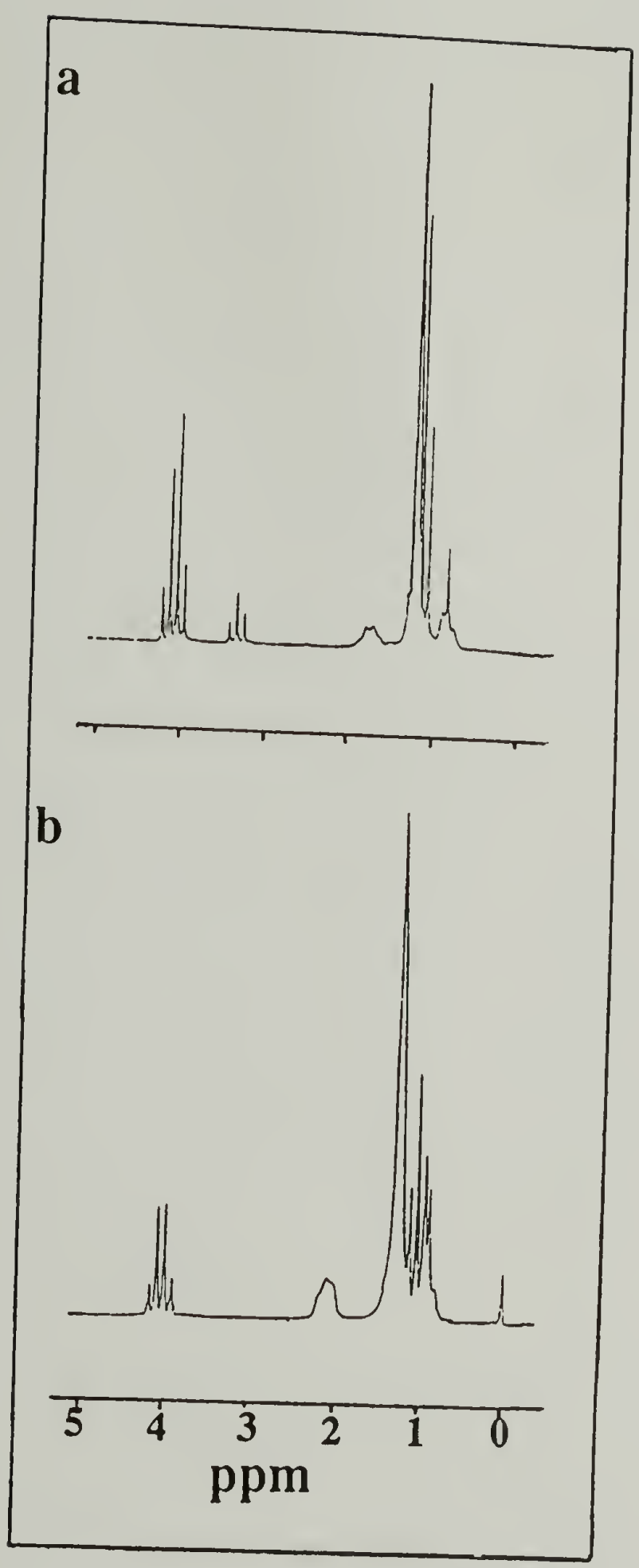


Figure 4.14 Proton Nuclear Magnetic Resonance Spectra of (a) Diethyl Octylmalonate, (b) Diethyl Dioctylmalonate.

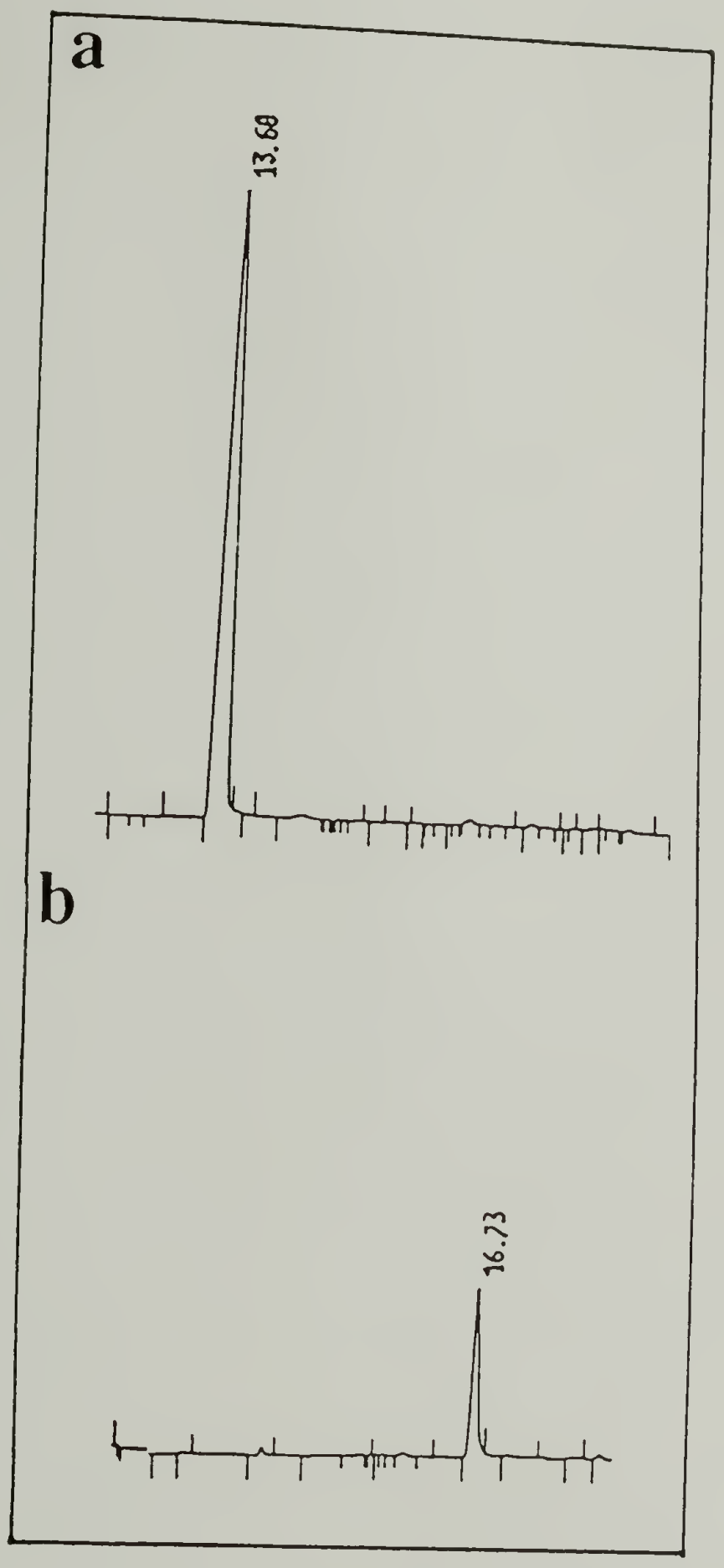


Figure 4.15 Gas Chromatograms of (a) Diethyl Octylmalonate, and (b) Diethyl Dioctylmalonate.

The information gained from $^1$H NMR, IR, GC, MP, and elemental analyses was used to verify both the synthesis and purity of intermediates. Proton nuclear magnetic resonance was useful in following the substitution of the octyl group for methylene protons (between the two ester groups) of diethyl malonate. The methine proton of diethyl octylmalonate at 3.4 ppm disappeared with conversion to diethyl dioctylmalonate as predicted. Infrared provided information on the nature of the carbonyl group; the $\nu_{(C=O)}$ of dioctylacetic acid at 1700 cm$^{-1}$ shifted to 1800 cm$^{-1}$ with conversion of the acid to dioctylacetyl chloride. Gas chromatograms, melting point data and elemental analyses substantiated the purity of the intermediates found by $^1$H NMR and IR.

Tripentylacetyl chloride was prepared from acetonitrile via several intermediates.[44] The synthetic procedure followed for tripentylacetyl chloride preparation is described in Scheme 4.3. The techniques used to characterize the intermediates and verify their purity are listed in Table 4.4 along with expected and observed elemental analyses. Infrared and proton nuclear magnetic resonance spectra which were used to follow these reactions are included in Figures 4.15 and 4.16, respectively. The first step of the synthetic procedure

Table 4.4 Elemental Analysis Results and Additional Techniques Used in Tripentylacetyl Chloride Synthesis.

| Sample | Expected (wt %) C : H : N : O : Cl | Observed (wt %) C : H : N : O : Cl | Additional Analyses |
|---|---|---|---|
| Tripentylaceto-nitrile | 81.20 : 13.23 : 5.57 | 80.25 : 13.50 : 6.25 | $^1$H NMR; IR; GC (1 peak) |
| Tripentylacet-amide | 75.77 : 13.09 : 5.20 : 5.94 | 76.01 : 13.11 : 5.28 : 5.60 | $^1$H NMR; IR; MP (60 - 64 °C) lit. 62.5-63.5 °C |
| Tripentylacetic acid | 75.50 : 12.07 : - :11.83 | 75.76 : 13.25 : 0.16 : 10.83 | $^1$H NMR; IR |
| Tripentylacetyl chloride | 70.68 : 11.51 : - :5.54 : 12.27 | 73.39 : 11.11 : 1.10 : 5.93 : 8.47 | $^1$H NMR; IR |

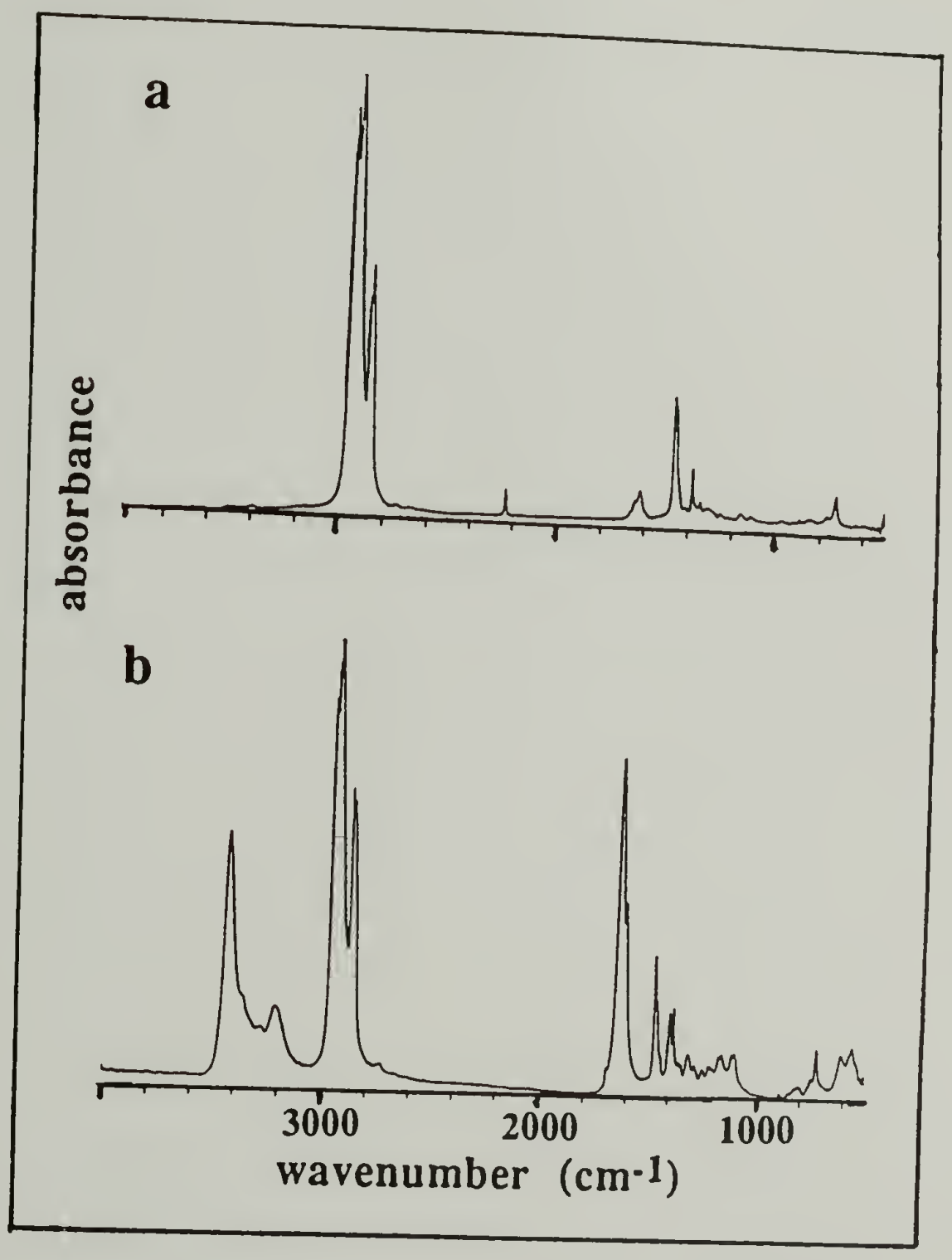


Figure 4.16 Infrared Spectra of (a) Tripentylacetonitrile, (b) Tripentylacetamide, (c) Tripentylacetic Acid, (d) Tripentylacetyl Chloride. Continued, next page.

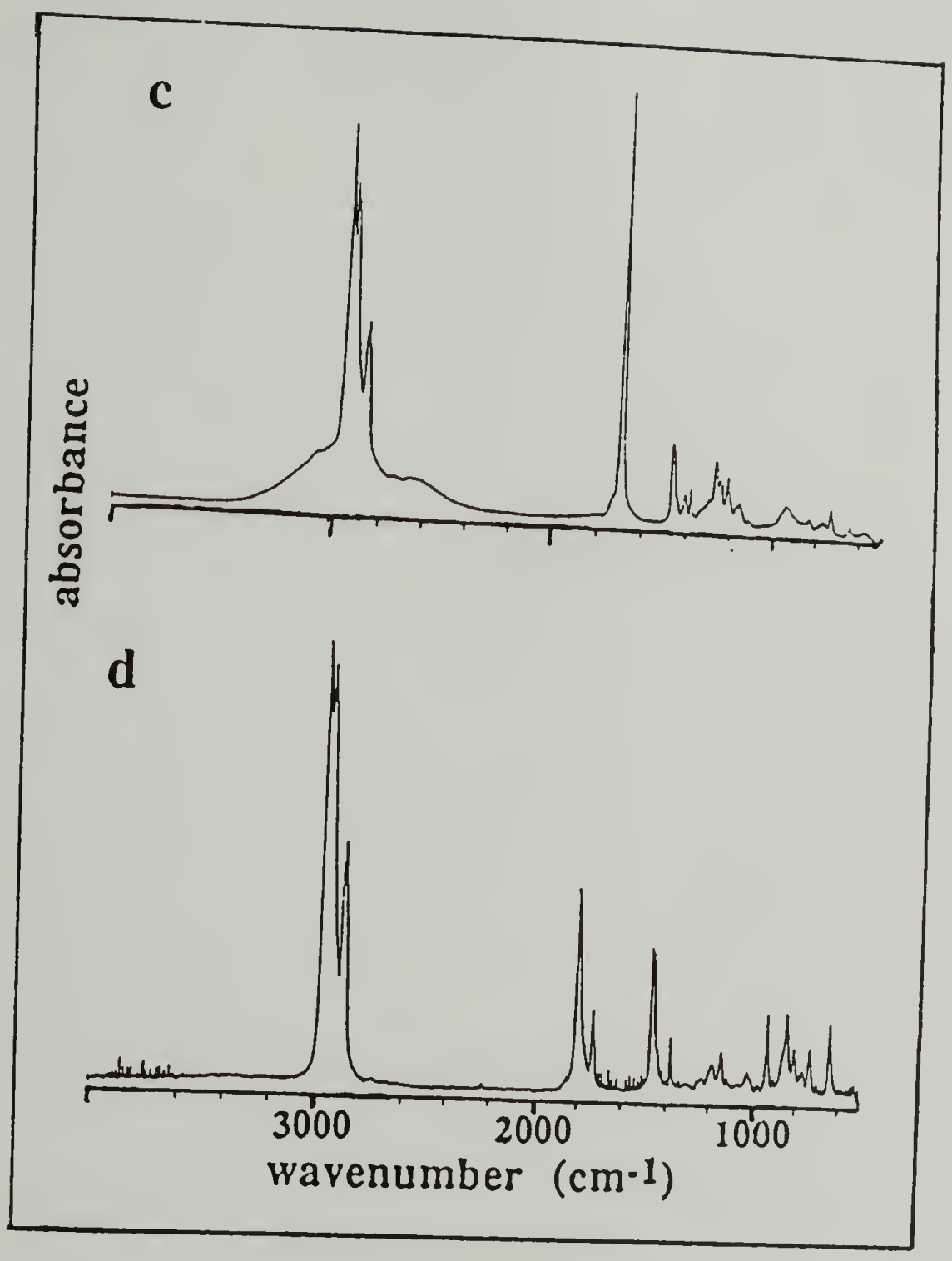


Figure 4.16 Continued.

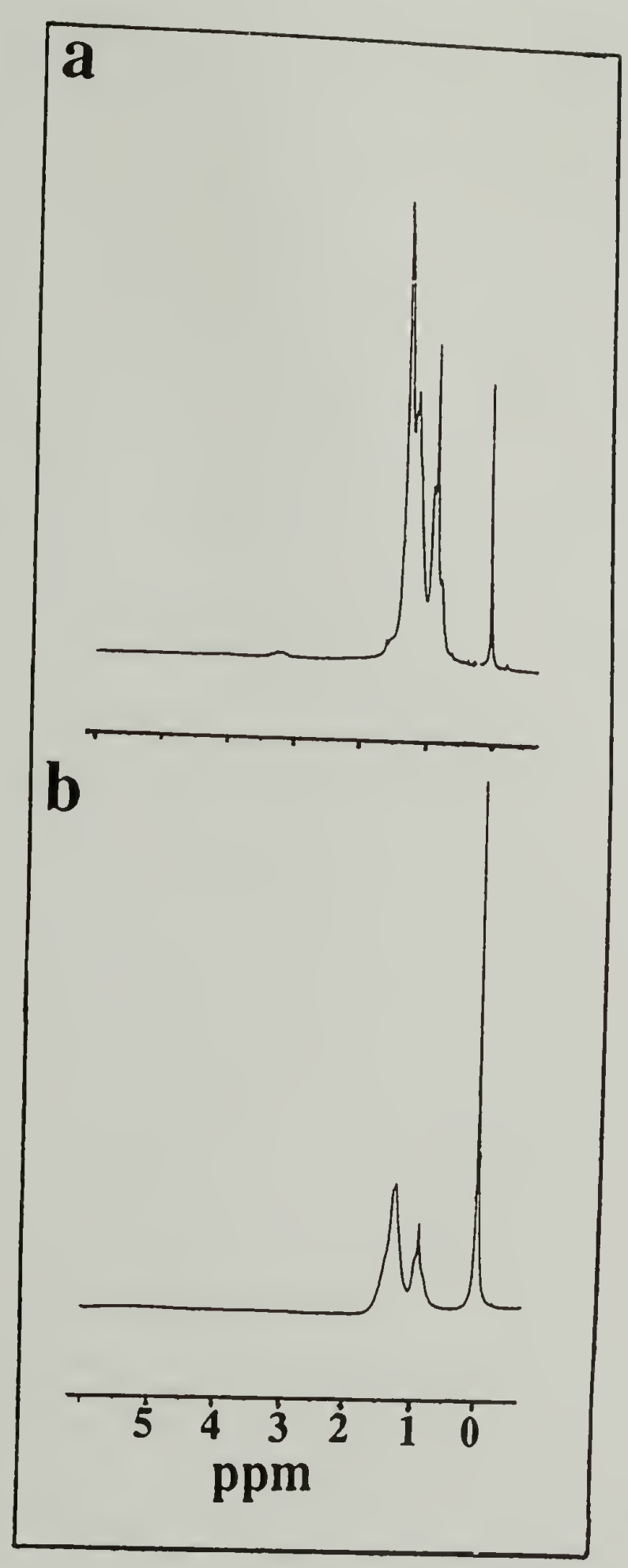


Figure 4.17 Proton Nuclear Magnetic Resonance Spectra of (a) Tripentylacetonitrile, (b) Tripentylacetamide, (c) Tripentylacetic Acid, (d) Tripentylacetyl Chloride. Continued, next page.

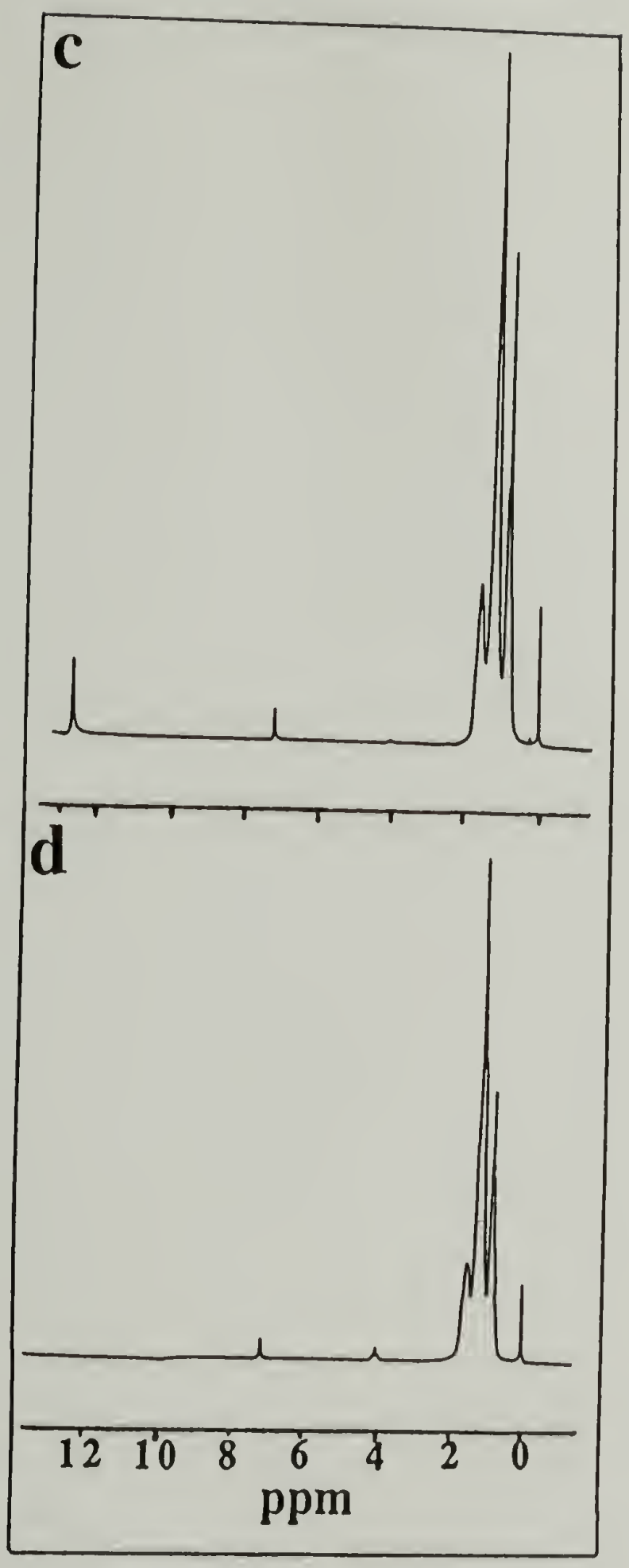


Figure 4.17 Continued.

involved trialkylation of acetonitrile; the nitrile peak at 2230 $cm^{-1}$ in the IR spectrum (Figure 4.15 (a)) indicates that trialkylation as opposed to ketenimine formation occurred.[52] GC indicates the presence of only one substance with only one detectable peak. With conversion of tripentylacetonitrile to tripentylacetamide, the IR peak at 2230 $cm^{-1}$ was removed; amide I (1637 $cm^{-1}$), amide II (1611 $cm^{-1}$) and $\nu_{(N-H)}$ between 3200 and 3400 $cm^{-1}$ were further evidence for amide formation. Tripentylacetamide reacted with butyl nitrite and hydrochloric acid to form tripentylacetic acid; the $\nu_{(C=O)}$ peak at 1699 $cm^{-1}$ and the $^1H$ NMR (from deuterated benzene) peak of the carboxylic acid proton at 12.8 ppm confirm this reaction. Evidence for tripentylacetyl chloride was obtained from the disappearance of the carboxylic acid proton from the $^1H$ NMR spectrum and the shift of the carbonyl peak $\nu_{(C=O)}$ to 1798 $cm^{-1}$.

The reaction of tripentylacetamide with butyl nitrite/hydrochloric acid to tripentylacetic acid requires further comment. Amides (and nitriles) have often been easily converted to acids.[53] However, the conversion of tripentylacetamide to tripentylacetic acid is complicated by tertiary substitution at the β carbon where steric hindrance inhibits the regular hydrolysis pathway.[54] Butyl nitrite and hydrochloric acid act in concert to convert the amide to the acid by a nitrosation reaction via an acyl diazonium salt.[55] The reaction relies upon the attack of the electrophilic nitrosating agent ($NO^+$) on the nucleophilic amide nitrogen.[56] By this mechanism, outlined in Scheme 4.5, nitrogen gas is evolved in the conversion of amide to acid.

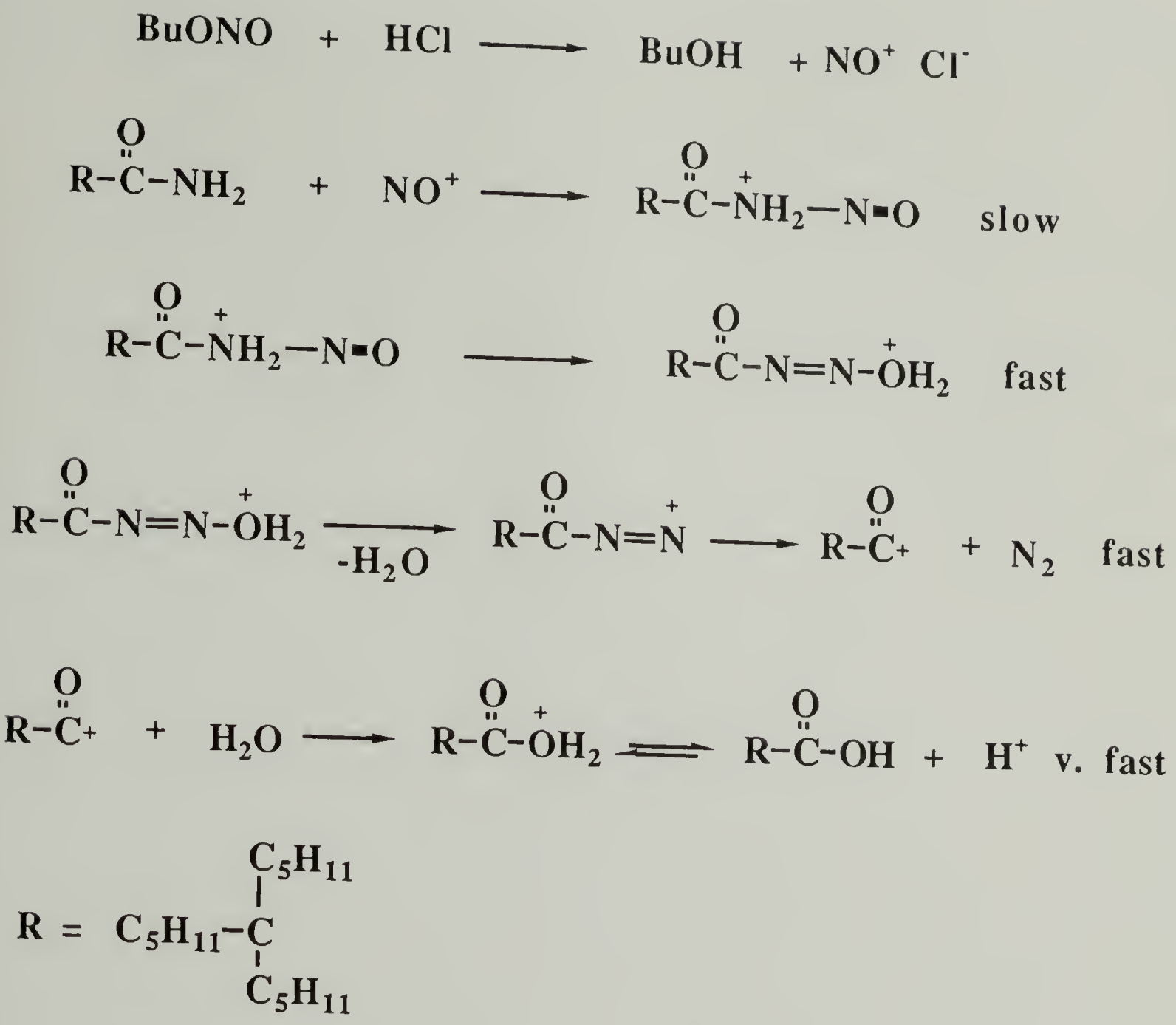


Scheme 4.5 Proposed Mechanism for Tripentylacetamide Reaction with Butyl Nitrite/Hydrochloric Acid to Form Tripentylacetic Acid.[56]

## Adsorption

The hydrophobic interaction as a driving force for adsorption from aqueous solution was studied with poly(ethylene oxide) (PEO) and end-capped poly(ethylene oxide) (PEO-R). An interaction between the hydrophobe (R) and a hydrophobic substrate was expected to enhance adsorption. Liberating water molecules from the hydrophobic substrate - water interface favors the hydrophobic interaction entropically. Neutral poly(L-

lysine) (PLL) adsorbed to FEP from an aqueous solution as a result of both a hydrophobic interaction and the high free energy at the water - fluoropolymer interface. As was detailed in Chapter II, the FEP-PLL adsorption was slow kinetically, likely as result of PLL polydispersity. In an attempt to overcome polydispersity effects, the hydrophobic interaction was studied with monodisperse PEO and PEO-R.

Poly(ethylene oxide) was chosen, amongst other water soluble polymers, for several reasons. Reports in the literature indicate that PEO could be synthesized to a range of molecular weights with narrow molecular weight distribution.[21] It was confirmed, as described in the previous section, that ethylene oxide could be polymerized to 50,000 g/mole with a narrow molecular weight distribution. In addition, literature precedence exists for using PEO in adsorption studies where the hydrophobic interaction was studied. For example, Char *et al.*[57] found that poly(ethylene glycol) (PEG) end-capped with pyrene, adsorbed preferentially over PEG to hydrophobic PS latex; the importance of the hydrophobic interaction was confirmed by Bohmer and Koopal.[58] Poly(ethylene oxide) and its copolymers are often used as "associative thickeners"[59] in paints, for example, where the hydrophobic moiety, by adsorbing preferentially to a latex particle, improves the rheology and viscosity of the system. Hoy and Hoy[60] described the phenomenon as micellar bridging where PEO of molecular weight 600 to 50,000 g/mole was sandwiched between two alkyl end groups of $C_{12}$ to $C_{16}$. Using the same polymer, Jenkins *et al.*[61] showed that association among the polymers' hydrophobic end groups improved the rheological properties of the system. PEO moieties of ~8200 g/mole were linked by diisocyanate groups to form polymers of molecular weights between 20,000 and 100,000 g/mole with alkyl end groups $C_{12}$ to $C_{16}$. In this study, PEO of 50,000 g/mole (an intermediate value in light of other work) was chosen for most of the adsorption studies.

The alkyl end groups used in this study were chosen in light of the work of Jenkins *et al.* and Hoy and Hoy. Four alkyl end groups on PEO-R were studied in terms of their enhanced adsorption to hydrophobic surfaces relative to that of PEO. From previous

studies, an alkyl group with at least $C_{12}$ to $C_{16}$ was likely to show differences in adsorption; stearoyl, $C_{18}$, was chosen for this reason. Dioctylacetyl ($C_{18}$) and tripentylacetyl ($C_{17}$) are essentially branched isomers of the stearoyl group. The effect of "branching" (while keeping the number of carbons essentially constant) on the effect of the hydrophobic interaction was studied. It was postulated that the configuration of the end group would affect the adsorption of PEO-R. The perfluorodecanoyl end group was chosen primarily for adsorption studies to fluoropolymer films because the latter are known to be oleophobic in addition to being hydrophobic.[62] The size of the perfluoroalkyl end group was limited by commercial availability ($C_{10}$).

PEO and PEO-R were adsorbed at three types of aqueous interfaces: fluoropolymer film, polystyrene latex, and air. The fluoropolymer films, $PVF_2$, PCTFE, and FEP, are hydrophobic surfaces which have high interfacial free energies when immersed in water. From PLL adsorption results, it was anticipated that adsorption to these films would result from a hydrophobic interaction between the PEO alkyl end group and the fluoropolymer film at the aqueous interface. Adsorption at the polystyrene latex was complicated by carboxylic acid groups which stabilized the latex electrostatically in water. At least two competing interactions resulted; (1) PEO-R could adsorb hydrophobically to the "hydrophobic" (PS) patches on the latex and (2) PEO could adsorb by a hydrogen bonding mechanism to polar carboxylic acid groups. Adsorption at the free or air interface indicated the enhanced surfactant properties of PEO-R over PEO. Surface tension measurements were also used to determine whether PEO-R formed micelles.

## Adsorption at the Fluoropolymer Film - Water Interface

Adsorption was studied at the fluoropolymer - water interface for several reasons. Because water could neither swell nor penetrate the film sample, the interface was well defined and sharp. The film samples provided a chemically homogeneous and smooth (to

at least 50 Å, as determined from SEM) surface for adsorption experiments. The hydrophobic nature of the fluoropolymer film coupled with its spectroscopic uniqueness facilitated analysis by contact angle and XPS. The three fluoropolymer films studied represent a range of critical surface tensions: FEP (18 dyn/cm), PCTFE (31 dyn/cm) and $PVF_2$ (25 dyn/cm).[63] Based on the assumption that PEO-R adsorption was enhanced by a hydrophobic interaction at a high free energy interface, adsorption to FEP would be favoured over the other two polymer films.

The hydrophobic interaction between the alkyl end group of PEO-R and the fluoropolymer film samples was investigated in terms of its enhanced adsorption, with respect to PEO, at the water interface. The adsorption was limited to physisorption because no specific interaction between film and PEO(-R) could be identified. Adsorption of PEO and PEO-R to the fluoropolymer film was likely concomitant with the release of water molecules from the interface. From a theoretical perspective, the adsorbing block (the alkyl end group) was expected to lie flat (a small train) on the film surface while the nonadsorbing block (the PEO) was expected to form a dangling tail extending from the surface.[64]

PEO and PEO-R adsorption to fluoropolymer films was characterized by XPS and contact angle measurements. Although not an in situ technique, XPS was indicative of the relative amounts of PEO(-R) adsorbed; contact angle represented the increased hydrophilicity of the modified polymer film. Figure 4.18 includes typical XPS survey and $C_{1s}$ (15° takeoff angle) spectra for $PVF_2$-PEO, PCTFE-PEO and FEP-PEO. PEO is evident in the XPS spectra by the $O_{1s}$ and low binding energy $C_{1s}$ peaks. By comparing the $O_{1s}/F_{1s}$ or the low to high binding energy $C_{1s}$ peaks, the relative amount of PEO adsorbed to fluoropolymer film can be determined. Little or no PEO adsorbed to FEP, more adsorbed to PCTFE, and the most adsorbed to $PVF_2$.

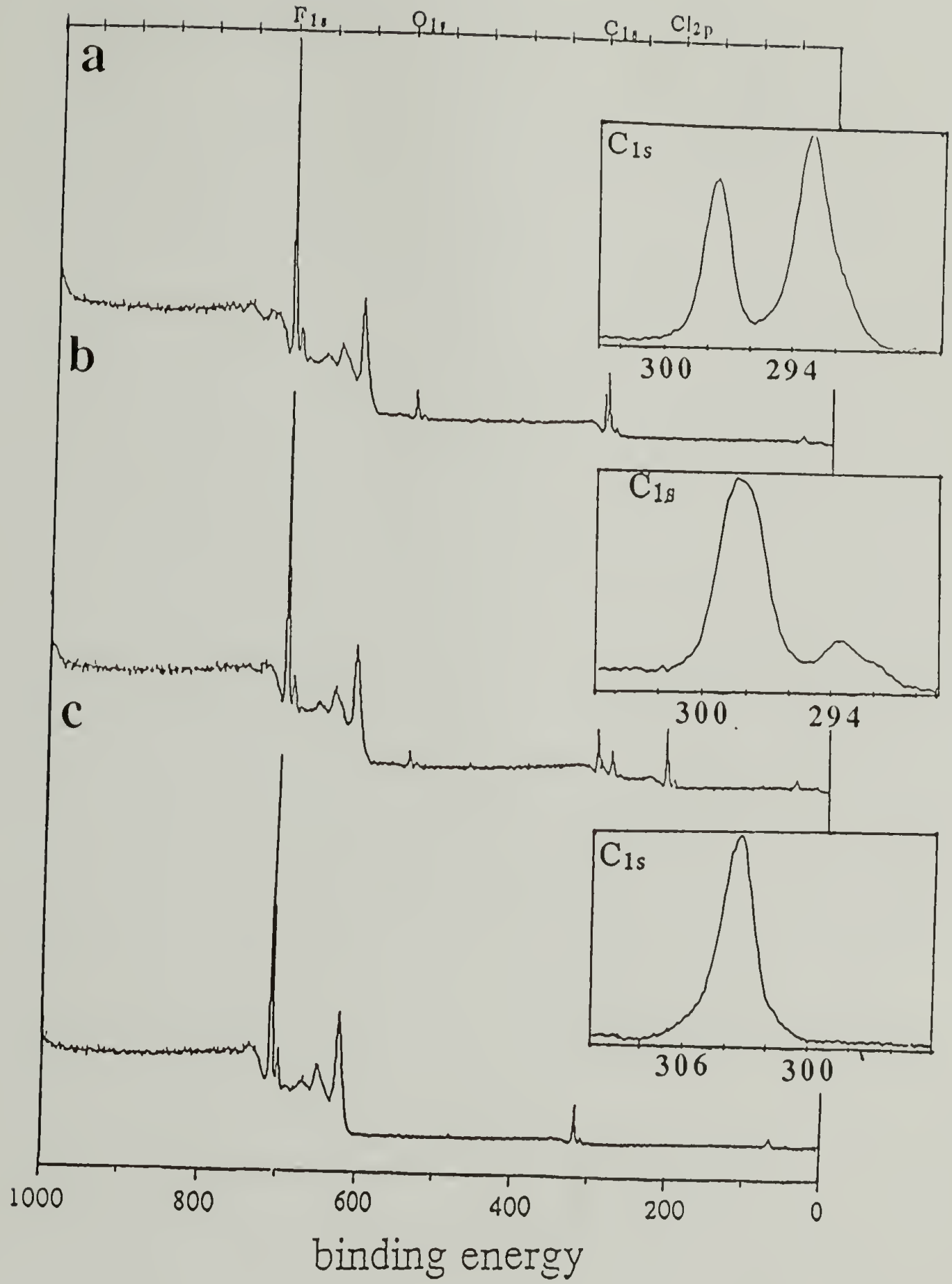


Figure 4.18 XPS Survey and $C_{1s}$ (15° takeoff angle) Spectra of (a) $PVF_2$-PEO, (b) PCTFE-PEO, (c) FEP-PEO.

The driving force for the adsorption of PEO to fluoropolymer film samples was more complicated than initially anticipated. The high interfacial free energy between the aqueous solution and the organic fluoropolymer film surface may have contributed to adsorption; however, other factors were at least equally important. The trend observed in the adsorption behavior followed that of the dielectric constants of the fluoropolymer film samples: FEP, 2.0,[65] PCTFE, 2.5,[66] $PVF_2$, 9.1.[67] A polar interaction between PEO(-R) and the fluoropolymer film sample likely enhanced adsorption.[68] In a similar experiment, Goddard *et al.*[69] found that the tenacity of PEO adsorption decreased in the order of decreasing polarity of the substrate mylar > polyethylene > PTFE-FEP. Low molecular weight PEO did not adsorb to FEP; the small amount of high molecular weight PEO that did adsorb to FEP was easily displaced by an advancing oil drop. The polar interaction likely outweighed any hydrophobic interaction between film sample and "R" group. Kronberg *et al.*[70] found that PEO adsorbed preferentially to PVC over PS by a polar interaction between ethylene oxide segments and the substrate. In addition, the hydrophobic interaction between nonylphenol and PS, expected to enhance adsorption, did not prevail; instead, the hydrophobic tail showed greater affinity to itself than to the polymer surfaces.

Adsorption to FEP

As was indicated in Figure 4.18, little or no PEO adsorbed to FEP. In Table 4.5 it is evident that end-capping PEO had little effect on its adsorption as determined from XPS and contact angle measurements. The $O_{1s}/F_{1s}$ ratios are too small for interpretation; contact angle data show that very little modification occurred. The hysteresis between advancing and receding contact angles indicates that perhaps a small amount of PEO adsorbed.

Table 4.5 Adsorption of PEO and PEO-R to the FEP - Water Interface: XPS and $\theta_A/\theta_R$ Data (24 h). [VI10-24,122-126,130-132,140-143]

| Sample | $C_{PEO}/C_{FEP}$ | $O_{1s}/F_{1s}$ | XPS (15°) | $\theta_A/\theta_R$ |
|---|---|---|---|---|
| FEP | | | $C_{34.88}F_{65.12}$ | 114°/102° |
| PEO 2 mg/ml (25k, V120) | | 0.005 | $C_{34.22}F_{65.45}O_{0.33}$ | 112°/95° |
| PEO 1 mg/ml | | 0.004 | $C_{34.19}F_{65.57}O_{0.24}$ | 112°/99° |
| PEO 0.5 mg/ml | | 0.004 | $C_{34.32}F_{65.39}O_{0.29}$ | 108°/94° |
| PEO 2 mg/ml (8k, V85) | | | $C_{37.12}F_{62.88}$ | 106°/92° |
| PEO-FD 2 mg/ml (25k, VII16) | | 0.013 | $C_{33.41}F_{65.74}O_{0.85}$ | 113°/93° |
| PEO-ST 1 mg/ml (50k, VII26) | 0.040 | 0.011 | $C_{34.20}F_{65.08}O_{0.72}$ | 109°/92° |

Although neither PEO nor PEO-R appeared to adsorb to FEP, a weak interaction between FEP and PEO(-R) may have been further decreased by the rinsing procedure (30 min in distilled water) causing PEO-(R) to desorb from FEP.

The captive bubble contact angle technique provided an in situ method to follow PEO and PEO-R adsorption at the fluoropolymer film - water interface. Although a detailed study using this technique was not done, preliminary results (Table 4.6) indicate that more PEO-FD than PEO adsorbed to FEP; this assessment was based on XPS analysis which shows a higher oxygen atomic concentration for FEP-PEO-FD than FEP-PEO. The captive bubble contact angle can be compared with the receding contact angle.[71]

Table 4.6 Captive Bubble Contact Angle and XPS Data for Adsorption to FEP. [VIII50-51]

| Sample | Air Contact Angle | XPS (15°) |
|---|---|---|
| FEP | 110° | $C_{34.88}F_{65.12}$ |
| FEP-PEO (VII24, 50k) | 102° | $C_{37.28}F_{60.64}O_{2.08}$ |
| FEP-PEOFD (VI16, 25k) | 83° | $C_{35.72}F_{60.96}O_{3.32}$ |

For FEP-PEO-FD (Table 4.5), the receding contact angle (93°) was greater than that measured by the captive bubble technique (83°). Captive bubble contact angle data indicate that PEO-FD adsorbed to FEP. Young's equation (4.1) can be solved for the

(4.1) $\gamma_{LS} = \gamma_{SV} - \gamma_{LV} \cos\theta$ (Young's equation)

three systems studied by the captive bubble technique, assuming that $\gamma_{SV}$ = 18 dyn/cm (FEP). $\gamma_{LS}$, $\gamma_{SV}$, and $\gamma_{LV}$ are the surface tensions at the liquid-solid, solid-vapor, and liquid-vapor interfaces, respectively; $\theta$ is the angle measured between the horizontal and the tangent of the air bubble at the solid-liquid-vapor intersection. (A flattened bubble shows a higher contact angle than a "beaded" bubble.) The data in Table 4.7 summarize the interfacial tension data used to calculate that of $\gamma_{LS}$.

Table 4.7 Interfacial Tension Data Used to Calculate the Free Energy at the FEP - Solution Interface ($\gamma_{LS}$).

| Sample | θ | cosθ | $\gamma_{LV}$ (dyn/cm) | $\gamma_{SV}$ (dyn/cm) | $\gamma_{LS}$ (dyn/cm) |
|---|---|---|---|---|---|
| Water | 110° | -0.342 | 72.1 | 18 | 42.66 |
| PEO | 102° | -0.208 | 60.78* | 18 | 30.64 |
| PEO-FD | 83° | 0.122 | 31.94* | 18 | 14.11 |

*Liquid-vapor interfacial tension values were obtained by surface tension measurements.

The captive bubble contact angle data and XPS (Table 4.6) indicate that both PEO and PEO-FD adsorbed to FEP whereas contact angle and XPS data of Table 4.5 indicate that neither PEO nor PEO-FD adsorbed to FEP. The latter were not useful in recognizing or distinguishing between adsorbed samples likely because only a small amount of polymer adsorbed which was desorbed by the washing technique (1/2 h in distilled water).

Adsorption to PCTFE [VI74-85,118-121,130-133,136-143,VII32-34]

The adsorption of PEO to PCTFE was studied in terms of (1) the time of interaction between PEO and PCTFE (Table 4.8, Figure 4.19), (2) PEO molecular weight (Table 4.9, Figure 4.20), and (3) PEO concentration (Table 4.10, Figure 4.21). The XPS ratios of both $C_{PEO}/C_{PCTFE}$ and $O_{1s}/F_{1s}$ are compared in the figures. Very little difference in the amount adsorbed was observed in any of the three studies indicating a weak interaction between PEO and PCTFE. The contact angle data corroborate XPS data that indicated that very little PEO adsorbed. The data in Figure 4.20 (Table 4.9) indicate that more low than

high molecular weight PEO adsorbed to PCTFE. This trend contradicts theoretical predictions and most experimental work. However, Kronberg *et al.*[70] observed a similar trend where lower molecular weight PEO adsorbed preferentially to PVC, by a polar interaction, because it occupied less area. The affinity between PEO and PCTFE is likely of a polar nature; more of the lower molecular weight PEO may have interacted with the PCTFE surface for similar reasons as outlined by Kronberg *et al.*

Table 4.8 Effect of Time of Interaction on the Adsorption of PEO (53k, 2 mg/ml) to PCTFE: XPS and $\theta_A/\theta_R$ Data. [VI78-81]

| Time (h) | $C_{PEO}/C_{PCTFE}$ | $O_{1s}/F_{1s}$ | $\theta_A/\theta_R$ |
|---|---|---|---|
| 0 (PCTFE + $dH_2O$) | 0.084 | 0.023 | 97°/75° |
| 1 | 0.196 | 0.074 | 88°/65° |
| 6 | 0.242 | 0.089 | 86°/64° |
| 12 | 0.211 | 0.083 | 86°/62° |
| 24 | 0.206 | 0.081 | 89°/63° |

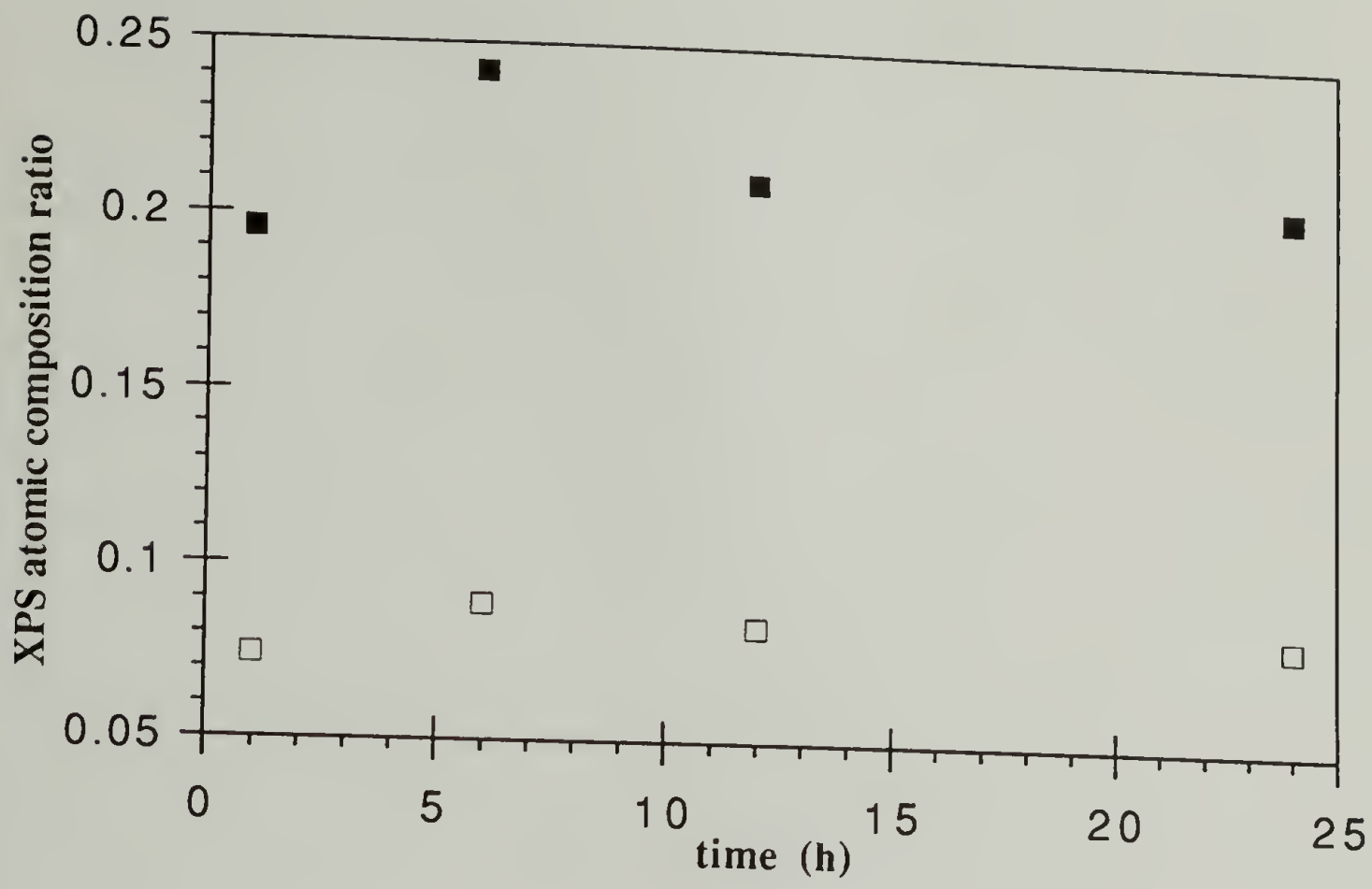


Figure 4.19 Effect of the Time of Interaction on the Amount of PEO (53k, 2 mg/ml) Adsorbed for PCTFE: (■) $C_{PEO}/C_{PCTFE}$, (□) $O_{1s}/F_{1s}$.

Table 4.9 Effect of PEO (2 mg/ml) Molecular Weight on the Adsorption to PCTFE: XPS and $\theta_A/\theta_R$ Data (24 h). [VI74-77]

| Molecular Weight (g/mole) | $C_{PEO}/C_{PCTFE}$ | $O_{1s}/F_{1s}$ | $\theta_A/\theta_R$ |
|---|---|---|---|
| 7k (V133) | 0.581 | 0.211 | 87°/62° |
| 16k (V44) | 0.330 | 0.142 | 87°/59° |
| 26k (V67) | 0.181 | 0.071 | 90°/63° |
| 53k (V40) | 0.206 | 0.081 | 89°/63° |

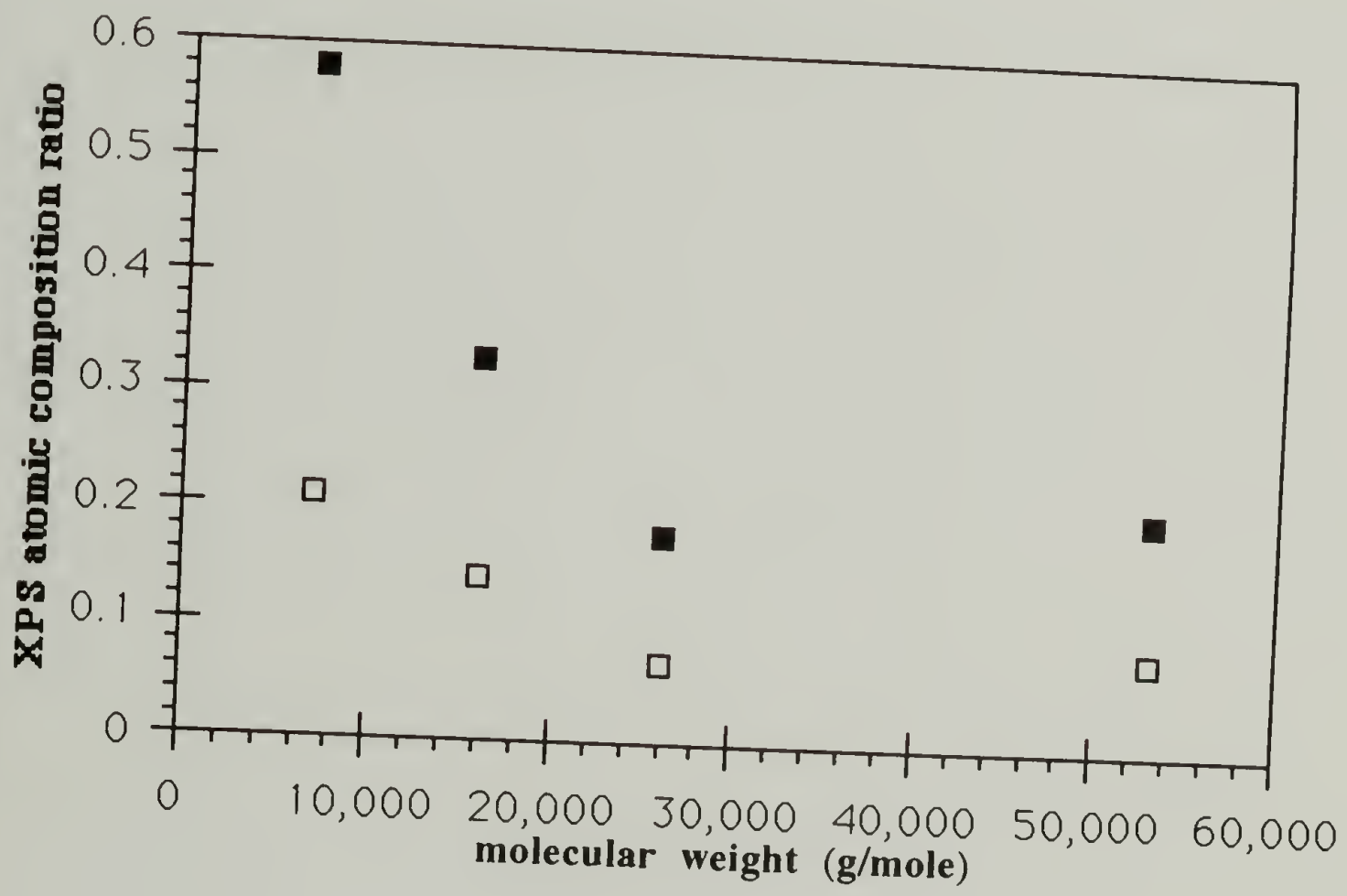


Figure 4.20 Effect of PEO Molecular Weight on the Amount Adsorbed to PCTFE: (■) $C_{PEO}/C_{PCTFE}$, (□) $O_{1s}/F_{1s}$.

Table 4.10 Effect of PEO (53k) Concentration on the Amount Adsorbed to PCTFE: XPS and $\theta_A/\theta_R$ Data (24 h). [VI82-85]

| Concentration (mg/ml) | $C_{PEO}/C_{PCTFE}$ | $O_{1s}/F_{1s}$ | $\theta_A/\theta_R$ |
|---|---|---|---|
| 0.05 | 0.124 | 0.053 | 90°/67° |
| 0.2 | 0.158 | 0.074 | 88°/63° |
| 0.5 | 0.189 | 0.072 | 89°/64° |
| 1.0 | 0.362 | 0.117 | 90°/67° |
| 2.0 | 0.206 | 0.081 | 89°/63° |

The amounts of PEO and PEO-R that adsorbed to PCTFE are compared in Figure 4.21; the data presented in this figure are included in Tables 4.10 (PEO), 4.11 (PEO-FD), 4.12 (PEO-ST), and 4.13 (PEO-TP). Although it was difficult to identify any trends in the adsorption data, the amount adsorbed seemed to increase with concentration of both PEO and PEO-R. It was more difficult to discern whether adsorption was enhanced with the alkyl end group. Of the data presented, there is some indication that PEO-TP enhanced adsorption to PCTFE at 0.5 and 2.0 mg/ml. However, due to the scatter in the data, no conclusion can be drawn.

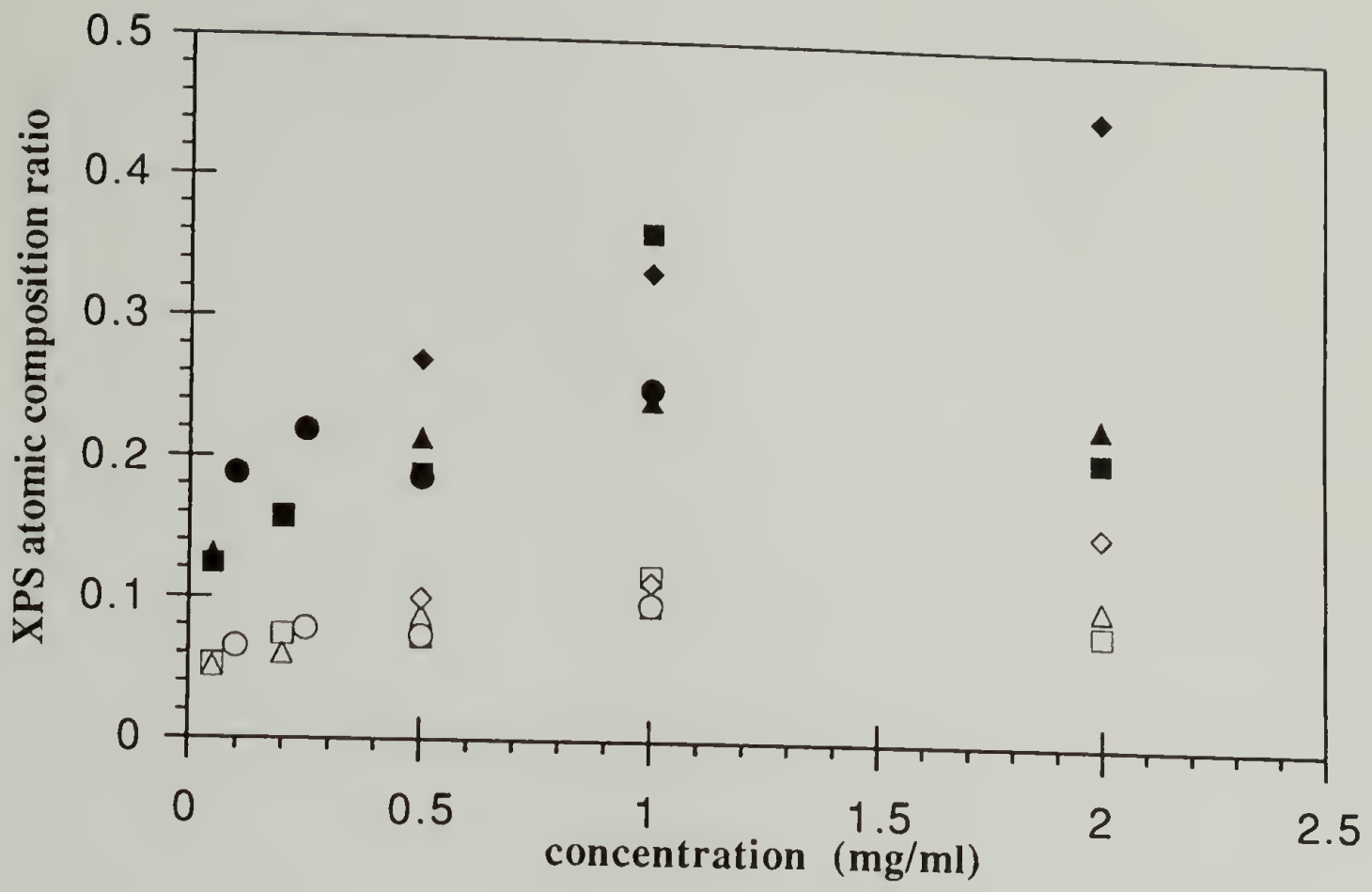


Figure 4.21 Effect of Concentration on the Amount Adsorbed to PCTFE of PEO - (■) $C_{PEO}/C_{PCTFE}$, (□) $O_{1s}/F_{1s}$; PEO-FD - (▲) $C_{PEO\text{-}FD}/C_{PCTFE}$, (△) $O_{1s}/F_{1s}$; PEO-ST - (●) $C_{PEO\text{-}ST}/C_{PCTFE}$, (○) $O_{1s}/F_{1s}$; and PEO-TP - (◆) $C_{PEO\text{-}TP}/C_{PCTFE}$, (◇) $O_{1s}/F_{1s}$.

Table 4.11 Effect of PEO-FD (24 h, 25k VII16) Concentration on its Adsorption to PCTFE: XPS and $\theta_A/\theta_R$ Data. [VI118-121]

| Concentration (mg/ml) | $C_{PEO\text{-}FD}/C_{PCTFE}$ | $O_{1s}/F_{1s}$ | $\theta_A/\theta_R$ |
|---|---|---|---|
| 0.05 | 0.131 | 0.051 | 89°/67° |
| 0.2 | 0.157 | 0.060 | 88°/66° |
| 0.5 | 0.214 | 0.088 | 87°/61° |
| 1.0 | 0.243 | 0.096 | 85°/56° |
| 2.0 | 0.231 | 0.099 | 85°/53° |

Table 4.12 Effect of PEO-ST (24 h, 50k VII26) Concentration on its Adsorption to PCTFE: XPS and $\theta_A/\theta_R$ Data. [VI130-133,136-143]

| Concentration (mg/ml) | $C_{PEO-ST}/C_{PCTFE}$ | $O_{1s}/F_{1s}$ | $\theta_A/\theta_R$ |
|---|---|---|---|
| 0.1 | 0.188 | 0.065 | 90°/69° |
| 0.25 | 0.219 | 0.078 | 91°/69° |
| 0.5 | 0.186 | 0.073 | 89°/66° |
| 1.0 | 0.251 | 0.097 | 88°/68° |

Table 4.13 Effect of PEO-TP (24 h, 50k VII74) Concentration on its Adsorption to PCTFE: XPS and $\theta_A/\theta_R$ Data. [VIII32-34]

| Concentration (mg/ml) | $C_{PEO-TP}/C_{PCTFE}$ | $O_{1s}/F_{1s}$ | $\theta_A/\theta_R$ |
|---|---|---|---|
| 0.5 | 0.270 | 0.100 | 88°/63° |
| 1.0 | 0.334 | 0.113 | 87°/62° |
| 2.0 | 0.453 | 0.152 | 87°/61° |

Adsorption to $PVF_2$ [VI62-73,114-117,126-128,130-133,136-143;VIII32-34]

The adsorptions of PEO and PEO-R at the $PVF_2$ - water interface were studied. The adsorption of PEO to $PVF_2$ was studied in terms of (1) the time of interaction between PEO and $PVF_2$ (Table 4.14, Figure 4.22), (2) PEO molecular weight (Table 4.15, Figure 4.23), and (3) PEO concentration (Table 4.16, Figure 4.24). The XPS ratios of both $C_{PEO}/C_{PVF2}$ and $O_{1s}/F_{1s}$ are compared in the figures. Very little difference in the amount

adsorbed was observed in any of the three studies. The contact angle data corroborate XPS results which indicate that only a small amount of PEO adsorbed to $PVF_2$. The receding contact angles are lower than those of PCTFE for two plausible reasons; (1) more PEO adsorbed to $PVF_2$ than to PCTFE; (2) the water contact angle is lower for unmodified $PVF_2$ than it is for unmodified PCTFE. The adsorption of PEO-R to $PVF_2$ is summarized in Figure 4.23 and Tables 4.16 (PEO), 4.17 (PEO-FD), 4.18 (PEO-ST) and 4.19 (PEO-TP). More lower than higher molecular weight PEO adsorbed to $PVF_2$ (Figure 4.23). PEO adsorbed to $PVF_2$ due to a weak polar interaction; more lower molecular weight PEO adsorbed to $PVF_2$ for reasons similar to those outlined previously for PEO adsorption to PCTFE. The difference between the amount of lower and higher molecular weight PEO adsorbed to $PVF_2$ was not as great as the difference observed for PCTFE. This likely results from the increased polarity of $PVF_2$ over PCTFE. There was little distinction in the amount of PEO-R adsorbed to $PVF_2$ for different R groups; the difference between PEO and PEO-R adsorptions were inconsistent and small. The differences were smaller than those observed for PCTFE confirming the effect of the polar interaction between PEO and $PVF_2$. This polar interaction likely overwhelmed any hydrophobic effect between PEO-R and $PVF_2$.

Table 4.14 Effect of Time of Interaction on the Amount of PEO (53k, 2 mg/ml) Adsorbed to $PVF_2$: XPS and $\theta_A/\theta_R$ Data. [VI66-69]

| Time (h) | *$C_{lbe}/C_{hbe}$ | $O_{1s}/F_{1s}$ | $\theta_A/\theta_R$ |
|---|---|---|---|
| 0 ($PVF_2$ + $dH_2O$) | 1.252 | 0.025 | 86°/66° |
| 1 | 1.548 | 0.106 | 85°/54° |
| 6 | 1.396 | 0.06 | 83°/54° |
| 12 | 1.376 | 0.066 | 82°/53° |
| 24 | 1.671 | 0.138 | 80°/47° |
| 100 | 1.644 | 0.107 | 84°/48° |

*The $C_{lbe}/C_{hbe}$ is the XPS $C_{1s}$ peak area ratio of that of low binding energy to that of high binding energy.

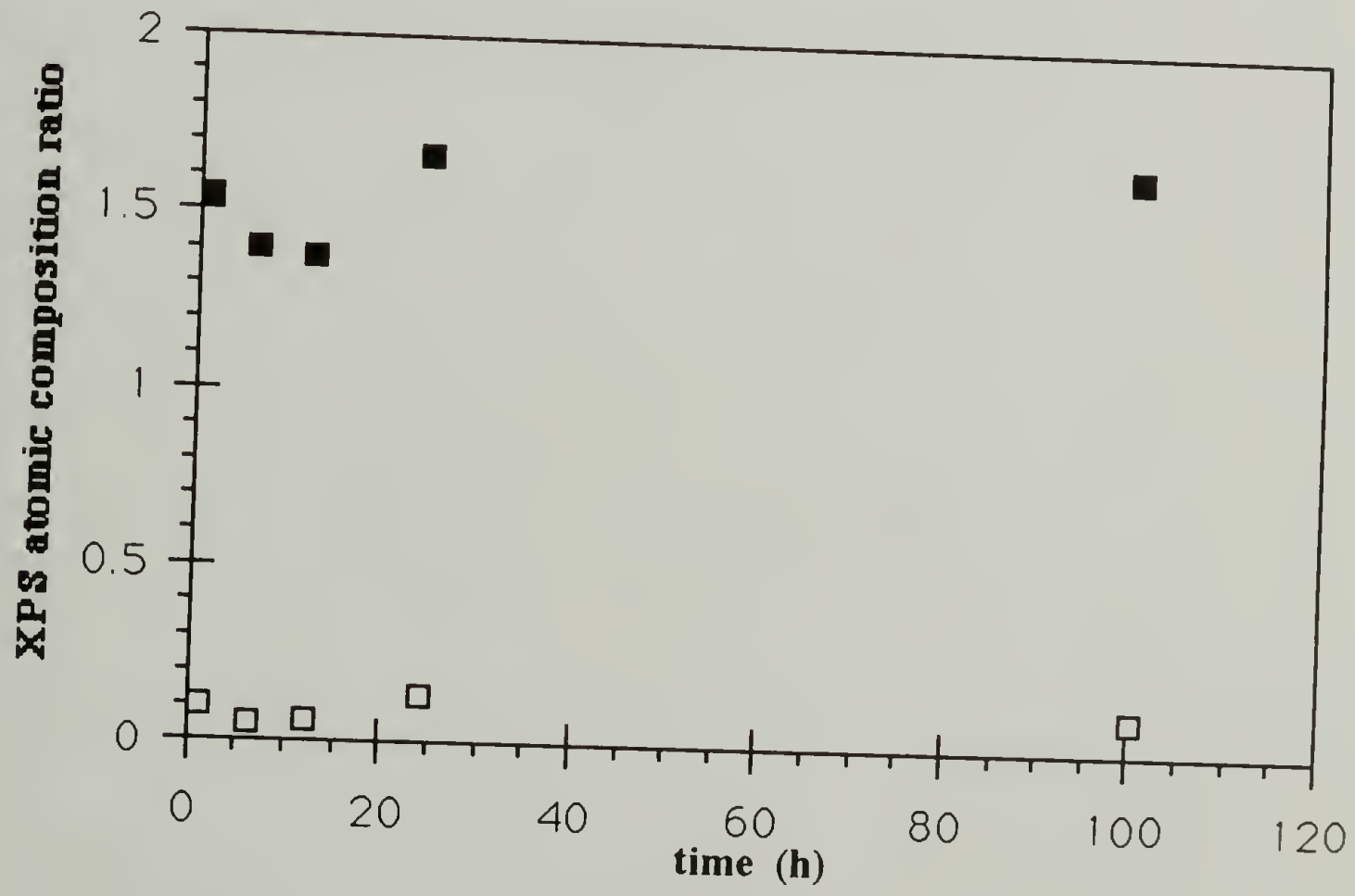


Figure 4.22 Effect of the Time of Interaction on the Amount Adsorbed for $PVF_2$-PEO: (■) $C_{lbe}/C_{hbe}$, (□) $O_{1s}/F_{1s}$.

Table 4.15 Effect of PEO (24 h, 2 mg/ml) Molecular Weight on the Amount Adsorbed to $PVF_2$: XPS and $\theta_A/\theta_R$ Data. [VI62-64]

| Molecular Weight (g/mole) | $C_{lbe}/C_{hbe}$ | $O_{1s}/F_{1s}$ | $\theta_A/\theta_R$ |
|---|---|---|---|
| 7k (V133) | 2.5 | 0.327 | 78°/46° |
| 16k (V44) | 1.43 | 0.075 | 82°/53° |
| 26k (V67) | 1.947 | 0.156 | 86°/63° |
| 53k (V40) | 1.671 | 0.138 | 84°/48° |

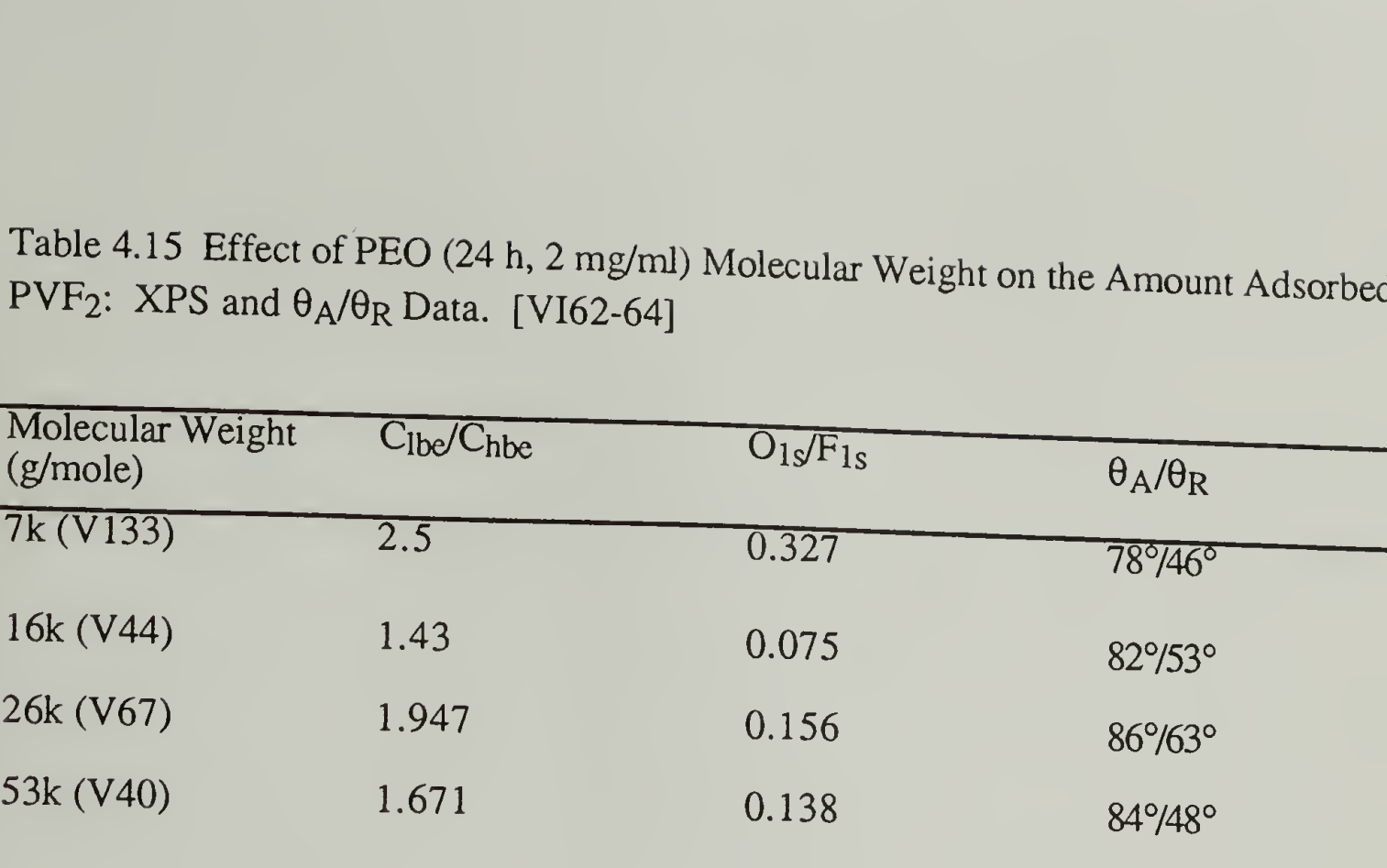


Figure 4.23 Effect of PEO Molecular Weight on the Amount Adsorbed for $PVF_2$-PEO: (■) $C_{lbe}/C_{hbe}$, (□) $O_{1s}/F_{1s}$.

Table 4.16 Effect of PEO (24 h, 53k) Concentration on the Amount Adsorbed to $PVF_2$: XPS and $\theta_A/\theta_R$ Data. [VI70-73]

| Concentration (mg/ml) | $C_{lbe}/C_{hbe}$ | $O_{1s}/F_{1s}$ | $\theta_A/\theta_R$ |
|---|---|---|---|
| 0.05 | 1.494 | 0.074 | 84°/55° |
| 0.2 | 1.423 | 0.077 | 83°/54° |
| 0.5 | 1.498 | 0.095 | 82°/52° |
| 1.0 | 1.805 | 0.147 | 82°/44° |
| 2.0 | 1.671 | 0.138 | 80°/48° |

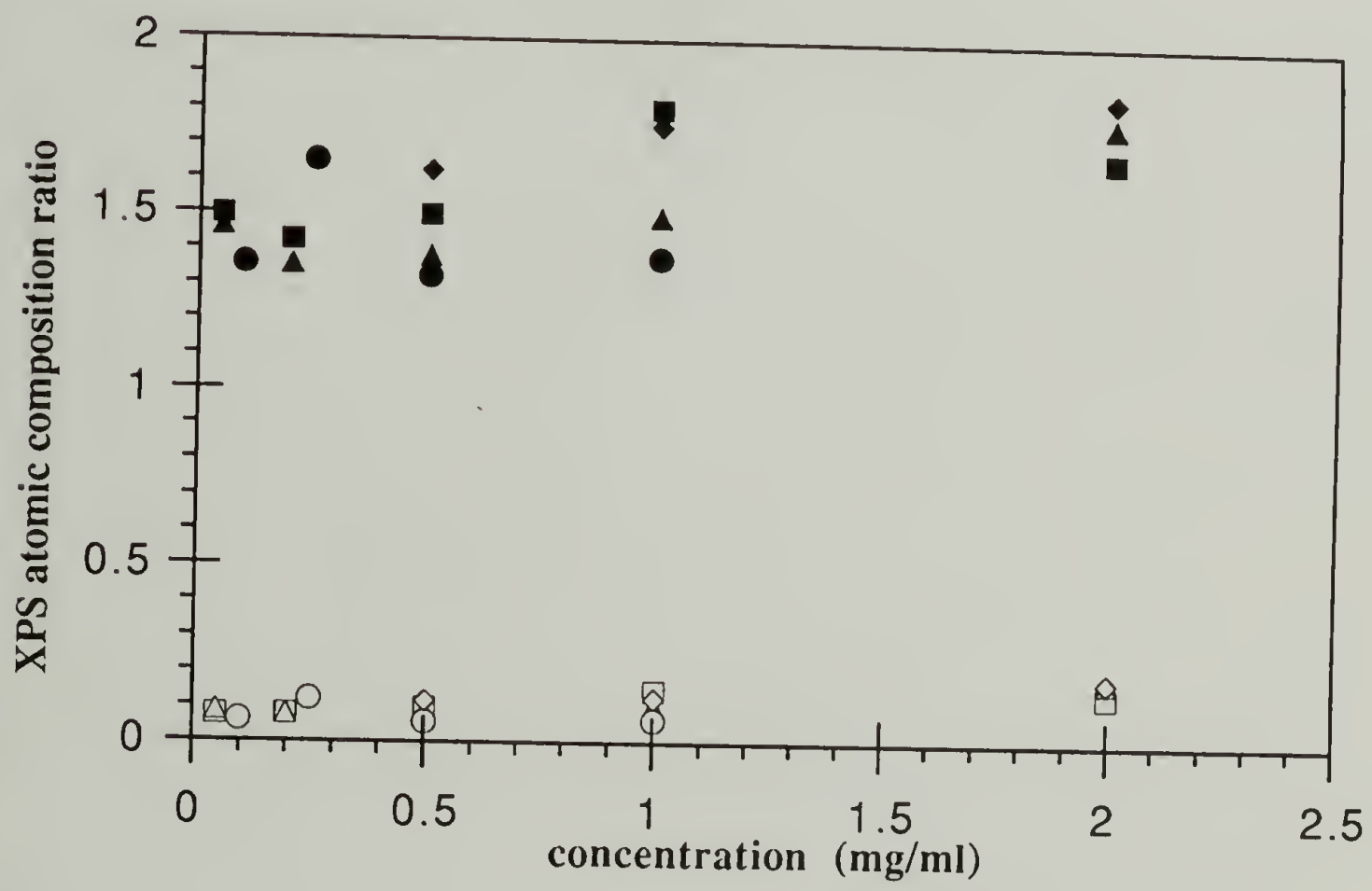


Figure 4.24 Effect of Concentration on the Amount Adsorbed to $PVF_2$ of PEO - (■) $C_{lbe}/C_{hbe}$, (□) $O_{1s}/F_{1s}$; PEO-FD - (▲) $C_{lbe}/C_{hbe}$, (△) $O_{1s}/F_{1s}$; PEO-ST - (●) $C_{lbe}/C_{hbe}$, (○) $O_{1s}/F_{1s}$; and PEO-TP - (◆) $C_{lbe}/C_{hbe}$, (◇) $O_{1s}/F_{1s}$.

Table 4.17 Effect of PEO-FD (24 h, 25k VII16) Concentration on the Amount Adsorbed to $PVF_2$: XPS and $\theta_A/\theta_R$ Data. [VI114-117]

| Concentration (mg/ml) | *$C_{lbe}/C_{hbe}$ | $O_{1s}/F_{1s}$ | $\theta_A/\theta_R$ |
|---|---|---|---|
| 0.05 | 1.462 | 0.087 | 83°/57° |
| 0.2 | 1.356 | 0.077 | 84°/55° |
| 0.5 | 1.380 | 0.082 | 83°/56° |
| 1.0 | 1.494 | 0.102 | 82°/55° |
| 2.0 | 1.773 | 0.181 | 78°/46° |

Table 4.18 Effect of PEO-ST (24 h, 50k VII26) Concentration on the Amount Adsorbed to $PVF_2$: XPS and $\theta_A/\theta_R$ Data. [VI130-133,136-143]

| Concentration (mg/ml) | *$C_{lbe}/C_{hbe}$ | $O_{1s}/F_{1s}$ | $\theta_A/\theta_R$ |
|---|---|---|---|
| 0.1 | 1.358 | 0.06 | 83°/63° |
| 0.25 | 1.652 | 0.119 | 84°/60° |
| 0.5 | 1.324 | 0.055 | 83°/57° |
| 1.0 | 1.378 | 0.061 | 83°/62° |

Table 4.19 Effect of PEO-TP (24 h, 50k VII74) Concentration on the Amount Adsorbed to $PVF_2$: XPS and $\theta_A/\theta_R$ Data. [VIII32-34]

| Concentration (mg/ml) | *$C_{lbe}/C_{hbe}$ | $O_{1s}/F_{1s}$ | $\theta_A/\theta_R$ |
|---|---|---|---|
| 0.5 | 1.623 | 0.115 | 83°/55° |
| 1.0 | 1.755 | 0.125 | 83°/52° |
| 2.0 | 1.842 | 0.182 | 81°/47° |

Despite former predictions, few trends were observed in the adsorption of PEO(-R) to the fluoropolymer film surface; little or no difference was observed in the amount of PEO or PEO-R adsorbed. From interfacial free energy arguments, the greatest amount of PEO-R was expected to adsorb to FEP which has the lowest critical surface tension. Instead, more PEO-R adsorbed to $PVF_2$ and PCTFE than to FEP. More PEO adsorbed to $PVF_2$ than to PCTFE as determined by the $O_{1s}/F_{1s}$ XPS atomic concentration data. The $O_{1s}/F_{1s}$ XPS ratio can be compared by multiplying that of PCTFE by 3/2; for a 2mg/ml solution of 53k PEO adsobed to PCTFE and $PVF_2$, $O_{1s}/F_{1s}$ is 0.121 (0.081 x 3/2, Table 4.8) and 0.138 (Table 4.14), respectively. The hydrophobic interaction between the alkyl end group of PEO-R and the $PVF_2$ film sample did not enhance adsorption of PEO nor was it an important driving force for adsorption. The adsorption likely depended more upon the polar interaction of PEO with $PVF_2$ than between that of PEO-R and the fluoropolymer film. The ratio of the alkyl end group to ethylene oxide repeat units was small: 1 end group : ~1,000 ethylene oxide repeat units. For PCTFE, where the polar interaction was decreased (relative to that of $PVF_2$), the hydrophobic interaction may have enhanced adsorption slightly, allowing more PEO-R to adsorb relative to PEO. For FEP, where there was no polar interaction, there was no adsorption. Although one would have expected that the hydrophobic interaction would be most prominent here, the polar interaction appears to be required for adsorption and the hydrophobic interaction to enhance the adsorbed amount. (The captive bubble contact angle experiment seemed to indicate a hydrophobic effect for adsorption.) A similar trend was observed for PEO where more polymer adsorbed to $PVF_2$ than to PCTFE than to FEP.

Adsorption at the PS Latex - Water Interface

Colloidal particles in a dispersion medium are stabilized by either electrostatic or steric interactions. Electrostatic stabilization is useful only at low ionic concentrations ($\sim 10^{-1}$ M) and at low solids contents. At higher electrolyte concentrations, the electrolyte compresses the spatial extension of the double layers leading to van der Waals attraction between the core particles and to coagulation. Steric stabilization is insensitive to the electrolytes present, is useful at both low and high solids content, and shows reversible flocculation. Steric stabilization depends upon repulsion between stabilizing moieties. The polystyrene latex used in this study was electrostatically stabilized by carboxylic acid groups. Although it was not specifically studied, adsorption of PEO(-R) likely enhanced the stability of the latex by providing steric stabilization. The best steric stabilizers are amphipathic, consisting of a non-soluble block which forms the anchor and a soluble block which forms the buoy. By end-capping PEO with an alkyl group (R), forming PEO-R, it was anticipated that the insoluble R group would form the anchor and that the soluble PEO the buoy on a hydrophobic latex. While PEO-R was soluble in water, the R group alone was insoluble.

The polystyrene latex that was used in adsorption studies was ~450 nm in diameter and resembled a plane[72] because of its low curvature. It was electrostatically stabilized in water with surface carboxylic acid groups which were separated by an average of ~202 $Å^2$ providing hydrophilic and hydrophobic (between the acid groups) patches on the surface. In addition, the latex was surfactant-free, providing a clean environment for adsorption. Although there are many potential latex variables - size, type, stabilization type (surfactant or charge), surface charge density (or type of charge) - adsorption studies were limited to the latex described. The objective of this work was to study the effect of the alkyl end group on adsorption.

The conformation of a polymer at an interface depends upon several variables:

(1) chemical constitution of the polymer, (2) chemical nature and geometrical shape of the interface, (3) chemical composition of the solvent, (4) mode of attachment, and (5) surface density of the polymer molecules at the interface. At high surface coverage, the stabilizing polymer moieties are extended from the surface giving rise to tails. In the adsorption study here, both latex and solvent were constant; however, the chemical constitution of the polymer changed with the end group. Addition of the end group likely affected the mode of attachment which in turn affected the surface density and packing of polymer molecules at the interface.

Adsorption of polymer chains from a dispersion medium to latex particles is a complicated system. Several factors contribute to the stability of the colloid and to the type of adsorption (flattened vs. extended) observed: concentration and molecular weight of the polymer, particle size, and solvency of the dispersion medium for the stabilizing polymer. The effects of these variables on colloid stability are summarized in Figure 4.25. Further details are not given because only the effect of the PEO-R end group was studied here. Particular attention was focussed on the hydrodynamic thickness of the adsorbed layer which reflects different modes of attachment of the stabilizing moieties.

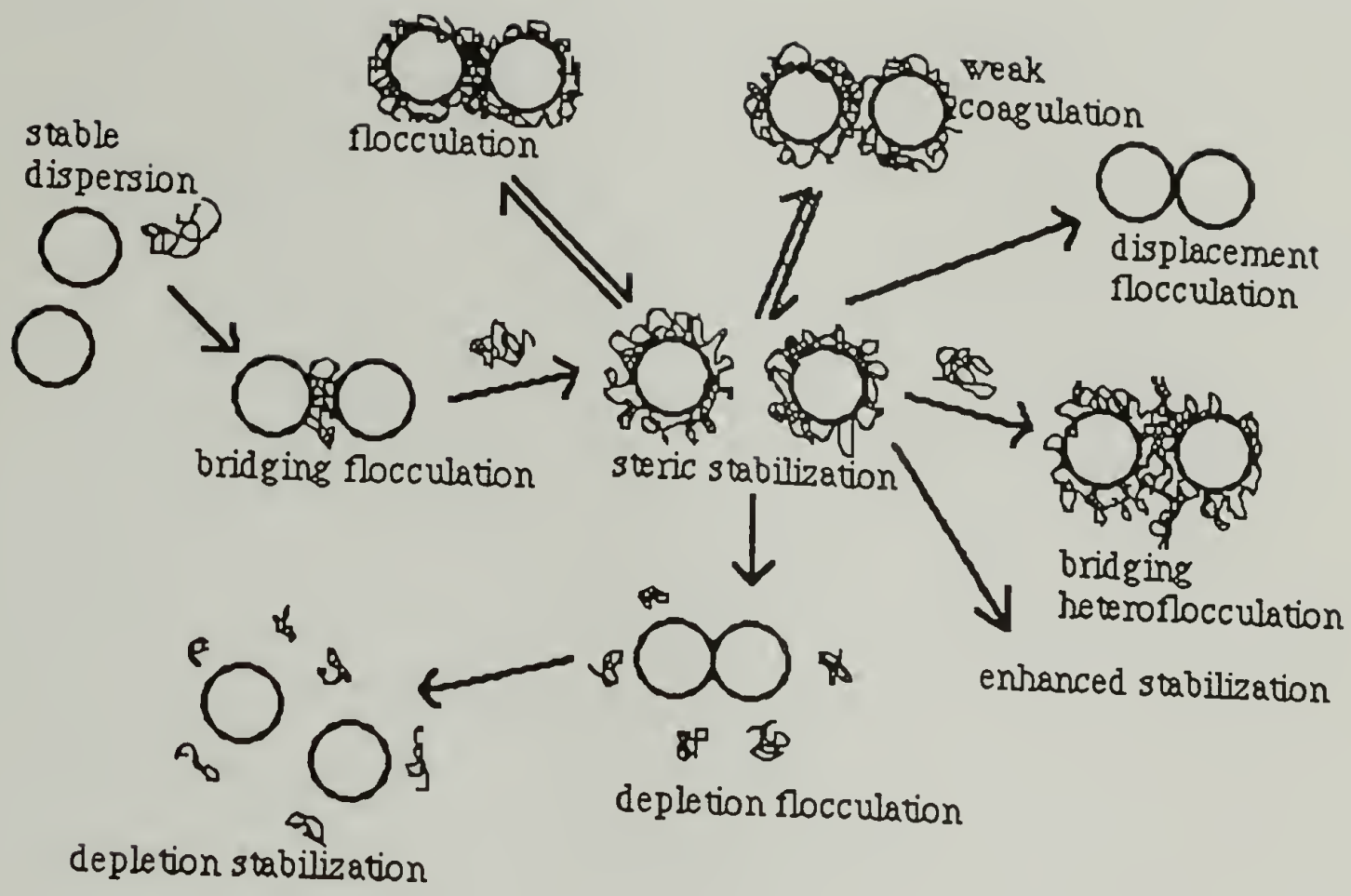


Figure 4.25 The Effect of Polymer Chains on Colloid Stability.[73]

The adsorption of PEO and PEO-R were compared at the polystyrene latex - water interface by photon correlation spectroscopy (PCS). The hydrodynamic thickness of the adsorbed PEO(-R) layer was determined by subtracting the radius of the PS latex. Table 4.20 and Figure 4.26 summarize the results for adsorption of PEO and PEO-R from water to PS latex (after 24 h). The values in Figures 4.27 - 4.30 are of the hydrodynamic thicknesses obtained after 1 h and 24 h of adsorption to PS for PEO, PEO-FD, PEO-TP, PEO-ST, respectively. The standard deviation of the values listed in Table 4.20 is $\pm$ 2, indicating that the differences in hydrodynamic thicknesses are more meaningful for the thicker adsorbed layers.

Table 4.20 Hydrodynamic Thickness for PEO and PEO-R Adsorbed to PS Latex Determined by PCS.

| Conc (mg/ml) | PEO 1 h | PEO 24 h | PEO-ST 1 h | PEO-ST 24 h | PEO-TP 1 h | PEO-TP 24 h | PEO-FD 1 h | PEO-FD 24 h |
|---|---|---|---|---|---|---|---|---|
| 0.05 | 4 | 7 | 31.5 | 33 | 16 | 24 | 7 | 5 |
| 0.1 | 5.5 | 10 | 25 | 25 | 13 | 24.5 | 5 | 5 |
| 0.2 | 12.5 | 18.5 | 20 | 33 | 29 | 27.5 | 16 | 4 |
| 0.5 | 13.5 | 16 | 34.5 | 37 | 25.5 | 27 | 24 | 9.5 |
| 0.8 | 18 | 19 | 33.5 | 40.5 | 30 | 33 | 25 | 15 |
| 1.0 | 25 | 18 | 42 | 48 | 43 | 45 | 48 | 25 |

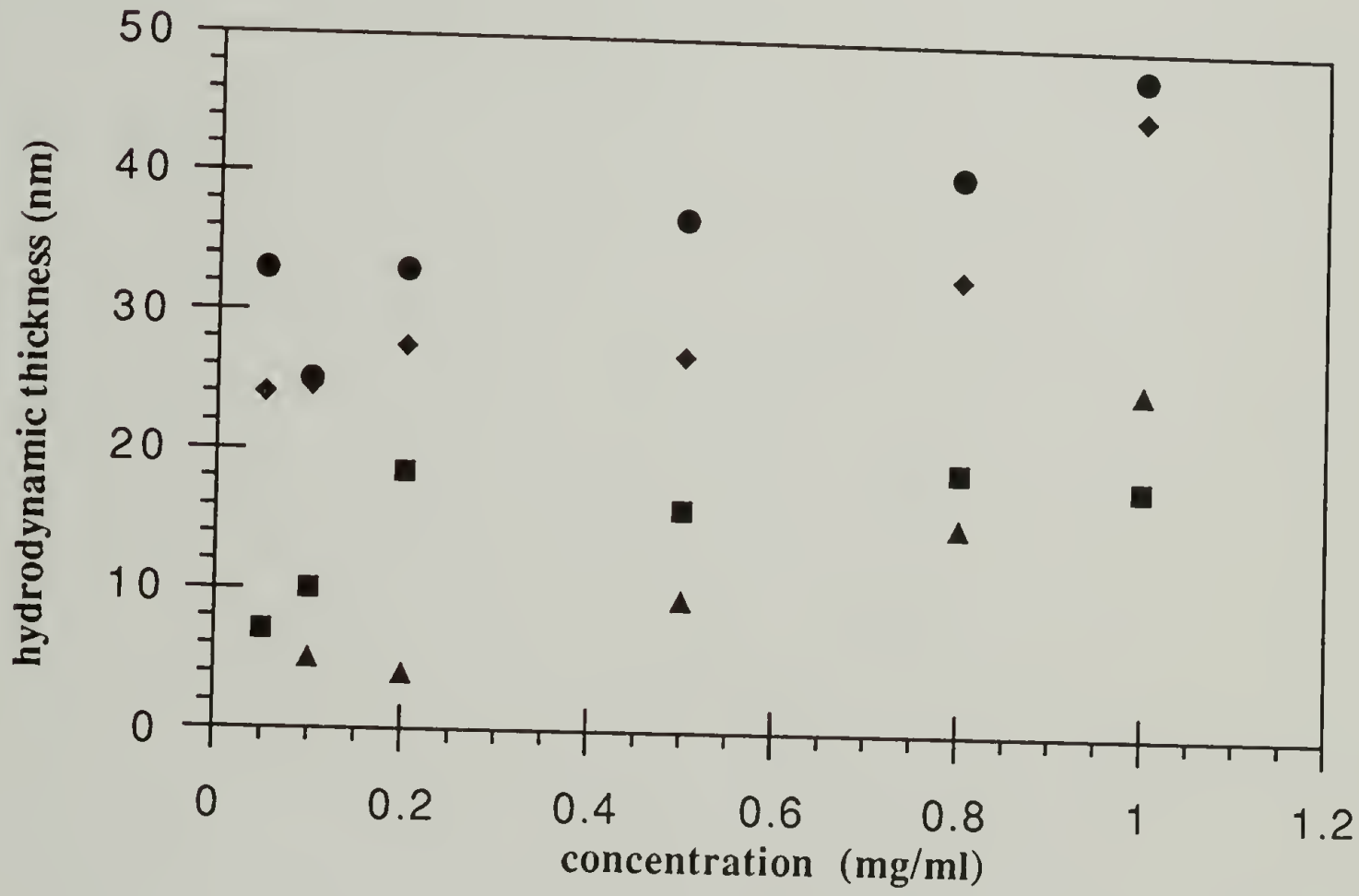


Figure 4.26 Adsorption at the PS Latex - Water Interface: Comparison of the Hydrodynamic Thickness after 24 h of (■) PEO, (▲) PEO-FD, (◆) PEO-TP, and (●) PEO-ST.

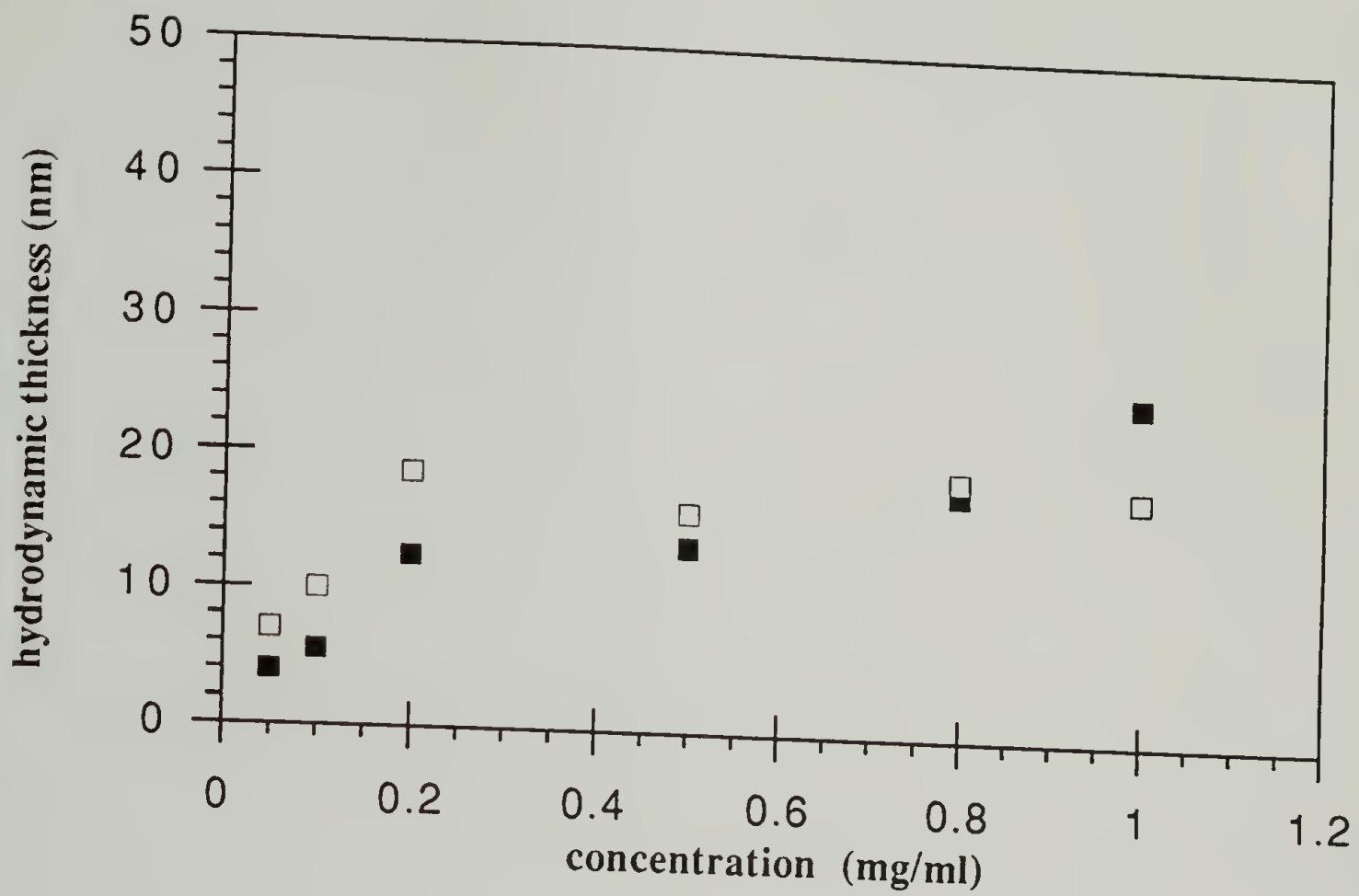


Figure 4.27 Adsorption of PEO at the PS Latex - Water Interface after (■) 1 h and (□) 24 h.

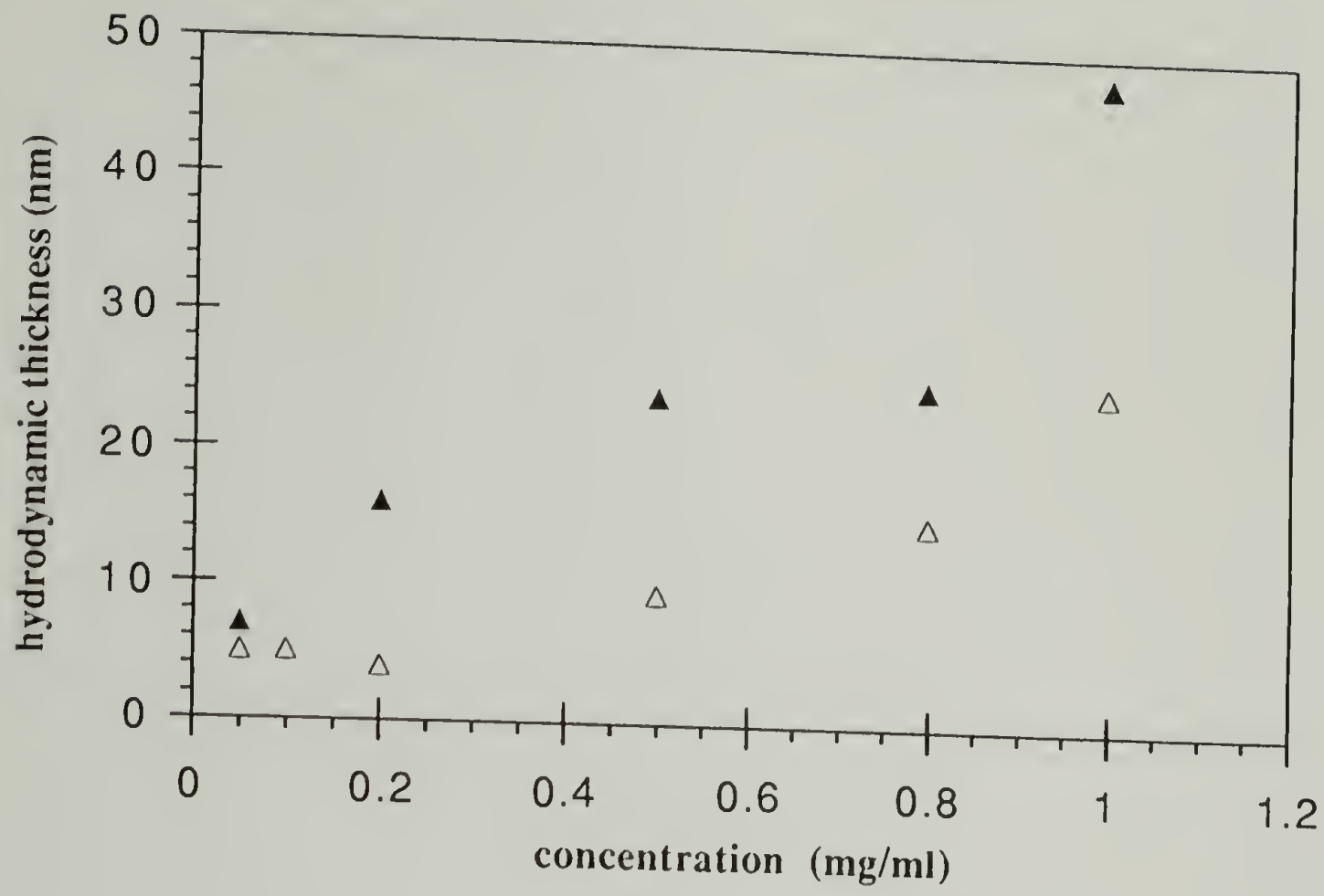


Figure 4.28 Adsorption of PEO-FD at the PS Latex - Water Interface after (▲) 1 h and (△) 24 h.

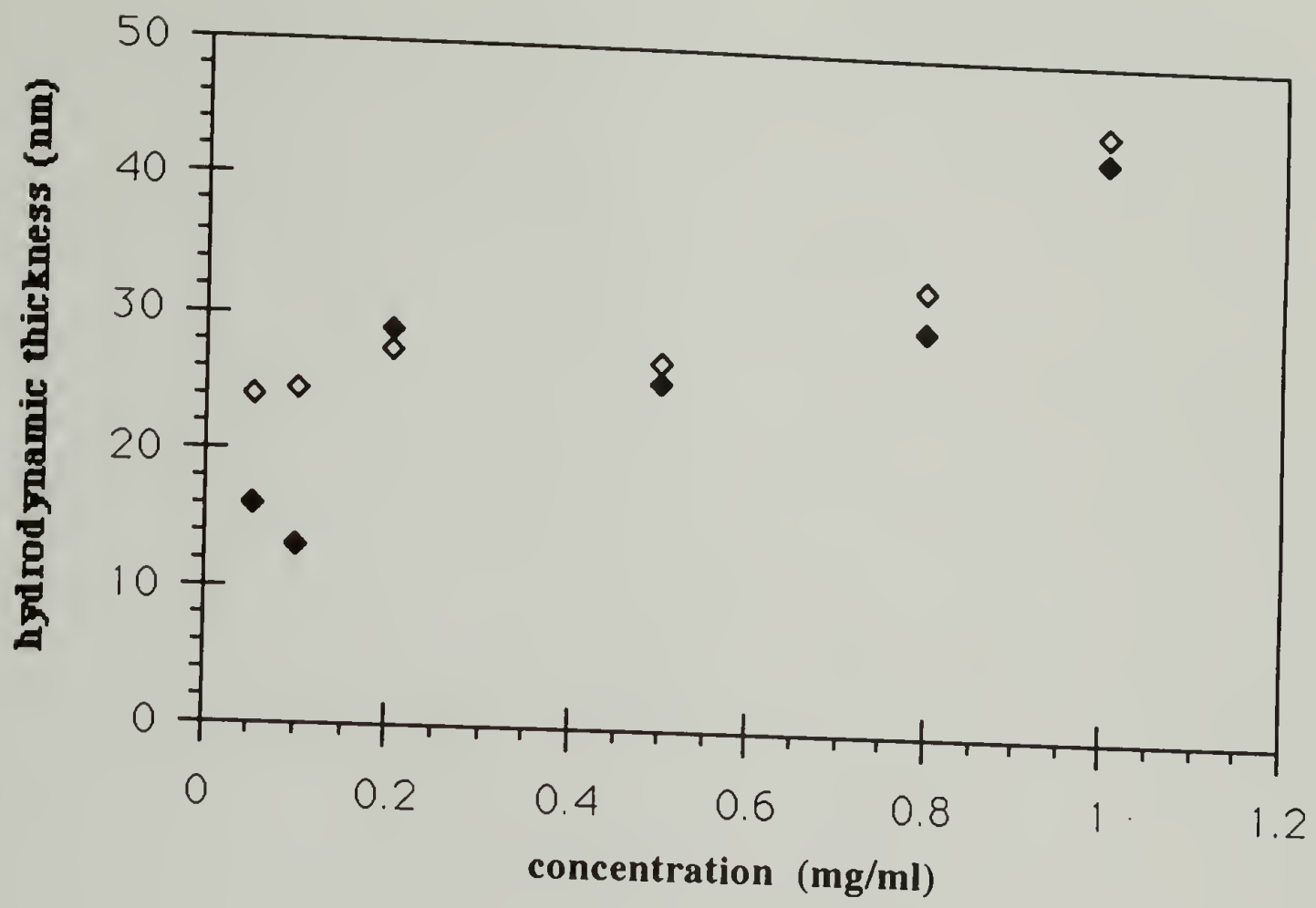


Figure 4.29 Adsorption of PEO-TP at the PS Latex - Water Interface after (◆) 1 h and (◇) 24 h.

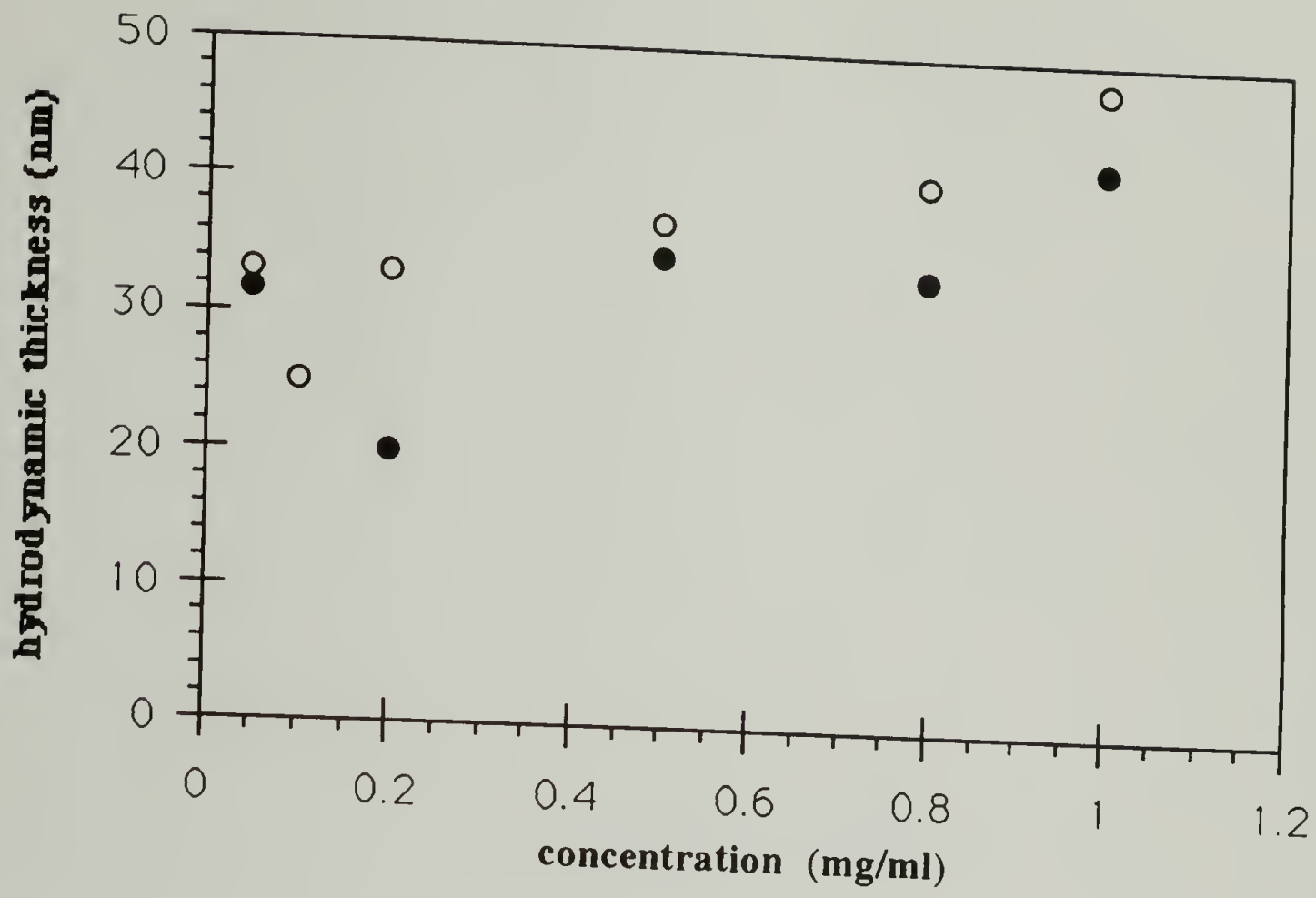


Figure 4.30 Adsorption of PEO-ST at the PS Latex - Water Interface after (●) 1 h and (○) 24 h.

From the data in Table 4.20 and Figure 4.26, it is apparent that the hydrodynamic thickness was greatest for PEO-ST and PEO-TP. The thickness of the adsorbed layer did not change significantly between 1 h and 24 h for all samples (Figures 4.27, 4.29, 4.30) excepting that of PEO-FD where the hydrodynamic thickness decreased substantially after 24 h (Figure 4.28). The data will be discussed first in terms of the effects that cause an increase in the adsorbed layer thickness and then in terms of the unusual behavior found for PEO-FD.

Adsorption of both PEO and PEO-R increased the hydrodynamic thickness of the PS latex with increasing concentration of the polymer dissolved in solution. The adsorption of PEO-R extended the hydrodynamic thickness of the PS latex further than that

of PEO. The alkyl end group affected the adsorption of PEO in terms of its adsorption conformation, mode of attachment to PS latex, and likely in terms of the surface density of adsorbed polymer. Poly(ethylene oxide) adsorbed to the latex by a hydrogen bonding interaction between the ether oxygen of the PEO repeat unit and the carboxylic acid proton.[31] In addition to the hydrogen bonding interaction, one of two possible modes of PEO-R interaction with the PS latex may account for the increased hydrodynamic thickness observed: (1) enhanced attraction of the alkyl end group to the hydrophobic "patches" between carboxylic acid groups on the PS latex or (2) repulsion of the hydrophobic group from the carboxylic acid surface. Figure 4.31 summarizes these possible modes of interaction.

(a)

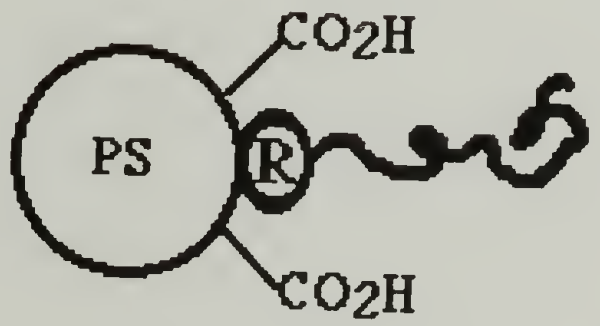


(b)

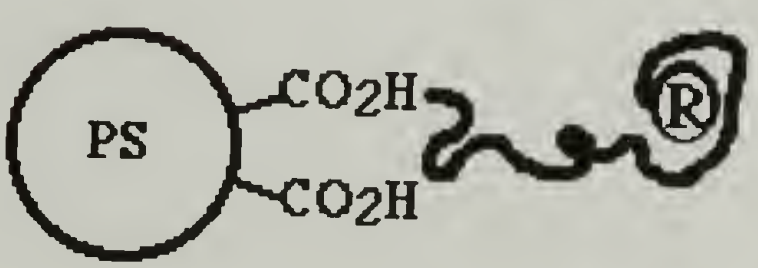


Figure 4.31 Adsorption of PEO-R to PS latex by either (a) a hydrophobic interaction or (b) a repulsion mechanism.

If it is assumed that PEO adsorbed to PS latex in the typical tail - loop - train conformation, PEO-R likely adsorbed with an extended tail. The hydrophobic interaction

between a hydrophobic surface and a hydrophobic moiety could enhance adsorption from an aqueous solution (Figure 4.31 (a)). The adsorption would be concomitant with the release of solvent molecules from the interface which would be entropically favorable. However, since the PS latex was carboxylic acid-stabilized with charge groups occupying approximately 202 $Å^2$, there were not large "hydrophobic patches" for this presumed hydrophobic interaction. Since, the R group could not interact with the latex in the same manner as did the hydroxyl end group of PEO, the R group may have formed a tail resulting in PEO-R being further extended from the PS surface. However, the R group was hydrophobic and unlikely to extend into the aqueous solution unless it was shielded (or surrounded) by the PEO backbone (Figure 4.31 (b)). In a separate study, Clunie *et al.*[74] found that the hydrophilic moiety (PEG) bound to the polar sites on the surface causing the hydrophobe (alkyl group) to be oriented out into the aqueous solution. From the information provided, it was difficult to discern whether either of the two proposed mechanisms had any merit and thus no conclusions were drawn.

The adsorption of PEO-FD to PS latex showed unusual behavior where the hydrodynamic thickness decreased from 1 h to 24 h. This unusual result may have arisen because the group was fluorinated or because it had a fewer number of carbon atoms in the end group. Initially (1 h) the FD group may have formed a tail extending from the PS latex as was observed for the other end groups; however, this effect diminished with time causing the thickness of the adsorbed layer to decrease. The thickness of the adsorbed PEO-FD layer was similar to that of PEO after 24 h. The fewer number of carbons in the hydrophobic group of FD ($C_{10}$) with respect to the other end groups ($C_{17}$ - $C_{18}$) was likely the reason for the unusual behavior. The end group could not sustain its effect on the adsorbed conformation and/or thickness over time. To determine if the end group could sustain its effect for lower molecular weight PEO-FD, the experiment was repeated with 25k PEO-FD which was half the molecular weight of the former sample studied. The ratio

of the FD group to EO repeat units doubled by using PEO of half the molecular weight. As shown in Figure 4.31, the adsorbed layer thickness did not decrease with time.

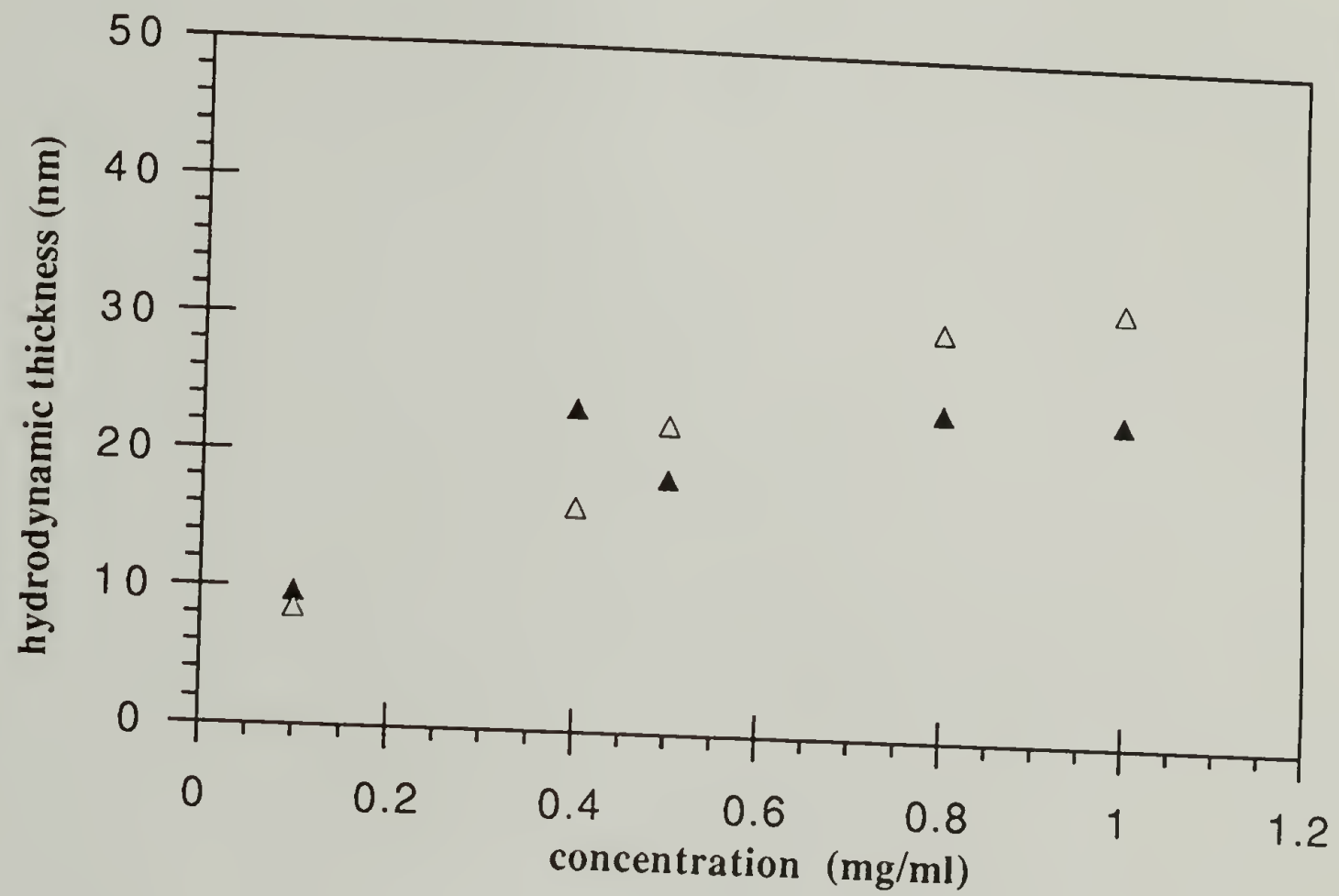


Figure 4.32 Adsorption of 25k PEO-FD at the PS Latex - Water Interface after (▲) 1 h and (△) 24 h.

In an attempt to determine the amount of PEO(-R) that had adsorbed to the PS latex, a turbidity measurement with potassium iodide/iodine solution was prepared.[47] The procedure relied upon measuring the amount of PEO left in solution after adsorbing it to PS latex and subtracting this amount from the amount of PEO originally added. This amount was determined by comparison to a calibration curve prepared with known amounts of polymer for each type of end group studied. The 'supernatant' was obtained by filtering

the PS-PEO latex solutions with a 0.22 μm filter. The latices (~450 nm) were effectively removed from solution by this technique. Unexpectedly, the filters retained some PEO (Rg ~6 - 10 nm[24,35]) as well. Because the amount adsorbed was calculated by difference, the results were not reproducible or consistent. An attempt to separate latex from non-adsorbed polymer in solution by centrifugation also gave results that were not interpretable, likely due to the interaction of $KI/I_2$ with hydrocarbon contaminants.

Adsorption at the Air -Water Interface

Surface tension measurements provided information on the adsorption of PEO(-R) at the air - water interface and lent some insight on possible micelle formation. Adsorption at the air - water interface was studied with the surface tensiometer, described in Figure 4.9, where the Du Nuoy Ring method[75] was used to measure the surface tension of water; a decrease in the surface tension of water was due to polymer adsorption at the air - water interface. The results are summarized in Figure 4.32 where the surface tension of water decreased by ~10 dyn/cm with the introduction of a low concentration of PEO (Mn ~50,000 g/mole). The surface tension appeared to be independent of PEO concentration but was further decreased with PEO-tripentylacetate (PEO-TP) and further with PEO-dioctylacetate (PEO-DO) and PEO-stearate (PEO-ST). The greatest decrease in water surface tension was observed for PEO-nonadecafluorodecanoate (PEO-FD) where the perfluoroalkyl group was likely present at the interface. Surface tension was calculated according to equation 4.2.

$$\gamma = \frac{\text{Force (h)}}{4\pi R} \times f(R^3/V, R/r) \qquad (4.2)$$

R is the ring radius; r is the wire radius; $f(R^3/V, R/r)$ was determined from tabulated results in terms of the indicated ratios. The force was calculated from the height, recorded on a chart recorder, required to pull the Du Nuoy ring through the air-water interface. Height was converted to mass by comparison with the calibration curve described by equation 4.3.

(4.3) $$y = 11.744x - 1.3036$$

y is the mass (mg); x is the height measured. The force ($gcm/s^2$) was calculated by multiplying the value of y by $980.7 \times 10^{-3}$ $cm/s^2$

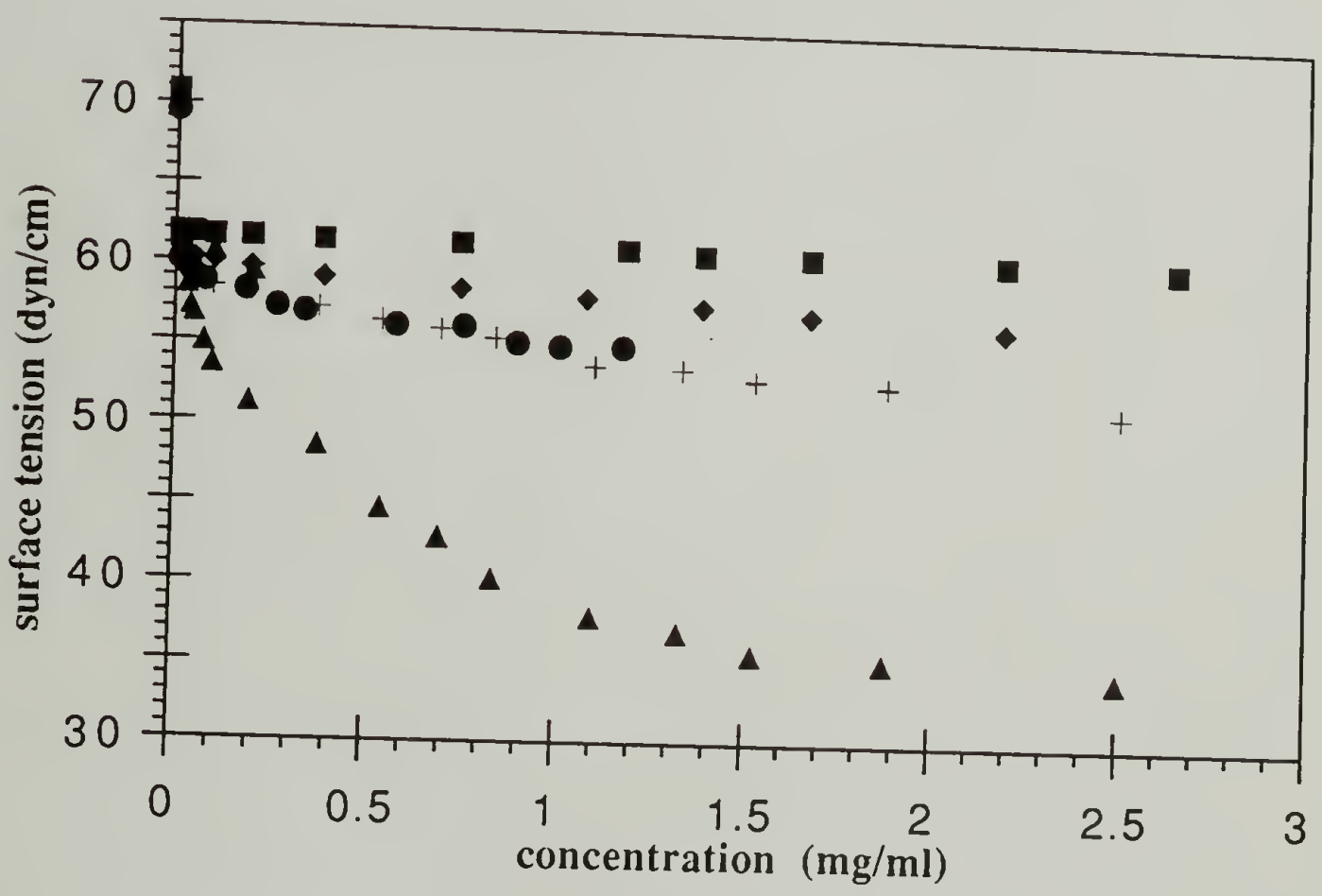


Figure 4.33 Adsorption at the Air - Water Interface of (■) PEO, (◆) PEO-TP, (●) PEO-ST, (+) PEO-DO, (▲) PEO-FD (Mn ~50,000 g/mole).

The perfluoroalkyl end group affects the surface tension of water dramatically. The perfluoroalkyl end group differs from the alkyl end group in two obvious ways: (1) it is a linear end group of 10 carbons and (2) it is perfluorinated. Perfluorinated polymers are known to have amongst the lowest surface tensions: FEP has a critical surface tension of 18 dyn/cm while that of $PVF_2$ is 25 dyn/cm. Although the perfluoroalkyl end group resembles the chemical structure of FEP most closely it is covalently bonded to PEO. Both PEO and FD are surface active; some competition between PEO and FD for the air - water interface likely exists. PEO-FD decreases the surface tension of water to a greater extent than PEO, indicating that the FD end groups are dominant at the interface. Because the perfluorodecanoate groups are attached to PEO of ~50,000 g/mole, the number of FD groups that can "pack" at the interface is limited by the packing of PEO directly below the interface.[76] The number of carbons in FD, 10, is less than the 18 (or 17) carbons of the other end groups studied; however, there is no evidence that this has a predominant effect. Studies are currently being conducted by Miriam Rafailovich (Queens College, CUNY) on the concentration profile at the air - water interface of PEO-FD using neutron reflectivity. Preliminary results indicate that a 60 Å layer formed at the water surface with a 4% concentration for a 1 mg/ml sample; this corresponds to a surface excess of 1.6 μM.

A small difference between the three alkyl end groups is observed for adsorption at the air-water interface. The alkyl end groups studied are essentially isomers with different hydrocarbon chain structures: ST is linear, DO is branched (bifurcated) with 2 alkyl groups of 8 carbons each, TP is branched with 3 alkyl groups of 5 carbons each. Unlike PEO adsorption at the air-water interface, a further decrease in the surface tension of water with PEO-R concentration is observed. As indicated for PEO-FD adsorption, the hydrophobic alkyl end group likely forms at the air-water interface. The alkyl end groups do not differ from the PEO backbone as substantially as the perfluoroalkyl group did. Although the alkyl end groups may have been predominant at the air-water interface, they were not as easily detected. The critical surface tension of polyethylene is 31 dyn/cm

whereas the surface tension of PEO was measured to be 61-62 dyn/cm. The difference between the three alkyl end groups in terms of reduced surface tension is very small. One can envision that the tripentylacetate group could form the most dense monolayer at the air-water interface because it is more compact than either the stearate or dioctylacetate groups. According to this argument, TP would form the most dense monolayer at the air - water interface followed by DO and then ST. However, because the alkyl groups are attached to PEO, their ability to "pack" at the interface depends upon that of PEO. The TP end group extended the least from PEO's backbone and the surface tension of PEO-TP resembled that of PEO most closely. The differences between the PEO-ST and PEO-DO surface tensions are very subtle. According to a study comparing stearic acid and dioctylacetic acid monolayers spread on the surface of water from benzene, a higher concentration of dioctylacetic acid formed over stearic acid at the air-benzene-water interface.[77] This was likely due to the compact nature of the dioctylacetic acid group with respect to that of stearic group. In a study on surface activity of polyelectrolytes, Okubo[78] showed that surface tension decreased as a function of the ability of the hydrophobic (surface active) and hydrophilic groups to separate. This should not be a factor in this study as the hydrophobic groups were attached to the polymer by the same chemistry. The difference was only in the extent to which the end group extended from the polymer chain. The stearyl group extended further than either tripentylacetyl or dioctylacetyl groups. In his study, Okubo equated a lowering in the surface tension of water with a reorganization of the water molecules at the interface.

Neither micellization nor time dependent surface pressure measurements were observed for these samples. Of the five samples studied, only PEO-ST showed time dependence (and this was minimal) and possible micelle formation; however, the data were inconclusive. (See Figure 4.33 for PEO-ST adsorption at the air - water interface showing possible time dependence.) From the hydrophilic - lipophilic balance (HLB) equation, the

polymers used in this study had HLB numbers (~20) greater than what is normally considered a solubilizer (15 - 18).[79]

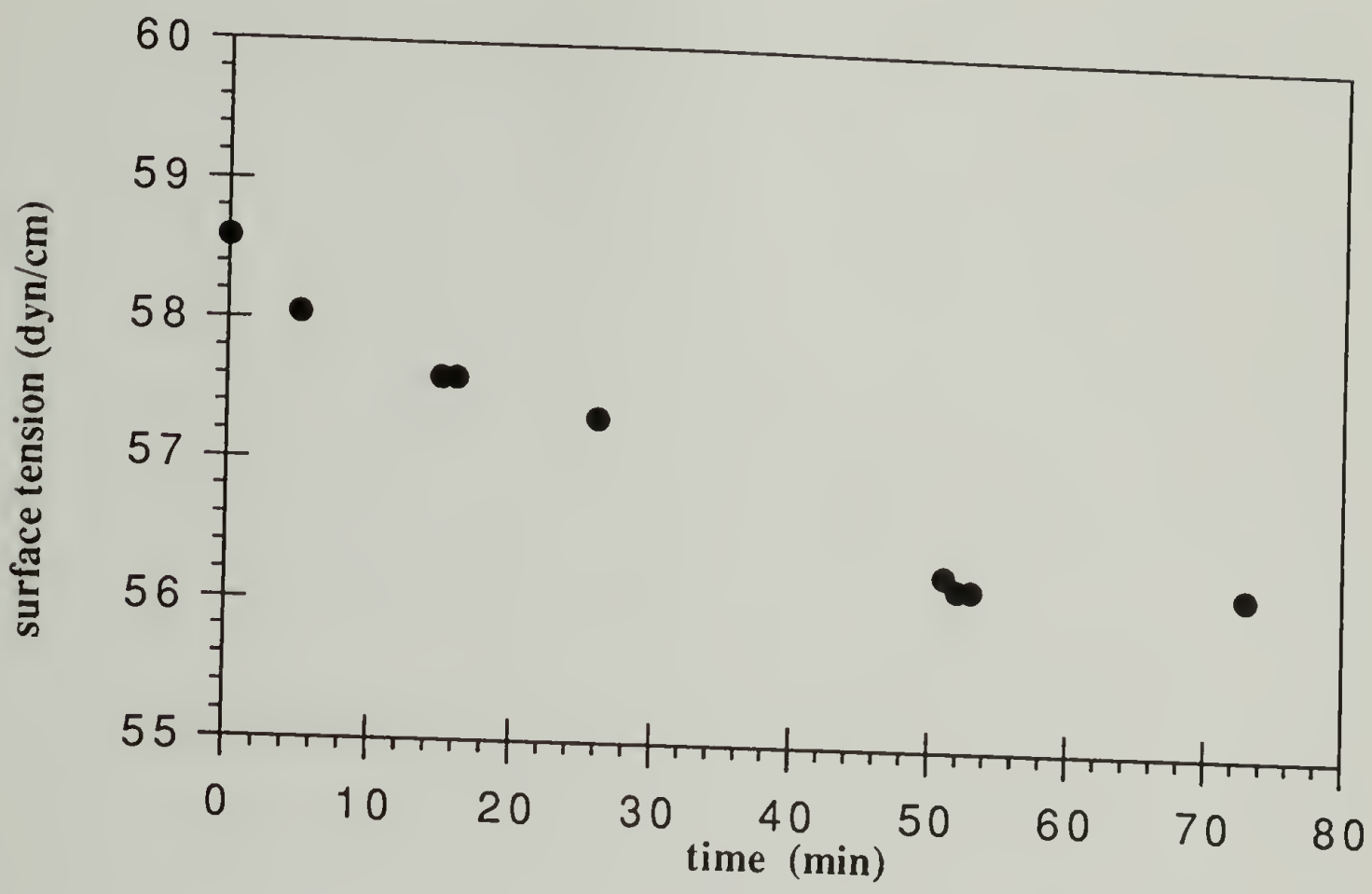


Figure 4.34 Adsorption of PEO-ST at the Air - Water Interface:
Dependence of Surface Tension on Time for a 0.57 mg/ml PEO-ST Solution.

## Conclusions

Ethylene oxide was polymerized anionically with triethylene glycol monomethyl ether potassium initiation. PEO, between 5,000 and 50,000 g/mole, was prepared with a narrow polydispersity of 1.07 to 1.17. PEO was end-capped by the reaction of its terminal hydroxyl group with an alkyl acid chloride, producing an ester linkage for PEO-R. The

effect of an alkyl end group on the adsorption of PEO-R with respect to that of PEO was investigated. The hydrophobic interaction as a driving force for adsorption from aqueous solution was investigated with three separate systems. Adsorption at the fluoropolymer film - water interface was affected neither by the presence nor the type of alkyl end group; adsorption appeared to be dominated by the PEO - film polar interaction rather than that of the hydrophobic PEO-R - film. The following trend was observed in amount adsorbed: FEP < PCTFE < $PVF_2$. The differences in adsorption between PEO-R and PEO were subtle and may have been diminished by the work up procedure. Captive bubble contact angle indicated that the adsorption of PEO and PEO-FD to FEP could be distinguished; further work in this area could lend insight on the hydrophobic interaction as a driving force for adsorption. Adsorption at the PS latex - water interface was complicated by the surface carboxylic acid groups and affected by the presence and type of the alkyl end group. An increase in the hydrodynamic thickness of the PS latex was observed for the adsorption of both PEO and PEO-R. The hydrodynamic thickness of PEO-R was greater than that of PEO; PEO-R interacted with the PS latex by either an attractive (hydrophobic) or repulsive interaction in addition to the hydrogen bonding interaction attributed to PEO adsorption. Adsorption at the air - water interface was affected by both the presence and the type of "R" group. The greatest decrease in surface tension was observed for PEO-FD where the perfluorodecanoate groups dominated the air - water interface.

## References


1. Bailey, F.E., Jr.; Koleske, J.V. *Alkylene Oxides and Their Polymers* (Surfactant Science Series, vol. 35) Marcel Dekker: New York, 1991.

2. Fuchs, O. in *Polymer Handbook*, 3rd ed. (Brandjup, J.; Immergut, E.H., Eds.); John Wiley and Sons: New York, 1989, p. 388.

3. Bailey, F.E.; Koleske, J.V. *Poly(ethylene oxide)* Academic Press, New York, 1976, ch. 5.

4. Szwarc, M. *Living Polymers and Mechanisms of Anionic Polymerization* (Adv. in Polym. Sci. vol. 49) Springer Verlag: Berlin, 1983.

5. Aida, T.; Inoue, S. *Macromolecules* **1981**, *14*, 1162.

6. Aida, T.; Inoue, S. *Macromolecules* **1981**, *14*, 1166.

7. Gee, G.; Higginson, C.E.; Levesley, P.; Taylor, K.J. *J. Chem Soc.* **1959**, 1338.

8. Wojtech, B. *Makromol. Chem.* **1966**, *66*, 180.

9. Price, C.C.; Carmelite, D.D. *J. Am. Chem. Soc.* **1966**, *88*, 4039.

10. Price, C.C.; Akkapeddi, M.K. *J. Am. Chem. Soc.* **1972**, *94*, 3972.

11. Figueruelo, J.E.; Worsfold, D.J. *Eur. Polym. J.* **1968**, *4*, 439.

12. Nenna, S.; Figueruelo, J.E. *Eur. Polym. J.* **1975**, *11*, 511.

13. Nenna, S.; Figueruelo, J.E. *Die Makromol. Chem.* **1975**, *176*, 3377.

14. Cabasso, I.; Zilkha, A. J. *Macromol. Sci.-Chem.* **1974**, *A8*, 1313.

15. Quirk, R.P.; Ma, J.-J. *J. Polym Sci. Part A: Polym. Chem.* **1988**, *26*, 2031.

16. Quirk, R.P.; Seung, N.S. in *Ring Opening Polymerization: Kinetics, Mechanism, and Synthesis* (J. E. McGrath, Ed.) **1985**, *286*, 37.

17. Kazanskii, K.S.; Solovyanov, A.A.; Entels, S.G. *Eur. Polym. J.* **1971**, *7*, 1421.

18. Deffieux, A.; Boileau, S. *Polymer* **1977**, *18*, 1047.

19. Eisenbach, C.D.; Peuscher, M. *Makromol. Chem., Rapid Commun.* **1980**, *1*, 105.

20. Eisenbach, C.D.; Peuscher, M.; Wegner, G.; Weiss, M. *Makromol. Chem.* **1983**, *184*, 2313.

21. Reuter, H.; Horing, S.; Ulbricht, J. *Eur. Polym. J.* **1989**, *25*, 1113.

22. Cohen Stuart, M.A.; Cosgrove, T.; Vincent, B. *Adv. Colloids Interface Sci.* **1986**, *24*, 143.

23. Cosgrove, T.; Vincent, B. in *Fluid Interfacial Phenomena* (Croxton, C.A., Ed.) John Wiley and Sons: New York, 1986, p. 607.

24. Klein, J.; Luckham, P.F. *Macromolecules* **1984**, *17*, 1041.

25. Kawaguchi, M.; Mikura, M.; Takahashi, A. *Macromolecules* **1984**, *17*, 2063.

26. (a) Marra, J.; Hair, M.L. *Colloids & Surfaces* **1989**, *34*, 215; (b) Hair, M.L.; Guzonas, D.; Boils, D. *Macromolecules* **1991**, *24*, 341.

27. Parnas, R.S.; Chaimberg, M.; Taepaisitphongse, V.; Cohen, Y. *J. Colloid Interface Sci.* **1989**, *129*, 441.

28. Killmann, E. *Polymer* **1976**, *17*, 864.

29. Kawaguchi, M.; Hada, T.; Takahashi, A. *Macromolecules* **1989**, *22*, 4045.

30. Kawaguchi, M.; Sakai, A.; Takahashi, A. *Macromolecules* **1986**, *19*, 2952.

31. Dobbie, J.W.; Evans, R.; Gibson, D.V.; Smitham, J.B.; Napper, D.H. *J. Colloid Interface Sci.* **1973**, *45*, 557.

32. Cosgrove, T.; Crowley, T.L.; Vincent, B. in *Adsorption From Solution* (Ottewill, R.H.; Rochester, C.H.; Smith, A.L., Eds.); Academic Press: New York 1983, p. 287.

33. Cosgrove, T.; Heath, T.G.; Ryan, K.; van Lent, B. *Polymer Commun.* **1987**, *28*, 64.

34. (a) Scheutjens, J.M.H.M.; Fleer, G.J. *J. Phys. Chem.* **1979**, *83*, 1619; (b) Scheutjens, J.M.H.M.; Fleer, G.J. *J. Phys. Chem.* **1980**, *84*, 178.

35. Cohen Stuart, M.A.; Waajen, F.H.W.H.; Cosgrove, T.; Vincent, B.; Crowley, T.L. *Macromolecules* **1984**, *17*, 1825.

36. Baker, J.A.; Berg, J.C. *Langmuir* **1988**, *4*, 1055.

37. Couture, L.; van de Ven, T.G.M. *Colloids & Surfaces* **1991**, *54*, 245.

38. (a) Kuzmenka, D.J.; Granick, S. *Macromolecules* **1988**, *21*, 779; (b) Kuzmenka, D.J.; Granick, S. *Polymer Commun.* **1988**, *29*, 64.

39. Kawaguchi, M; Komatsu, S.; Matsuzumi, M.; Takahashi, A. *J. Colloid Interface Sci.* **1984**, *102*, 356.

40. For an overview see *Nonionic Surfactants: Physical Chemistry* (Schick, M.J., Ed.) (Surfactant Science Series vol. 23) Marcel Dekker: New York, 1987.

41. Filler, R.; O'Brien, J.F.; Fenner, J. V.; Hauptschein, M. *J. Am. Chem. Soc.* **1953**, *75*, 966.

42. (a) Lopez, A.; Fidel, J.; Alonso Cermenco, F. *An. Quim.* **1969**, *55*, 153; (b) Midgley, G.; Thomas, C.B. *J. Chem. Soc., Perkin Trans. II* **1984**, *(9)*, 1537.

43. General reaction conditions for producing an acid chloride from an acid by reaction with thionyl chloride can be found in the following references. (a) Rabjohn, N.; Harbert, C.A. *J. Org. Chem.* **1970**, *35*, 3726; (b) Cason, *J. Org. Synth. Coll. vol. III* (Horning, E.C., Ed.) John Wiley & Sons: New York, **1955**, p. 169; (c) Barnes, P. *ibid.* p. 555; (d) Womack, E.B.; McWhirter, J. *ibid.* p. 714.

44. Sperber, N.; Papa, D.; Schwenk, E. *J. Am. Chem. Soc.* **1948**, *70*, 3091.

45. Noyes, W.A. *Org. Synth. Coll. vol. III* (Blatt, A.H., Ed.); John Wiley & Sons: New York, **1955**, p. 108.

46. Tripentylacetyl chloride was reported and characterized but no experimental details were given for its synthesis by Gasparani, G.M.; Polidori, E. *J. Chem. Eng. Data* **1976**, *21*, 504.

47. Baleux, B. *C.R. Acad. Sci., Ser. C. Paris* **1972**, *274*, 1617.

48. Kazanskii, K.S. *Pure & Appl. Chem.* **1981**, *53*, 1645.

49. Lehn, J.M. *Pure & Appl. Chem.* **1980**, *52*, 2303.

50. For example see Kevill, D.N.; Daum, P.H.; Sapre, R. *J. Chem. Soc., Perkin II* **1975**, 963.

51. Fersht, A.R.; Jencks, W.P. *J. Am. Chem. Soc.* **1970**, *92*, 5432.

52. Newman, M.S.; Fukunaga, T.; Miwa, T. *J. Am. Chem. Soc.* **1960**, *82*, 873.

53. For example see Rabinovitch, B.S.; Winkler, C.A. *Canad. J. Res.* **1942**, *20*, 221.

54. Zil'berman, E.N. *Russ. Chem. Rev.* **1962**, *31*, 615.

55. Other reagents have been used for this reaction, for example see Wade, L.G., Jr.; Silvey, W.B. *Org. Prep. Proc. International* **1982**, *14*, 357.

56. Ladenheim, H.; Bender, M.L. *J. Am. Chem. Soc.* **1960**, *82*, 1895.

57. Char, K.; Frank, C.W.; Gast, A.P. *Langmuir* **1989**, *5*, 1335.

58. Bohmer, M.R.; Koopal, L.K. *Langmuir* **1990**, *6*, 1478.

59. Sperry, P.R.; Thibeault, J.C.; Kostansek, E. C. in *Eleventh International Conference in Organic Coating Science and Technology Proceedings* (Patsis, A.V., Ed.) Advanced Orgainc Coatings Science and Technology Series 1985; Technomic Publishing: Lancaster, PA, **1987**, *9*, 1.

60. Hoy, K.K.; Hoy, R.C. United States Patent #4,426,485 1/17/84.

61. The polymers studied were provided by Union Carbide with polydispersities between 2.1 and 7.1. For more information see (a) Jenkins, R.D.; Silebi, C.A.; El-Aasser, M.S. in *Polymers as Rheology Modifiers* (Schulz, D.N.; Glass, J.E., Eds.) **1991**, ACS Symposium Series *462*, ch. 13, p. 222; (b) Jenkins, R.D.; Sinha, B.R.; Bassett, D.R. *Proc. Am. Chem. Soc., Div. Polym. Mater. Sci. Eng.* **1991**, *65*, 72; (c) Jenkins, R.D. Ph.D. dissertation, Lehigh University 1990.

62. Gangal, S.V. in *Encyclopedia of Polymer Science and Engineering* (Mark, H.F.; Bikales, N.M.; Overberger, C.G.; Menges, G.; Kroschwitz, J.I., Eds.); John Wiley and Sons: New York, **1989**, *16*, 587.

63. Shafrin, E.G.; Zisman, W.A. *J. Phys. Chem.* **1960**, *64*, 519.

64. Evers, O.A.; Scheutjens, J.M.H.M.; Fleer, G.J. *Macromolecules* **1990**, *23*, 5221.

65. Gangal, S.V. in *Encyclopedia of Polymer Science and Engineering*, 2nd ed. (Mark, H.F.; Bikales, N.M.; Overberger, C.G.; Menges, G.; Kroschwitz, J.I., Eds.); John Wiley and Sons: New York, 1989, vol. 16, p. 608.

66. Chandrasekaran, S. in *Encyclopedia of Polymer Science and Engineering*, 2nd ed. (Mark, H.F.; Bikales, N.M.; Overberger, C.G.; Menges, G.; Kroschwitz, J.I., Eds.); John Wiley and Sons: New York, 1985, vol. 3, p. 468.

67. Dohany, J.E.; Humphrey, J.S. in *Encyclopedia of Polymer Science and Engineering*, 2nd ed. (Mark, H.F.; Bikales, N.M.; Overberger, C.G.; Menges, G.; Kroschwitz, J.I., Eds.); John Wiley and Sons: New York, 1989, vol. 17, p. 539.

68. Goddard, E.D.; Aronson, M.P.; Gum, M.L. in *The Effect of Polymers on Dispersion Properties* (Tadros, Th. F., Ed.) Academic Press, London, 1982, p. 252.

69. Goddard, E.D.; Aronson, M.P.; Gum, M.L. *ibid.* p. 59.

70. Kronberg, B.; Kall, L.; Stenius, P. *J. Dispersion Sci. Tech.* **1981**, *2*, 215.

71. Andrade, J.D.; Ma, S.M.; King, R.N.; Gregonis, D.E. *J. Colloid Interface Sci.* **1979**, *72*, 488.

72. Baker, J.A.; Pearson, R.A.; Berg, J.C. *Langmuir* **1989**, *5*, 339.

73. Napper, D.W. *Polymeric Stabilization of Colloidal Dispersions Colloid Science* (Ottewill, R.H.; Rowell, R.L., Eds.) Academic Press: London, 1989.

74. Clunie, J.S.; Ingram, B.T. in *Adsorption from Solution at the Solid/Liquid Interface* (Parfitt, G.D.; Rochester, C.H., Eds.) Academic Press: London, 1983, p. 105.

75. Harkin, W.D.; Jordan, H.F. *J. Am. Chem. Soc.* **1930**, *52*, 1751.

76. Riess, G; Nervo, J.; Rogez, D. *Polym. Eng. Sci.* **1977**, *17*, 634.

77. Minc, S. *Electroanal. Chem. Int. Electrochem.* **1975**, *62*, 291.

78. Okubo, T. *J. Colloid Interface Sci.* **1988**, *125*, 386.

79. Becher, P.; Schick, M.J. in *Nonionic Surfactants Physical Chemistry* (Schick, M.J., Ed.) (Surfactant Science Series volume 23) Marcel Dekker, Inc.: New York, 1987, p. 435.

# BIBLIOGRAPHY


Aida, T.; Inoue, S. *Macromolecules* **1981**, *14*, 1162.

Airhart, J.; Sibiga, S.; Sanders, H.; Khairallah, E. A. *Anal. Biochem.* **1973**, *53*, 132;

Allmer, K.; Feiring, K. A. *Macromolecules* **1991**, *24*, 5487.

Andrade, J. D. in *Surface and Interfacial Aspects of Biomedical Polymers: Surface Chemistry and Physics* (Andrade, J. D., Ed.); Plenum: New York, 1985, vol. 1, p. 184.

Andrade, J. D.; Smith, L. M.; Gregonis, D. E. in *Surface and Interfacial Aspects of Biomedical Polymers: Surface Chemistry and Physics*. (Andrade, J. D., Ed.); Plenum: New York, 1985, vol. 1, chap. 7, pp. 276-7.

Andrade, J. D.; Ma, S. M.; King, R. N.; Gregonis, D. E. *J. Colloid Interface Sci.* **1979**, *72*, 488.

Andrews, D. W.; Ottensmeyer, F. P. *Ultramicroscopy* **1982**, *9*, 337.

Antohi, S.; Brumfeld, V. *Rev. Roum. Morphol., Embryol. Physiol., Physiol.* **1984**, *21*, 213.

Arnold, L. J., Jr. *Methods Enzymol.* **1985**, *112*, 270.

Asako, S.; Hirai, Y.; Okita, K.; Matsubara, H.; Niwa, S.; Takashina, M. *Jpn Kokai Tokkyo Koho* JP 63,196,282 [88,196,282] **1987**. [CA 110:113245s]

Asako, S.; Hirai, Y.; Okita, K.; Matsubara, H.; Niwa, S.; Takashira, M. *Jpn Kokai Tokkyo Koho* JP 63,198,978 [88,198,978] **1987**. [CA 110:113252s]

Bailey, F. E., Jr.; Koleske, J. V. *Alkylene Oxides and Their Polymers* (Surfactant Science Series, vol. 35) Marcel Dekker: New York, 1991.

Bailey, F. E.; Koleske, J. V. *Poly(ethylene oxide)* Academic Press: New York, 1976, ch. 5.

Baker, J. A.; Berg, J. C. *Langmuir* **1988**, *4*, 1055.

Baker, J. A.; Pearson, R. A.; Berg, J. C. *Langmuir* **1989**, *5*, 339.

Balazs, A. C.; Gempe, M.; Zhou, Z. *Macromolecules* **1991**, *24*, 4918.

Baleux, B. *C.R. Acad. Sci., Ser. C. Paris* **1972**, *274*, 1617.

Barnes, P. *J. Org. Synth. Coll. vol. III* (Horning, E.C., Ed.) John Wiley and Sons: New York, **1955**, p. 555;

Baszkin, A.; Terminassian-Seraga, L. *Polymer* **1974**, *15*, 759.

Batich, C. D.; Wendt, R. C. in *Photon, Electron and Ion Probes of Polymer Structure and Properties* (Dwight, D. W.; Fabish, T. J.; Thomas, H. R., Eds.) American Chemical Society: Washington, D. C. 1981, (ACS Symposium Series 162), p. 221.

Becher, P.; Schick, M. J. in *Nonionic Surfactants Physical Chemistry* (Schick, M. J., Ed.) (Surfactant Science Series volume 23) Marcel Dekker, Inc.: New York, 1987, p. 435.

Bee, T. G.; McCarthy, T. J. *Macromolecules* **1992**, *25*, 2093.

Bening, R. C.; McCarthy, T. J. *Macromolecules* **1990**, *23*, 2648.

Blaakmeer, J.; Bohmer, M. R.; Cohen Stuart, M. A.; and Fleer, G. J. *Macromolecules* **1990**, *23*, 2301.

Bohmer, M. R.; Koopal, L. K. *Langmuir* **1990**, *6*, 1478.

Bomben, K. D.; Dev, S. B. *Anal. Chem.* **1988**, *60*, 1393.

Bonekamp, B. C. *Colloids Surfaces* **1989**, *41*, 267.

Bonekamp, B. C.; Alvarez, R. H.; De Fas Nieves, F. J.; Bijsterbosch, B. H. *J. Colloid Interface Sci.* **1987**, *118*, 366.

Bonekamp, B. C.; Lyklema, J. *J. Colloid Interface Sci.* **1986**, *113*, 67.

Brennan, J. V. Ph.D. dissertation, University of Massachusetts, 1991.

Brennan, J. V.; McCarthy, T. J. *Polym. Prepr. (Am. Chem. Soc., Div. Polym. Chem.)* **1988**, *29* (2), 338.

Brennan, J. V.; McCarthy, T. J. *Polym. Prepr. (Am. Chem. Soc., Div. Polym. Chem.)* **1989**, *30* (2), 152.

Briggs, D.; Brewis, D. M.; Konieczo, M. B. *J. Mater. Sci.* **1976**, *11*, 1270.

Burdon, J.; Tatlow, J. C. *J. Appl. Chem.* **1958**, *8*, 293.

Cabasso, I.; Zilkha, A. J. *Macromol. Sci.-Chem.* **1974**, *A8*, 1313.

Cason,J. *J. Org. Synth. Coll. vol. III* (Horning, E.C., Ed.) John Wiley and Sons: New York, **1955**, p. 169.

Chandrasekaran, S. in *Encyclopedia of Polymer Science and Engineering*, 2nd ed. (Mark, H. F.; Bikales, N. M.; Overberger, C. G.; Menges, G.; Kroschwitz, J. I., Eds.); John Wiley and Sons: New York, 1985, vol. 3, p. 468.

Char, K.; Frank, C. W.; Gast, A. P. *Langmuir* **1989**, *5*, 1335.

Clark, D. T.; Thomas, H. R. *J. Polym. Sci., Polym. Chem. Ed.* **1977**, *15*, 2843.

Clunie, J. S.; Ingram, B. T. in *Adsorption from Solution at the Solid/Liquid Interface* (Parfitt, G. D.; Rochester, C. H., Eds.) Academic Press: London, 1983, p. 105.

Cohen Stuart, M. A. *J. Phys. France* **1988**, *49*, 1001.

Cohen Stuart, M. A.; Cosgrove, T.; Vincent, B. *Adv. Colloids Interface Sci.* **1986**, *24*, 143.

Cohen Stuart, M. A.; Fleer, G. J.; Lyklema, J.; Norde, W.; Scheutjens, J. M. H. M. *Adv. Colloid Interface Sci.* **1991**, *34*, 477.

Cohen Stuart, M. A.; Scheutjens, J. M. H. M.; Fleer, G. J. *J. Polym. Sci.: Polym. Phys. Ed.* **1980**, *18*, 559.

Cohen Stuart, M. A.; Waajen, F. H. W. H.; Cosgrove, T.; Vincent, B.; Crowley, T. L. *Macromolecules* **1984**, *17*, 1825.

Cosani, A.; Terbojevich, M.; Romanin-Jacur, L.; Peggion, E. in *Peptides, Polypeptides and Proteins* (Blout, E. R.; Bovey, F. A.; Goodman, M.; Lotan, N., Eds.); John Wiley and Sons: New York, 1974, p. 166.

Cosgrove, T.; Crowley, T. L.; Vincent, B. in *Adsorption From Solution* (Ottewill, R. H.; Rochester, C. H.; Smith, A. L., Eds.); Academic Press: New York, 1983, p. 287.

Cosgrove, T.; Heath, T. G.; Ryan, K.; van Lent, B. *Polymer Commun.* **1987**, *28*, 64.

Cosgrove, T.; Vincent, B. in *Fluid Interfacial Phenomena* (Croxton, C. A., Ed.) John Wiley and Sons: New York, 1986, p. 607.

Costello, C. A.; McCarthy, T. J. *Macromolecules* **1984**, *17*, 2940.

Costello, C. A.; McCarthy, T. J. *Macromolecules* **1987**, *20*, 2819.

Couture, L.; van de Ven, T. G. M. *Colloids & Surfaces* **1991**, *54*, 245.

Crabb, H. J.; Jackson, R. C. *J. Membr. Biol.* **1986**, *91*, 85.

Danielson, N. D.; Taylor, R. T.; Huth, J. A.; Siergiej, R. W.; Galloway, J. G.; Paperman, J. B. *Ind. Eng. Chem. Prod. Res. Dev.* **1983**, *22*, 303.

Dann, J. R. *J. Colloid Interface Sci.* **1970**, *32*, 302.

Davies, R. J.; Dix, L. R.; Toprakcioglu, C. *J. Colloid Interface Sci.* **1989**, *129*, 145.

Deffieux, A.; Boileau, S. *Polymer* **1977**, *18*, 1047.

Dias, A. J.; McCarthy, T. J. *Macromolecules* **1984**, *17*, 2529.

Dias, A. J.; McCarthy, T. J. *Macromolecules* **1985**, *18*, 1826.

Dias, A. J.; McCarthy, T. J. *Macromolecules* **1987**, *20*, 2068.

Dobbie, J. W.; Evans, R.; Gibson, D. V.; Smitham, J. B.; Napper, D. H. *J. Colloid Interface Sci.* **1973**, *45*, 557.

Dohany, J. E.; Humphrey, J. S. in *Encyclopedia of Polymer Science and Engineering*, 2nd ed. (Mark, H. F.; Bikales, N. M.; Overberger, C. G.; Menges, G.; Kroschwitz, J. I., Eds.); John Wiley and Sons: New York, 1989, vol. 17, p. 539.

Dwight, D. W. *Chemtech* **1982**, *March*, 166.

Dwight, D. W.; Riggs, W. M. *J. Colloid Interface Sci.* **1974**, *47*, 650.

Eagland, D. *Chemtech* **1990**, *April*, 248.

Eisenbach, C. D.; Peuscher, M. *Makromol. Chem., Rapid Commun.* **1980**, *1*, 105.

Eisenbach, C. D.; Peuscher, M.; Wegner, G.; Weiss, M. *Makromol. Chem.* **1983**, *184*, 2313.

Epand, R. F.; Scheraga, H. A. *Biopolymers* **1968**, *6*, 1383.

Evers, O. A.; Scheutjens, J. M. H. M.; Fleer, G. J. *Macromolecules* **1990**, *23*, 5221.

Evers, O. A; Fleer, G. J; Scheutjens, J. M. H. M.; Lyklema, J. *J. Colloid Interface Sci.* **1985**, *111*, 446.

Fersht, A. R.; Jencks, W. P. *J. Am. Chem. Soc.* **1970**, *92*, 5432.

Figueruelo, J. E.; Worsfold, D. J. *Eur. Polym. J.* **1968**, *4*, 439.

Filler, R.; O'Brien, J.F.; Fenner, J. V.; Hauptschein, M. *J. Am. Chem. Soc.* **1953**, *75*, 966.

Fleer, G. J.; Lyklema, J. in *Adsorption from Solution at the Solid/Liquid Interface* (Parfitt, G. D.; Rochester, C. H., Eds.); Academic Press: New York, 1983, p. 153.

Fuchs, O. in *Polymer Handbook*, 3rd ed. (Brandjup, J.; Immergut, E. H., Eds.); John Wiley and Sons: New York, 1989, p. 388.

Furusawa, K.; Kanesaka, M.; Yamashita, S. *J. Colloid Interface Sci.* **1984**, *99*, 341.

Gagnon, D. R.; McCarthy, T. J. *J. Appl. Polym. Sci.* **1984**, *29*, 4335.

Gangal, S. V. in *Encyclopedia of Polymer Science and Engineering* (Mark, H. F.; Bikales, N. M.; Overberger, C. G.; Menges, G.; Kroschwitz, J. I., Eds.); John Wiley and Sons: New York, 1989, *16*, 587, 608.

Gasparani, G. M.; Polidori, E. *J. Chem. Eng. Data* **1976**, *21*, 504.

Gee, G.; Higginson, C. E.; Levesley, P.; Taylor, K. J. *J. Chem Soc.* **1959**, 1338.

Goddard, E. D.; Aronson, M. P.; Gum, M. L. in *The Effect of Polymers on Dispersion Properties* (Tadros, Th. F., Ed.) Academic Press, London, 1982, pp. 59, 252.

Golander, C.-G.; Kiss, E. *J. Colloid Interface Sci.* **1988**, *121*, 240.

Greenfield, N.; Fasman, G. D. *Biochemistry* **1969**, *8*, 4108.

Hair, M. L.; Guzonas, D.; Boils, D. *Macromolecules* **1991**, *24*, 341.

Hardebo, J. E. *J. Kaahrstroem Acta Physiol. Scand.* **1985**, *125*, 495.

Harkin, W. D.; Jordan, H. F. *J. Am. Chem. Soc.* **1930**, *52*, 1751.

Holmes Farley, S. R.; Bain, C. D.; Whitesides, G. M. *Langmuir* **1988**, *4*, 921.

Holmes Farley, S. R.; Whitesides, G. M. *Langmuir* **1986**, *2*, 266.

Holmes Farley, S. R.; Whitesides, G. M. *Langmuir* **1987**, *3*, 62.

Holmes, Farley, S. R.; Reamey, R. H.; McCarthy, T. J.; Deutch, J.; Whitesides, G. M. *Langmuir* **1985**, *1*, 725.

Homes Farley, S. R.; Reamey, R. H.; Nuzzo, R.; McCarthy, T. J.; Whitesides, G. M. *Langmuir* **1987**, *3*, 799.

Hommel, M.; Sun, A. M. F.; Goosen, M. F. A. *Eur. Pat. Appl. EP 167690* **1984**. [CA 104:174704]

Hoy, K. K.; Hoy, R. C. United States Patent #4,426,485 1/17/84.

Huang, W. M.; Gibson, S. J.; Facer, P.; Gu, J.; Polak, J. M. *Histochemistry* **1983**, *77*, 275.

Iyengar, D. R.; Brennan, J. V.; McCarthy, T. J. *Macromolecules* **1991**, *24*, 5886.

Iyengar, D. R.; McCarthy, T. J. *Macromolecules* **1990**, *23*, 4344.

Jacobsen, C.; Jacobsen, J. *Biochem. J.* **1979**, *181*, 251.

Jacobson, B. S. *Adv. Cell Biol.* **1988**, *2*, 91.

Jacobson, B. S.; Branton, D. *Science*, **1977**, *195*, 302.

Jacobson, B. S.; Ryan, U. S. *Tissue and Cell* **1982**, *14*, 69.

Jenkins, R. D. Ph.D. dissertation, Lehigh University 1990.

Jenkins, R. D.; Silebi, C. A.; El-Aasser, M. S. in *Polymers as Rheology Modifiers* (Schulz, D. N.; Glass, J. E., Eds.) **1991**, ACS Symposium Series *462*, ch. 13, p. 222.

Jenkins, R. D.; Sinha, B. R.; Bassett, D. R. *Proc. Am. Chem. Soc., Div. Polym. Mater. Sci. Eng.* **1991**, *65*, 72.

Johnson, R. E., Jr.; Dettre, R. H. *J. Phys. Chem.* **1964**, *68*, 1744.

Johnson, R. E., Jr.; Dettre, R. H. in *Surface and Colloid Science* (Matijevic, E., Ed.) Wiley-Interscience: New York; **1969**, *2*, 85.

Kawaguchi, M.; Hada, T.; Takahashi, A. *Macromolecules* **1989**, *22*, 4045.

Kawaguchi, M.; Mikura, M.; Takahashi, A. *Macromolecules* **1984**, *17*, 2063.

Kawaguchi, M.; Sakai, A.; Takahashi, A. *Macromolecules* **1986**, *19*, 2952.

Kawaguchi, M; Komatsu, S.; Matsuzumi, M.; Takahashi, A. *J. Colloid Interface Sci.* **1984**, *102*, 356.

Kazanskii, K. S. *Pure & Appl. Chem.* **1981**, *53*, 1645.

Kazanskii, K. S.; Solovyanov, A. A.; Entels, S. G. *Eur. Polym. J.* **1971**, *7*, 1421.

Kevill, D. N.; Daum, P. H.; Sapre, R. *J. Chem. Soc., Perkin II* **1975**, 963.

Killmann, E. *Polymer* **1976**, *17*, 864.

Klein, J.; Luckham, P. F. *Macromolecules* **1984**, *17*, 1041.

Kolb, B. U.; Patton, P. A.; McCarthy, T. J. *Macromolecules* **1990**, *23*, 366.

Kolthoff, I. M.; Sandel, E. B.; Meehan, E. J.; Bruckenstein, S. *Quantitative Chemical Analysis*, 4th ed. The MacMillan Co.: Toronto, 1969, p. 1163.

Kronberg, B.; Kall, L.; Stenius, P. *J. Dispersion Sci. Tech.* **1981**, *2*, 215.

Kurami, M.; Shirakami, Y.; Takahashi, K.; Ueda, N. *Eur. Pat. Appl. EP 233,619* **1987**. [CA 108:34189g]

Kuzmenka, D. J.; Granick, S. *Macromolecules* **1988**, *21*, 779.

Kuzmenka, D. J.; Granick, S. *Polymer Commun.* **1988**, *29*, 64.

Ladenheim, H.; Bender, M. L. *J. Am. Chem. Soc.* **1960**, *82*, 1895.

Lazar, A.; Silverstein, L.; Margel, S.; Mizrahi, A. *Dev. Biol. Stand.* **1985**, *60*, 457.

Lee, K.-W.; McCarthy, T. J. *Macromolecules* **1988**, *21*, 2318.

Lehn, J. M. *Pure & Appl. Chem.* **1980**, *52*, 2303.

Lenher, V.; Stone, H. W.; Skinner, H. H. *J. Am. Chem. Soc.* **1922**, *44*, 143.

Lide, D. R., Ed. *Handbook of Chemistry and Physics*, 72nd ed.; CRC Press: Boca Raton, 1991-1992, p. VIII-39.

Lipton, M. F.; Sorensen, C. M.; Sadler, A. C.; Shapiro, R. H. *J. Organometallic Chem.* **1980**, *186*, 155.

Lopez, A.; Fidel, J.; Alonso Cermenco, F. *An. Quim.* **1969**, *55*, 153.

Losse, G.; Raddatz, H.; Naumann, W. *J. Kossowicz Pharmazie* **1988**, *43*, 105.

Lundblad, R. L.; Robert, H. R. *Thromb. Res.* **1982**, *25*, 319.

Marra, J.; Hair, M. L. *Colloids & Surfaces* **1989**, *34*, 215.

McKillop, A.; Bromley, D.; Taylor, E. C. *J. Org. Chem.* **1968**, *34*, 1172.

Midgley, G.; Thomas, C. B. *J. Chem. Soc., Perkin Trans. II* **1984**, *(9)*, 1537.

Minc, S. *Electroanal. Chem. Int. Electrochem.* **1975**, *62*, 291.

Miyazawa, T. in *Poly(α-amino acids): Protein Models for Conformational Studies* (Fasman, G. D., Ed.); Marcel Dekker: New York, 1967, p. 90.

Mobashery, S.; Johnston, M. *J. Org. Chem.* **1985**, *50*, 2200.

Morra, M.; Occhiello, E.; Garbassi, F. *Langmuir* **1989**, *5*, 872.

Napper, D. W. *Polymeric Stabilization of Colloidal Dispersions Colloid Science* (Ottewill, R. H.; Rowell, R. L., Eds.) Academic Press: London, 1989.

Nemec, J. W.; Bauer, W., Jr. in *Encyclopedia of Polymer Science and Engineering*, 2nd ed. (Mark, H.F.; Bikales, N. M.; Overberger, C. G.; Menges, G.; Kroschwitz, J. I., Eds.); John Wiley and Sons: New York, 1985, p. 285.

Nenna, S.; Figueruelo, J. E. *Die Makromol. Chem.* **1975**, *176*, 3377.

Nenna, S.; Figueruelo, J. E. *Eur. Polym. J.* **1975**, *11*, 511.

Newman, M. S.; Fukunaga, T.; Miwa, T. *J. Am. Chem. Soc.* **1960**, *82*, 873.

Noyes, W. A. *Org. Synth. Coll. vol. III* (Blatt, A. H., Ed.); John Wiley and Sons: New York, **1955**, p. 108.

Nuzzo, R. G.; Smolinsky, G. *Macromolecules* **1984**, *17*, 1013.

Okubo, T. *J. Colloid Interface Sci.* **1988**, *125*, 386.

Owens, D. K.; Wendt, R. C. *J. Appl. Polym. Sci.* **1969**, *13*, 1741.

Panitz, J. A. *Ultramicroscopy* **1983**, *11*, 161.

Papenhuijzen, J.; Fleer, G. J.; Bijsterbosch, B. H. *J. Colloid Interface Sci.* **1985**, *104*, 530.

Papenhuijzen, J.; Van der Schee, H. A.; Fleer, G. J. *J. Colloid Interface Sci.* **1985**, *104*, 540.

Parnas, R. S.; Chaimberg, M.; Taepaisitphongse, V.; Cohen, Y. *J. Colloid Interface Sci.* **1989**, *129*, 441.

Pease, J. P.; Tsang, W.-G.; Magee, A. S.; Konopacki, D. B. *Macromol. Synth.* **1989**, *11*, in press.

Pederson, D.; Gabriel, D.; Hermans, J., Jr. *Biopolymers* **1971**, *10*, 2133.

Pirkle, W. H.; Hyun, M. H. *J. Org. Chem.* **1984**, *49*, 3043.

Price, C. C.; Akkapeddi, M. K. *J. Am. Chem. Soc.* **1972**, *94*, 3972.

Price, C. C.; Carmelite, D. D. *J. Am. Chem. Soc.* **1966**, *88*, 4039.

Quirk, R. P.; Ma, J.-J. *J. Polym Sci. Part A: Polym. Chem.* **1988**, *26*, 2031.

Quirk, R. P.; Seung, N. S. in *Ring Opening Polymerization: Kinetics, Mechanism, and Synthesis* (J. E. McGrath, Ed.) **1985**, *286*, 37.

Rabinovitch, B. S.; Winkler, C. A. *Canad. J. Res.* **1942**, *20*, 221.

Rabjohn, N.; Harbert, C. A. *J. Org. Chem.* **1970**, *35*, 3726.

Rasmussen, J. R.; Bergbreiter, D. E.; Whitesides, G. M. *J. Am. Chem. Soc.* **1977**, *19*, 4746.

Rasmussen, J. R.; Stedronsky, E. R.; Whitesides, G. M. *J. Am. Chem. Soc.* **1977**, *99*, 4736.

Reilley, C. N.; Everhart, D. S.; Ho, F. F.-L. in *Applied Electron Spectroscopy for Chemical Analysis* (Windawi, H.; Ho, F. F.-L., Eds.) John Wiley and Sons: New York, 1982, ch. 6.

Reuter, H.; Horing, S.; Ulbricht, J. *Eur. Polym. J.* **1989**, *25*, 1113.

Rha, C.; Rodriguez-Sanchez, D. *Eur. Pat. Appl. EP 152,898* **1984**. [CA 104:18670u]

Riess, G; Nervo, J.; Rogez, D. *Polym. Eng. Sci.* **1977**, *17*, 634.

Roe, R. J. *J. Chem. Phys.* **1974**, *60*, 4192.

Rosenhack, K.; Doty, P. *Biochemistry* **1961**, *47*, 1775.

Ryser, H. J. P.; Shen, W. C.; Morad, N. *Polym. Prepr. (Am. Chem. Soc., Div. Polym. Chem.)* **1986**, *27*, 15.

Satoh, M.; Matsumoto, N.; Komiyama, J.; Iijima, T. *Polym. Comm.* **1987**, *28*, 71.

Scheutjens, J. M. H. M.; Fleer, G. J. *J. Chem. Phys.* **1979**, *83*, 1619;

Scheutjens, J. M. H. M.; Fleer, G. J. *J. Chem. Phys.* **1980**, *84*, 178.

Schick, M. J., Ed. *Nonionic Surfactants: Physical Chemistry* (Surfactant Science Series vol. 23) Marcel Dekker: New York, 1987.

Sepulveda, C. A.; Schlager, S. I. *Methods Enzymol.* **1983**, *93*, 260.

Shafrin, E. G.; Zisman, W. A. *J. Phys. Chem.* **1960**, *64*, 519.

Shen, S.; Kibat, P. G.; Chow, M. B.; Langer, R. S. *Polym. Prepr. (Am. Chem. Soc., Div. Polym. Chem.)* **1989**, *30 (1)*, 478.

Shih, L. B.; Primus, F. J.; Goldenberg, M. D. *PCT Int. Appl. WO 8705031* **1987**. [CA 108:68965x]

Shima, S.; Fukuhara, Y.; Sukai, H. *Agric. Biol. Chem.* **1982**, *46*, 1917.

Shima, S.; Matsuoka, H.; Iwamoto, T.; Sakai, H. *J. Antibiot.* **1984**, *37*, 1449.

Shoichet, M. S.; McCarthy, T. J. *Macromolecules* **1991**, *24*, 982.

Shoichet, M. S.; McCarthy, T. J. *Macromolecules* **1991**, *24*, 1441.

Shoichet, M. S; McCarthy, T. J. in *Materials Synthesis Based on Biological Processes*; (Alper, M.; Calvert, P.; Frankel, R.; Rieke, P.; Tirrell, D., Eds.); Materials Research Society Symposium Proceedings, 1990, vol. 218, Materials Research Society: Pittsburgh, 1991, p. 57.

Skinner, J. F.; Calkins, H. H.; Liles, W. C, Jr.; Kaplan, L. J. *Biopolymers* **1982**, *21*, 833.

Skutelsku, E.; Roth, J. *J. Histochem. Cytochem.* **1986**, *34*, 693.

Sperber, N.; Papa, D.; Schwenk, E. *J. Am. Chem. Soc.* **1948**, *70*, 3091.

Sperry, P. R.; Thibeault, J. C.; Kostansek, E. C. in *Eleventh International Conference in Organic Coating Science and Technology Proceedings* (Patsis, A. V., Ed.) Advanced Orgainc Coatings Science and Technology Series 1985; Technomic Publishing: Lancaster, PA, **1987**, *9*, 1.

Stouffer, J. M.; McCarthy, T. J. *Macromolecules* **1988**, *21*, 1204.

Szwarc, M. *Living Polymers and Mechanisms of Anionic Polymerization* (Adv. in Polym. Sci. vol. 49) Springer Verlag: Berlin, 1983.

Tanaka, S.; Fukagawa, O.; Baba, Y.; Kagemoto, A.; Fujishiro, R. *Netsu Sokutei* **1982**, *9*, 2.

van den Beld, C. M. B.; Lingeman, H.; van Ringen, G. J.; Tjaden, U. R.; van der Greef, J. *Anal. Chim. Acta* **1988**, *205*, 15.

Van der Schee, H. A.; Lyklema, J. *J. Phys. Chem.* **1984**, *88*, 6661.

Wade, L. G., Jr.; Silvey, W. B. *Org. Prep. Proc. International* **1982**, *14*, 357.

Walz, D. A.; Penner, J.; Barnhart, M. I. *Scanning Electron Microsc.* **1984**, *(1)*, 303.

Ward, W. J.; McCarthy, T. J. in *Encyclopedia of Polymer Science and Engineering*, 2nd ed.; (Mark, H. F.; Bikales, N. M.; Overberger, C. G.; Menges, G.; Kroschwitz, J. I., Eds.); Wiley: New York, 1989, supplement, p. 674.

Weiler, J. M. *Immunopharmacology* **1983**, *6*, 245.

Wilson, M. D.; Ferguson, G. S.; Whitesides, G. M. *J. Am. Chem. Soc.* **1990**, *112*, 1244.

Wilson, M. D.; Whitesides, G. M. *J. Am. Chem. Soc.* **1988**, *110*, 8718.

Wojtech, B. *Makromol. Chem.* **1966**, *66*, 180.

Womack, E. B.; McWhirter, J. *J. Org. Synth. Coll. vol. III* (Horning, E.C., Ed.) John Wiley and Sons: New York, **1955**, p. 714.

Wu, S. *Polymer Interface and Adhesion* Marcel Dekker: New York, **1982**, pp. 337, 359.

Yang, J. T.*Abs. Pap. (Am. Chem. Soc.)* **1982**, *183*, 147.

Yasui, S. C.; Keiderling, T. A. *J. Am. Chem. Soc.* **1986**, *108*, 5576.

Yoon, N. M.; Pak, C. S.; Brown, H. C.; Krishnamurthy, S.; Stocky, T. P. *J. Org. Chem.* **1973**, *38*, 2786.

Young, P. R.; Vacante, D. A.; Snyder, W. R. *J. Am. Chem. Soc.* **1982**, *104*, 7287.

Yu, T. J.; Peticolas, W. L. in *Peptides, Polypeptides, and Proteins* (Blout, E.R.; Bovey, F. A.; Goodman, M.; Lotan, N., Eds.); John Wiley and Sons: New York, 1974, p. 370.

Zil'berman, E. N. *Russ. Chem. Rev.* **1962**, *31*, 615.